Unconventional particle behaviours in supersymmetric theories and gravity

Luc Darmé

LPTHE
LABORATOIRE DE PHYSIQUE THEORIQUE ET HAUTES ENERGIES

Institut Lagrange de Paris

UPMC
SORBONNE UNIVERSITÉS

THÈSE DE DOCTORAT
DE L'UNIVERSITÉ PIERRE ET MARIE CURIE

Spécialité : Physique

École doctorale : Physique en Île-de-France

réalisée au

LPTHE

présentée par

Luc DARMÉ

pour obtenir le grade de :

DOCTEUR DE L'UNIVERSITÉ PIERRE ET MARIE CURIE

Sujet de la thèse :

Unconventional particle behaviours in supersymmetric theories and gravity

soutenue le 09/06/2016

devant le jury composé de :

Mme	Geneviève Bélanger	Examinateur
M.	Karim Benakli	Directeur de thèse
M.	Emilian Dudas	Rapporteur
M.	Bertrand Laforge	Examinateur
M.	Yann Mambrini	Examinateur
Mme	Veronica Sanz	Rapporteur

À ma famille et mes amis

Remerciements

Mes premiers remerciements vont à mon directeur de thèse Karim Benakli. Son sens physique extraordinaire, sa disponibilité permanente et son soutien sans faille m'ont donné les clés de ce doctorat. Je veux également le remercier pour son aide patiente et considérable lors de l'organisation de cette soutenance, ainsi que pour sa bonne humeur et tous les moments mémorables passés lors de nos visites, conférences et repas communs.

Je remercie tout particulierement Mark Goodsell et Pietro Slavich, qui ont non seulement pris le temps de guider et d'accueillir le jeune doctorant que j'étais, mais qui m'ont aussi énormément appris lors de ces trois dernières années, par leurs conseils, leurs explications et leur gentillesse. Je voudrais aussi remercier spécialement Yaron Oz pour son accueil chaleureux à Tel Aviv, son fort soutien et les discussions passionnantes lors de nos projets commun. Je suis de plus profondément redevable envers Shira Chapman et Julia Harz pour leur aide et tous les bons moments passés lors de nos travaux communs.

Je tiens à remercier également mes rapporteurs Emilian Dudas et Veronica Sanz pour m'avoir permis de soutenir en temps et heure. Je suis infiniment reconnaissant envers les membres de mon jury de thèse, Geneviève Bélanger, Karim Benakli, Emilian Dudas, Bertrand Laforge, Yann Mambrini et Veronica Sanz qui ont pris le temps de se déplacer pour assister à ma soutenance.

Je remercie toute l'équipe de LPTHE pour leur travail exceptionnel qui m'a permis de mener ma thèse dans un cadre harmonieux. Plus particulièrement, un grand merci aux directeurs successifs Olivier Babelon et Benoît Doucot ainsi qu'aux secrétaires Françoise Got, Isabelle Nicolaï et Annie Richard qui ont toujours été présents pour m'aider et résoudre les nombreux problèmes administratifs. J'aimerais également remercier de tout cœur Lionel Pihery pour son aide dans mon installation informatique, sa gentillesse et son extrême compétence. Sa disparition a laissé un vide.

Je tiens à remercier les laboratoires et instituts qui m'ont accueilli au fil de ma thèse ainsi que tous les chercheurs croisés durant ces trois années pour leur aide et leurs conseils, en particulier ceux du LPTHE ainsi que Ben Allanach, Marco Cirelli, Emilian Dudas, Joerg Jaeckel, Marios Petropoulos, Mariano Quiros et Leszek Roszkowski. Un grand merci à Jean-Bernard Zuber pour avoir accepté de me parrainer durant cette thèse et pour les discussions toujours intéressantes et agréables.

Je remercie également l'équipe de l'UE 3P021 (ex-LP348), particulièrement Christophe Claveau, Géraldine Féraud, Samuel Gresillon, Rémy Le Breton et bien évidement Jean-Hugues Fillion. L'entraide et la bonne humeur de cette équipe ont fait de cet enseignement (et des réunions pédagogiques) un plaisir et un très bon souvenir.

J'aimerais exprimer ma gratitude à mes professeurs pour m'avoir donné le goût de la physique théorique, et spécialement à Denis Bernard, Christoph Kopper, Marios Petropoulos et Ben Allanach.

Je remercie de plus les allocations AMX qui m'ont donné la possibilité de réaliser cette thèse dans les meilleures conditions, ainsi que le soutien financier de l'Institut Lagrange de Paris qui m'a permis de participer à de nombreux séminaires et conférences.

Merci aux postdocs du labo pour leur gentillesse et les nombreux et riches échanges que j'ai pu avoir avec eux. En particulier un grand merci à Julia Harz, Diego Redigolo, Robert Ziegler, Marco Zaro, Filippo Sala, Kalliopi Petraki et Bradley Kavanagh. Je voudrais ensuite remercier les doctorants, présents et passés, du laboratoire ou d'ailleurs qui m'ont aidé à passer ces trois années le plus agréablement possible : Emanuele, Harold, Jérémy, Sasha, Thibault, Thomas V., Tianhan, Tresa, Pierre, Gauthier, Antoine, Laetitia, Matthieu, Frédéric, Hugo, Johannes, Oscar, Thomas D., Chrysoula, Alessandro et Gyorgy.

Finalement, je suis profondément redevable envers tous ceux qui m'ont permis d'arriver là où je suis. D'abord mes amis qui m'ont toujours donné leur appui et leur confiance, mes frères et sœurs pour m'avoir patiemment écouté et aider, ma famille et ma belle-famille pour leur présence réconfortante, et surtout mes parents qui m'ont fait monter une à une les marches de la vie. Mon dernier et plus grand merci va à ma femme Claire qui a illuminé ma vie depuis notre rencontre et à ma fille Gabrielle dont le sourire m'a porté pendant ces derniers mois.

Contents

Introduction

"It doesn't make any difference how beautiful your guess is, it doesn't make any difference how smart you are, who made the guess, or what his name is. If it disagrees with experiment, it's wrong."[1]

An important lesson from history is that Nature rarely complies graciously with the theories carefully crafted by scientists. Successful theories are usually built over a graveyard of rejected ideas. The discovery of the Higgs boson in 2012 therefore marked a milestone in modern physics. For once Nature had complied with the theoretical predictions. This Brout–Englert–Higgs boson (or Higgs boson for short) had indeed been expected as the keystone of the Standard Model of particle physics for decades.

The Standard Model of particle, which describes the physics of three fundamental forces mediated by gauge bosons shaping the interactions between elementary particles has been incredibly successful in experiments. It has predicted successfully thousands of measurements during the past four decades. Despite these tremendous achievements, it has however been known for an equally long time to be incomplete. Apart from the obvious fact that it does not provide us with a quantum theory of gravity, it has a major consistency puzzle known as the hierarchy problem. In a nutshell, this issue arises when one computes the quantum corrections to the Higgs boson mass. The integral involving loops of Standard Model particles depends quadratically on the ultraviolet cut-off which measures the scale up to which the Standard Model is valid. If the Standard Model is all which exists up to the quantum gravity scale, then the Higgs boson mass should be very close to the Planck mass. Since we actually measured it to be roughly thirty order of magnitude smaller, a miracle must be occurring which protects its mass against these radiative corrections up to a precision of 10^{-30}. As physicists do not like miracles, numerous mechanisms have been introduced to explain this conundrum.

Among these mechanisms, supersymmetry (SUSY) has been arguably the most studied. It is based on the idea that fermions and bosons should be treated on a morally equal footing by fitting them into a bigger object, called a supermultiplet. Supersymmetry associates with each bosonic divergent loop diagram a fermionic loop diagram precisely cancelling the divergence. Unfortunately, Nature did not follow this beautiful picture and all Standard Model particles come without a supersymmetric partner with the same mass. Supersymmetry therefore needs to be broken at a scale above the current detection capability, effectively making the supersymmetric particles

[1] Richard Feynman, pronounced during one of the famous lectures from the serie "The Character of Physical Law" delivered in 1964 at Cornell University

too heavy to be seen. The price to pay is the re-introduction of a new fine-tuning, usuall called the *little hierarchy problem*. We have in fact traded the question "Why is the Higgs mass so much lighter than the Planck scale?" for "Why is the Higgs mass lighter than the SUSY scale?". As the collider experiments push to ever higher scale the hypothetic SUSY particles, this little hierarchy problem becomes more pressing and the most basic supersymmetric realisation are now severly fine-tuned.

There are, however, two main reasons why we would like to retain supersymmetry close the electroweak scale. The first one is a long-standing problem arising from cosmology: there are overwhelming evidence that most of the mass of the universe is composed by some ellusive "dark matter". The point is that supersymmetry gives a upstanding candidate for such dark matter: the Lightest Supersymmetric Particle (LSP), which is expected to be stable in most supersymmetric model due to a residual discrete symmetry called R-parity. The small miracle is that such particle has precisely the right characteristics to provide us with the correct relic density of dark matter through a simple process called freeze-out. The second reason is more theoretical. In the Standard Model gauge couplings which measure the strength of the three elementary forces almost reach a similar value at a scale close the Planck scale. This is a frustrating property as equal couplings are precisely what is needed to unify the three gauge groups into a single, Grand Unified Theory (GUT). Supersymmetry cures this issue and allows for a near-perfect unification, opening the way for a GUT.

In a nutshell, there are now increasing evidence that we should be looking beyond the basic SUSY models which have shaped Beyond Standard Model physics in the past decades, and look for new, unconventional ideas to describe Nature. In this thesis, I will present two phenomenological setups where the fields contents or couplings are not the one we would have expected, but where supersymmetry has still an important role to play.

In the first part of this thesis, after reviewing the basics of the Higgs mechanism and of the hierarchy problem, I will consider two unconventional applications of supersymmetry to Beyond Standard Model phenomenology. The first one is that idea that, after all, supersymmetry may not be the symmetry protecting the mass of the Standard Model Higgs, but will still be realised at higher energy. This amounts to suppose that while supersymmetry may protect the masses of scalar particles above the SUSY scale M_S, one should find another solution to the little hierarchy problem. However, it can be shown that such scenarios, and in particular a variation called Fake Split SUSY models introduced in [1,2,3], have nonetheless numerous advantages. In particular they can give an incredibly robust prediction of the Higgs mass and have simple dark matter candidates as Weakly Interacting Massive Particles. In the second place, I will describe how to use the Dirac Gauginos framework to build a well-motivated supersymmetric scenario explaining the diphoton channel resonance possibly observed by ATLAS and CMS in the first dataset of LHC run-2. This model will retain perturbativity up to the GUT scale, vacuum stability and gauge couplings unification, while being "minimal" in the sense that it will not be necessary to introduce new "ad-hoc" fields to fit the data [4].

Another fundamental symmetry, which contrary to supersymmetry has been tested to an incredible precision is the Lorentz symmetry. Among its main consequences, Lorentz symmetry fixes the form of the dispersion relation of a momentum eigenstates,

effectively linking spatial momentum with the energy carried by the field. Interestingly, global Lorentz symmetry is also a blatantly broken one. Indeed, it is broken by the curvature of spacetime and by every fluids fixing a particular direction of time.

In a second part of this work, I will study two cases where, particles do not propagate the way one could naively expect from Lorentz symmetry, namely with a relativistic dispersion relation. Instead these particles propagates unconventionally because Lorentz symmetry will be broken, either by an underlying fluid [5, 3] or by the curvature of spacetime in extended gravity theories in [6]. The first setup, known as the "slow gravitino" ([5]) focus on the Lagrangian resulting from the breaking of Lorentz symmetry as well as supersymmetry by a fluid. Similarly to what happen in the Higgs-mechanism the pseudo-particle generated by this breaking, called *phonino*, will be absorbed in local supersymmetry gauge fermion, the gravitino, and become its longitudinal degrees of freedom. The end product of this super-Higgs mechanism in fluid is a Lorentz violating Lagrangian for a massive spin-3/2 particle, that we will thoroughly study "per se". The second setup, refered to as the "swift graviton"([6]), is obtained from extended gravity theories where the usual Hilbert-Einstein Lagrangian is supplemented by various terms constructed from Riemann tensors. It can be shown that, when the spacetime is curved by a particular axisymmetric background, gravitons can be accelerated faster than the speed of light in a suitably corresponding flat spacetime, a feature we called "swift graviton". As the effect depends on the polarisation, the graviton experienced a form of "birefringence" with certain modes propagating swiftly while others remain unaffected.

Chapter 1

Higgs and Super-Higgs Mechanism

We present in the chapter a short review of the Higgs mechanism, its consequences and extensions. We start in Section 1 by reviewing the Higgs mechanism in the Standard Model. Then we present in Section 2 its extension to the so-called super-Higgs mechanism arising in local supersymmetry (namely supergravity). The two last Sections 3 and 4 present how this mechanism generalise to the supersymmetric case of the Minimal Supersymmetric Standard Model and study a related development: the issue of the hierarchy problem and Split SUSY.

1 Higgs Mechanism in the Standard Model

A keystone of the Standard Model of particle physics is the spontaneous breaking of the $SU(2) \times U(1)_Y$ gauge symmetry down to $U(1)_{em}$ of electromagnetism by the Higgs boson.

The Standard Model Higgs is a complex scalar doublet Φ transforming under a $(\mathbf{2}, 1/2)$ representation of $SU(2) \times U(1)_Y$ as:

$$\Phi \to e^{i\alpha_a \tau^a} e^{i\beta/2} \Phi \ , \tag{1.1}$$

where we used the usual notation $\tau^a = \sigma^a/2$ with σ^a are the Pauli matrices. Let us note W^a_μ the $SU(2)$ gauge bosons, B_μ the $U(1)_Y$ one and further introduce the covariant derivative

$$D^\mu \Phi = \partial_\mu - igW^a_\mu \tau_a - \frac{i}{2} g' B^\mu \tag{1.2}$$

so that the kinetic and potential terms of the Higgs doublet are given by

$$\mathcal{L}_{SM} \supset D^\mu \Phi D_\mu \Phi^\dagger - V(\Phi\Phi^\dagger). \tag{1.3}$$

with a scalar potential V

$$V = -\mu^2 \Phi\Phi^\dagger + \frac{\lambda}{2}(\Phi\Phi^\dagger)^2 \ . \tag{1.4}$$

This scalar potential for the Higgs contains a *negative* mass term which will trigger the spontaneous breaking. Minimising the scalar potential, we find that the Higgs doublet acquires a Vacuum Expectation Value (VEV) such that

$$\langle \Phi \Phi^\dagger \rangle \equiv \frac{v^2}{2} = \frac{\mu^2}{\lambda} \ . \tag{1.5}$$

Without loosing generality we can parametrise Φ as

$$\Phi = U \frac{1}{\sqrt{2}} \begin{pmatrix} 0 \\ v+h \end{pmatrix} \ , \tag{1.6}$$

where h is a real valued field called Higgs boson and U is a unitary matrix. We can subsequently use our $SU(2) \times U(1)$ gauge freedom to eliminate U (since $e^{i\alpha_a \tau^a} e^{i\beta/2}$ precisely generate the group of unitary matrices) . In this gauge choice, called the *unitary gauge*, the Higgs doublet takes the simple form

$$\Phi = \frac{1}{\sqrt{2}} \begin{pmatrix} 0 \\ v+h \end{pmatrix} \ , \tag{1.7}$$

and we see easily that the gauge transformation (1.1) is broken down to the $U(1)$ subgroup of transformations such that $\alpha_1 = \alpha_2 = 0$ and $\alpha_3 = \beta$.

A crucial point is that in the unitary gauge, the $SU(2) \times U(1)_Y$ gauge bosons will acquire a mass and a longitudinal component. From $D^\mu \Phi D_\mu \Phi^\dagger$ of (1.1) we get

$$\begin{aligned} \mathcal{L}_{SM} \supset & \frac{1}{2} \begin{pmatrix} 0 & v \end{pmatrix} \left(i g W^a_\mu \tau_a + \frac{i}{2} g' B^\mu \right) \left(-i g W^a_\mu \tau_a - \frac{i}{2} g' B^\mu \right) \begin{pmatrix} 0 \\ v \end{pmatrix} \\ & = \frac{v^2}{4} \left[g^2 W^+_\mu W^{-\mu} + (g^2 + g'^2) Z^0_\mu Z^{0\mu}) \right] \ , \end{aligned} \tag{1.8}$$

where we have defined the fields

$$\begin{aligned} W^\pm_\mu &= \frac{1}{\sqrt{2}} (W^1_\mu \mp W^2_\mu) \\ Z^0_\mu &= \cos\theta_W W^3_\mu - \sin\theta_W B_\mu \ , \end{aligned} \tag{1.9}$$

and the Weinberg angle

$$\cos\theta_W = \frac{g}{\sqrt{g^2 + g'^2}} \qquad\qquad \sin\theta_W = \frac{g'}{\sqrt{g^2 + g'^2}} \ . \tag{1.10}$$

We see that the fields $W^\pm$ and Z^0 obtain masses $m_W = vg/2$ and $m_Z = m_W / \cos\theta_W$ respectively. In contrast, the photon field A_μ given by the combination

$$A^\mu = \sin\theta_W W^3_\mu + \cos\theta_W B_\mu \ , \tag{1.11}$$

remains massless as required by electromagnetism. Simultaneously to their masses, the bosons $W^\pm$ and Z^0 have acquired a longitudinal component. Indeed, we can write the unitary matrix U as

$$U(x^\mu) = e^{i\zeta/(2v)} e^{i \frac{\xi_a(x^\mu)}{v} \tau^a} \ ,$$

When taking the unitary gauge, we have therefore (suppressing $SU(2)$ indices)

$$W_\mu \to W'_\mu = e^{-i\frac{\xi_a(x^\mu)}{v}\tau^a} W_\mu e^{i\frac{\xi_a(x^\mu)}{v}\tau^a} + \frac{i}{g} e^{-i\frac{\xi_a(x^\mu)}{v}\tau^a} \partial_\mu (e^{i\frac{\xi_a(x^\mu)}{v}\tau^a})$$
$$B_\mu \to B'_\mu = B_\mu - \frac{1}{vg'}\partial_\mu \zeta,$$

and consequently the gauge boson have absorbed the Goldstone bosons, giving them the longitudinal part fitting their massive spin-1 status. Using the fact that we are considering small gauge transformations as ζ and ξ are constructed from the Goldstone bosons, we can simplify (1.12) for the W^3_μ and Z^0 fields to

$$W^3_\mu \to W^{3\prime}_\mu = W^3_\mu - \frac{1}{vg}\partial_\mu(\xi^3 + \eta) - \frac{1}{v} f^3_{ab} W^a_\mu \xi^b \tag{1.12}$$
$$B_\mu \to B'_\mu = B_\mu - \frac{1}{vg'}\partial_\mu(\zeta + \eta),$$

where f^a_{bc} are the $SU(2)$ structure constant. Notice that since (1.7) is invariant under transformations of the form $e^{i\eta}e^{i\eta\tau^3}$, eq. (1.12) are only defined up to this transformation. The combination defining the Z^0 boson in (1.9) is precisely the one required to cancel the residual η gauge freedom, whereas for A^0 we can set η to cancel the additional piece generated by the unitary transformation. In this way the photon field which remains massless and does not acquire a longitudinal component.

2 Super-Higgs Mechanism

This mechanism can be extended to the case of spin-3/2 and spin-1/2 particles. In this section we will use the following conventions. The metric will have the mostly plus signature $(-,+,+,+)$. We take the Clifford algebra to be

$$\left\{\gamma^a, \gamma^b\right\} = 2\eta^{ab} \ . \tag{1.13}$$

Our basis for this algebra is obtained by adding to γ^a the two matrices γ^{ab} and γ^{abc} defined by

$$\gamma^{ab} = \frac{[\gamma^a, \gamma^b]}{2} \qquad\qquad \gamma^{abc} = \frac{\{\gamma^a, \gamma^{bc}\}}{2} \ .$$

We further define the γ^5 gamma matrices with $\gamma^5 = i\gamma^0\gamma^1\gamma^2\gamma^3$ and have $\gamma^{abc} = i\epsilon^{abcd}\gamma^5\gamma_d$ .. The two chiral projector are then

$$P_L \equiv \frac{1+\gamma^5}{2} \qquad\qquad P_R \equiv \frac{1-\gamma^5}{2} \ . \tag{1.14}$$

Furthermore, the Dirac adjoint is defined as $\bar{\psi} = i\psi^\dagger\gamma^0$.

The super-Higgs mechanism describes the absorption of a massless spin-1/2 particle, the Goldstino, by the gauge fermion of local supersymmetry: the gravitino, after this local supersymmetry is broken. As a first step, we will start by considering the

case of a spontaneous breaking of global supersymmetry in a toy-model where we can easily exhibit the goldstino. We take a set of chiral supermultiplets with scalars ϕ_i, fermions $P_L\psi_i$ and auxiliary fields F_i. Given a superpotential W and a diagonal Kähler metric, the fermionic mass terms in the Lagrangian are

$$\mathcal{L} \supset -\frac{1}{2}W_{ij}\bar{\psi^i}P_L\psi^j - \frac{1}{2}\bar{W}_{ij}\bar{\psi^i}P_L\psi^j \ , \tag{1.15}$$

where we used the notation $W_i = \frac{\partial W}{\partial \phi^i}$ and $W_{ij} = \frac{\partial^2 W}{\partial \phi^i \partial \phi^j}$. The scalar potential V derived from the superpotential is given by

$$V = W_i(\phi)\bar{W}_i(\phi). \tag{1.16}$$

If we suppose that the theory has a SUSY-breaking vacuum state, then V is non-zero at its minimum. The minimisation condition leads to

$$W_{ij}(\phi_0)\bar{W}^j(\phi_0) = 0 \tag{1.17}$$

where ϕ_0 are the scalar fields VEV in the vacuum state. We therefore conclude that $v^i \equiv \bar{W}^i(\phi_0)$ is a non-zero eigenvector for the matrix W_{ij} with null eigenvalue. Consequently there is a fermionic state with zero mass given by

$$P_L G \equiv \ v^j P_L \Psi_j \ . \tag{1.18}$$

This mode is called a Goldstino. We see that as for bosonic Goldstone fields which are derived from the components of the Higgs doublet, the Goldstino is defined as a linear combination of the fermions in the theory.

We now consider local supersymmetry (supergravity). When supersymmetry is broken in supergravity, one obtains the following Lagrangian

$$\mathcal{L} \ = \ \frac{1}{2}e\left[\mathcal{L}_{\text{gravitino}} - \frac{F^2}{M_P^2} + \mathcal{L}_{\text{phonino}} + \mathcal{L}_{\text{mixing}}\right], \tag{1.19}$$

where e is the square root of the metric determinant, F^2 is a cosmological constant term originating from the vacuum value of the scalar potential and M_P is the reduced Planck mass. Note that as we are a priori in curved space-time, we need to use covariant derivatives ∇. The other three contributions are

$$\begin{aligned}
\mathcal{L}_{\text{gravitino}} &= R - \bar{\psi}_\mu \gamma^{\mu\nu\rho}\nabla_\nu\psi_\rho \\
\mathcal{L}_{\text{phonino}} &= -\bar{G}\gamma_{\ \mu}\nabla^\nu G \\
\mathcal{L}_{\text{mixing}} &= +\sqrt{2}\frac{F}{M_P}\bar{G}\gamma_{\ \mu}\psi_\nu \ .
\end{aligned}$$

The mixing between the gravitino and goldstino originates from the mixing terms between the original fermions in the theory (from which the Goldstino is derived) and the gravitino. The Lagrangian (1.19) transforms linearly as a total derivative under the transformations:

$$\begin{cases}
\delta e_\mu^a &= \frac{1}{2}M_P\bar{\epsilon}\gamma^{\ a}\psi_\mu \\
\delta\psi_\mu &= M_P\nabla_\mu\epsilon \\
\delta G &= \frac{F}{\sqrt{2}}\epsilon \ .
\end{cases} \tag{1.20}$$

However, we see that the resulting cosmological constant is of the order of the SUSY breaking term F^2. Since supersymmetric particles have not been observed yet, this scale must immensely bigger than the cosmological constant required to account for the near flatness of space-time. This is nothing but an example of the *cosmological constant problem*. One therefore need to cancel F^2, this can be achieved by adding to the above Lagrangian

$$\frac{eF^2}{M_P^2} + \frac{e}{2}\left[\frac{1}{2}m_{\frac{3}{2}}\bar{\psi}_\mu\gamma^{\mu\nu\rho}\gamma_\nu\psi_\rho + 2m_{\frac{3}{2}}\bar{G}G\right] .$$

with the price of introducing a gravitino mass

$$m_{\frac{3}{2}} = \frac{F}{\sqrt{3}M_P} \tag{1.21}$$

The resulting Lagrangian is given by:

$$\begin{aligned}\mathcal{L} = \frac{1}{2}e\Big[\, R - \bar{G}\gamma_\mu\nabla^\mu G - \frac{\sqrt{2}}{M_P}\bar{G}\gamma_\mu\psi_\nu - \bar{\psi}_\mu\gamma^{\mu\nu\rho}\nabla_\nu\psi_\rho \\ + \frac{1}{2}m_{\frac{3}{2}}\bar{\psi}_\mu\gamma^{\mu\nu\rho}\gamma_\nu\psi_\rho + 2m_{\frac{3}{2}}\bar{G}G\,\Big] .\end{aligned} \tag{1.22}$$

with the supergravity transformations obtained from the previous ones by replacing $\nabla_\mu \to \nabla_\mu - \frac{1}{2}m_{\frac{3}{2}}\gamma^\nu$

$$\begin{cases}\delta e_\mu^a &= \frac{1}{2}M_P\bar{\epsilon}\gamma^a\psi_\mu \\ \delta\psi_\mu &= M_P(\nabla_\mu\epsilon - \frac{1}{2}m_{\frac{3}{2}}\gamma_\mu\epsilon) \\ \delta G &= \frac{F}{\sqrt{2}}\epsilon\ .\end{cases} \tag{1.23}$$

Similarly to the spin-0/spin-1 case of the Higgs mechanism, we can now choose the unitary gauge to remove the Goldstino from the Lagrangian by making the SUSY transformation

$$\begin{cases}\delta e_\mu^a &= -\frac{1}{\sqrt{2}F}M_P\bar{G}\gamma^a\psi_\mu \\ \delta\psi_\mu &= -M_P(\nabla_\mu - \frac{1}{2}m_{\frac{3}{2}}\gamma^\nu)\frac{\sqrt{2}G}{F} \\ \delta G &= -G\ ,\end{cases}$$

which cancels the Goldstino contribution in the Lagrangian and simultaneously add a Longitudinal component to the gravitino.

We find finally that the gravitino follows the Rarita-Schwinger Lagrangian for a massive spin-3/2 boson:

$$\mathcal{L} = \frac{1}{2}e\left[\, R - \bar{\psi}_\mu\gamma^{\mu\nu\rho}(\partial_\nu - \frac{1}{2}m_{\frac{3}{2}}\gamma_\nu)\psi_\rho\,\right] , \tag{1.24}$$

where we replaced the covariant derivatives by partial ones as we are now in flat space-time. To summarise, the super-Higgs mechanism describe how a massless spin-3/2 particle absorbs the massless Goldstino and acquires a mass, in perfectly similar fashion to the usual Higgs mechanism. In Chapter 6 we will present a non-relativistic version of this result which can be applied when supersymmetry is broken by thermal effect. The resulting Lagrangian will generalise the Rarita-Schwinger Lagrangian to the non-relativistic case.

3 Toward the MSSM

We will now expand the Standard Model Higgs mechanism to the more complex case of the Minimal Supersymmetric Standard Model (MSSM). While there is no additional theoretical mechanisms involved, the fact that the MSSM has two Higgs doublets make calculations more subtle. We will start by considering the slightly simpler case of a Two-Higgs Doublet Model before pushing to the MSSM.

3.1 Two-Higgs Doublets Model

As a first step toward the MSSM, let us briefly consider how the Standard Model picture is modified in the presence of a second Higgs doublet with the same quantum number as the Standard Model one. We will note Φ_1, Φ_2 the two doublets and use the usual short notation for the sinus and cosinus $\cos\beta = c_\beta$ and $\sin\beta = s_\beta$.

If we make the simplifying assumption that the Lagrangian for these doublets is CP-conserving and that a discrete symmetry forces the doublet to come by pairs, one possible scalar potential V is now[1]

$$\begin{aligned} V =& m_{11}^2 \Phi_1 \Phi_1^\dagger + m_{22}^2 \Phi_2 \Phi_2^\dagger - m_{12}^2 (\Phi_1 \Phi_2^\dagger + \Phi_2 \Phi_1^\dagger) + \frac{\lambda_1}{2} (\Phi_1 \Phi_1^\dagger)^2 + \frac{\lambda_2}{2} (\Phi_2 \Phi_2^\dagger)^2 \\ & \lambda_3 \Phi_1 \Phi_1^\dagger \Phi_2 \Phi_2^\dagger + \lambda_4 \Phi_1 \Phi_2^\dagger \Phi_2 \Phi_1^\dagger \ . \end{aligned} \tag{1.25}$$

As one could expect, minimisation of this potential in general is more difficult than in the Standard Model case. Let us suppose the existence of a CP-conserving and charge-preserving vacuum of the form

$$\langle \Phi_1 \rangle = \frac{1}{\sqrt{2}} \begin{pmatrix} 0 \\ v_1 \end{pmatrix} \qquad \langle \Phi_2 \rangle = \frac{1}{\sqrt{2}} \begin{pmatrix} 0 \\ v_2 \end{pmatrix} \tag{1.26}$$

we will define the angle β as

$$\tan\beta \equiv \ \frac{v_2}{v_1} \ , \tag{1.27}$$

and the overall VEV v as $v^2 = v_1^2 + v_2^2 \sim 246^2 \mathrm{GeV}^2$. After electroweak symmetry breaking , three degrees of freedom out of the eight from the two doublets become Goldstone bosons. We will find these modes by searching for massless fields. With the field convention

$$\Phi_i = \begin{pmatrix} \phi_i^+ \\ (v_i + \phi_i + i\eta_i) \Big/ \sqrt{2} \end{pmatrix}, \tag{1.28}$$

the charged scalar mass matrix is given in the basis $(\phi_1^\pm, \phi_2^\pm)$ by

$$\mathcal{M}_{\phi^\pm} = \left[m_{12}^2 - \lambda_4 \frac{v_1 v_2}{2} \right] \begin{pmatrix} \dfrac{v_2}{v_1} & -1 \\ -1 & \dfrac{v_1}{v_2} \end{pmatrix} \ , \tag{1.29}$$

[1] we choose this particular form to make contact with the MSSM one easier.

the pseudo-scalar one in the basis (η_1, η_2) by

$$\mathcal{M}_\eta = (\frac{2m_{12}^2}{s_{2\beta}} \begin{pmatrix} v_2^2 & -v_1 v_2 \\ -v_1 v_2 & v_1^2 \end{pmatrix} , \tag{1.30}$$

and finally the scalar one in the basis (ϕ_1, ϕ_2) by

$$\mathcal{M}_\phi = \begin{pmatrix} m_{12}^2 \frac{v_2}{v_1} + \lambda_1 v_1^2 & -m_{12}^2 + \lambda_{34} v_1 v_2 \\ -m_{12}^2 + \lambda_{34} v_1 v_2 & m_{12}^2 \frac{v_1}{v_2} + \lambda_2 v_2^2 \end{pmatrix}, \tag{1.31}$$

with the standard notation $\lambda_{34} = \lambda_3 + \lambda_4$. In deriving this expression, one needs to use the minimisation condition

$$\begin{aligned} m_{11}^2 + \frac{\lambda_1 v_1^2}{2} \frac{\lambda_3 v_2^2}{2} &= m_{12}^2 \frac{v_2}{v_1} - (\lambda_4) \frac{v_2^2}{2} \\ m_{22}^2 + \frac{\lambda_2 v_2^2}{2} \frac{\lambda_3 v_1^2}{2} &= m_{12}^2 \frac{v_1}{v_2} - (\lambda_4) \frac{v_1^2}{2} \ . \end{aligned} \tag{1.32}$$

We can now rotate the two doublets in the so-called Higgs basis by

$$\begin{pmatrix} H_1 \\ H_2 \end{pmatrix} \equiv \begin{pmatrix} \cos\beta & \sin\beta \\ -\sin\beta & \cos\beta \end{pmatrix} \begin{pmatrix} \Phi_1 \\ \Phi_2 \end{pmatrix} , \tag{1.33}$$

so that the lower component of H_2 gets a zero VEV while the lower component H_1 has a VEV $v/\sqrt{2}$. From (1.29) and (1.30) we see that the Godstone modes $G^\pm$ and G^0 correspond to the components of H_1 introduced in (1.33). We can therefore write

$$H_1 = \begin{pmatrix} G^\pm \\ \frac{1}{\sqrt{2}} (v + h + iG^0) \end{pmatrix} \qquad H_2 = \begin{pmatrix} H^\pm \\ \frac{1}{\sqrt{2}} (H + iA^0) \end{pmatrix} , \tag{1.34}$$

where $H^\pm$ are the physical charged Higgs bosons and A^0 the pseudoscalar Higgs boson which are also eigenstates of the mass matrices (1.29) and (1.30). We note h and H the scalar Higgs bosons. We can straightforwardly deduce the masses for $H^\pm$ and A^0 from the previous matrices, leading to

$$\begin{aligned} m_{H^\pm}^2 &= M^2 - \frac{v^2}{2} \lambda_4 \\ m_A^2 &= M^2 \ . \end{aligned} \tag{1.35}$$

where we used the usual notation $M^2 = \frac{2m_{12}^2}{s_{2\beta}}$. The Higgs scalars matrix can be diagonalised using a rotation matrix with angle α defined by

$$\tan 2\alpha = \frac{(M^2 - \lambda_{34} v^2) s_{2\beta}}{(M^2 - \lambda_1 v^2) c_\beta^2 - (M^2 - \lambda_2 v^2) s_\beta^2} \tag{1.36}$$

leading to the two mass eigenstate m_1 and m_2

$$m_{1,2} = \frac{1}{2} \left[\mathcal{M}_{\phi,11} + \mathcal{M}_{\phi,22} \mp \sqrt{(\mathcal{M}_{\phi,11} - \mathcal{M}_{\phi,22})^2 + 4\mathcal{M}_{\phi,12}^2} \right] \tag{1.37}$$

In particular the would-be Standard Model Higgs boson h is now a linear combination of the two eigenstates, except if one takes the limit case $\alpha = \beta$ (decoupling limit). Of particular interest is the quartic coupling λ_{SM} of the Standard Model-like Higgs h. Given that $\phi_1 \supset c_\beta h$ and $\phi_2 \supset s_\beta h$, we obtain from (1.25) and (1.31):

$$\lambda_{SM} = \frac{s_{2\beta}^2}{2}\lambda_{34} + (\lambda_1 c_\beta^4 + \lambda_2 s_\beta^4) \tag{1.38}$$

3.2 Higgs Mechanism in the MSSM

We are now ready to consider the MSSM case. The Higgs sector is in fact precisely the one of a Two-Higgs Doublet Model, albeit with two doublets of opposite hypercharge $+1$ and -1. We now have H_u and H_d such that:

$$H_u = \begin{pmatrix} H_u^+ \\ H_u^0 \end{pmatrix} \qquad\qquad H_d = \begin{pmatrix} H_d^0 \\ H_d^- \end{pmatrix} \ . \tag{1.39}$$

As we are considering a supersymmetric theory, these two doublets are bundled with two doublets of fermions with the same quantum number: the Higgsinos. A first sight, including two doublets in a "minimal" realisation may seem arbitrary, there are in fact two reasons for that:

- In order to prevent the $U(1)_Y$ gauge symmetry to be anomalous, one needs to ensure that

$$A \equiv \sum_{LHf_i} Y_i^3 + \sum_{RHf_i} Y_i^3 = 0 \ , \tag{1.40}$$

  where the first sum runs over all left-handed fermions with hypercharge Y_i and the second over right-handed fermions. This is verified for each fermion family in the Standard Model. As we have introduced new fermions, the higgsinos, we must ensure that we add them in pairs of opposite hypercharge, therefore leading to two doublets.

- The superpotential in a SUSY theory is written in term of *chiral* superfields. Hence a positively hypercharged Higgs doublet can only couple to up-type quarks and left-handed leptons. Therefore an additional negatively hypercharged doublet is required to give a mass to the down-type quarks and right-handed leptons.

Using the superspace formalism and noting θ and $\bar{\theta}$ the Grassmanian anti-commuting coordinates, we can write the Higgs/Higgsino part of the MSSM Lagrangian as:

$$\mathcal{L}_{MSSM} \supset \int d^4\theta \, (\mathbf{H_u} e^{V_u} \mathbf{H_u}^\dagger + \mathbf{H_d} e^{V_d} \mathbf{H_d}^\dagger) + \int d^2\theta W_H + h.c. \ , \tag{1.41}$$

where the bold symbols $\mathbf{H_u}$ denote superfieds with scalar part H_u, fermionic one $\tilde{H}_u$ and auxiliar field F_u as:

$$\mathbf{H_u} = H_u(y^\mu) + \sqrt{2}\theta\tilde{H}_u(y^\mu) + \theta\theta F_u(y^\mu) \text{ with} \qquad y^\mu = x^\mu + i\theta\sigma^\mu\overline{\theta} \ , \tag{1.42}$$

and similarly for $\mathbf{H_d}$. The Kähler potential includes gauge interactions with the Higgs and Higgsinos through V_u and V_d given by

$$\begin{aligned} V_u &= g' V_Y + g\sigma_a V^a \\ V_d &= -g' V_Y + g\sigma_a V^a \ , \end{aligned} \tag{1.43}$$

where V_Y, V^a are the gauge vector multiplets which can be expressed in the Wess-Zumino gauge as a function of the gauge bosons and gauginos $\tilde{B}$ and $\tilde{W}^a$ as

$$\begin{aligned} V_Y &= \theta\sigma^\mu\overline{\theta} B_\mu + (\theta\theta)\overline{\theta}\overline{\tilde{B}} + (\overline{\theta\theta})\theta\tilde{B} + \frac{1}{2}(\theta\theta)(\overline{\theta\theta}) D_Y \\ V^a &= \theta\sigma^\mu\overline{\theta} W^a_\mu + (\theta\theta)\overline{\theta}\overline{\tilde{W}}^a + (\overline{\theta\theta})\theta\tilde{W}^a + \frac{1}{2}(\theta\theta)(\overline{\theta\theta}) D^a \ . \end{aligned} \tag{1.44}$$

Finally, the Higgs part of the superpotential W_H is simply

$$W = \mu\, \mathbf{H_u} \cdot \mathbf{H_d} \ , \tag{1.45}$$

where we use the dot notation for the $SU(2)$ invariant combination $\mathbf{H_u}\cdot\mathbf{H_d} \equiv \epsilon_{ij}\mathbf{H_u}^i\mathbf{H_d}^j$.

The scalar potential derived from this Lagrangian after integration of the auxilliary fields is given by

$$\begin{aligned} V \supset \sum_i \left|\frac{\partial W}{\partial H_u}\right|^2 + \sum_i \left|\frac{\partial W}{\partial H_d}\right|^2 + \frac{g^2}{8}(H_u^\dagger \sigma_a H_u + H_d^\dagger \sigma_a H_d)^2 \\ + \frac{g'^2}{8}(H_u^\dagger H_u - H_d^\dagger H_d)^2 \ , \end{aligned} \tag{1.46}$$

and is supplemented by the SUSY-breaking soft-terms V_{SB}

$$V_{SB} = m^2_{H_u} H_u^\dagger H_u + m^2_{H_d} H_d^\dagger H_d + (B_\mu H_d \cdot H_u + h.c.) \ , \tag{1.47}$$

leading to the 2HDM-like scalar potential V_H

$$\begin{aligned} V_H =& (m^2_{H_u} + \mu^2) H_u^\dagger H_u + (m^2_{H_d} + \mu^2) H_d^\dagger H_d - B_\mu (H_d \cdot H_u + h.c.) \\ &+ \frac{g^2 + g'^2}{8}(H_u^\dagger H_u - H_d^\dagger H_d)^2 + \frac{g^2}{2}|H_d^\dagger H_u|^2 \ . \end{aligned} \tag{1.48}$$

Comparing (1.48) with (1.25), we see that we have the following dictionary

$$\begin{aligned} H_u &\leftrightarrow \Phi_2 \\ H_d &\leftrightarrow i\sigma_2 \Phi_1^* \\ B_\mu &\leftrightarrow m^2_{12} \\ m^2_{H_d} + \mu^2 &\leftrightarrow m^2_{11} \\ m^2_{H_u} + \mu^2 &\leftrightarrow m^2_{22} \\ \lambda_1 = \lambda_2 &\leftrightarrow \frac{g^2 + g'^2}{4} \\ \lambda_3 &\leftrightarrow -\frac{g^2 + g'^2}{4} - \frac{g^2}{2} \\ \lambda_4 &\leftrightarrow \frac{g^2}{2} \ . \end{aligned} \tag{1.49}$$

We are now in position to deduce the scalar spectrum of the MSSM from the calculations done in the 2HDM case. Apart from the three Goldstone bosons absorbed by the gauge field, we find a pseudo-scalar A^0 with mass

$$m_{A^0}^2 = M^2 = 2\frac{B_\mu}{\sin 2\beta} \tag{1.50}$$

and a charged scalar $H^\pm$ with mass

$$m_{H^\pm}^2 = m_{A^0}^2 + \frac{v^2 g^2}{4} \tag{1.51}$$

where the second contribution is the W-boson mass $m_W^2 = \frac{v^2 g^2}{4}$. Introducing the Z-boson mass $m_Z^2 = (g^2 + g'^2)\frac{v^2}{2}$, we obtain the two eigenvalues of the neutral scalar mass matrix:

$$m_{h_1,h_2} = \frac{1}{2}\left(m_{A^0}^2 + m_Z^2 \pm \sqrt{(m_{A^0}^2 - m_Z^2)^2 + 4m_Z^2 m_{A^0}^2 s_{2\beta}^2}\right) . \tag{1.52}$$

We can finally find the quartic coupling of the Standard Model-like Higgs h, which will be important in the next section:

$$\begin{aligned}\lambda_{SM} &= -\frac{s_{2\beta}^2}{2}\frac{g^2 + g'^2}{4} + \frac{g^2 + g'^2}{4}(c_\beta^4 + s_\beta^4) \\ &= \frac{g^2 + g'^2}{4}c_{2\beta}^2\end{aligned} \tag{1.53}$$

4 Hierarchy and Split SUSY

4.1 The Hierarchy Problem

The point of introducing the Higgs mechanism is to give a mass to the chiral fermions (and to the massive gauge bosons). This is achieved by adding Yukawa couplings with the Higgs doublet for the leptons and quarks of the form:

$$\mathcal{L}_Y = -(Y_e \overline{L}\Phi e_R + Y_d \overline{Q}_L \Phi d_R + Y_u \overline{Q}_L \cdot \Phi^\dagger u_R + h.c) \tag{1.54}$$

where Y_e, Y_d and Y_u are 3×3 matrices and we have suppressed generation indices. It is quite clear from the decomposition (1.7) that these couplings will simultaneously give a mass to the quarks and leptons and generate Yukawa couplings with the Higgs boson h. For instance, calling y_t the top-top component of Y_u, we see that the top quarks gets a mass $m_t = y_t v/\sqrt{2}$ as well as a coupling m_t/v with the Higgs boson.

However, one may now want to take into account the quantum corrections to the Higgs pole mass by computing the self-energy $\Sigma(p^2)$ of the Standard Model Higgs. The dominant contributions are represented in Figure 1.1, they consist in a fermionic top loop and bosonic Higgs and gauge boson loops. Let us focus on the top loop first. Making the (very) rough approximation that the top quark is heavy compared to the

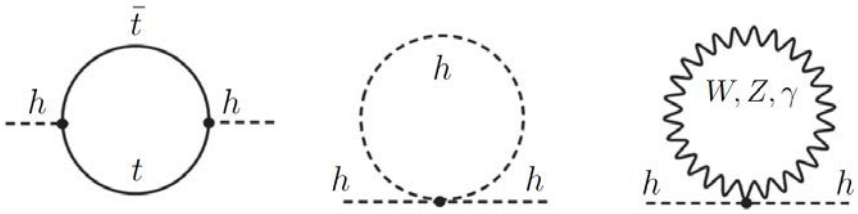

Figure 1.1: Dominant one-loop diagrams contributing to the Standard Model Higgs self-energy. We note t and $\bar{t}$ the left-handed and right-handed top respectively.

Higgs mass, we get

$$\begin{aligned}\Sigma(p^2) \supset & -3i \int \frac{d^4k}{(2\pi)^4} \mathrm{tr}\left[\frac{(\not{k}+m_t)(\not{k}+\not{p}+m_t)}{(k^2-m_t^2)((k+p)^2-m_t^2)}\right] \\ \sim & \ \frac{3y_t}{4\pi^2}\int_0^1 dx \int_0^{\Lambda^2} dy \frac{y(m_t^2-y)}{(y+m_t^2)^2} \\ \supset & -\frac{3y_t^2}{8\pi^2}\Lambda^2 \ ,\end{aligned} \tag{1.55}$$

where we have included an UV cut-off Λ to regularise the divergent integral. The self energy also includes subdominant – but still quadratically divergent – contributions from the bosonic loops $\Sigma(p^2) \supset \frac{1}{16\pi^2} g^2\Lambda^2 + \frac{1}{16\pi^2}\lambda^2\Lambda^2$.

A priori Λ can be vastly different from the Electroweak Scale, therefore in order for the physical Higgs mass

$$M_h^2 = m_h^2 + \Sigma(p^2)$$

to be around 125 GeV, one must precisely organise the cancellation between m_h^2 and $\Sigma(p^2)$. This fine-tuning, which can be as big as 10^{-30} when Λ is the Planck scale, is the called the *hierarchy problem*.

Let us now study the same one-loop corrections in the MSSM. The Yukawa couplings (1.54) are now included in the superpotential as

$$W_Y = Y_u\, \mathbf{U^c}\, \mathbf{Q} \cdot \mathbf{H_u} - Y_d\, \mathbf{D^c}\, \mathbf{Q} \cdot \mathbf{H_d} - Y_e\, \mathbf{E^c}\, \mathbf{L} \cdot \mathbf{H_d} \ , \tag{1.56}$$

where we used the notation summarised in Table 1.1 for the superfields. Crucially, these terms do not only re-generate couplings similar to (1.54), but also new quartic couplings with the scalar superpartner, the squarks and sleptons. Furthermore, the new couplings are precisely the one required to cancel the fermionic loops from quarks and leptons. For instance, let us focus on the top again, its coupling to the Standard Model-like Higgs is given by $\tilde{y}_t \equiv \frac{\cos\alpha}{\sin\beta} Y_u(3,3)$. The superpotential contribution to the scalar potential (similar to (1.46)) for the stops is of the form

$$\sum_i \left|\frac{\partial W}{\partial \tilde{t}_L}\right|^2 + \sum_i \left|\frac{\partial W}{\partial \tilde{t}_R}\right|^2 \tag{1.57}$$

Names		Spin 0	Spin 1/2	Spin 1	$(SU(3), SU(2), U(1)_Y)$
Quarks	$\mathbf{Q}$	$\tilde{Q} = (\tilde{u}_L, \tilde{d}_L)$	(u_L, d_L)		$(\mathbf{3}, \mathbf{2}, 1/6)$
	$\mathbf{U^c}$	$\tilde{u}_L^c$	u_L^c		$(\overline{\mathbf{3}}, \mathbf{1}, -2/3)$
(×3 families)	$\mathbf{D^c}$	$\tilde{d}_L^c$	d_L^c		$(\overline{\mathbf{3}}, \mathbf{1}, 1/3)$
Leptons	$\mathbf{L}$	$(\tilde{\nu}_{eL}, \tilde{e}_L)$	(ν_{eL}, e_L)		$(\mathbf{1}, \mathbf{2}, -1/2)$
(×3 families)	$\mathbf{E^c}$	$\tilde{e}_L^c$	e_L^c		$(\mathbf{1}, \mathbf{1}, 1)$
Higgs	$\mathbf{H_u}$	(H_u^+, H_u^0)	$(\tilde{H}_u^+, \tilde{H}_u^0)$		$(\mathbf{1}, \mathbf{2}, 1/2)$
	$\mathbf{H_d}$	(H_d^0, H_d^-)	$(\tilde{H}_d^0, \tilde{H}_d^-)$		$(\mathbf{1}, \mathbf{2}, -1/2)$
Gluons	$\mathbf{W_{3\alpha}}$		$\lambda_{3\alpha}$ $[\equiv \tilde{g}_\alpha]$	g	$(\mathbf{8}, \mathbf{1}, 0)$
W	$\mathbf{W_{2\alpha}}$		$\lambda_{2\alpha}$ $[\equiv \tilde{W}^\pm, \tilde{W}^0]$	$W^\pm, W^0$	$(\mathbf{1}, \mathbf{3}, 0)$
B	$\mathbf{W_{1\alpha}}$		$\lambda_{1\alpha}$ $[\equiv \tilde{B}]$	B	$(\mathbf{1}, \mathbf{1}, 0\ )$

Table 1.1: Chiral and gauge multiplet fields in the Minimal Supersymmetric Standard Model.

So that the interactions between the Standard Model-like Higgs, the tops and the stops are now given by

$$\mathcal{L} \supset -\tilde{y}_t h t\bar{t} - \tilde{y}_t^2(\tilde{t_L} h \tilde{t_L}^* + \tilde{t_R} h \tilde{t_R}^*) \tag{1.58}$$

The one-loop diagram involving the left and right-handed tops is now balanced by the one showed in Figure 1.2 involving both right-handed $\tilde{t}_L$ and left-handed $\tilde{t}_R$ stops, coupling to h with coupling y_t^2. Indeed, evaluating the stops loops showed in Figure 1.2 is straightforward and lead to the quadratically divergent contribution

$$\Sigma(p^2) \supset +\frac{3\tilde{y}_t^2}{4\pi^2}\Lambda^2 \ , \tag{1.59}$$

which is precisely what is needed to cancel the quadratic divergence of the tops loop (1.55).

Fascinatingly, the mass of the stops did not enter the previous argument. This is a crucial point as in order to lift the squark masses above detection capability of the current experiment, we need to add scalar mass terms $m_{\tilde{t}_L}$ and $m_{\tilde{t}_R}$ which could naively spoil the cancellation as they explicitly break supersymmetry. We just saw however that these terms do in fact not participate in the quadratic corrections to the Higgs. Similar Lagrangian operators which explicitly breaks SUSY but do not introduce a quadratic divergence in the one-loop self-energy for scalars are called *soft terms*. Every scalar squared mass terms and trilinear scalar couplings are soft.[2]

Let us define the SUSY scale $M_S = \sqrt{m_{\tilde{t}_R} m_{\tilde{t}_L}}$ as the geometric mean of the stops masses, which is used as the generic mass scale for all supersymmetric particles. The

[2]One can also consider gauginos masses as well as tadpole couplings, the latest being soft only if the scalar is a gauge singlet.

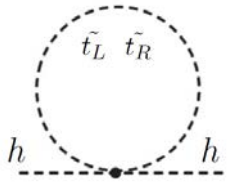

Figure 1.2: One-loop stops diagrams contributing to the Standard Model-like Higgs self-energy.

actual loop corrections in the top/stops sector in the MSSM give the well-known expression for the lightest Higgs boson at large B_μ (decoupling limit)

$$m_h^2 \simeq m_Z^2 c_{2\beta}^2 + \frac{3m_t^4}{2\pi^2 v^2}\left[\log\frac{M_S^2}{m_t^2} + \frac{X_t^2}{M_S^2}\left(1 - \frac{X_t^2}{12M_S^2}\right)\right] \tag{1.60}$$

where we have defined the stop mixing parameter: $X_t = A_t + \mu\cot\beta$ and A_t is the stop trilinear coupling. We stress that in light of the Higgs mass measurement, such correction terms are in fact desirable. Indeed, without these logarithmic corrections, supersymmetry would be unable to generate a heavy-enough Higgs boson. Given the experimentally measured 125 GeV Higgs mass, one needs either large trilinear or stops of the order of the TeV. However, this comes with a price: when we increase the SUSY scale M_S we re-introduce a fine-tuning in the theory as soft terms feeds into the Higgs bosons self-energy through the logarithmic contributions. This tension between naturalness and the absence of SUSY signal at experiments is called the *little hierarchy problem.*

4.2 Split Supersymmetry

On top of the hierarchy problem we discuss in the previous section, Beyond Standard Model physics faces two main open problems (i) the issues of unification – the fact that the three gauge couplings does not unify at a certain scale in the Standard Model –, and of (ii) Dark Matter – the fact that observations seems to indicate that we are missing a good part of the matter in the universe –.

Split SUSY scenarios [7,8,9], which consider heavy supersymmetric scalar particles but keep the gauginos and the higgsinos at the electroweak scale, have a severe little hierarchy problem, but still solve (i) and (ii). Particularly, as it was shown in [8], a crucial property of the MSSM: the natural unification of gauge couplings (without the need of fine-tuning the particle mass thresholds), is conserved in Split SUSY. Further, it was argued to be the simplest extension of the Standard Model with such natural unification. A Split spectrum with heavy scalar also reduces the constraints on Flavour Changing Neutral Currents (FNCN) which can plague SUSY scenarios (a somehow related solution is the so-called inverted hierarchy setup where only the third generation of SUSY scalars are light, which is more resilient to FCNC [10] and have also improved Higgs mass prediction with respect to the MSSM [11]).

In Split SUSY scenarios, the scalar particles, except for the lightest Higgs boson, are a priori arbitrarily heavy at a scale M_S but the fermionic supersymmetric particles

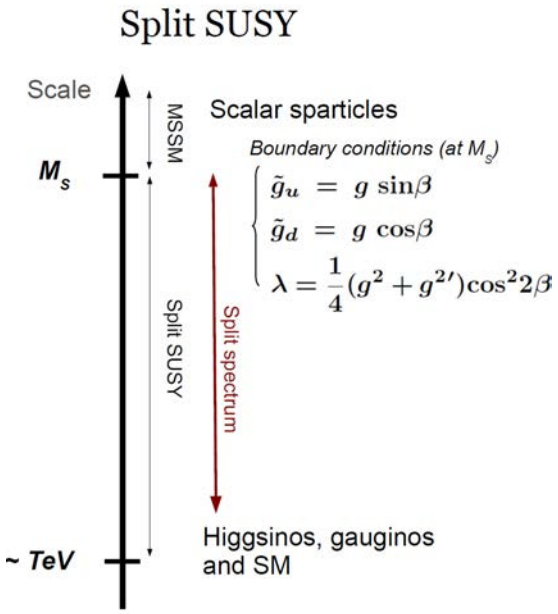

Figure 1.3: Spectrum of Split SUSY theory and matching procedure.

are kept at the electroweak scale, usually protected by an approximate R-symmetry. R-symmetries are global symmetries which do not commute with the SUSY generators. In practice, we consider $U(1)$ R-symmetries under which the anti-commuting variable θ and $\theta^\dagger$ transform as:

$$\theta \to e^{i\alpha}\theta \qquad\qquad \theta^\dagger \to e^{-i\alpha}\theta^\dagger \ . \tag{1.61}$$

As a consequence, if a superfield carries a R-charge r_X, the scalar components will have R-charge r_X and the fermionic ones R-charge $r_X - 1$. It also follows that the superpotential must carry a R-charge +2. Notice that scalar soft SUSY-breaking mass terms automatically preserve R-symmetry whereas the Gauginos masses do not. Schematically, a small breaking ϵ of this symmetry will then generate a split spectrum with heavy scalars at the SUSY scale M_S but light fermions with masses $\epsilon^2 M_S$.

When dealing with the Higgs mass, the key point of such scenarios is that even if the SUSY scale is not related to the electroweak scale anymore, Split SUSY models nonetheless yield the Standard Model Higgs mass as a function of the supersymmetric scale M_S. We will explore the relationship between these two parameters in the rest of the section.

Split SUSY models are best studied in an effective field theory approach summarised in Figure 1.3. We therefore consider a simplified field content, with only Standard Model particles along with the gauginos and higgsinos, below the supersymmetric scale M_S and the rest of the supersymmetric spectrum above M_S. Using the field notation of (1.1) and writing the Standard-Model like Higgs doublet h, the

Lagrangian below the SUSY scale is given by [12]

$$\begin{aligned}\mathcal{L} \supset\ & m^2 h^\dagger h - \frac{\lambda}{2}\left(h^\dagger h\right)^2 - \Big[Y_e \overline{L} h e_R + Y_d \overline{Q}_L h d_R + Y_u \overline{Q}_L \cdot h^\dagger u_R \\ & + \frac{1}{2} M_3\, \tilde{g}^A \tilde{g}^A + \frac{1}{2} M_2\, \tilde{W}^a \tilde{W}^a + \frac{1}{2} M_1\, \tilde{B}\tilde{B} + \mu\, \tilde{H}_u^T \epsilon \tilde{H}_d \\ & + \frac{h^\dagger}{\sqrt{2}}\left(\tilde{g}_u \sigma^a \tilde{W}^a + \tilde{g}'_u \tilde{B}\right) \tilde{H}_u + \frac{h^T \epsilon}{\sqrt{2}}\left(-\tilde{g}_d \sigma^a \tilde{W}^a + \tilde{g}'_d \tilde{B}\right) \tilde{H}_d + \text{h.c.}\Big]\,, \end{aligned} \tag{1.62}$$

where we used the notation $\epsilon = i\sigma_2$. The second line contains the masses for the SUSY fermions: higgsinos (superpartners of the higgs doublets) and gauginos (superpartners of the gauge bosons). The third contains the four new couplings $\tilde{g}_u, \tilde{g}_d, \tilde{g}'_d$ and$\tilde{g}'_u$ between these fermions and the Standard Model Higgs. They will modify the Renormalisation Group Evolution of the Higgs quartic during its running between the SUSY scale and the Electroweak scale. Matching the effective low energy theory with the full supersymmetric one at M_S gives a boundary condition for the Higgs quartic λ, which is precisely at tree level the one we derived previously in eq. (1.53) (usually supplemented with the one-loop threshold corrections). Furthemore the four new couplings are matched with the gauge couplings as:

$$\begin{aligned} \tilde{g}_u(M_S) &= g(M_S)\sin\beta & \tilde{g}_d(M_S) &= g(M_S)\cos\beta \\ \tilde{g}'_u(M_S) &= g'(M_S)\sin\beta & \tilde{g}'_d(M_S) &= g'(M_S)\cos\beta\ . \end{aligned} \tag{1.63}$$

Finally, one must add the requirement that the Standard Model-like Higgs is light, which translate in a relation on the determinant of the tree-level MSSM scalar mass matrices for H_u and H_d:

$$\det\begin{pmatrix} m_{H_u}^2 + |\mu|^2 & -B_\mu \\ -B_\mu & m_{H_d}^2 + |\mu|^2 \end{pmatrix} \simeq 0 \quad \rightarrow \quad \tan\beta = \sqrt{\frac{m_{H_d}^2 + |\mu|^2}{m_{H_u}^2 + |\mu|^2}}. \tag{1.64}$$

This last relation gives a boundary condition for $\tan\beta$. However from a low-energy point of view, one can simply focus on the Split SUSY phase below M_S and treat $\tan\beta$ as a free parameter. The Higgs boson pole mass is then obtained by solving the Renormalisation Group Equations (RGEs) down to the electroweak scale and calculate the loop corrections in the effective Split SUSY theory. The result is presented in Figure 1.4. We see that the measurement of the Standard Model Higgs mass can give conversely a bound on M_S, since the 125 GeV Higgs can be obtained only for M_S in the 10^4-10^8 GeV region in most of the parameter space (see also [13, 14]). Further limits arise when considering unified Higgs sector soft masses and considering their evolution above the SUSY scale. Indeed unification in Split SUSY requires μ to be < 10 TeV at 1σ or < 100 TeV at 2σ [15] and thus for much larger values of M_S we would have $\tan\beta \approx \sqrt{\frac{m_{H_u}^2}{m_{H_d}^2}}$. For high values of M_S to match the known value of the Higgs mass is is necessary to have a small $\tan\beta$; in [15] it was found that the largest value of M_S thus compatible with unification and the correct Higgs mass was 10^8 GeV, and that required $\tan\beta = 1$ – if $\tan\beta = 2$ instead it becomes 10^6 GeV – but a tuning

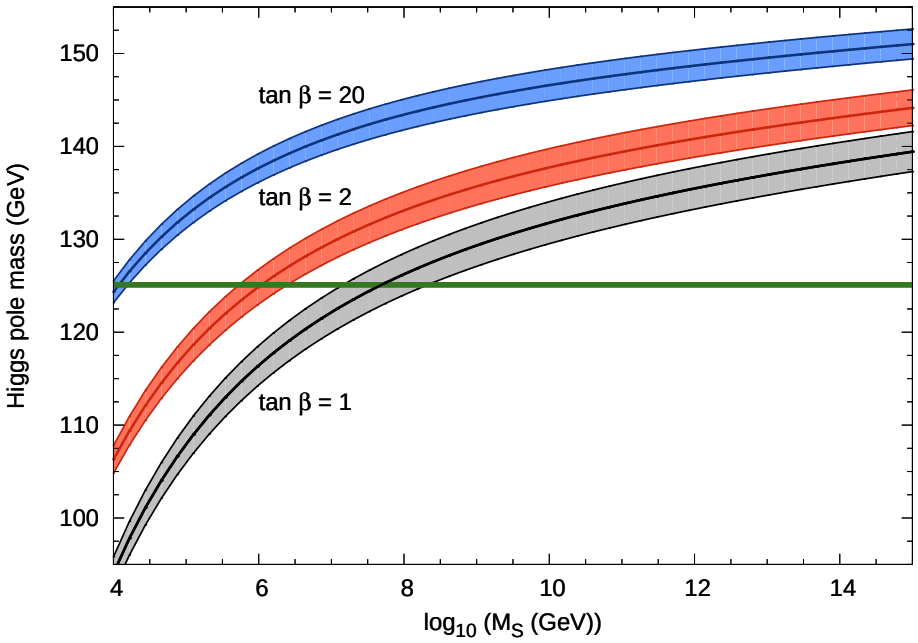

Figure 1.4: Prediction of the Higgs mass in Split SUSY as a function of the SUSY scale M_S for various values of $\tan\beta$. The shaded regions give a 2σ variation in the top pole mass.

of the Higgs soft masses to achieve such a value of $\tan\beta$ is not justifiable; just as in the MSSM the RGE running from any given mediation scale tends to drive $m_{H_u}^2 < 0$ via

$$16\pi^2 \frac{d}{d\log\mu} m_{H_u}^2 = 6|y_t|^2(m_{H_u^2} + m_Q^2 + m_U^2) + ... \tag{1.65}$$

and this is exacerbated since the gaugino masses are much smaller than the scalar masses, so they cannot compensate. The conclusion is that without additional tuning $\tan\beta$ should be somewhat different from 1, the SUSY scale should be low, and the amount of running from the scale at which the soft masses is generated cannot be too large (potentially problematic for gravity mediation). This is the "Mini-Split" scenario, for which the SUSY scale is below $10^5 - 10^6$ GeV [15, 16, 17].

In the coming chapter on Fake Split SUSY models, we will show that it is easy to engineer models with the same advantages as Split SUSY and equally simple effective theory below M_S, for which the previous bounds do not apply.

Chapter 2

An Introduction to Dirac Gauginos

The fermionic masses generated by the Higgs mechanism in the Standard Model are of Dirac type, namely they are constructed from four-components Dirac fermions,

$$\Psi = \begin{pmatrix} \bar{\psi} \\ \chi \end{pmatrix} \qquad\qquad \overline{\Psi} = \begin{pmatrix} \overline{\chi} & \psi \end{pmatrix}$$

as

$$\mathcal{L} \supset m_D \overline{\Psi}\Psi = \chi\psi + \bar{\psi}\overline{\chi}$$

where ψ and χ are two-components Weyl spinors, and the conjugate is defined by $\bar{\psi}_{\dot{\alpha}} = (\psi_\alpha)^*$.

In contrast, the new supersymmetric fermions related to the gauge boson, the gauginos are Majorana fermions with only two degrees freedom. Consequently, they can only be given Majorana masses (such masses break supersymmetry softly, as defined in the previous chapter).

In this chapter, we will investigate the consequences of giving a Dirac mass to the gauginos. In section 1 we introduce this mechanism, before reviewing some of its main consequences in section 2 and presenting an explicit model in section 3.

1 Dirac Fermions and Gauginos

The idea of adding Dirac masses to SUSY gauginos by considering additional fermionic degrees of freedom is an old one, already present in [18, 19, 20]. However, this setup has regained more attention during the past decade after it was realised that such Dirac masses were *supersoft* in the sense that while such masses are explicitly breaking supersymmetry, they do not even introduce logarithmic divergences.

Let us start by pointing out that the maximal amount of supersymmetry consistent with the chirality of the matter fields and gauge couplings perturbativity up to the GUT scale is a $N = 1$ SUSY for matter multiplets (as indicated from the fact that the Standard Model is a chiral theory) and $N = 2$ for gauge multiplets (as more supersymmetry would lead to a Landau pole before the Grand Unification Theory – GUT – scale). Such a SUSY setup implies adding $N = 1$ chiral multiplets $\mathbf{S}$, $\mathbf{T}^i$ and $\mathbf{O}^a$ to the usual gauge multiplets, namely one complex scalar and one Majorana

fermion for each gauge field. The two fermionic degrees of freedom of the original gauginos can then be combined with the two new ones from the additional multiplet to form a Dirac fermion. Notice that this additional multiplet must transform under *adjoint* representations of the gauge groups. For this reason we will sometimes called the scalars from these multiplets "adjoint scalars". Furthermore, one may additionally fit the two Higgs supermultiplet in a $N = 2$ hypermultiplet, slightly reducing the parameter space.

The key point of this construction is that on top of the usual soft SUSY breaking terms (bilinears and trilinears in scalar fields and gauginos' Majorana mass terms) SUSY can be broken by gauginos *Dirac* masses. These terms takes the schematic form (suppressing all indices)

$$\mathcal{L} \supset \int d^2\theta \sqrt{2}\theta^\alpha m_D \mathrm{tr}\, \mathbf{\Sigma} W \ , \tag{2.1}$$

where m_D is the Dirac mass, $\mathbf{\Sigma}$ is the additional Dirac gaugino supermultiplet (with scalar component Σ) and W is the field multiplet of the corresponding gauge group. Such term is called *supersoft* as it does not introduce logarithmic divergences like the usual soft terms. Indeed, the superpotential contribution (2.1) not only introduce Dirac masses for the gauginos, but also additional D-term-generated trilinear interactions for the new "adjoint" scalar Σ of the form

$$\mathcal{L} \supset -\sqrt{2} m_D (\Sigma + \Sigma^*) D \tag{2.2}$$

where D is the D-term of the gauge group corresponding to S. After integrating out the D-terms, the trilinears take the form

$$\mathcal{L} \supset -\sqrt{2} m_D (\Sigma + \Sigma^*) \sum_i (\phi_i^* T_i \phi_i) \tag{2.3}$$

where ϕ_i are the matter scalar fields charged under the gauge group and T_i is the matrix of their gauge group representations. When calculating the loop contributions to the scalar ϕ_i masses, these trilinears are the precise couplings required so that the purely scalar loops including one adjoint scalar S cancels the fermionic loop including one gaugino. While this can be checked by direct calculations, let us illustrate this by an argument from [21]. The spurion giving the Dirac mass θm_D in (2.1) originate from the D-term VEV of a gauge field strength: $W'_\alpha/\Lambda \equiv \theta m_D$ where Λ is the new-physics scale where W'_α acquires its VEV (and consequently the cut-off scale of the divergent integrals). If this term generates a divergence in the self-energy of any matter scalar field, then one need to add a supersymmetric counterterm function of the spurion. However, the only possible gauge-invariant term giving a scalar mass is of the form

$$\int d^4\theta \ \frac{(W'^\alpha W'_\alpha)^\dagger (W'^\alpha W'_\alpha)}{M^6} \overline{\theta}^2) \frac{m_D^4}{\Lambda^2} \mathbf{Q_i}^\dagger \mathbf{Q_i} \tag{2.4}$$

which we can re-write as

$$\int d^4\theta \ (\theta^2 \overline{\theta}^2) \frac{m_D^4}{\Lambda^2} \mathbf{Q_i}^\dagger \mathbf{Q_i} \tag{2.5}$$

with $\mathbf{Q_i}$ the matter supermultiplet containing ϕ_i. Such term vanishes in the limit $\Lambda \to \infty$, implying that the radiative correction to the scalar ϕ_i are finite.

Let us close this introductory section by some comments:

- Supersymmetric models allowing Dirac gauginos masses can be realised relatively easily in String Theory (see for instance [22, 23, 24, 25])
- An interesting characteristic of SUSY breaking Dirac masses is that contrary to Majorana masses, such terms do not break R-symmetry. This opens the possibility to either preserve it completely (the so-called MRSSM), or limit the R-symmetry breaking to the Higgs sector [26]. We will focus on the second case in the following sections.
- The supersoftness property is weakened when introducing explicit R-symmetry breaking in the Higgs sector as it is customary done: the logarithms re-appear from higher order radiative corrections.
- The early attempt [18] at constructing Dirac Gauginos model faced the issue that when a proper mediation mechanism, like gauge mediation, was specified, the simplest interactions lead to tachyonic masses for the adjoint scalars, requiring an additional stabilising Majorana mass. This obstacle was overcome in [27, 28].

2 A Brief Phenomenology of Dirac Gauginos Models

Dirac Gauginos models have a very rich phenomenology, we give here a brief overview of the various aspects which will be developed in particular cases in the following chapters.

Electroweak Sector Observables and Naturalness Let us start with electroweak precisions tests. The main constraints in Dirac gauginos comes from the mixing between the Higgs sector and the adjoint scalar ones.

Let us note v_S and v_T the Vacuum Expectation Values (VEV) of the scalar singlet S and of the neutral component of the adjoint triplets T respectively. As v_T gives a contribution to the W boson mass ([29] – see also [30, 31] –), one must examine the induced correction $\Delta\rho$ to the Veltman ρ-parameter:

$$\rho \equiv \frac{M_W^2}{c_{\theta_W}^2 M_Z^2} = 1 + \Delta\rho \ , \tag{2.6}$$

with, for v the Standard Model Higgs VEV:

$$\Delta\rho \sim \frac{4v_T^2}{v^2} \tag{2.7}$$

in the Minimal Dirac Gaugino Supersymmetric Standard Model (MDGSSM) for instance (see [29]). This implies that v_T must be at a few GeV at most, which can be typically obtained either with large triplet soft masses m_T (few TeV) or large triplet Dirac mass m_{2D}(also few TeV), or small λ_T and small $\tan\beta$.

This requirement can often be at odd with a natural electroweak scale which prefers smaller triplet and singlet soft masses. Indeed, radiative corrections induced by the adjoint scalars to $m_{H_{u,d}}^2$ are [29]:

$$\delta m_{H_{u,d}}^2 \supset -\frac{1}{16\pi^2}(2\lambda_S^2 m_S^2 + 2\lambda_T^2 m_T^2)\log\left\{\frac{\Lambda}{\text{TeV}}\right\} \tag{2.8}$$

with Λ the UV cut-off, $m^2_{H_{u,d}}, m^2_S, m^2_T$ the squared masses for Higgses, scalar singlet S and scalar triplet T, and λ_S, λ_T are the couplings defined below in (2.12) which gives the superpotential interaction bewteen the new adjoint scalars and the Higgs doublets. Let us stress that generally, Dirac Gauginos models are less fine-tuned than the minimal SUSY models. Indeed, the supersoftness of the Dirac gauginos terms lifts the constraint on the Gluinos masses as they only contribute to the squark masses via a finite corrections (which can mean heavy gluinos escaping LHC detection while keeping relatively light stops). Furthermore, the tree-level Higgs mass is also modified by two competing effects: an enhancement from the new couplings λ_S and λ_T, but a reduction through mixing with the scalar singlet proportional to $\frac{v_S}{v}$ and with the scalar triplet proportional to $\frac{v_T}{v}$ ([21, 32, 33, 29, 30]). Depending on the model set-up one does not have necessarily to push the Higgs mass through heavy squarks, thereby increasing the naturalness. Furthermore, as Dirac gluinos have reduced one-loop contribution to the stops masses, one can easily have heavy Dirac masses while keeping light stops, thereby improving naturalness and respecting LHC lower bounds on the gluinos mass [34]. Overall, Dirac gauginos models fare better than the (N-)MSSM when dealing with naturalness, a point which also explains their popularity.

Finally, with the discovery of the Higgs boson, it becomes possible to analyse its decay channels and compare them with the Standard Model prediction. For Higgs tree-level decay, these constraints basically boils down to the mixing between the Higgs and the adjoint scalar we already discussed above. For loop-induced decays, one must further consider the contribution from loops of adjoint scalars. Staying in line with the current absence of deviation from the predicted Standard Model rate will generically require smaller couplings and larger adjoint scalar masses. A precise study for the Higgs di-photon channel can be found in [29].

EDM and flavour constraints In most SUSY theories, one can have numerous new sources of flavour and CP violations which can be for example constrained from electron dipole moment searches, B-mesons decays and Kaons oscillations. Essentially, for rather light squarks and gluinos as naturalness should require, the SUSY breaking mediation mechanism should be flavor-blind. Interestingly, it was noticed by [35, 36] that replacing the gluino Majorana mass terms by Dirac ones significantly weakens the constraints from both electric dipole moments and Kaons oscillations. The crux of the arguments lie in the preserved R-symmetry which forbids numerous effective operators usually present in SUSY models. For instance, the effective operator between the strange and down quarks and squarks which contributes to Kaons oscillations

$$\frac{1}{M_{\tilde{g}}} \tilde{d}^*_R \tilde{s}^*_L \bar{d}_R s_L$$

usually arising after integrating gluinos with Majorana masses $M_{\tilde{g}}$ is no longer allowed. Other flavour-violating observables can be similarly reduced [37, 38].

This result nevertheless suffers from some limitations. First of all, when the Higgs sector explicitly breaks R-symmetry through the higgsinos μ/B_μ term, the effective operators mediated by higgsinos will not be suppressed. Secondly, as it was shown in [39], when considering simultaneously Majorana and Dirac gauginos masses this

effect is dramatically reduced and remains strong only in the so-called "mass-insertion approximation" (near-degeneracy of the SUSY scalar masses).

Dark Matter One of the early reasons Dirac Gauginos were studied was to make the Bino a viable Dark matter candidate. Indeed, while Majorana Binos do not decay fast enough in the MSSM, pure Dirac Bino dark matter can co-annihilate, enhancing the decay rate.

Such Dirac spinor will have a vector-vector coupling induced by Z-boson with nucleons, putting strong constraints on such model from direct detection experiments. However, pseudo-Dirac Dark matter with simultaneously a small Majorana mass and large Dirac one can still decay through co-annihilation while possibly avoiding direct detection if the splitting is large enough. This makes the (pseudo-Dirac Bino) a suitable Dark matter candidate [40] (we will discuss in the coming section a related issue in the Fake Split SUSY models).

More generally, Dirac Gauginos models have six neutralinos: Bino, wino, two Higgsinos and the adjoint fermions. Extracting the LSP and its relic density is thus a more involved process than in the ususal MSSM. In [41], it was found that on top of the usual MSSM scenarios, one could in fact have also pure Dirac Bino (escaping direct detection assuming above TeV right-handed squarks and higgsinos). Mixed LSP Bino/Higgsinos are still possible with both Majorana Bino/Higgsinos states.

Gauge couplings unification It was early realised that adding the adjoint chiral multiplets would spoil the hardly-fought natural gauge coupling unification (namely unification without mass-threshold tunings) obtained in the MSSM. In order to recover natural unification, one needs to add bachelor fields to form complete multiplets of the GUT gauge group [21]. Fascinatingly, while a $SU(5)$ unification is perfectly possible at one-loop by adding states in a $(\mathbf{3},\mathbf{2})_{-5/6} + (\overline{\mathbf{3}},\mathbf{2})_{5/6}$, it was latter found in [42, 43] that at a Landau Pole appears at two loop before the GUT scale. The second possibility is a $(SU(3))^3$ GUT. In this case one must add states in $(\mathbf{1},\mathbf{2})_{\pm 1/2} + 2 \times (\mathbf{1},\mathbf{1})_{\pm 1}$, loosely speaking, they are two Higgs-like doublets, and two pairs of right-handed electron-like fields. A priori, such fields can have masses at the same scale that the other supersymmetric fields, allowing for diverse model-building possibilities which will be explored in the coming chapters. In order to avoid numerous new couplings, one can additionally charge these fields under lepton number or impose an exact R-symmetry [43].

Detection at LHC The study of the phenomenology of Dirac gauginos models at LHC has so far focused on the color particles.

In particular, the Dirac gluino case has been studied in [44, 34]. The general idea is that one could not use directly the LHC searches for Majorana gluinos and that lightest squarks are generally allowed.

The case of the scalar octet (also called sgluon) has been studied mainly in the context of Dirac gauginos models with a totally preserved R-symmetry (MRSSM) [45, 46, 47] and a NLO calculation of its production is avaible [48]. Typically, they are pair-produced from gluons fusion and decay either into gluinos or squarks if kinematically

opened or into quark pairs or gluons through one-loop interactions [49,50]. As the loops contains gluinos and squarks, the decay amplitude decreases when they are heavy.

The (pseudo-)scalar octet is a crucial element of the explanation of the diphoton excess we will present in chapter 5. Therefore, more details concerning the constraints lying on such particle can be found in [4].

3 Minimal Dirac Gauginos SUSY Model : a Step by Step Approach

As a particular example, we will construct here step by step the Minimal Dirac Gaugino Supersymmetric Standard Model (MDGSSM for short) presented in [29]. This model can be seen as the minimal set of fields which allows a Dirac mass for the gauginos, preserves one-loop natural unification of gauge couplings and allows to easily reproduce the measured Higgs mass.

3.1 Field Content

We start with the MSSM field content, summarised in Table 1.1. As we have described above, in order to have Dirac Gauginos masses, we must add the adjoint supermultiplets, presented in Table 2.1. More precisely, we associate to $U(1)_Y$ the singlet supermultiplet $\mathbf{S}$, to $SU(2)$ the triplet supermultiplets $\mathbf{T}$ and to $SU(3)$ the octet supermultiplets $\mathbf{O}$. These new multiplets contain new complex adjoint scalars, S, T and O:

$$
\begin{aligned}
S &= \frac{S_R + iS_I}{\sqrt{2}} \\
T &= \frac{1}{2\sqrt{2}} \begin{pmatrix} T_R + iT_I & \sqrt{2}(T_{+R} + iT_{+I}) \\ \sqrt{2}(T_{-R} + iT_{-I}) & -(T_R + iT_I) \end{pmatrix} \\
O^{(a)} &= \frac{O_R^{(a)} + iO_I^{(a)}}{\sqrt{2}}
\end{aligned} \tag{2.9}
$$

where the $S_R, O_R^{(a)}, T_R, T_{-R}, T_{+R}$ and the $S_I, O_I^{(a)}, T_I, T_{-I}, T_{+I}$ are respectively real scalar fields and real pseudo-scalar fields.

However, we have now broken the natural unification of the MSSM. As we discussed previously, the simplest unification group for this model is $(SU(3))^3$. The new adjoint fields must therefore fit in a **24** adjoint representation[1] which include several new "unification" bachelor fields. They consist in an extra Higgs-like doublets [2] $\mathbf{R}_u, \mathbf{R}_d$ as well as two pairs of vector-like right-handed electron superfields $\mathbf{E'}_{1,2}$ in $(\mathbf{1},\mathbf{1})_1$ and $\tilde{\mathbf{E}}'_{1,2}$ in $(\mathbf{1},\mathbf{1})_{-1}$. The unifications fields are summarised in Table 2.2

[1] This representation also contain four additional singlets which we will not include here for simplicity, as they are not necessary for gauge couplings unifications.

[2] The hypercharge are opposite with respect to the Higgs doublet in the MSSM to make comparison with the MRSSM easier

Names		Spin 0	Spin 1/2	Spin 1	$(SU(3), SU(2), U(1)_Y)$
DG-octet	**O**	O	χ_g $[\equiv \tilde{g}']$		(**8**, **1**, 0)
DG-triplet	**T**	$\{T^0, T^\pm\}$	$\{\chi_T^0, \chi_T^\pm\}$ $[\equiv \{\tilde{W}'^\pm, \tilde{W}'^0\}]$		(**1**,**3**, 0)
DG-singlet	**S**	S	χ_S $[\equiv \tilde{B}']$		(**1**, **1**, 0)

Table 2.1: Adjoint chiral multiplet fields.

Names		Spin 0	Spin 1/2	Spin 1	$(SU(3), SU(2), U(1)_Y)$
Higgs-like Leptons	$\mathbf{R_u}$	R_u	$\tilde{R}_u$		(**1**, **2**, -1/2)
	$\mathbf{R_d}$	R_d	$\tilde{R}_d$		(**1**, **2**, 1/2)
Fake electrons	$\hat{\mathbf{E}}(\times 2)$	$\hat{E}$	$\hat{\tilde{E}}$		(**1**, **1**,1)
	$\hat{\mathbf{E}}'(\times 2)$	$\hat{E}'$	$\hat{\tilde{E}}'$		(**1**, **1**,-1)

Table 2.2: Chiral and gauge multiplet fields in the model.

In order to restrain the possible couplings between the unification fields (which we will refer to sometimes as "fake" fields in relation with the Fake Split SUSY models which will be introduced in the following chapters) and the MSSM ones, we will give them a lepton number. We can therefore view these fields as a vector-like pair of left-handed leptons and two vector-like pairs of right-handed leptons, together with their companion sleptons.

3.2 Lagrangian

We will sort the various terms in the Lagrangian according to whether or not they preserve R-symmetry. We remind that the superpotential must carry a R-charge +2. Therefore, in order for the gauge fields kinetic terms to be R-conserving, one needs to give R-charge +1 to the gauge field-strength superfields and consequently R-charge +1 for the gauginos. An important consequence of this simple algebra is that the SUSY-breaking Majorana mass term for the gaugino also breaks R-symmetry. As we have already pointed out above, this is not the case for Dirac masses as one can give R-charge −1 to the additional adjoint fermions. In this case, we conclude that the supermultiplets $\mathbf{S}, \mathbf{T}$ and $\mathbf{O}$ must have R-charge 0. We can use these results to sort the different terms in our Lagrangian, as we will see below.

Let us now write the superpotential for our model. It can be decomposed as

$$W = W_{Yukawa} + W_{DG} + W_{RV} + W_{unif} \tag{2.10}$$

where W_{Yukawa} contains the usual MSSM Yukawas part

$$W_{Yukawa} = Y_u^{ij} U_i Q_j H_u - Y_d^{ij} D_i Q_j H_d - Y_e^{ij} E_i L_j H_d \tag{2.11}$$

W_{DG} contains the a priori R-symmetric contributions of the adjoint superfields

$$W_{DG} = (\mu + \lambda_S S) H_d H_u + \sqrt{2}\lambda_T H_d T H_u \tag{2.12}$$

while W_{RV} gathers the R-symmetry violating terms

$$\begin{aligned} W_{RV} =& L S + \frac{\hat{M}_1}{2} S^2 + \frac{\kappa}{3} S^3 + \hat{M}_2 \mathrm{tr}(TT) + \hat{M}_3 \mathrm{tr}(OO) \\ &+ \lambda_{ST} S \mathrm{tr}(TT) + \lambda_{SO} S \mathrm{tr}(OO) + \frac{\kappa_O}{3} \mathrm{tr}(OOO) \\ \underset{\mathrm{R-symmetry}}{\longrightarrow}& 0 \end{aligned} \tag{2.13}$$

and W_{unif} the terms with the unification superfields:

$$\begin{aligned} W_{unif} =& (\mu_R + \lambda_{SR} S) R_u R_d + 2\lambda_{TR} R_u T R_d \\ &+ (\mu_{\hat{E}\,ij} + \lambda_{S\hat{E}\,ij} S) \hat{E}_i \hat{E}'_j + \lambda_{SEij} S E_i \hat{E}'_j \\ &+ \lambda_{SLRi} S L_i R_d + 2\lambda_{TLRi} L_i T R_d - Y_{\hat{E}i} R_u H_d \hat{E}_i \\ &- Y_{\hat{E}'i} R_d H_u \hat{E}'_i - Y_{LFV}^{ij} L_i \cdot H_d \hat{E}_j - Y_{EFV}^{j} R_u H_d E_j \ , \end{aligned} \tag{2.14}$$

for which we did not fix a priori the R-charge. Notice in particular that the contributions of the last two last lines of (2.12) couples the new "fake" leptons with the usual Standard Model ones.

We turn now to the soft SUSY-breaking terms. Suppressing all gauge indices while retaining generation indices and denoting the complex conjugation of fields by upper versus lower indices we can have:

- Dirac gaugino masses:

$$W_{\mathrm{supersoft}} = \int d^2\theta \sqrt{2}\theta^\alpha \Big[m_{D1} \mathbf{S} W_{Y\,\alpha} + 2 m_{D2} \mathrm{tr}(\mathbf{T} W_{2\,\alpha}) + 2 m_{D3} \mathrm{tr}(\mathbf{O} W_{3\,\alpha}) \Big]. \tag{2.15}$$

- soft terms associated with the adjoint scalars

$$\begin{aligned} -\Delta\mathcal{L}^{\text{scalar soft}}_{\text{adjoints}} =& + m_S^2 |S|^2 + \frac{1}{2} B_S (S^2 + h.c.) + 2 m_T^2 \mathrm{tr}(T^\dagger T) + (B_T \mathrm{tr}(TT) + h.c.) \\ &+ 2 m_O^2 \mathrm{tr}(O^\dagger O) + (B_O \mathrm{tr}(OO) + h.c.) \\ &+ [T_S S H_u \cdot H_d + 2 T_T H_d \cdot T H_u + \frac{1}{3} \kappa A_\kappa S^3 + h.c.] + (t_S S + h.c.) \end{aligned} \tag{2.16}$$

- soft terms involving the new vector-like leptons:

$$\begin{aligned} -\Delta\mathcal{L}^{\text{scalar soft}}_{\text{vector-like}} =& m_{R_u}^2 |R_u|^2 + m_{R_d}^2 |R_d|^2 + [B_R R_d R_u + h.c.] \\ &+ \hat{E}_i (m^2_{\hat{E}})^i_j \hat{E}^j + \hat{E}'^i (m^2_{\hat{E}'})^j_i \hat{E}'_j + [B^{ij}_{\hat{E}} \hat{E}_i \hat{E}'_j + h.c.] \\ &+ [T^{ij}_{SE} S \hat{E}_i \hat{E}'_j + T_{SR} S R_d R_u + h.c.] \ . \end{aligned} \tag{2.17}$$

Overall, this model have even more parameters than the MSSM. It is therefore particularly important to constrain the parameter space from experimental and theoretical reasons.

In the following, we will consider that the couplings between the fake and true leptons, which are given in the two last lines of (2.12) are negligible. Notice that there are important constraints on them from rare leptons decay and electron dipole moment [43]. Furthermore, we will suppose that the terms in the last line of (2.16) are small so that we will not study their phenomenology. Finally, in a R-symmetry conserving model, one cannot have simultaneously the trilinears T_{SE} (respectively T_{SR}) and the superpotential couplings λ_{SE} (respectively λ_{SR}) as each term requires a different R-charge for the fields $\hat{E}$ and $\hat{E}'$ (respectively R_u and R_d) to be R-invariant.

Chapter 3

Fake Split Supersymetric Models

Split supersymmetry is generally thought to be the simplest extension of the Standard Model with natural, MSSM-like unification of gauge couplings [8]. However, as we have shown in chapter 1, constraints from the Higgs mass measurement severely limit the available parameter space, and particularly the SUSY scale M_S is bounded to be below $10^5 - 10^6$ GeV [15, 16, 17].

Fake Split SUSY models [1,2] (FSSM) were build from the observation that the previous conclusion of minimality for Split SUSY *only applies to the spectrum of particles and not to their couplings*. Indeed, we will show that by considering the same low-energy particle content but with different couplings one can alleviate the constraints on the SUSY scale, leading potentially to a "Mega-Split" spectrum.

We will start by studying in detail the model building of Fake Split SUSY Models in Section 1 by considering two possible realisations, called type-I and type-II. In Section 2, we show that contrary to the Split SUSY the Higgs mass does not lead to *any* upper bound on M_S. Section 3 summarises our results and draws a comparison with the usual Split SUSY case.

1 Constructing Fake Split SUSY Models

A strength of Split SUSY-related models is their exceedingly simple low energy field content. On top of the usual Standard Model particles, one simply adds the fermionic supersymetric particles, namely the gauginos and higgsinos while the scalar SUSY particles are heavy. An approximate symmetry is then needed to protect the desired split spectrum against radiative corrections which could re-instate the light SUSY fermions at the heavy SUSY scale.

In this section, we present the full supersymmetric field contents of two types of Fake Split SUSY Models (FSSM) and describe the approximate global symmetries leading to the splitting. We then further describe the generic Fake Split SUSY effective theory below the SUSY scale.

1.1 The Full Supersymmetric Theory

We introduce in this section two realisations of the above idea, called FSSM-I and FSSM-II. They have both a different field content above the SUSY scale and a different

approximate symmetry protecting the splitting. We will then describe their common low-energy effective below the SUSY, the Fake Split SUSY setup.

a Type I FSSM

In the case of the FSSM-I, the complete supersymmetric theory above the SUSY scale is related to the MDGSSM we introduced in section 3 of chapter 2 but for the treatment of R-symmetry and with a different mass hierarchy as we will see below.

Let us start by reminding briefly its field content shown in Table 2.1 and Table 2.2. We will group the fields in three sets. In the following bold-face symbols denote superfields.

1. *Fake gauginos* (henceforth, F-gauginos) are fermions χ_Σ in the adjoint representation of each gauge group, which sit in a chiral multiplet $\mathbf{\Sigma}$ having scalar component Σ. These consist of: a singlet $\mathbf{S} = S + \sqrt{2}\theta\chi_S + \dots$; an $SU(2)$ triplet $\mathbf{T} = \sum_a \mathbf{T}^a \sigma^a/2$, where $\mathbf{T}^a = T^a + \sqrt{2}\theta\chi_T^a + \dots$ and σ^a are the three Pauli matrices; an $SU(3)$ octet $\mathbf{O} = \sum_a \mathbf{O}^a \lambda^a/2$, where $\mathbf{O}^a = O^a + \sqrt{2}\theta\chi_O^a + \dots$ and λ^a are the eight Gell-Mann matrices.

In order to preserve natural unification we further need to add the bachelor fields described in section 3. For $M_S \lesssim M_{\rm GUT}$ these fields restore the possibility of gauge coupling unification, because they equalise the shifts in the one-loop beta functions at M_S of all of the gauge groups relative to the MSSM [51]. They consist in

2. Higgs-like $SU(2)_W$ doublets $\mathbf{H'_u}$ and $\mathbf{H'_d}$ (henceforth, F-Higgs doublets) with fermions appearing as *fake higgsinos* (henceforth, F-higgsinos).

3. Two pairs of vector-like electron superfields (i.e. two pairs of superfields with charges ± 1 under $U(1)_Y$) with a supersymmetric mass M_S.

We stress that in contrast to the usual Split-SUSY case – and also in contrast to the model we introduced in chapter 2 – we do not preserve an R-symmetry. This means that the gauginos have masses at M_S, moreover the higgsino mass is not protected, thus a μ term of order M_S will be generated for the higgsinos.

However, we introduce an approximate $U(1)_F$ symmetry under which all the adjoint superfields and the F-Higgs fields $\mathbf{H'_u}$ and $\mathbf{H'_d}$ have the same charge. The breaking of this symmetry is determined by a small parameter ε which may correspond to the expectation value of some charged field divided by the fundamental mass scale of the theory (at which Yukawa couplings are generated); in this case we can suppose it to have charge -1 under $U(1)_F$, this reasoning is familiar from flavour models. The charge assignments are the following:

Superfield	$U(1)_F$ charge
$\mathbf{H'_u}, \mathbf{H'_d}$; $\mathbf{S}, \mathbf{T}, \mathbf{O}$	1
$\mathbf{E'}_{1,2}, \tilde{\mathbf{E}}'_{1,2}$	0

As consequence of this approximate symmetry, the superpotential contains a hierarchy of couplings due to suppressions by different powers of ε:

$$\begin{aligned} W \;\supset\;& W_{\rm unif} + \mu_0\, \mathbf{H_u}\cdot\mathbf{H_d} + Y_u\, \mathbf{U^c}\,\mathbf{Q}\cdot\mathbf{H_u} - Y_d\, \mathbf{D^c}\,\mathbf{Q}\cdot\mathbf{H_d} - Y_e\, \mathbf{E^c}\,\mathbf{L}\cdot\mathbf{H_d} \\ &+ \varepsilon\, \left(\hat{\mu}'_d\, \mathbf{H_u}\cdot\mathbf{H'_d} + \hat{\mu}'_u\, \mathbf{H'_u}\cdot\mathbf{H_d} + \hat{Y}'_u\, \mathbf{U^c}\,\mathbf{Q}\cdot\mathbf{H'_u} - \hat{Y}'_d\, \mathbf{D^c}\,\mathbf{Q}\cdot\mathbf{H'_d} - \hat{Y}'_e\, \mathbf{E^c}\,\mathbf{L}\cdot\mathbf{H'_d}\right) \\ &+ \varepsilon\, \left(\hat{\lambda}_S\, \mathbf{S}\,\mathbf{H_u}\cdot\mathbf{H_d} + 2\,\hat{\lambda}_T\, \mathbf{H_d}\cdot\mathbf{T}\,\mathbf{H_u}\right) \\ &+ \varepsilon^2\, \left(\hat{\lambda}'_{Sd}\, \mathbf{S}\,\mathbf{H_u}\cdot\mathbf{H'_d} + \hat{\lambda}'_{Su}\, \mathbf{S}\,\mathbf{H'_u}\cdot\mathbf{H_d} + 2\,\hat{\lambda}'_{Tu}\, \mathbf{H_d}\cdot\mathbf{T}\,\mathbf{H'_u} + 2\,\hat{\lambda}'_{Td}\, \mathbf{H'_d}\cdot\mathbf{T}\,\mathbf{H_u}\right) \\ &+ \varepsilon^2\, \hat{\mu}''\, \mathbf{H'_u}\cdot\mathbf{H'_d} \;+\; \varepsilon^2\, \left[\frac{1}{2}\, \hat{M}_S\, \mathbf{S}^2 + \hat{M}_T\, \mathrm{Tr}(\mathbf{TT}) + \hat{M}_O\, \mathrm{Tr}(\mathbf{OO})\right] + \mathcal{O}(\varepsilon^3)\ , \end{aligned} \tag{3.1}$$

where $\mathbf{Q}, \mathbf{U^c}, \mathbf{D^c}, \mathbf{L}$ and $\mathbf{E^c}$ are the quarks and leptons superfields, $\mathbf{H_u}$ and $\mathbf{H_d}$ the usual MSSM two Higgs doublets. We have explicitly written the ε factors so that all mass parameters are expected to be generated at M_S and all dimensionless couplings are either of order one or suppressed by loop factors. The additional superpotential $W_{\rm unif}$ contains the interactions involving the pairs $\mathbf{E'}_{1,2}$ and $\tilde{\mathbf{E}}'_{1,2}$; these fields are irrelevant for the low energy theory because their masses are not protected, so are of order M_S.

We shall not explicitly write all of the soft terms in the model for reasons of brevity, since they can simply be inferred from the flavour assignments. For example, for the gauginos, allowing all terms permitted by the symmetries we have unsuppressed Majorana masses for the gauginos, and then the suppressed Majorana masses for the F-gauginos $\varepsilon^2 \hat{M}_{S,T,O}$ – and Dirac masses mixing the two suppressed only by ε, giving a generic mass matrix of

$$\mathcal{M}_{1/2} \;\sim\; \mathcal{O}(M_S) \begin{pmatrix} 1 & \mathcal{O}(\varepsilon) \\ \mathcal{O}(\varepsilon) & \mathcal{O}(\varepsilon^2) \end{pmatrix}. \tag{3.2}$$

We have a heavy eigenstate of mass $\mathcal{O}(M_S)$ and a light one, the F-gaugino at leading order, of mass $\mathcal{O}(\varepsilon^2 M_S)$. Requiring that the F-gauginos have a mass at the TeV scale (for unification and, as we shall later see, dark matter) then fixes ε:

$$\varepsilon = \mathcal{O}(\sqrt{\frac{\rm TeV}{M_S}})\ . \tag{3.3}$$

For the adjoint scalars we shall define the explicit soft terms:

$$\begin{aligned} -\mathcal{L}_{\rm scalar\ soft} \supset\; & m_S^2 |S|^2 + 2 m_T^2 \mathrm{tr}\, T^\dagger T + 2 m_O^2 \mathrm{tr}\, O^\dagger O \\ & + \frac{1}{2}\varepsilon^2 B_S [S^2 + h.c] + \varepsilon^2 B_T [\mathrm{tr}\, TT + h.c] + \varepsilon^2 B_O [\mathrm{tr}\, OO + h.c]\ . \end{aligned} \tag{3.4}$$

We see that the B parameters are ε^2-suppressed. This resolves in a very straightforward way the problem, typical of Dirac gaugino models, of having tachyonic adjoints [27, 52, 53].

The Higgs mass matrix can be written in terms of the four-vector

$v_H \equiv (H_u, {H_d}^*, H'_u, {H'_d}^*)$ as

$$-\frac{1}{M_S^2}\mathcal{L}_{soft} \supset v_H^\dagger \begin{pmatrix} \mathcal{O}(1) & \mathcal{O}(1) & \mathcal{O}(\varepsilon) & \mathcal{O}(\varepsilon) \\ \mathcal{O}(1) & \mathcal{O}(1) & \mathcal{O}(\varepsilon) & \mathcal{O}(\varepsilon) \\ \mathcal{O}(\varepsilon) & \mathcal{O}(\varepsilon) & \mathcal{O}(1) & \mathcal{O}(\varepsilon^2) \\ \mathcal{O}(\varepsilon) & \mathcal{O}(\varepsilon) & \mathcal{O}(\varepsilon^2) & \mathcal{O}(1) \end{pmatrix} v_H. \tag{3.5}$$

In the spirit of Split SUSY we tune the weak scale to its correct value and define the SM-like Higgs boson H as

$$H_u \approx \sin\beta\, H + \dots\,, \qquad H_d \approx \cos\beta\, i\sigma^2\, H^* + \dots\,, \tag{3.6}$$

$$H'_u \approx \varepsilon\, H + \dots\,, \qquad H'_d \approx \varepsilon\, i\sigma^2\, H^* + \dots\,, \tag{3.7}$$

where β is a mixing angle and the ellipses represent terms at higher order in ε. Notice that in comparison with 2HDM, MSSM and Split SUSY case, the Standard Model-like Higgs is now a mixed state of four doublets. However, due to the suppression of the mixing between the eigenstates by the $U(1)_F$ symmetry, we can safely neglect the influence of the fake Higgs doublets. Thus, the Yukawa couplings are unaffected compared to the usual Split-SUSY scenario. Note that, if we wanted to simplify the model, we could impose an additional unbroken symmetry under which the F-Higgs fields transform and are vector-like – for example, lepton number – . In this way we would remove the mixing between the Higgs and F-Higgs fields. This is unimportant in what follows, since we are only interested in the light fields that remain.

Furthermore, the presence of a light SM-like Higgs implies at first order in ε

$$B_\mu \simeq \sqrt{(m_{H_u}^2 + \mu_0^2)(m_{H_d}^2 + \mu_0^2)} + \mathcal{O}(\varepsilon)\,. \tag{3.8}$$

From the discussion above we can then read off the mass matrices after electroweak symmetry breaking. In the basis $(\tilde{B}', \tilde{W}'^0, \tilde{H'_d}^0, \tilde{H'_u}^0)$ the neutralino mass matrix is [1]

$$\mathcal{M}_{\chi^0} = \begin{pmatrix} m_{\tilde{B}'} & 0 & \varepsilon^2 M_Z & \varepsilon^2 M_Z \\ 0 & m_{\tilde{W}'} & \varepsilon^2 M_Z & \varepsilon^2 M_Z \\ \varepsilon^2 M_Z & \varepsilon^2 M_Z & 0 & -\mu \\ \varepsilon^2 M_Z & \varepsilon^2 M_Z & -\mu & 0 \end{pmatrix}. \tag{3.9}$$

We see that there is a mixing suppressed by $\varepsilon^2 = \frac{\text{TeV}}{M_S}$. For example, if the F-higgsino is the lightest eigenstate, it will be approximately Dirac with a splitting of the eigenvalues of order $\varepsilon^4 M_Z^2/\mu \sim \left(\frac{\text{TeV}}{M_S}\right)^2 M_Z$.

We then write the chargino mass matrix involving the $\tilde{H}'^+$, $\tilde{H}'^-$ and the charged F-gauginos $\tilde{W}'^+$ and $\tilde{W}'^-$. The mass terms for the charginos can be expressed in the form

$$-(v^-)^T \mathcal{M}_{\chi^\pm} v^+ \;+\; \text{h.c.}\,, \tag{3.10}$$

where we have adopted the basis $v^+ = (\tilde{W}'^+, \tilde{H'}_u^+)$, $v^- = (\tilde{W}'^-, \tilde{H'}_d^-)$. This gives

$$\mathcal{M}_{\chi^\pm} = \begin{pmatrix} m_{\tilde{W}'} & \varepsilon^2 M_W \\ \varepsilon^2 M_W & \mu \end{pmatrix}. \tag{3.11}$$

[1] From now on, given the smallness of ε, we shall not keep explicit track of the numerical coefficients in front of it, thus we will use ε^n as a shorthand for $\mathcal{O}(\varepsilon^n)$.

Again we have very little mixing.

Clearly, the mixing coefficients of order ε^2 in the mass matrices are dependent on quantities in the high-energy theory that we cannot determine. However, because they are so small, they have essentially no bearing on the mass spectrum of the theory (although they will be relevant for the lifetimes).

b Type II FSSM

Having F-gauginos in the low-energy spectrum will in fact be a drawback when dealing with cosmology, as we will show in the next chapter. We therefore present a second model which realises the FSSM below M_S, where only the higgsinos become fake. We shall refer to this as the type II FSSM (or FSSM-II for short).

Since we do not have fake gauginos, the ultraviolet model building is much more conservative than the FSSM-I; in particular one does not have to appeal to Dirac gauginos. Instead, we just add two pairs of Higgs-like doublets, $\mathbf{H}'_u, \mathbf{H}'_d$ and $\mathbf{R}_u, \mathbf{R}_d$. Unification of the gauge couplings at one-loop above M_S is recovered by adding two pairs of supermultiplets in the representations $(\mathbf{3},\mathbf{1})_{1/3} \oplus (\overline{\mathbf{3}},\mathbf{1})_{-1/3}$. In total, we have therefore added two vector-like pairs of $\mathbf{5}+\overline{\mathbf{5}}$ of $SU(5)$. This should be reminiscent of gauge mediation scenarios, except that here the doublets mix with the Higgs fields.

In order to create a split spectrum, we introduce an approximate R-symmetry with charges:

Superfields	R-charge
$\mathbf{H}_u, \mathbf{H}_d$	0
$\mathbf{R}_u, \mathbf{R}_d$	2
$\mathbf{H'_u}, \mathbf{H'_d}$	$+1, -1$

Parametrising the breaking of this R-symmetry by a small parameter ε, the part of the superpotential containing the μ terms of the three Higgs-like multiplets is

$$\begin{aligned} W \supset\ & \varepsilon^2(\mu \mathbf{H}_u\, \mathbf{H}_d + \mu_{H'} \mathbf{H}'_u\, \mathbf{H}'_d) \\ +\ & [\mu_u \mathbf{H}_u\, \mathbf{R}_d + \mu_d \mathbf{R}_u\, \mathbf{H}_d] \\ +\ & \varepsilon \mu_{fdr} \mathbf{R}_u\, \mathbf{H}'_d + \varepsilon \mu_{df} \mathbf{H}'_u\, \mathbf{H}_d + \varepsilon^3 \mu_{uf} \mathbf{H}_u\, \mathbf{H}'_d. \end{aligned}$$

The R-charges have been chosen so that the mixing terms between $\mathbf{H}_{u,d}$ and $\mathbf{R}_{u,d}$ fields are unsuppressed. This allows the particles described mainly by $\mathbf{H}_{u,d}$ and $\mathbf{R}_{u,d}$ to have masses of order M_S, while $\mathbf{H}'_{u,d}$ provide a pair of light F-higgsinos with a mass of $\mathcal{O}(\varepsilon^2 M_S)$. The Yukawa part of the superpotential is given by

$$\begin{aligned} W \supset\ & [Y_u\, \mathbf{U^c}\, \mathbf{Q} \cdot \mathbf{H_u} - Y_d\, \mathbf{D^c}\, \mathbf{Q} \cdot \mathbf{H_d} - Y_e\, \mathbf{E^c}\, \mathbf{L} \cdot \mathbf{H_d}] \\ & + \varepsilon [- Y_d\, \mathbf{D^c}\, \mathbf{Q} \cdot \mathbf{H'_d} - Y_e\, \mathbf{E^c}\, \mathbf{L} \cdot \mathbf{H'_d}] \end{aligned}$$

which allows a successful mass generation for the quarks and leptons, the SM-like Higgs obtained from fine-tuning at the electroweak scale must originate from the $\mathbf{H}_u$ and $\mathbf{H}_d$ multiplets.

Imposing the R-symmetry on the soft terms leads to the suppression of the Majorana gauginos mass by ε^2 factors (this mechanism is similar to the usual Split SUSY

one). In the term of the vector $v_H \equiv (H_u, {H_d}^*, H'_u, H'^*_d, R_u, R^*_d)$, the Higgs mass matrix has the following hierarchy

$$-\frac{1}{M_S^2}\mathcal{L}_{soft} \supset v_H^\dagger \begin{pmatrix} \mathcal{O}(1) & \mathcal{O}(1) & \mathcal{O}(\varepsilon) & \mathcal{O}(\varepsilon) & \mathcal{O}(\varepsilon^2) & \mathcal{O}(\varepsilon^2) \\ \mathcal{O}(1) & \mathcal{O}(1) & \mathcal{O}(\varepsilon) & \mathcal{O}(\varepsilon) & \mathcal{O}(\varepsilon^2) & \mathcal{O}(\varepsilon^2) \\ \mathcal{O}(\varepsilon) & \mathcal{O}(\varepsilon) & \mathcal{O}(1) & \mathcal{O}(1) & \mathcal{O}(\varepsilon) & \mathcal{O}(\varepsilon^3) \\ \mathcal{O}(\varepsilon) & \mathcal{O}(\varepsilon) & \mathcal{O}(1) & \mathcal{O}(1) & \mathcal{O}(\varepsilon) & \mathcal{O}(\varepsilon^3) \\ \mathcal{O}(\varepsilon^2) & \mathcal{O}(\varepsilon^2) & \mathcal{O}(\varepsilon) & \mathcal{O}(\varepsilon) & \mathcal{O}(1) & \mathcal{O}(\varepsilon^4) \\ \mathcal{O}(\varepsilon^2) & \mathcal{O}(\varepsilon^2) & \mathcal{O}(\varepsilon^3) & \mathcal{O}(\varepsilon^3) & \mathcal{O}(\varepsilon^4) & \mathcal{O}(1) \end{pmatrix} v_H. \quad (3.12)$$

We can tune the SM-like Higgs from the scalar components of $\mathbf{H}_u$ and $\mathbf{H}_d$ to get

$$H_u \approx \sin\beta\, H + \dots\,, \qquad H_d \approx \cos\beta\, i\sigma^2\, H^* + \dots\,, \quad (3.13)$$

and the other Higgs-like scalars only enters the linear combination with ε suppression. The fine-tuning condition can therefore be applied on the B_μ term similarly, with the exception that the μ terms are not ε-suppressed compared to the soft masses, leading to

$$B_\mu \simeq \sqrt{(m^2_{H_u} + \mu_u^2)(m^2_{H_d} + \mu_d^2)} + \mathcal{O}(\varepsilon)\,. \quad (3.14)$$

The parameter ε is here also fixed by the requirement that the gauginos obtain a mass at the TeV scale

$$\varepsilon = \mathcal{O}(\sqrt{\frac{\text{TeV}}{M_S}}). \quad (3.15)$$

1.2 The Low-Energy Theory: Fake Split SUSY

Focusing on the effective theory below the supersymmetry scale M_S, we can integrate out all of the heavy states and find that the particle content of the theory appears exactly the same as in Split SUSY: this is why we call the scenario Fake Split SUSY.

The following discussion will be made for the FSSM type I, but could be made in a completely similar fashion for FSSM type-II by replacing the F-gauginos by the usual gauginos. The only difference is that the couplings $\tilde{g}_{u,d}$ and $\tilde{g}'_{u,d}$ will be suppressed by ϵ instead of ϵ^2 which does not modify our results.

Above the electroweak scale, we have F-Binos $\tilde{B}'$, F-Winos $\tilde{W}'$ and F-gluinos $\tilde{g}'$ with (Majorana) masses $m_{\tilde{B}'}$, $m_{\tilde{W}'}$ and $m_{\tilde{g}'}$, respectively, and F-higgsinos $\tilde{H}'_{u,d}$ with a Dirac mass μ.

We can also determine the effective renormalisable couplings. The F-gauginos and F-higgsinos have their usual couplings to the gauge fields. The F-gluinos have only gauge interactions, whereas there are in principle renormalisable interactions between the Higgs, F-higgsinos and F-electroweakinos. The allowed interactions take the form

$$\mathcal{L}_{\text{eff}} \supset -\frac{H^\dagger}{\sqrt{2}}(\tilde{g}_u\, \sigma^a\, \tilde{W}'^a + \tilde{g}'_u\, \tilde{B}')\ \tilde{H}'_u - \frac{H^T i\sigma^2}{\sqrt{2}}(-\tilde{g}_d\, \sigma^a\, \tilde{W}'^a + \tilde{g}'_d\, \tilde{B}')\ \tilde{H}'_d\,. \quad (3.16)$$

Since the gauge couplings of all the particles are the same as in the usual Split-SUSY case, the allowed couplings take the same form. However, the values differ greatly. Indeed in our model the couplings are *doubly* suppressed:

$$\tilde{g}'_u \sim \tilde{g}'_d \sim \tilde{g}_u \sim \tilde{g}_d \sim \varepsilon^2, \quad (3.17)$$

since the terms in (3.16) violate the approximate global symmetry. We recall that, in the usual Split-SUSY case, we would have instead: $\tilde{g}_u = g \sin\beta$, $\tilde{g}_d = g \cos\beta$, $\tilde{g}'_u = g' \sin\beta$ and $\tilde{g}'_d = g' \cos\beta$, where β is the angle that rotates the Higgs doublets H_u and H_d into one light, SM-like doublet and a heavy one.

The remaining renormalisable coupling in the theory is the Higgs quartic coupling λ, which at tree level is determined by supersymmetry to be

$$\lambda \;=\; \frac{1}{4}\left(g^2 + g'^2\right)\cos^2 2\beta \;+\; \mathcal{O}(\varepsilon^2)\;. \tag{3.18}$$

The tree-level corrections at $\mathcal{O}(\varepsilon^2)$ come from the superpotential couplings $\hat{\lambda}_S$ and $\hat{\lambda}_T$, and from the $\mathcal{O}(\varepsilon)$ mixing between the Higgs and F-Higgs fields. Additional $\mathcal{O}(1)$ contributions to this relation could arise if the SUSY model above M_S included new, substantial superpotential (or D-term) interactions involving the SM-like Higgs, but this is not the case in our models. Similarly, the introduction of Dirac masses can modify this relation [21], but they are negligible compared to the Majorana ones (see eq (3.2)). There are, however, small loop-level corrections to eq. (3.18), which we will discuss in the next section.

The $\mathcal{O}(\varepsilon^2)$ corrections to the $\tilde{g}_{(u,d)}$, $\tilde{g}'_{(u,d)}$ and λ couplings are not determined from the low-energy theory and are thus unknown from the low-energy perspective. However, in this study we focus on models where the set of F-gauginos and F-higgsinos lies in the TeV mass range, which corresponds to values of ε of the order of

$$\varepsilon \sim \sqrt{\frac{\text{TeV}}{M_S}}\;, \tag{3.19}$$

which gives a ε^2 ranging between 10^{-13} to 10^{-2} when M_S goes from the highest GUT scale of 10^{16} GeV down to 100 TeV, the lowest scale considered here. With such values of ε, we have verified that we can safely neglect the contribution of $\tilde{g}_{(u,d)}$ and $\tilde{g}'_{(u,d)}$to the running of the Higgs quartic coupling, and that the shift in the Higgs mass due to the tree-level corrections to λ is less than 2 GeV for $M_S > 100$ TeV, falling to a negligibly small amount for $M_S > 1000$ TeV.

2 Higgs Mass Prediction in Fake Split Models

We will study the Higgs mass prediction in Fake Split SUSY models in two steps. First, we focus on the low energy effective theory, with most input parameters at the electroweak scales with the exception of $\tan\beta$ which is considered a free parameter at the SUSY scale. In the second place, we will include the full supersymmetric theories above the SUSY scale with unified input parameters at the GUT scale. We will show that contrary to the Split SUSY case, this does not lead to stronger constraints on the SUSY scale.

2.1 An Effective Theory Approach

Our low-energy effective theory has a remarkably small number of parameters. Namely, the gluino pole mass, the F-Higgsino μ term,$\tan\beta$ and the SUSY scale, with the Higgs

mass depending mainly of $\tan\beta$, M_S and the gluino mass. This limited parameter space is however perfectly sufficient since, as we will see now, it is in fact hard *not to get* a 125 GeV Higgs in Fake Split SUSY models.

a Implementation

Our procedure for the determination of the Higgs-boson mass is based on the one described in ref. [13] for the regular Split-SUSY case. We impose boundary conditions on the $\overline{\text{MS}}$-renormalised parameters of the FSSM, at the high scale M_S for $\tan\beta$ (and the electroweak gauginos masses, defined from a GUT relation as we will described below), where we match our effective theory with the full supersymmetric theory, and at the low scale M_Z for the other parameters, where we match the effective theory with the SM. We then use RG evolution iteratively to obtain all the effective-theory parameters at the weak scale, where we finally compute the radiatively corrected Higgs mass. However, in this analysis we improved several aspects of the earlier calculation, by including the two-loop contributions to the boundary condition for the top Yukawa coupling, the two-loop contributions to the RG equations for the Split-SUSY parameters, as well as some two- and three-loop corrections to the Higgs-boson mass.

At the high scale M_S, the boundary condition on the quartic coupling of the light, SM-like Higgs doublet is determined by supersymmetry and given by eq. (3.18). In contrast with the Split-SUSY case, a large μ_0-term and A-terms are no longer forbidden by R-symmetry (as the latter is broken at the scale M_S), and the threshold corrections proportional to powers of $|A_t - \mu_0 \cot\beta|^2/M_S^2$ can in principle alter the boundary condition in eq. (3.18). For very large values of M_S, the top Yukawa coupling that controls these corrections is suppressed, and their effect on the Higgs mass is negligible. For lower values of M_S, on the other hand, the effect becomes sizable, and it can shift the Higgs mass by up to 6 GeV when $M_S \sim 10^5$ GeV [14]. This allows us to obtain the desired Higgs mass for a lower value of $\tan\beta$ for fixed M_S, or a lower M_S for a given value of $\tan\beta$. As our main purpose in this work is to study the possibility of pushing M_S to its highest values, in the following we shall take the stop-mixing parameter to be vanishing, and we will neglect all of the one-loop corrections described in refs [13, 14].

As mentioned in section 1.2, the effective Higgs–(F-)higgsino–(F-)gaugino couplings $\tilde{g}_u$, $\tilde{g}_d$, $\tilde{g}'_u$ and $\tilde{g}'_d$ are of $\mathcal{O}(\varepsilon^2)$ for the FSSM-I and $\mathcal{O}(\varepsilon)$ for the FSSM-II, we therefore set them to zero at the matching scale M_S. The RG evolution down to the weak scale does not generate non-zero values for those couplings, therefore, in contrast with the case of the regular Split SUSY, the F-higgsinos and (F-)gauginos have negligible mixing upon electroweak symmetry breaking, and they do not participate in the one-loop corrections to the Higgs-boson mass. Consequently their precise nature, fake in FSSM-I and true in FSSM-II does not modify the low-energy effective theory.

Indeed, the electroweak (F-)gauginos and the F-higgsinos affect our calculation of the Higgs mass only indirectly, through their effect on the RG evolution and on the weak-scale boundary conditions for the electroweak gauge couplings, and we find that the precise values of their masses have very little impact on the prediction for the Higgs mass. On the other hand, the choice of the (F-)gluino mass is more important due to its effect on the boundary conditions for the strong and top Yukawa couplings.

To fix the soft SUSY-breaking (F-)gaugino masses, we take as input the physical

(F-)gluino mass $M_{\tilde{g}'}$, and convert it to the $\overline{\rm MS}$ parameter $m_{\tilde{g}'}$ evaluated at the scale $M_{\tilde{g}'}$ according to the one-loop relation

$$m_{\tilde{g}'}(M_{\tilde{g}'}) \;=\; \frac{M_{\tilde{g}'}}{1+\frac{3\,g_3^2}{4\,\pi^2}}\;, \tag{3.20}$$

where g_3 is the strong gauge coupling of the FSSM. We then evolve $m_{\tilde{g}'}$ up to the scale M_S, where, for simplicity[2], we impose on the other two F-gaugino masses the GUT-inspired relations

$$m_{\tilde{B}'}(M_S) \;=\; \left[\frac{g_1(M_S)}{g_3(M_S)}\right]^2 m_{\tilde{g}'}(M_S)\;, \qquad m_{\tilde{W}'}(M_S) \;=\; \left[\frac{g_2(M_S)}{g_3(M_S)}\right]^2 m_{\tilde{g}'}(M_S)\;. \tag{3.21}$$

We can then evolve all of the (F-)gaugino masses down to the weak scale. For what concerns the F-higgsino mass μ, we take it directly as an $\overline{\rm MS}$ input parameter evaluated at the scale M_Z.

We use the experimental Higgs mass $M_h = 125.09 \pm 0.24$ from the combined ATLAS and CMS results [54]. The gauge and third-family Yukawa couplings, as well as the vacuum expectation value v of the SM-like Higgs (normalised as $v \approx 174$ GeV in our code), are extracted from the following set of SM inputs [55,56]: the strong gauge coupling $\alpha_s(M_Z) = 0.1184$ (in the $\overline{\rm MS}$ scheme with five active quarks); the electromagnetic coupling $\alpha(M_Z) = 1/127.944$; the Z-boson mass $M_Z = 91.1876$ GeV; the Fermi constant $G_F = 1.16638\times10^{-5}$ GeV^{-2}; the physical top and tau masses $M_t = 173.2\pm0.9$ GeV and $M_\tau = 1.777$ GeV; and the running bottom mass $m_b(m_b) = 4.18$ GeV. We use the one-loop formulae given in the appendix A of ref. [13] to convert all the SM inputs into $\overline{\rm MS}$ running parameters of the FSSM evaluated at the scale M_Z.

In view of the sensitivity of λ to the precise value of the top Yukawa coupling g_t, we include the two-loop QCD contribution to the relation between the physical top mass M_t and its $\overline{\rm MS}$ counterpart m_t. In particular, we use:

$$m_t(M_Z) \;=\; \frac{M_t}{1+\frac{g_3^2}{(4\pi)^2}\,C_1 \;+\; \frac{g_3^4}{(4\pi)^4}\left(C_2^{\rm SM}+C_2^{\tilde{g}'}\right)} \;+\; \Sigma_t(m_t)^{\rm EW}\;, \tag{3.22}$$

where g_3 is computed at the scale M_Z using eq. (A.1) of ref. [13], $\Sigma_t(m_t)^{\rm EW}$ denotes the terms in the one-loop top self energy that do not involve the strong interaction, and

$$C_1 \;=\; \frac{16}{3} - 4\,\ln\frac{M_t^2}{M_Z^2}\;, \tag{3.23}$$

$$C_2^{\rm SM} \;=\; \frac{2821}{18} + \frac{16}{3}\,\zeta_2\,(1+\ln 4) - \frac{8}{3}\,\zeta_3 - \frac{338}{3}\,\ln\frac{M_t^2}{M_Z^2} + 22\,\ln^2\frac{M_t^2}{M_Z^2}\;, \tag{3.24}$$

$$C_2^{\tilde{g}'} \;=\; \frac{89}{9} + 4\,\ln\frac{m_{\tilde{g}'}^2}{M_Z^2}\left(\frac{13}{3} + \ln\frac{m_{\tilde{g}'}^2}{M_Z^2} - 2\,\ln\frac{M_t^2}{M_Z^2}\right)\;. \tag{3.25}$$

The boundary condition for the top Yukawa coupling of the FSSM is then given by $g_t(M_Z) = m_t(M_Z)/v(M_Z)$. The two-loop SM contribution $C_2^{\rm SM}$ in eq. (3.24) is from

[2] Although the patterns of neutralino and chargino masses are important for collider searches, in our model they have negligible impact on the Higgs mass and so the exact relation is not important.

ref. [57], while to obtain the two-loop (F-)gluino contribution $C_2^{\tilde{g}'}$ in eq. (3.25) we adapted the results of ref. [58] to the case of a heavy Majorana fermion in the adjoint representation of $SU(3)$. For an (F-)gluino mass of a few TeV, the inclusion of $C_2^{\tilde{g}'}$ in the boundary condition for g_t becomes crucial, as it changes the prediction for the Higgs mass by several GeV. Alternatively, one could decouple the (F-)gluino contribution from the RG evolution of the couplings below the scale $M_{\tilde{g}'}$, include only the SM contributions in the boundary conditions for g_t and g_3 at the scale M_Z, and include the non-logarithmic part of $C_2^{\tilde{g}'}$ as a threshold correction to g_t at the scale $M_{\tilde{g}'}$. We have checked that the predictions for the Higgs mass obtained with the two procedures are in very good agreement with each other.

To improve our determination of the quartic coupling λ at the weak scale, we use two-loop renormalisation-group equations (RGEs) to evolve the couplings of the effective theory between the scales M_S and M_Z. Results for the two-loop RGEs of Split SUSY have been presented earlier in refs [59,14,60]. Since there are discrepancies between the existing calculations, we used the public codes `SARAH` [61] and `PyR@TE` [62] to obtain independent results for the RGEs of Split SUSY in the $\overline{\text{MS}}$ scheme. Taking into account the different conventions, we agree with the RGE for λ presented in ref. [59], and with all the RGEs for the dimensionless couplings presented in section 3.1 of ref. [60]. However, we disagree with ref. [60] in some of the RGEs for the mass parameters (our results for the latter are collected in the appendix). Concerning the RGEs for the dimensionless couplings presented in ref. [14], we find some discrepancies [3] in two-loop terms proportional to g_2^4 and g_2^6.

At the end of our iterative procedure, we evolve all the parameters to a common weak scale Q_W, and obtain the physical squared mass for the Higgs boson as

$$\begin{aligned} M_H^2 &= \frac{\lambda(Q_W)}{\sqrt{2}\,G_F}\left[1-\delta^{1\ell}(Q_W)\right] \\ &+ \frac{g_t^4\,v^2}{128\,\pi^4}\left[16\,g_3^2\,(3\,\ell_t^2+\ell_t)-3\,g_t^2\left(9\,\ell_t^2-3\,\ell_t+2+\frac{\pi^2}{3}\right)\right] \\ &+ \frac{g_3^4\,g_t^4\,v^2}{64\,\pi^6}\,\ln^3\frac{m_{\tilde{g}'}^2}{Q_W^2}\,, \end{aligned} \tag{3.26}$$

where $\ell_t = \ln(m_t^2/Q_W^2)$. The one-loop correction $\delta^{1\ell}(Q_W)$, which must be computed in terms of $\overline{\text{MS}}$ parameters, is given in eqs (15a)–(15f) of ref. [63], while the two-loop corrections proportional to $g_3^2 g_t^4$ and to g_t^6 come from ref. [64]. We have also included the leading-logarithmic correction arising from three-loop diagrams involving F-gluinos, which can become relevant for large values of $m_{\tilde{g}'}/Q_W$. This last term must of course be omitted if the F-gluinos are decoupled from the RGE for λ below the scale $M_{\tilde{g}'}$. In our numerical calculations we set $Q_W = M_t$ to minimise the effect of the radiative corrections involving top quarks, but we have found that our results for the physical Higgs mass are remarkably stable with respect to variations of Q_W.

[3] In particular, in ref. [14] the coefficient of g_2^4 in the RGEs for g_t, g_b, g_τ, $\tilde{g}'_u$ and $\tilde{g}'_d$ should be changed from $-15/4$ to $-17/4$, while the coefficient of g_2^4 in the RGEs for $\tilde{g}_u$ and $\tilde{g}_d$ should be changed from $-121/4$ to $-409/12$. In the RGE for λ, the terms proportional to g_2^6, λg_2^4 and $g_2^4 g_1^2$ should be corrected in accordance with ref. [59]. We thank A. Strumia for confirming these corrections.

b Results

Before presenting our result for the Higgs mass, we stress that at the one-loop level, the running of gauge couplings in our model is the same as in Split SUSY because the (suppressed) Yukawa couplings only enter at two-loop level. We have verified that the gauge-coupling unification of Split SUSY scenario is maintained at two loops in our model.

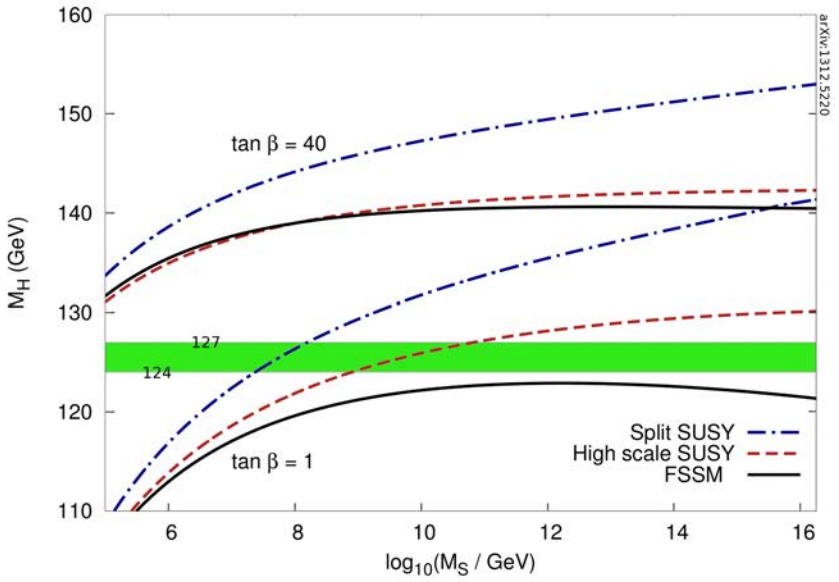

Figure 3.1: Higgs-mass predictions as a function of the SUSY scale M_S for FSSM, High-Scale SUSY and Split SUSY. We set $M_{\tilde{g}'} = \mu = 2$ TeV and $\tan\beta = 1$ or 40. The green-shaded region indicates a Higgs mass in the range $[124, 127]$ GeV.

Higgs mass in FSSM: We find that, in the FSSM, the dependence of the physical Higgs mass on the SUSY scale M_S differs markedly from the cases of regular Split SUSY or High-Scale SUSY (where all superparticle masses are set to the scale M_S). Figure 3.1 illustrates this discrepancy, showing M_H as a function of M_S for $M_{\tilde{g}'} = \mu = 2$ TeV. The solid (black) curves represent the prediction of the FSSM, the dashed (red) ones represent the prediction of High-Scale SUSY, and the dot-dashed (blue) ones represent the prediction of regular Split SUSY (the predictions for the latter two models were obtained with appropriate modifications of the FSSM calculation described in section 2.1). For each model, the lower curves were obtained with $\tan\beta = 1$, resulting in the lowest possible value of M_H for a given M_S, while the upper curves were obtained with $\tan\beta = 40$.

As was shown earlier in ref. [14], the Higgs mass grows monotonically with the SUSY scale M_S in the Split-SUSY case, while it reaches a plateau in High-Scale SUSY. In both cases, the prediction for the Higgs mass falls between 124 and 127 GeV only for a relatively narrow range of M_S, well below the unification scale $M_{\rm GUT} \approx 2{\times}10^{16}$ GeV. In the FSSM, on the other hand, the Higgs mass reaches a maximum and then starts

decreasing, remaining generally lower than in the other models. It is therefore much easier to obtain a Higgs mass close to the experimentally observed value even for large values of the SUSY scale. For example, as will be discussed later, when $\tan\beta \approx 1.5$ we find that the FSSM prediction for the Higgs mass falls between 124 and 127 GeV for all values of M_S between 10^8 GeV and $M_{\rm GUT}$.

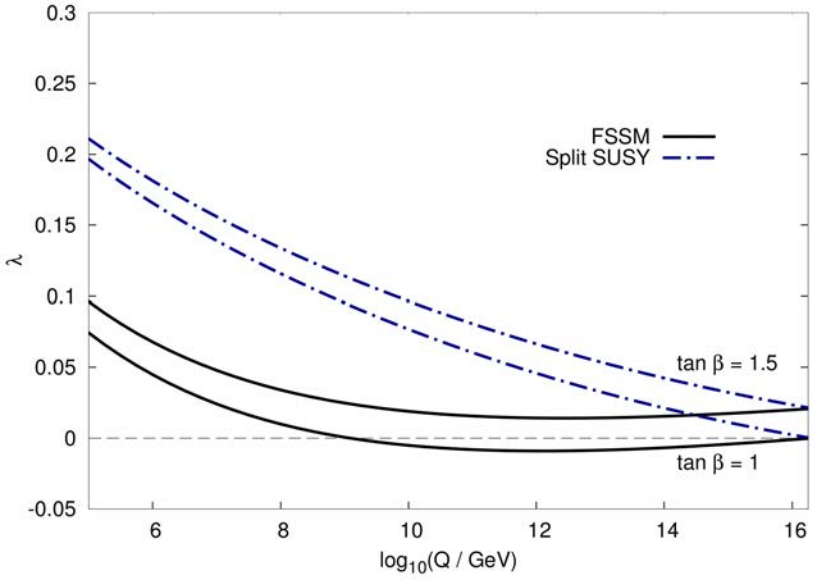

Figure 3.2: Running of the Higgs quartic coupling λ in the FSSM and in the usual Split-SUSY case for $\tan\beta = 1$ and 1.5. We set $M_S = 2\times10^{16}$ GeV and $M_{\tilde{g}'} = \mu = 2$ TeV.

This new behaviour originates in the RG evolution of λ in the FSSM, which differs from the case of Split SUSY. In figure 3.2 we show the dependence of λ on the renormalisation scale Q in the two theories, imposing the boundary condition in eq. (3.18) at the scale $M_S = 2\times10^{16}$ and setting $\tan\beta$ to either 1 or 1.5. Even though we impose the same boundary condition in both theories, the fact that the effective Higgs–higgsino–gaugino couplings are zero in the FSSM induces a different evolution. Indeed, in Split SUSY the contributions proportional to four powers of the Higgs–higgsino–gaugino couplings enter the one-loop part of β_λ with negative sign, as do those proportional to four powers of the top Yukawa coupling, whereas the contributions proportional to four powers of the gauge couplings enter with positive sign. For $M_S \gtrsim 10^{12}$ GeV, the top Yukawa coupling is sufficiently suppressed at the matching scale that removing the Higgs–higgsino–gaugino couplings makes β_λ positive. This prompts λ to decrease with decreasing Q, until the negative contribution of the top Yukawa coupling takes over and λ begins to increase. We will analyse this result in more detail in section 3.

Vacuum stability: Figure 3.2 also shows that, for values of $\tan\beta$ sufficiently close to 1, the quartic coupling λ can become negative during its evolution down from the scale M_S, only to become positive again when Q approaches the weak scale. This points to an unstable vacuum, and a situation similar to the one described in ref. [65]. However, it

was already clear from figure 3.1 that, for $\tan\beta = 1$, the FSSM prediction for the Higgs mass is too low anyway. For the values of $\tan\beta$ large enough to induce a Higgs mass in the observed range, the theory is stable. This is illustrated in figure 3.3, where we show the contours of equal Higgs mass on the $M_S - \tan\beta$ plane, setting $M_{\tilde{g}'} = \mu = 2$ TeV. The green-shaded region corresponds to a Higgs mass in the observed range between 124 and 127 GeV, while the yellow-shaded region is where λ becomes negative during its evolution between M_S and the weak scale, and the vacuum is unstable. It can be seen that, for $M_S \gtrsim 10^8$ GeV, a Higgs mass around 126 GeV can be comfortably obtained for $\tan\beta \approx 1.5$. The unstable region is confined to values of $\tan\beta$ very close to 1, and only for $M_S \gtrsim 10^{12}$ GeV. For lower values of M_S, the top Yukawa coupling is not sufficiently suppressed at the matching scale and β_λ is always negative, therefore there is no region of instability.

We investigated how our results are affected by the experimental uncertainty on the top mass. An increase (or decrease) of 1 GeV from the central value $M_t = 173.2$ GeV used in figure 3.3 translates into an increase (or decrease) in our prediction for the Higgs mass of 1–2 GeV, depending on M_S. For larger values of M_t, the observed value of M_H is obtained for $\tan\beta$ closer to 1, and the green regions in figure 3.3 approach the unstable region. The size of the unstable region is itself dependent on M_t (i.e. the region shrinks for larger M_t) but the effect is much less pronounced. Consequently, raising the value of the top mass may lead to instability for large M_S (e.g. for $M_S \gtrsim 10^{12}$ GeV when $M_{\tilde{g}'} = 2$ TeV). Considering an extreme case, for $M_t = 175$ GeV we would see a substantial overlap of the experimentally acceptable regions with the unstable region around $M_S \approx M_{\rm GUT}$. On the other hand, for values of M_t lower than 173.2 GeV the green regions in figure 3.3 are shifted towards values of $\tan\beta$ further away from 1, and the vacuum is always stable for the correct Higgs mass.

Finally, in figure 3.4 we show the contours of equal Higgs mass on the $M_{\tilde{g}'} - \tan\beta$ plane, setting $M_S = 2\times10^{16}$ GeV and $\mu = 2$ TeV. The colour code is the same as in figure 3.3. It can be seen that the region where the FSSM prediction for the Higgs mass is between 124 and 127 GeV gets closer to the unstable region when the F-gluino mass increases. However, the dependence of M_H on $M_{\tilde{g}'}$ is relatively mild, and only when $M_{\tilde{g}'}$ is in the multi-TeV region do the green and yellow regions in figure 3.4 overlap. We conclude that if we insist on enforcing exact stability and setting $M_S \approx 2\times10^{16}$ GeV, then obtaining a Higgs mass compatible with the observed value constrains the gluino mass to the few-TeV region.

Strongly-coupled fake fermions As a related development, one could wonder from a purely bottom-up approach what could be the effect of relaxing the constraints on $\tilde{g}_u$, $\tilde{g}_d$, $\tilde{g}'_u$ and $\tilde{g}'_d$ and simply choose to fix them at the SUSY scale as

$$\begin{aligned} \tilde{g}_{1u} &= \tilde{\epsilon} g' \sin\beta & \tilde{g}_{1d} &= \tilde{\epsilon} g' \cos\beta \\ \tilde{g}_{2u} &= \tilde{\epsilon} g \sin\beta & \tilde{g}_{2d} &= \tilde{\epsilon} g \cos\beta \end{aligned} \tag{3.27}$$

where $\tilde{\epsilon}$ is a free parameter, which we can use to interpolate between the FSSM case ($\tilde{\epsilon} \sim 0$) and the Split SUSY one ($\tilde{\epsilon} \sim 1$). For bigger values of $\tilde{\epsilon} > 1$, we have a new region of the parameter space, in which the running of the Higgs quartic runs very quickly to zero (which could hypothetically allow to fit this low-energy model in a Gauge-Higgs

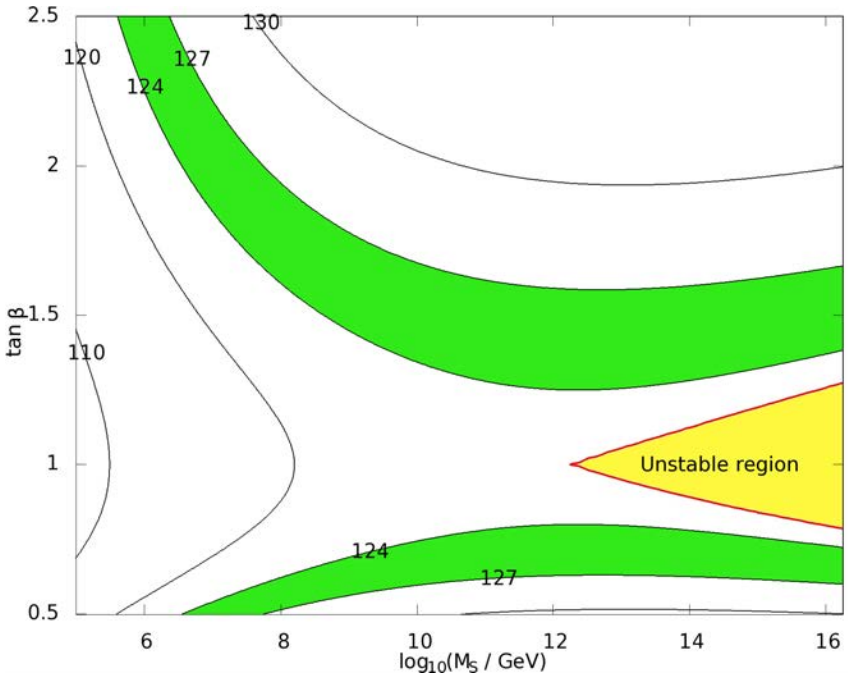

Figure 3.3: Contour plot of the prediction for the Higgs mass on the $M_S - \tan\beta$ plane, for $M_{\tilde{g}'} = \mu = 2$ TeV. The yellow-shaded region indicates where λ becomes negative during its running between M_Z and M_S. The green-shaded region indicates a Higgs mass in the range $[124, 127]$ GeV.

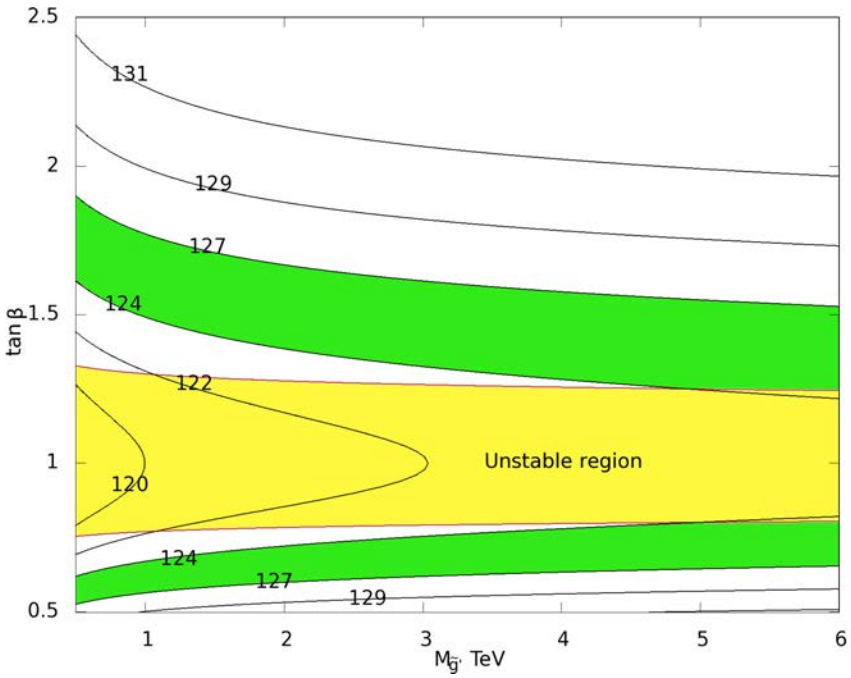

Figure 3.4: Same as figure 3.3 on the $M_{\tilde{g}'} - \tan\beta$ plane, with $M_S = 2\times10^{16}$ GeV and $\mu = 2$ TeV.

unification approach, with the SUSY scale M_S replaced by a compactification scale). The Higgs mass can be easily determined as a function of the UV scale M_C and of the parameter $\tilde{\epsilon}$, this is shown in Figure 3.5.

2.2 A Complete Treatment

Let us summarise our results so far. We have defined a model – the FSSM – which has the same particle content at low energies as Split SUSY, but has a substantially different ultraviolet completion and also low-energy phenomenology:

We have found that a standard-model-like Higgs boson with a mass around 125 GeV can be obtained for low values of $\tan\beta$. For low values of M_S, the exact value of $\tan\beta$ is subject to modification that we estimated when considering the presence of additional contributions to the quartic Higgs coupling from the unsuppressed A-terms. For larger values of M_S, the latter contributions are negligible.

One crucial element is missing in this picture though: we have left aside the theory above the SUSY scale and focused directly on the low-energy effective theory. Indeed, we know from the works on the Mini-Split [15, 16, 17] that the RGE of the complete theory above M_S constrains the allowed range of values for $\tan\beta$, therefore increasing the constraints on the Higgs mass. We will now show that in Fake Split SUSY Models, including the full SUSY theory above M_S does not lead to increased constraints.

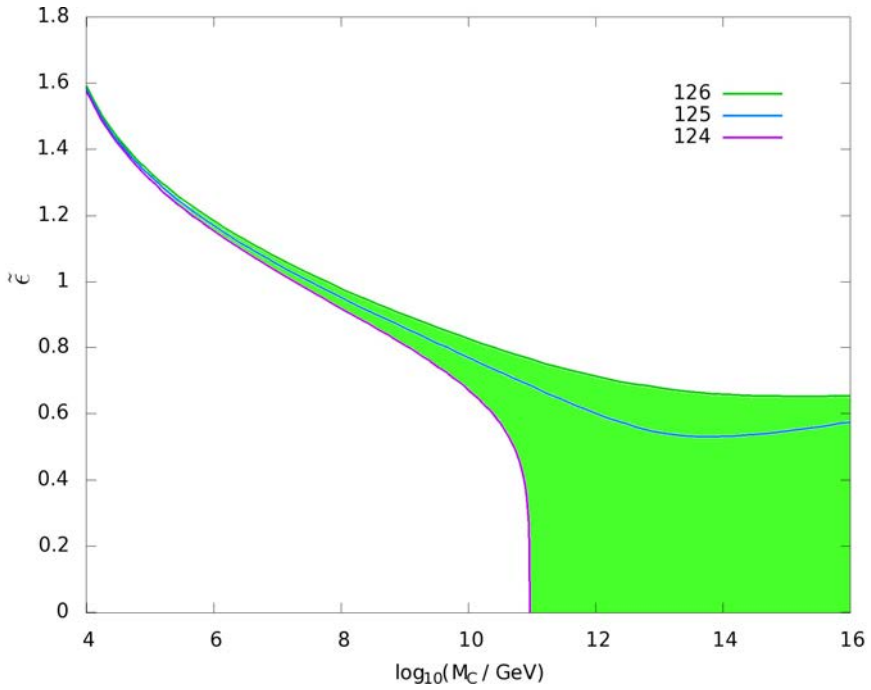

Figure 3.5: Higgs pole mass as a function of the UV scale M_C and of the strength of the Yukawas coupling for F-Higgsinos $\tilde{\epsilon}$. We have chosen $\tan\beta = 1$.

a Obtaining $\tan\beta$

In Fake Split SUSY, the situation is different from the Split SUSY tension between unification and Higgs mass we presented in the last chapter although the details depend upon the high-energy theory:

- In the FSSM-I, we have

$$\det\begin{pmatrix} m_{H_u}^2 + |\mu_0|^2 & -B_\mu \\ -B_\mu & m_{H_d}^2 + |\mu_0|^2 \end{pmatrix} \simeq 0 \quad \rightarrow \quad \tan\beta = \sqrt{\frac{m_{H_d}^2 + |\mu_0|^2}{m_{H_u}^2 + |\mu_0|^2}} \tag{3.28}$$

  as above but now unification only requires the *fake-higgsino* mass parameter μ to be small which differs from μ_0. This means that provided μ_0 is sufficiently large it is not important whether $m_{H_u}^2$ becomes negative; we will always have a stable vacuum solution, and generically $\tan\beta \sim \mathcal{O}(1)$.

  In addition, there is no R-symmetry protecting the masses and thus the RGEs take on the full dependence:

$$16\pi^2 \frac{d}{d\log\mu} m_{H_u}^2 \simeq 6|y_t|^2(m_{H_u^2} + m_Q^2 + m_U^2 + A_t^2) - 6g_2^2 M_2 - 2g_Y^2 M_1 + 2g_Y^2 \mathrm{tr}(Y m^2) \tag{3.29}$$

  where the trilinear mass A_t and gaugino masses $M_{1,2}$ are not suppressed. These can reduce the tendency for $m_{H_u}^2$ to become tachyonic in Split SUSY models.

- In the FSSM-II, we have instead an R-symmetry which protects the trilinear scalar masses and gaugino masses, and neglecting terms of $\mathcal{O}(\varepsilon)$ we have

$$\det \begin{pmatrix} m_{H_u}^2 + |\mu_u|^2 & -B_\mu \\ -B_\mu & m_{H_d}^2 + |\mu_d|^2 \end{pmatrix} \simeq 0 \quad \rightarrow \quad \tan\beta = \sqrt{\frac{m_{H_d}^2 + |\mu_d|^2}{m_{H_u}^2 + |\mu_d|^2}}. \quad (3.30)$$

  As in the FSSM-I, since $\mu_{u,d} \sim M_S$ there is no incompatibility with unification and obtaining $\tan\beta \sim \mathcal{O}(1)$.

Therefore there should be no impediment from taking the soft masses to be generated at the unification scale. In the following, we will consider the predictions from a scenario where this is the case: we will take a common scalar mass m_0, common gaugino mass $M_{1/2}$ and (in the FSSM-I) a common trilinear mass A_0 at that scale and investigate the consequences for the Higgs mass and dark matter.

b Implementation

The Higgs mass along with the low-energy spectrum are computed using a two-fold procedure. On one side, we compute the running between the electroweak scale and M_S. On the other side we compute the running between M_S and the unification scale. The consistency of the computation is insured through proper matching of the boundary conditions at M_S.

Running parameters between the electroweak and the SUSY scale are obtained using the code described in the previous section where boundary conditions are imposed both at M_S to match the SUSY region predictions and at the electroweak scale to match the SM inputs. RGEs are then solved iteratively (using numerical routines from SPheno [66,67]) until we reach a solution satisfying both boundary conditions at the required precision.

The RGEs above the SUSY scale have been obtained using the public code `SARAH` (see ref. [68,69,70,71,61] and ref. [72]).

Our input parameters are the following

- The F-Higgsino μ-term, μ_f
- The true Higgsino μ-term, $\mu \sim M_S$
- The unified F-gaugino Majorana mass m_{fg} and the usual unified gaugino mass $M_{1/2}$. In the FSSM-I, only the F-gaugino mass is at the TeV scale while the gauginos are at the SUSY scale. In the FSSM-II, the gaugino mass is suppressed down to the TeV scale as seen in the previous section.
- The SUSY scale M_S, which also serves as a unified mass scale for all SUSY-breaking scalar mass terms (but those for the Higgs doublet in the NUHM case)
- The unified trilinear coupling A_0.

The small parameter ε is defined from the (F-)gauginos mass

$$\varepsilon = \begin{cases} \sqrt{\frac{m_{fg}}{M_S}} & \text{in the FSSM-I} \\ \sqrt{\frac{M_{1/2}}{M_S}} & \text{in the FSSM-II} \end{cases} \quad (3.31)$$

so that the mass of the light gauginos-like particle is $\mathcal{O}(M_s\varepsilon^2) \simeq \mathcal{O}(1)$ TeV.

Since the low-energy spectrum contains only F-higginos and (F-)gauginos, most of the parameter space in the UV is redundant. As a simplifying assumption, we use μ as a common scale for all unsuppressed superpotential μ-like and B_μ-like terms, μ_f/ε for all superpotential terms ε-suppressed and μ_f for the ε^2-suppressed terms.

One subtlety is that even if the F-higgsinos are to leading order in ε directly derived from their UV counterparts, their masses should formally be obtained by diagonalising the mass matrix for the higgsino-like particles. In order to make sure that our simplifying assumptions do not turn into fine-tuning (which happens when the determinant of the mass matrix becomes zero), we made the following choice in the FSSM-I (the FSSM-II being free from this issue): the F-higgsino μ-term is μ_f and the mixing between fake and usual Higgs doublets are defined as $\frac{\mu_f}{5\varepsilon}$. We take $B_{\mu_f} = \mu_f^2$. This choice does not modify the low-energy physics and allows us to make sure that μ_f really controls the mass of the F-higgsinos in the low-energy theory.

A similar issue arises when diagonalising the gaugino mass matrix, so in the FSSM-I the gauginos' Dirac masses are defined suppressed by a loop factor at $\frac{1}{16\pi^2}m_{fg}$. This choice similarly allows us to make sure that m_{fg} controls the mass of the F-gauginos in the low-energy theory.

The B_μ-term for the Higgs doublets is fixed at the SUSY scale by the requirement of having a light SM-like Higgs

$$B_\mu \simeq \sqrt{(m_{H_u}^2 + \mu_u^2)(m_{H_d}^2 + \mu_d^2)} \tag{3.32}$$

where $\mu_u = \mu_d = \mu$ in the FSSM-I case and we have neglect ϵ-suppressed contributions.

The light eigenstates are predominantly composed of the original Higgs doublets and contain fake doublets only at $\mathcal{O}(\varepsilon)$. Hence, the mixing angle β is given by

$$\tan\beta = \sqrt{\frac{m_{H_d}^2 + \mu_u^2}{m_{H_u}^2 + \mu_d^2}}\,, \tag{3.33}$$

and it is used to parameterise the Higgs observables, mass and Yukawa couplings. The variation of $\tan\beta$ allows to reproduce the cases with $\mu_u \neq \mu_d$ as well as non-universal Higgs masses (NUHM) set-up, where $m_{H_d}^2$ and $m_{H_u}^2$ have different values at M_{GUT}.

Supersymmetry predicts the SM-like tree-level Higgs quartic coupling at M_S via equation:

$$\lambda(M_S) \;=\; \frac{1}{4}\left(g^2 + g'^2\right)\cos^2 2\beta \;+\; \Delta^{(\ell)}\lambda \;+\; \Delta^{(\overline{MS})}\lambda \;+\; \mathcal{O}(\varepsilon^2). \tag{3.34}$$

The corrections $\mathcal{O}(\varepsilon)$ are always negligible in this work, however the loop contributions can play a role. At one loop, we have the leading stop contribution given by

$$\Delta^{(1)}\lambda \supset \frac{3y_t^4}{16\pi^2}\left[\log\frac{m_{Q_3}^2 m_{U_3}^2}{M_S^4} + \mathcal{O}(\tilde{X}_t)\right] \tag{3.35}$$

where y_t is the top Yukawa coupling, $\tilde{X}_t \equiv \frac{|A_t - \overline{\mu}\cot\beta|^2}{m_{Q_3}m_{U_3}}$ and the dependence on this can be found e.g. in [16]. Since the stop contribution is the most important, we make the

standard convenient choice of using it to define $M_S \equiv \sqrt{m_{Q_3} m_{U_3}}$. In the FSSM-II , A_t and μ term are suppressed by the R-symmetry, so we can safely take $\tilde{X}_t \simeq 0$. In the FSSM-I, however, both are in general quite large; we have estimated the shift of the Higgs mass to be at most 4.5 GeV when when $M_S \sim 100$ TeV and at most to 1 GeV when $M_S \sim 10^8$ GeV. In most of our plots, A_t and μ are chosen to be equal to M_S at the GUT scale so the shift is further reduced to circa 2 GeV even for $M_S \sim 100$ TeV.

Other threshold corrections include terms from decoupling the heavy MSSM particles and changes of the renormalisation schemes from $\overline{DR}$ to $\overline{MS}$. For the case of Split SUSY, the expressions are given in [16]. We have found the effects in our models to lead to a sub-GeV contribution to the Higgs mass so they have been neglected; however it would be interesting to be able to compute these contributions for our model to completely assess their effect.

c Results

The Higgs mass as a function of M_S is shown in Figure 3.6 (where all heavy mass parameters have been taken to be equal to the SUSY scale). We first observe that we obtain a slightly higher Higgs mass than in Figure 3.1 as the running from the GUT scale produces somewhat heavier gluinos which in turn increases the Higgs mass as shown in Figure 3.4. In the plot, it is useful to note that the curves exhibit plateaux so that by choosing the right value of $\tan\beta$ between 1 and 5 we can reproduce the desired Higgs mass for any SUSY scale up to the GUT scale.

If we suppose unification of the Higgs masses at the GUT scale (so that $m^2_{H_u} \simeq m^2_{H_d}$ and $\mu_u \simeq \mu_d$), then $\tan\beta$, all parameters in (3.33) are of the same order, and we predict that generically the value of $\tan\beta$ is close to 1. This can be seen in Figure 3.7 where we have plotted $\tan\beta$ in the FSSM-I as a function of the SUSY scale M_S and the A-term at the GUT scale A_0. We see that in most of the parameter space $\tan\beta$ is between 1 and 1.4. The increase in the right part of the plot show that for a larger value of A_0, $m^2_{H_u} + \mu_0^2$ can run close to zero. In principle, by varying m_0 and A_0 in the FSSM-I we can find values of $\tan\beta > 2$, potentially allowing values of the SUSY scale lower than 10^9 GeV without requiring a breaking of the universality of the soft masses at the GUT scale. Figure 3.8 illustrates the effect of the running of the Higgs soft masses: in both the FSSM-I and the FSSM-II the renormalisation group evolution does not greatly separate these masses leading to a $\tan\beta \simeq \mathcal{O}(1)$. Note that the longer the running above M_S, the higher the predicted $\tan\beta$, which in turn raises the Higgs mass at tree level. Hence for small values of M_S it is natural to have larger values of $\tan\beta$, and for larger M_S we expect $\tan\beta \sim 1$, both compatible in this model with the observed Higgs mass.

As we discussed above, unification in both models is ensured at one-loop. At two-loops it is also well preserved, as can be seen from Figure 3.9 where we have plotted the unification scale as a function of the SUSY scale M_S, along with $|g_1 - g_3|/g_3$ at the unification scale of g_1 and g_2. A percent level unification can be obtained for all M_S for FSSM-I and above 10^7 GeV for FSSM-II. The unification scale itself remains of the order of 10^{16} GeV.

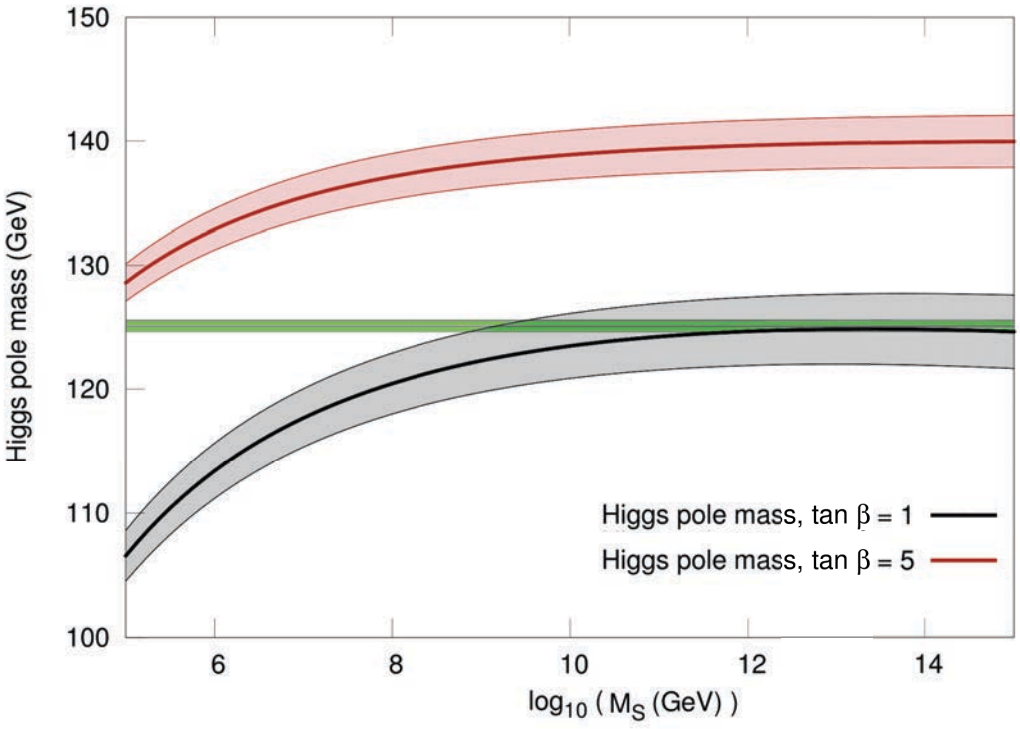

Figure 3.6: Higgs pole mass as a function of the SUSY scale, all parameters at the GUT scale have been set to be equal to the SUSY scale. The low energy spectrum is taken as $m_{\rm fg} = 1$ TeV and $\mu_f = 1$ TeV. We consider a Non Universal Higgs Mass (NUHM) scenario in FSSM-II so that we fix directly $\tan\beta$ at M_S to 1 for the lower curve and 5. for the upper one. The shaded region gives the variation from a 2σ variation in the top pole mass. The green band corresponds to the measured Higgs mass.

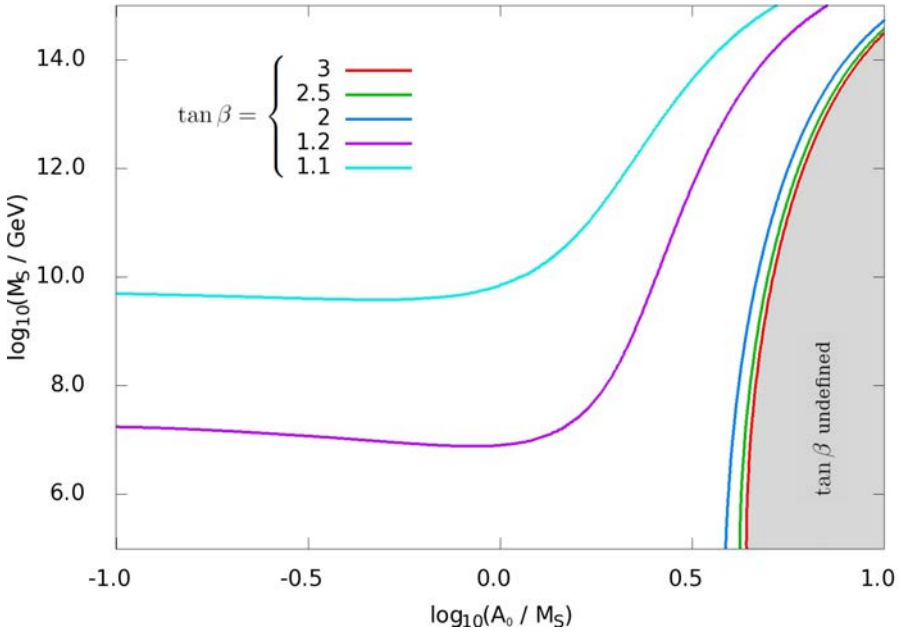

Figure 3.7: Contours of the value of $\tan\beta = \sqrt{\frac{m_{H_d}^2+\mu_0^2}{m_{H_u}^2+\mu_0^2}}$ found to match the observed Higgs mass in the FSSM-I varying the scalar unification mass m_0 and trilinear mass A_0.

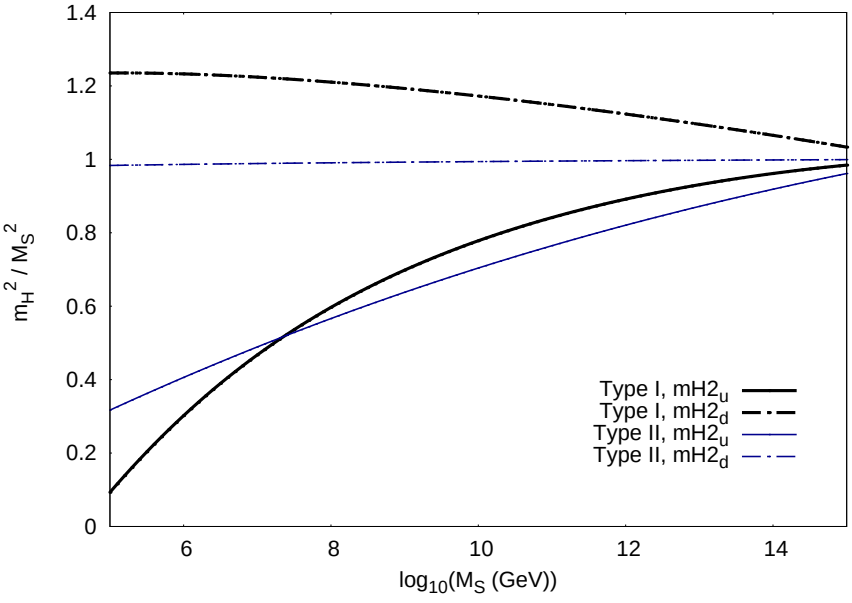

Figure 3.8: Running masses $m_{H_u}^2/M_S^2$ and $m_{H_d}^2/M_S^2$ in the FSSM-I (bold lines) and the FSSM-II (normal line) at the SUSY scale as a function of the M_S. All UV parameters are set to be equal to the SUSY scale.

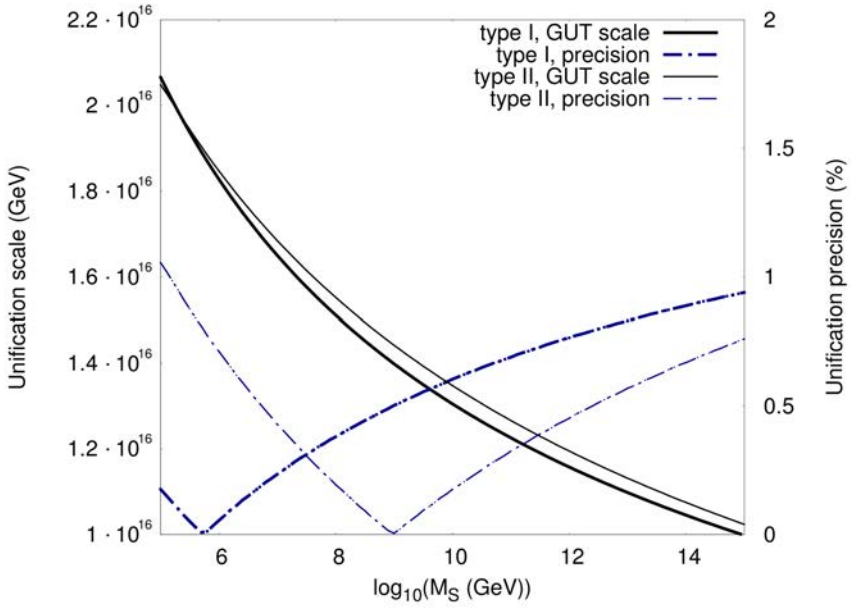

Figure 3.9: Evolution of the unification scale as well as the precision of the unification ($|g_1 - g_3|/g_3$ in percent at the point where g_1 and g_2 unify) as a function of the SUSY scale M_S. All UV parameters are set to be equal to the SUSY scale.

3 Summary and Conclusions

Let us close this chapter by briefly reviewing the main aspects of the Higgs mass prediction in Fake Split SUSY models and comparing them with the usual Split SUSY case.

3.1 Easing the Split SUSY Higgs Mass Constraints with FSSM

We have presented a way to rescue the original idea of Split SUSY: allowing an arbitrary value of M_S and an arbitrarily large splitting in the sparticles masses. This is one aim of FSSM [1] and [2]. There are different realisations of the FSSM scenario (see also [39] for yet another different realisation and for a motivation of fake gluinos):

- FSSM-I: both the higgsinos and gauginos are swapped for fake gauginos (henceforth F-gauginos) and fake higgsinos (henceforth F-higgsinos).

    1. The fermions remain light because of a $U(1)$ flavour symmetry
    2. The F-gauginos are Dirac partners of the gauginos
    3. Higgs-F-higgsino-F-gaugino Yukawa couplings $\tilde{g}_{u,d}, \tilde{g}'_{u,d}$ are suppressed by $(\mathrm{TeV}/M_S)^2$
    4. Two pairs of vector-like electron superfields need to be added at M_S to insure unification.

- FSSM-II: Only the higgsinos are swapped for fake higgsinos.

    1. The fermions remain light because of R-symmetry charges
    2. Higgs-F-higgsino-gaugino Yukawa couplings $\tilde{g}_{u,d}, \tilde{g}'_{u,d}$ are suppressed by (TeV/M_S)
    3. Two pairs of Higgs-like doublets needed for the F-higgsinos
    4. Two pairs of $(\mathbf{3},\mathbf{1})_{1/3} \oplus (\overline{\mathbf{3}},\mathbf{1})_{-1/3}$. In total we have added a vector-like pair of $\mathbf{5}+\overline{\mathbf{5}}$ of $SU(5)$ to insure unification.

The success of FSSM is illustrated in Figure 3.1. Here, we would like to pinpoint the origin of the differences in the predictions for the Higgs mass. While in Split SUSY, the Higgs mass regularly increases with M_S, the increase is way flatter in High Scale SUSY and the curve even exhibits a plateau for the FSSM.

In order to understand the hurdles met when trying to reproduce the correct Higgs mass with an arbitrary high M_S, let us understand the way λ evolves, shown in Figure 3.2. The various contributions to β_λ at one-loop can be roughly classified as[4]:

$$\beta_\lambda = \frac{1}{16\pi^2}\left[\underbrace{12\lambda^2 + \lambda(12y_t^2 + (\cdots \tilde{g}^2 \cdots) - (\cdots g^2 \cdots))}_{\equiv\, \beta_{\text{quartic}}} + \underbrace{(\cdots g^4 \cdots)}_{\equiv\, \beta_g} \underbrace{-(\cdots \tilde{g}^4 \cdots)}_{\equiv\, \beta_{\tilde{g}}} \underbrace{-12y_t^4}_{\equiv\, \beta_t}\right], \tag{3.36}$$

where $(\cdots g^n \cdots)$ and $(\cdots \tilde{g}^n \cdots)$ contains contributions from contains gauge couplings and Higgs-higgsino-gaugino Yukawa couplings, respectively. Fixing λ at M_S and evolving it down to the electroweak scale, positive contributions tend to bring λ towards lower values while negative contributions increases the Higgs mass. Two different effects explain the discrepancies between Split SUSY, High-Scale SUSY and FSSM:

1. Compared to Split SUSY, we see that both FSSM and High scale SUSY have vanishing $(\cdots \tilde{g}^n \cdots)$ terms. This decreases $\beta_\lambda(M_S)$ in the Higgs scale SUSY and FSSM case.

2. High scale SUSY has smaller gauge couplings than FSSM and Split SUSY: these have extra fermions below M_S which contribute in RGEs to push the couplings towards higher values.

These corrections are enhanced by a "domino" effect. At one-loop the top Yukawa coupling y_t beta function β_t has a positive contribution from $(\cdots \tilde{g}^n \cdots)$ terms and a negative one from g_3. Since y_t is fixed at the electroweak scale, a smaller β_{y_t} means a smaller y_t at M_S. The split between different contributions to the β-functions is presented in Figure 2.

To summarise, the success of FSSM rests on simultaneously switching off the higgsinos Yukawa couplings while conserving stronger gauge couplings than High scale SUSY thanks to the presence of extra states at the TeV-scale.

[4]Studying β_λ at one-loop is enough to understand the two main mechanisms discriminating the three cases in Figure 1.

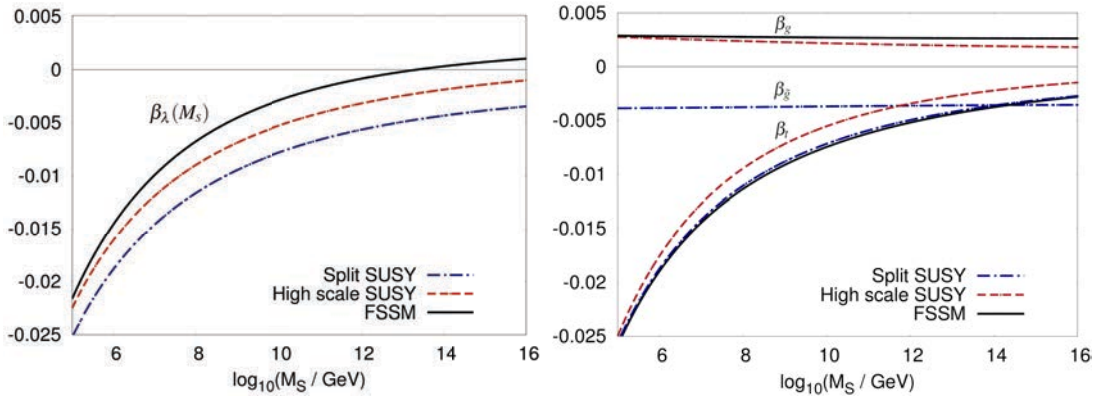

Figure 3.10: Left plot : β_λ at M_S for $\tan\beta = 1$ in the case of Split SUSY, High scale SUSY and FSSM-I as a function of M_S. **Right plot :** Decomposition of β_λ at M_S into its various components β_t, β_g (superposed for FSSM and Split SUSY) and $\beta_{\tilde{g}}$ as a function of M_S.

Finally, it is easy to see that low value of $\tan\beta$ are natural in FSSM, while this is not the case the Split SUSY models. At the SUSY scale, $\tan\beta$ is defined fixed by the requirement that one Higgs has a mass at the electroweak scale. In Split SUSY this fixes

$$\tan\beta \;=\; \sqrt{\frac{m_{H_d}^2 + |\mu|^2}{m_{H_u}^2 + |\mu|^2}} \;\simeq\; \sqrt{\frac{m_{H_d}^2}{m_{H_u}^2}}$$

since higgsinos are light. Renormalisation group evolution of $m_{H_d}^2$ and $m_{H_u}^2$, particularly due to the large top Yukawa coupling, then generates a $\tan\beta \gg \mathcal{O}(1)$. On the contrary, in FSSM, we have

$$\tan\beta \;=\; \sqrt{\frac{m_{H_d}^2 + |\mu_d|^2}{m_{H_u}^2 + |\mu_u|^2}}\,,$$

with $\mu_d = \mu_u$ in the FSSM-I and $\mu_u, \mu_d \simeq M_S$ since they are unrelated to the low energy spectrum. Note that the longer the running above M_S, the higher the predicted $\tan\beta$, which in turn raises the Higgs mass at tree level. Hence for small values of M_S it is natural to have larger values of $\tan\beta$, and for larger M_S we expect $\tan\beta \sim 1$.

3.2 Conclusive Words

In this chapter, we have investigated Fake Split-Supersymmetry Models (FSSM). The main motivation is their extremely robust prediction of the correct Higgs mass in an impressive range of values of the SUSY scale M_S, something that can not be obtained in the original Split SUSY or High scale SUSY models.

We have presented two realisations of such models. The original FSSM-I which in the UV is a Dirac gaugino model with an extra flavour symmetry, and the FSSM-II where only the higgsinos are fake but not gauginos. While the first type is based on the Dirac Gauginos framework, the second type involved a much simpler UV completion

with a small number of additional matter fields and the hierarchy in the spectrum which is ensured by an approximate R-symmetry.

Next, we implemented both models, along with their UV completions in a code to determine the pole Higgs mass and all of the spectrum at low-energy. Once again, we stress that the Higgs mass prediction in these models is very robust. For unified masses at the GUT scale, $\tan\beta \sim 1$, all SUSY scales above 10^9 GeV give a 125 GeV Higgs. If one allows values of $\tan\beta$ between 1 and 5, we have show that a 125 Gev Higgs can be "predicted" without constraints on the SUSY scale. We have finally checked that unification was preserved at a percent level at two-loops.

Overall, it seems very difficult to constrain the SUSY scale in Fake Split SUSY model from the Higgs mass measurement in stark contrast to the usual Split SUSY case.

Chapter 4

Fake Fermions and Cosmology

Since Fake Split SUSY models are incredibly effective in predicting the accurate Higgs mass, one should look for other ways of constraining their parameter space. In this chapter, we will give a closer look on the cosmology of FSSMs, investigating various Dark Matter candidates and showing how the (F-)gluinos life-time can be used to put strong bounds on the SUSY scale.

We shall assume that the universe has a standard cosmology, i.e. any hidden sector heavy particles decay well before dark matter freezes out – since we are considering high SUSY scales this is typically the case. We then populate the dark matter abundance of the universe with the lightest neutral stable fermion in our model, or at least do not overpopulate (as in the case of underabundant dark matter, the remainder could consist of axions or other hidden-sector particles).

We recall here that the field contents below the SUSY scale is simple and consists of: the Standard Model field contents; Fake Higgsinos, with the same quantum numbers $(\mathbf{1},\mathbf{2},1)$ and $(\mathbf{1},\mathbf{2},-1)$ than usual Higgsinos doublets; gauginos-like particle which can be either the true gauginos or new, fake gauginos (henceforth written F-gauginos) with quantum numbers similar to the usual supersymmetric gauginos. We stressed that while we have adopted names reminiscent of a supersymmetric setup, the Yukawas between the (F-)gauginos, (F-)higgsinos and the Standard Model Higgs are not constrained by supersymmetry. Our Lagrangian contains:

$$\mathcal{L}_{\text{eff}} \supset -\frac{H^\dagger}{\sqrt{2}}(\tilde{g}_u\,\sigma^a\,\tilde{W}'^a + \tilde{g}'_u\,\tilde{B}')\;\tilde{H}'_u - \frac{H^T i\sigma^2}{\sqrt{2}}(-\tilde{g}_d\,\sigma^a\,\tilde{W}'^a + \tilde{g}'_d\,\tilde{B}')\;\tilde{H}'_d\;, \qquad (4.1)$$

where $\tilde{W}'$ and $\tilde{B}'$ are the (F-)Winos and (F-)Binos, $\tilde{H}'$ the F-Higgsinos and the couplings $\tilde{g}$ are fixed at the SUSY scale as:

$$\begin{aligned} \tilde{g}'_u &= \tilde{\epsilon} g' \sin\beta & \tilde{g}'_d &= \tilde{\epsilon} g' \cos\beta \\ \tilde{g}_u &= \tilde{\epsilon} g \sin\beta & \tilde{g}_d &= \tilde{\epsilon} g \cos\beta \end{aligned} \qquad (4.2)$$

where β and $\tilde{\epsilon}$ are free parameters of our model.

In the rest of this chapter, except when dealing with baryogenesis and when we explicitely mentioned it, we will consider $\tilde{\epsilon} \sim 0$. More precisely, if the gauginos-like particles are F-gauginos (a situation refered to as type-I), we will have $\tilde{\epsilon} \sim \frac{\text{TeV}}{M_S}$ and

if they are the original gauginos (type-II), $\tilde{\epsilon} \sim \sqrt{\frac{\text{TeV}}{M_S}}$. While the two types were behaving similarly when dealing with the Higgs mass, we will see that assuming a standard cosmology, the life-time of the gluino-like particle will put distinct bounds on them.

We start this chapter by presenting the relic density of various dark matter candidates in Fake Split SUSY models in section 1. Then we consider other cosmology-related bounds on FSSMs in section 2. Finally we deal with the possibility of Electroweak Baryogenesis in the context of FSSMs in section 3

1 Dark Matter Relic Density in FSSM

1.1 The WIMP Idea

Supersymmetry is well-known for providing plenty of Dark Matter candidates in the form of Weakly-Interacting Massive Particles (WIMPs). Such particles can explain the current Dark Matter relic density measurement from Planck $\Omega h^2 = 0.1188 \pm 0.0010$ (see [73]) by a mechanism called freeze-out. We will review briefly this mechanism and highlight the so-called WIMP miracle.

Let us start with a WIMP particle with mass m and an annihilation cross-section to any final state of Standard Model particle noted σ. We use the FLRW[1] metric with the scale factor a and Hubble scale $H = \frac{\dot{a}}{a}$ to describe the expanding universe.

The Boltzman equations on the phase space density f for the WIMP particle can be written in the symbolic form [74]

$$L[f] = C[f] \ , \tag{4.3}$$

where L is the Liouville operator which measures the change in time of the phase space density and C is the collision operator which quantifies the creation of annihilation of particles from interactions.

Since we are only interested in the dependence of the phase density as a function of time, we can integrate this equation in the spatial components of the WIMP momentum. Supposing that the phase space density is spatially homogeneous and isotropic, we define the number density $n(t)$ by

$$n(t) = \sum_s \int \frac{d^3p}{(2\pi)^3} f(E,t) \ , \tag{4.4}$$

where the sum runs over all the spin configurations and basically counts the number of degrees of freedom of our WIMP. After a bit of algebra the Boltzmann equation leads to the standard result

$$\dot{n} + 3Hn = -\langle \sigma v \rangle (n^2 - n_{eq}^2) \tag{4.5}$$

where n_{eq} is the equilibrium number density and $\langle \sigma v \rangle$ is the thermally-averaged cross-section times velocity. Supposing that decay products are in thermal equilibrium and

[1] Friedmann–Lemaître–Robertson–Walker

that all particles obey Maxwell-Boltzmann statistics, we have

$$f_{eq}(E,T) = e^{-\frac{E}{T}} \tag{4.6}$$

$$n_{eq} = g \int \frac{d^3p_1}{(2\pi)^3} e^{-\frac{E_1}{T}} \tag{4.7}$$

and

$$\langle \sigma v \rangle = \frac{g^2}{n_{eq}^2} \int\int \frac{d^3p_1}{(2\pi)^3} \frac{d^3p_2}{(2\pi)^3} (\sigma v) e^{-\frac{E_1+E_2}{T}} \tag{4.8}$$

with

$$v = \frac{\sqrt{(p_1 \cdot p_2)^2 - m^4}}{E_1 E_2} \ , \tag{4.9}$$

and we have replaced the sum over the spin states by the number of degrees of freedom g. Traditionally, one then trade the variable n for $Y = \frac{n}{s}$ where s is the total entropy density of the universe. Indeed, expansion of the universe naturally dilutes the number density as a^3. Supposing expansion to be isentropic, the entropy per comoving element $S \propto sa^3$ is constant leading to $s \propto a^{-3}$. The variable Y is therefore proportional to the number density of WIMP per comoving volume element. Furthermore, during the radiation-dominated era, time and temperature are related by

$$t = 0.301 \frac{m_{pl}}{T^2} g_*^{-1/2} \tag{4.10}$$

with m_{pl} is the Planck mass and g_* the effective number of relativistic degrees of freedom in the thermal bath defined as

$$g_*(T) = \sum_b g_b + \frac{7}{8} \sum_f g_f \tag{4.11}$$

with the first (second) sum running over all bosonic (fermionic) relativistic degrees of freedom. For example $g_* = 106.75$ in the complete Standard Model. One can therefore further replace t by $x \equiv \frac{m}{T}$ so that eq. (4.5) now reads

$$\frac{\partial Y}{\partial x} = -\frac{\langle \sigma v \rangle}{xH} (Y^2 - Y_{eq}^2) \tag{4.12}$$

This equations tells us that when the annihilation rate $\langle \sigma v \rangle$ fall below the Hubble rate during inflation, the number density for comoving volume element essentially "freeze-out".

The analytic approximate solution for the temperature at "freeze-out" is given by

$$x_f \simeq \frac{T_f}{m} = \left[\ln(0.038 \frac{g}{\sqrt{g_*}} M_P \langle \sigma v \rangle) \right]^{-1} \sim 20 \tag{4.13}$$

where the approximate value of x_f use the usual cross-section for a WIMP. After the freeze-out, if there is a residual annihilation of relic particle, one needs to use

$$J(x_f) = \int_{x_f}^{\infty} \frac{\langle \sigma v \rangle}{x^2} dx \ , \tag{4.14}$$

to finally obtain the present day number density

$$Y_\infty \simeq 3.8\frac{\sqrt{g_*}}{g}\frac{1}{m_{pl}J(x_f)m} \ . \tag{4.15}$$

We can now report the result in the relic abundance to find:

$$\Omega h^2 = \frac{\rho h^2}{\rho_c} = 3.8\frac{\sqrt{g_*}}{g}\frac{s_0 h^2}{\rho_c}\frac{1}{m_{pl}J(x_f)} \ . \tag{4.16}$$

Using the numerical values for the entropy density $s_0 = 2890\ \mathrm{cm}^2$ and the critical mass density $\rho_c = 1.05 \times 10^{-5} h^2\ \mathrm{GeV\ cm}^{-3}$ and supposing that there is no effective annihilation after freeze-out, we can directly integrate J and find

$$\Omega h^2 \simeq \frac{10^{-37}\ \mathrm{cm}^2}{\langle\sigma v\rangle} \ . \tag{4.17}$$

Now consider a simple scenario in which the WIMP candidate can only decay through a coupling y to a heavy mediator of mass m_Φ, the s-wave annihilation cross-section is given by

$$\begin{aligned}\langle\sigma v\rangle &\sim \frac{y^4}{\pi}\frac{m^2}{m_\Phi^4} \\ &\sim 10^{-36}\mathrm{cm}^2 y^4 \left(\frac{m}{400\mathrm{GeV}}\right)^2 \left(\frac{2\mathrm{TeV}}{m_\Phi}\right)^4 \ ,\end{aligned} \tag{4.18}$$

so that SUSY neutralino are exactly in the right ballparks to reproduce the observed relic density of Dark Matter. This is such an impressive coincidence that it has earned the name of *WIMP miracle*.

We close this review by discussing a famous exception to the previous result which will be used in the next section: the co-annihilation setup. We consider two Dark Matter candidates χ_1 and χ_2 with a small positive mass difference $\delta m = m_2 - m_1 \ll (m_2 + m_1)/2$ (usually below 10%). We now have also the following available processes

$$\begin{aligned}\chi_j &\leftrightarrow \chi_i X X' \\ \chi_i X &\leftrightarrow \chi_i X' \\ \chi_j \chi_i &\leftrightarrow \ X' X\end{aligned} \tag{4.19}$$

where X, X' is any Standard Model particles, supposed to be relativistic at freeze-out. We note the cross-section for the first processes σ_{ij}. Ultimately, all χ_2 will decay in the lightest particle χ_1. It was shown in [75] that in this case, one must replace in previous calculation the annihilation cross-section σ by

$$\sigma_{eff} = \sum_{ij} \sigma_{ij} r^i r^j \ , \tag{4.20}$$

where r^i is the proportion of χ_i in the Dark Matter density at equilibrium, namely

$$r^i \equiv \ \frac{n_{eq}^i}{\sum_k n_{eq}^k} = \frac{g_i(1+\Delta_i)^{3/2}\exp(-x\Delta_i)}{\sum_k g_k(1+\Delta_k)^{3/2}\exp(-x\Delta_k)} \tag{4.21}$$

with $\Delta_i = (m_i - m_1)/m_1$. This effective cross-section can be vastly different from the original one. For instance, suppose we have $\sigma_{22} \propto a\sigma_{22} \propto a^2\sigma_{11}$, for $a > 1$ this leads for almost degenerate particle to as sizeable enhancement of the cross-section

$$\sigma_{eff} = \sigma_{11}\frac{a^2}{(1+g_1/g_2)^2} \tag{4.22}$$

and reciprocally to a decrease of the cross-section for $a < 1$. This co-annihilation region is particularly important for (F-)Bino dark matter as we will see below.

1.2 Application to FSSM

Being derived from a supersymmetric theories, Fake Split SUSY models have natural WIMP candidate in the form of the lightest SUSY particle, called Lightest SuperPartner (LSP). We present in this section the possible candidates and determine their relic density.

a Dark Matter Candidates

At low energies, the non-SM fields in the FSSM are organised into a set of neutral fermions – neutralinos – and charged ones – charginos. In the basis $(\tilde{B}', \tilde{W}'^0, \tilde{H}_d'^0, \tilde{H}_u'^0)$ the neutralino mass matrix is

$$\mathcal{M}_{\chi^0} = \begin{pmatrix} m_{\tilde{B}'} & 0 & -\frac{\tilde{g}_d' v}{\sqrt{2}} & \frac{\tilde{g}_u' v}{\sqrt{2}} \\ 0 & m_{\tilde{W}'} & \frac{\tilde{g}_d v}{\sqrt{2}} & -\frac{\tilde{g}_u v}{\sqrt{2}} \\ -\frac{\tilde{g}_d' v}{\sqrt{2}} & \frac{\tilde{g}_d v}{\sqrt{2}} & 0 & -\mu \\ \frac{\tilde{g}_u' v}{\sqrt{2}} & -\frac{\tilde{g}_u v}{\sqrt{2}} & -\mu & 0 \end{pmatrix}. \tag{4.23}$$

We can express the chargino mass matrix involving the F-higgsinos $\tilde{H}'^+$, $\tilde{H}'^-$ and the charged (F-)gauginos $\tilde{W}'^{\pm}$ in the form

$$-(v^-)^T \mathcal{M}_{\chi^\pm} v^+ \; + \; \text{h.c.}\,, \tag{4.24}$$

where we have adopted the basis $v^+ = (\tilde{W}'^+, \tilde{H}_u'^+)$, $v^- = (\tilde{W}'^-, \tilde{H}_d'^-)$. This reads

$$\mathcal{M}_{\chi^\pm} \; = \; \begin{pmatrix} m_{\tilde{W}'} & \tilde{g}_{2u} v \\ \tilde{g}_{2u} v & \mu \end{pmatrix}. \tag{4.25}$$

Here the crucial difference to Split SUSY is the suppression of the F-higgsino Yukawa couplings $\tilde{g}_{u,d}$ and $\tilde{g}'_{u,d}$ (by ε for the FSSM-II and ε^2 for the FSSM-I), which results in rather different dark matter phenomenology. Our WIMP candidate will be the lightest eigenstate of the neutralino mass matrix (4.23). We will consider three standard possible scenarios for a viable Dark Matter candidates:

- Scenario $\tilde{H}|_{\text{DM}}$: F-higgsino LSP.

- Scenario $\tilde{W}|_{\rm DM}$: (F-)Wino LSP.
- Scenario $\tilde{B}/\tilde{H}|_{\rm DM}$: a mixed F-Bino/F-higgsino LSP, with a small splitting.

Notice that a priori, one can also have a mixed Bino/Wino dark matter which gives the correct relic density. But since we expect generically that the gaugino mass hierarchy is fixed by the chosen mechanism of supersymmetry breaking, one does not have the freedom to tune the (F-)Bino / (F-)Wino mass ratio as can the (F-)Bino and the F-higgsinos masses in the scenario $\tilde{B}/\tilde{H}|_{\rm DM}$. We shall not discuss here such a scenario.

In the setup of $\tilde{W}|_{\rm DM}$, since the RG running would naturally induced a Bino LSP, one has to consider non-universal gaugino masses (NUGM) mass hierarchy at the GUT scale. For practical purposes, we will consider unification at M_{GUT} between the Wino and gluino masses but suppose that the SUSY breaking mechanism induces a larger Bino mass. The latter becomes an extra parameter which has no impact on the Higgs mass and on the Dark Matter constraint, as long as it is heavy enough not to be the LSP. In the following, when dealing with scenario $\tilde{W}|_{\rm DM}$, we take Majorana mass for the (F-)Bino $M_1 = 10$ TeV at the GUT scale, which translates into a Bino of roughly 5 TeV at the electroweak scale.

Finally the scenario $\tilde{B}/\tilde{H}|_{\rm DM}$ relies on co-annihilation between the higgsinos and Binos to avoid overproduction of the latter. This implies that the Bino mass must be chosen precisely to reproduce the correct relic density. Evaluating fine-tuning from the simplest definition:

$$\Delta = \frac{\partial \Omega h^2}{\partial m_{\tilde{B}}} \frac{m_{\tilde{B}}}{\Omega h^2} \ , \tag{4.26}$$

we found $\Delta \sim 20 - 40$ in the scenario $\tilde{B}/\tilde{H}|_{\rm DM}$ (depending on M_S and on wether or not one consider FSSM-I or FSSM-II), while we have $\Delta \sim 1$ in the scenarios $\tilde{H}|_{\rm DM}$ and $\Delta \sim 2$ in $\tilde{W}|_{\rm DM}$, indicating that this scenarios is ten to forty times more fine-tuned than the two others. It however offers other virtues, such as avoiding the constraints from direct detection which apply for $\tilde{H}|_{\rm DM}$.

b Relic Density Results

In Split SUSY models, the LSP abundances are governed mainly by gauge interactions that are the same for true and fake gauginos/higgsinos. The suppressed Yukawa couplings are expected to play a minor role. In that case, one can use the standard expressions [76] to obtain a rough estimate

$$\Omega_{\tilde{W}} h^2 = 0.13 \left(\frac{M_2}{2.5 \text{ TeV}} \right)^2 \ , \tag{4.27}$$

for Wino-like DM and

$$\Omega_{\tilde{H}} h^2 = 0.10 \left(\frac{\mu}{1 \text{ TeV}} \right)^2 \ , \tag{4.28}$$

for higgsino-like dark matter.

In order to compute the relic density with a better precision, we have used routines from the public code `micrOMEGAs` [77] to compute the relic density in the three scenarios

described above. We used `SARAH` [70] to generate the CalcHep file which was taken as an input by `micrOMEGAs`. We take for the relic density the Planck 2015 value [73] $\Omega h^2 = 0.1188 \pm 0.0010$; clearly the *theoretical* uncertainty stemming from higher-order corrections is many times larger than this – the contours could potentially move by potentially as much as 50%. However, we do not show this uncertainty in the plots because it is difficult to estimate, and because the important point is the relationship between the parameters.

In scenarios $\tilde{H}|_{\rm DM}$ and $\tilde{W}|_{\rm DM}$, our results are fully consistent with the previous approximate formulas. In order to recover the correct relic density at 3σ, we need to have an F-higgsino pole mass between 1110 GeV and 1140 GeV or a (F-)Wino pole mass between 2390 GeV and 2450 GeV.

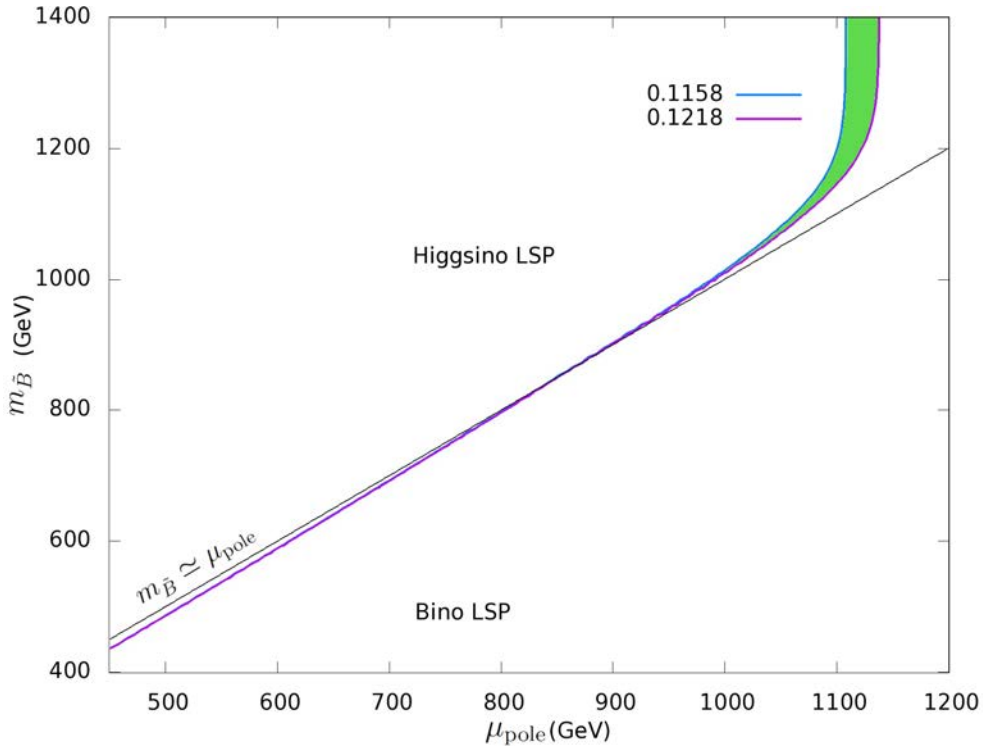

Figure 4.1: Visualisation of the constraints coming from gluino life-time, from the requirement of a 125 GeV Higgs pole mass, and from obtaining the correct relic density. We furthermore represent the separation (Black diagonal line) between a Bino LSP and a Higgsino LSP We use a $\mu_{\rm pole}$ - $m_{\tilde{B}}$ plane, where $m_{\tilde{B}}$ is the Bino pole mass and $\mu_{\rm pole}$ is the Fake Higgsinos pole mass. The SUSY scale M_S has been chosen at 10^{10} GeV. Calculations has been done in the FSSM-II.

Since the (F-)Bino cannot annihilate except through mixing, in the $\tilde{B}/\tilde{H}|_{\rm DM}$ scenario we therefore require co-annihilation to obtain the correct relic density. However, differently to other SUSY scenarios, when we have co-annihilation so that $|\mu_{\rm pole} - m_{\tilde{B}}| \lesssim T_f$, the mixing is in general still very small. Indeed in the FSSM it is controlled

by

$$\frac{\tilde{g}'_{u,d} v}{|\mu| - |M_1|} \ . \tag{4.29}$$

For example, if we take $M_S = 10^9$ GeV then $\varepsilon \sim 10^{-3}$ so for $(|\mu| - m_{\tilde{B}}) \sim v$ we have mixing in the FSSM-II of $\sim 10^{-3}$ and in the FSSM-I of $\sim 10^{-6}$. Since as usual $T_f \sim m/20 \sim \mathcal{O}(10)$ GeV for m the LSP mass, the enhancement of the mixing is only $\mathcal{O}(10)$ – which for small values of ε still leads to negligible mixing of the Bino/F-higgsino. Only when M_S is rather low and in the FSSM-II, or in the case of very small mass differences, smaller than that required to allow co-annihilation, will we find appreciable mixing. Overall, we conclude that in the scenario $\tilde{B}/\tilde{H}|_{\rm DM}$, the LSP is in fact almost a pure (F-)Bino dark matter.

We now show that (F-)Bino is nonetheless interacting enough to be kinetically thermalised in most of the interesting parameter space of the FSSM. Pure higgsinos have an annihilation cross-section given by

$$\langle \sigma_{\tilde{H}\tilde{H}} v \rangle \simeq \frac{g^4}{512\pi\mu^2}(21 + 3\tan^2\theta_W + 11\tan^4\theta_W) \tag{4.30}$$

and their interactions freeze out at the typical temperature of $T_f \sim \mu/x_f$ where $x_f \equiv m/T_f \simeq 25$. So if the Bino has a similar mass but weakly mixes, let us approximate the ratio $\Gamma/H \equiv n\langle\sigma v\rangle/H$ for processes involving it near the freezeout temperature and put $m \sim M_W$:

$$\begin{aligned} \frac{\Gamma(\tilde{B} + \tilde{H} \to \text{SM fermions})}{H} &\sim \frac{\tilde{g}'^2_{u,d}}{M_W^2} \frac{(mT)^{3/2} e^{-m/T}}{1.66\sqrt{g_*}T^2/M_P} \sim 10^4 \times \tilde{g}'^2_{u,d} \\ \frac{\Gamma(\tilde{B} + \text{SM} \to \tilde{H} + \text{SM})}{H} &\sim \frac{\tilde{g}'^2_{u,d}}{M_W^2} \frac{T^3}{T^2/M_P} \sim 10^{16} \times \tilde{g}'^2_{u,d} \end{aligned} \tag{4.31}$$

so the first process is always frozen out well before the higgsino interactions, but the second will remain important for $M_S \lesssim 10^{11}$ GeV in the FSSM-I and for *any* value of M_S up to the Planck scale in the FSSM-II. This means that the Bino remains thermalised even if its annihilations are ineffective. Notice that $M_S \gtrsim 10^{11}$ is at any rate generically ruled out in the FSSM-I by constraints on the F-gluino life-time, as we will see below.

We can therefore calculate the relic density rather straightforwardly following the procedure described at the end of section 1.1:

$$\Omega h^2 \simeq \frac{8.7 \times 10^{-11} \text{GeV}^{-2}}{\sqrt{g_*} \int_{x_f}^{\infty} dx x^{-2} \langle \sigma_{eff} v \rangle}. \tag{4.32}$$

The integral over temperatures *after* the freezeout (in the denominator) can be important as there can be a significant reduction of the dark matter density.

Let us define $\Omega_c h^2 (= 0.1188)$ as the observed dark matter density fraction, and μ_c the value of μ that matches this for a pure higgsino. Then for our case we can approximate

$$\langle \sigma_{eff} v \rangle = r_{\tilde{H}}^2 \langle \sigma_{\tilde{H}\tilde{H}} v \rangle \simeq r_{\tilde{H}}^2 \times 8.7 \times 10^{-11} x_f/\sqrt{g_*} \times \left(\frac{\mu_c}{\mu}\right)^2 \times \frac{1}{\Omega_c h^2} \tag{4.33}$$

so that

$$\frac{\Omega h^2}{\Omega_c h^2} \simeq \left(\frac{\mu}{\mu_c}\right)^2 \frac{1}{x_f \int_{x_f}^{\infty} dx \; r_{\tilde{H}}^2/x^2}. \tag{4.34}$$

Therefore if we plot the contour matching the relic density in the Bino-higgsino mass plane, as we have done in Figure 4.1, we are plotting the contour of the right hand side of the above equal to one. We find in the FSSM, since we shall typically require $\Delta_i \ll 1$, that we can well approximate

$$r_{\tilde{H}} \simeq \left(1 + \frac{1}{4}\exp\left[-x\left(\frac{m_{\tilde{B}} - m_{\tilde{H}}}{m_{\tilde{H}}}\right)\right]\right)^{-1}. \tag{4.35}$$

The immediate observation is that when $m_{\tilde{B}} = m_{\tilde{H}}$ we have $r_{\tilde{H}} = 4/5$ and so we require $\mu = \frac{4}{5}\mu_c$; on figure 4.1 we see that the curves cross at 900 GeV which is exactly four fifths of 1125 GeV, the critical value for a pure higgsino. This crossing point can be of importance, since F-higgsino dark matter is a perfect example of inelastic dark matter and therefore direct detection experiments can be sensitive to it. Numerically evaluating equation (4.34) then gives a curve in excellent agreement with the results of `micrOMEGAs`. For a Bino LSP we find a linear approximation to fit rather well in the range of values considered $m_{\tilde{B}} \simeq \mu_{\text{pole}} - (4\mu_c/5 - \mu_{\text{pole}})/x_f$, i.e. the mass difference required is of order T_f.

c Enhanced F-Bino Annihilation

When relaxing the constraints that $\tilde{\epsilon} \sim 0$, we have observed that the conclusion that Fake Split SUSY models have several good dark matter candidates is not modified. In fact an interesting side-effect of the case $\tilde{\epsilon} > 1$ is the (F-)Bino can further become a good WIMP without relying on co-annihilation.

Indeed for large $\tilde{\epsilon}$, the couplings between the F-gauginos, the F-higgsino and the Higgs is sufficiently enhanced so that a F-Bino Dark Matter can now annihilate through F-higgsinos exchange. Thus we have a more effective Bino annihilation into two SM-like Higgses H or one Z and one H, which for high enough $\tilde{\epsilon}$ allows the F-Bino to be a valuable Dark Matter candidate. This behaviour is illustrated in Figure 4.2 and Figure 4.3. In particular, the bottom-right corner of these Figures represent an almost pure F-Bino dark matter, which becomes viable for $\tilde{\epsilon} \gtrsim 1.5$.

2 Other Cosmological Constraints on FSSM

Returning to the case $\tilde{\epsilon} \sim 0$, we will consider in this section the constraints on FSSM from direct detection experiments and from the fact that (F-)gluinos tend to have a long life-time.

2.1 Direct Detection and Inelastic Scattering

We have computed the conventional direct detection constraints for our model and found that, when the dark matter can be treated as a Majorana particle, due to

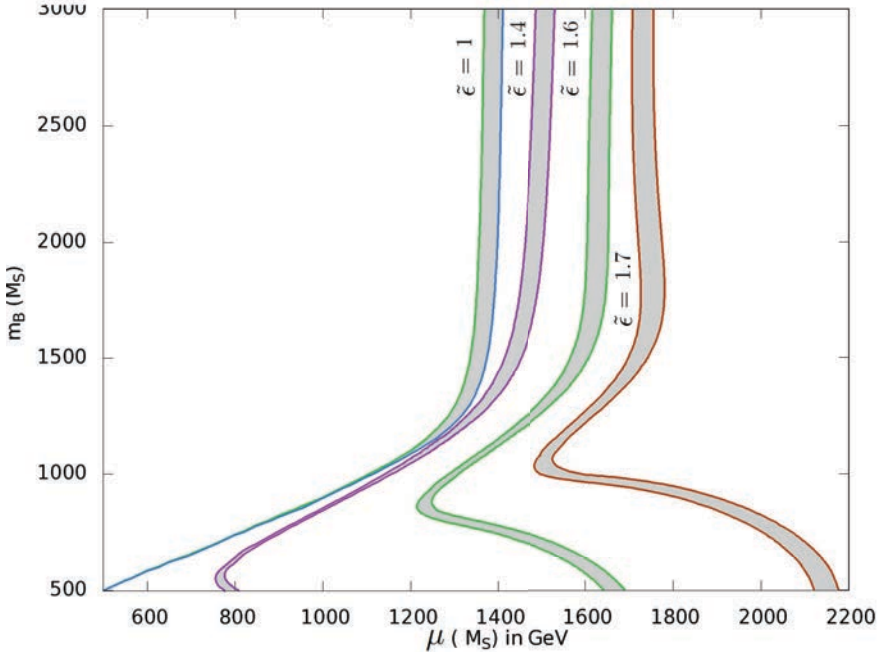

Figure 4.2: Relic density for mixed Bino/F-Higgsinos Dark Matter as a function of mass parameter μ for the F-Higgsinos and m_B for the Binos. From left to right, the curves gives the region where we obtained the correct relic density for $\tilde{\epsilon} = 1, 1.4, 1.6$ and 1.7.

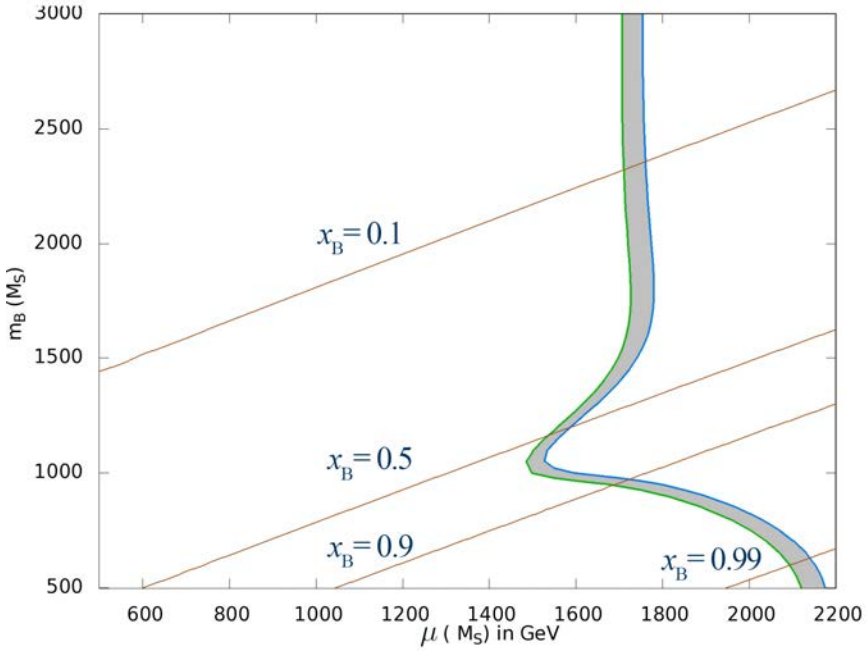

Figure 4.3: Right plot: Relic density for $\tilde{\epsilon} = 1.7$, the straight lines gives the fraction of Bino in the ligtest neutralino, from top to bottom : $0.1, 0.5, 0.9, 0.99$.

the highly suppressed Higgs/(F-)gaugino/F-higgsino interactions, they barely restrict the parameter space. However, since those same interactions determine the splitting between the F-higgsino mass eigenstates, when it is small enough the fake higgsinos can be treated as a Dirac fermion. In that case one can have vector-vector couplings with nucleons through the exchange of a Z boson, leading to inelastic scattering. The spin-independent cross-section implied by this process is so large that direct detection experiments have already ruled these out by many orders of magnitude. This effect has been studied in [78] where they find that the XENON100 [79] and LUX [80] experiments constrained the splitting to be larger than 210 keV for a 1 TeV higgsino LSP. We will consider below a conservative bound of 300 keV for the splitting.

Given the mass matrices for neutralino (3.9) the splitting δ between the two higgsinos can be estimated as :

$$\delta \simeq -\frac{v^2}{4}\left[\frac{(\tilde{g}'_d+\tilde{g}'_u)^2}{M_1-\mu}+\frac{(\tilde{g}_d+\tilde{g}_u)^2}{M_2-\mu}+\frac{(\tilde{g}'_d-\tilde{g}'_u)^2}{M_1+\mu}+\frac{(\tilde{g}_d-\tilde{g}_u)^2}{M_2+\mu}\right] . \tag{4.36}$$

This analytic formula agrees with the numerical mass difference between the two higgsinos pole masses at a few percent level accuracy when estimated using $\overline{\text{MS}}$ running parameter at the electroweak scale. This gives

$$\delta \simeq \begin{cases} 200 \text{ keV}\cdot\mathcal{O}(1)\cdot\left(\dfrac{400 \text{ TeV}}{M_S}\right)^2\left(\dfrac{m_{fg}}{4 \text{ TeV}}\right) & \text{for the FSSM-I} \\ 200 \text{ keV}\cdot\mathcal{O}(1)\cdot\left(\dfrac{10^7 \text{ GeV}}{M_S}\right)\left(\dfrac{\mu}{1 \text{ TeV}}\right)\left(\dfrac{4 \text{ TeV}}{m_{fg}}\right) & \text{for the FSSM-II ,} \end{cases} \tag{4.37}$$

where m_{fg} gives the typical scale of the F-gaugino masses. The extra $\mathcal{O}(1)$ terms come from the uncertainty on the precise suppression of the $\tilde{g}_u, \tilde{g}_d, \tilde{g}'_u$ and $\tilde{g}'_d$ couplings. We see that for F-gauginos of several TeV and for a μ term around 1 TeV (as required from relic density constraints), the SUSY scale M_S is bounded below roughly $5\cdot 10^8$ GeV for the FSSM-II and $5\cdot 10^6$ GeV for the FSSM-I if the $\mathcal{O}(1)$ is taken to be 10. The constraints are far more stringent than in Split SUSY because of the extra-suppression in ε^2 for the FSSM-I and in ε for the FSSM-II.

2.2 The (F-)gluino Lifetime

The gluino lifetime is crucial for determining the cosmology of the Split SUSY model [7,81]. In the standard Split-SUSY case, if the gluino has a lifetime above 100 seconds then it would be excluded when assuming a standard cosmology [81] due to constraints from Big Bang Nucleosynthesis (BBN).

In the FSSM-I, fake gluinos are even more long-lived than gluinos in usual Split Supersymmetry ([82], [39]). Indeed, the decay of F-gluinos to the lightest F-neutralino must proceed via mixing with the usual gluinos in order to have couplings to sfermions. And since the mixing is suppressed by factors of ϵ, the overall F-gluino lifetime in the FSSM-I is therefore enhanced by a factor of $\epsilon^{-4} \simeq \frac{M_S^2}{m_{fg}^2}$.

$$\tau_{\tilde{g}'} \sim 4 \text{ sec} \times \left(\frac{M_S}{10^7 \text{GeV}}\right)^6 \times \left(\frac{1 \text{ TeV}}{m_{fg}}\right)^7 . \tag{4.38}$$

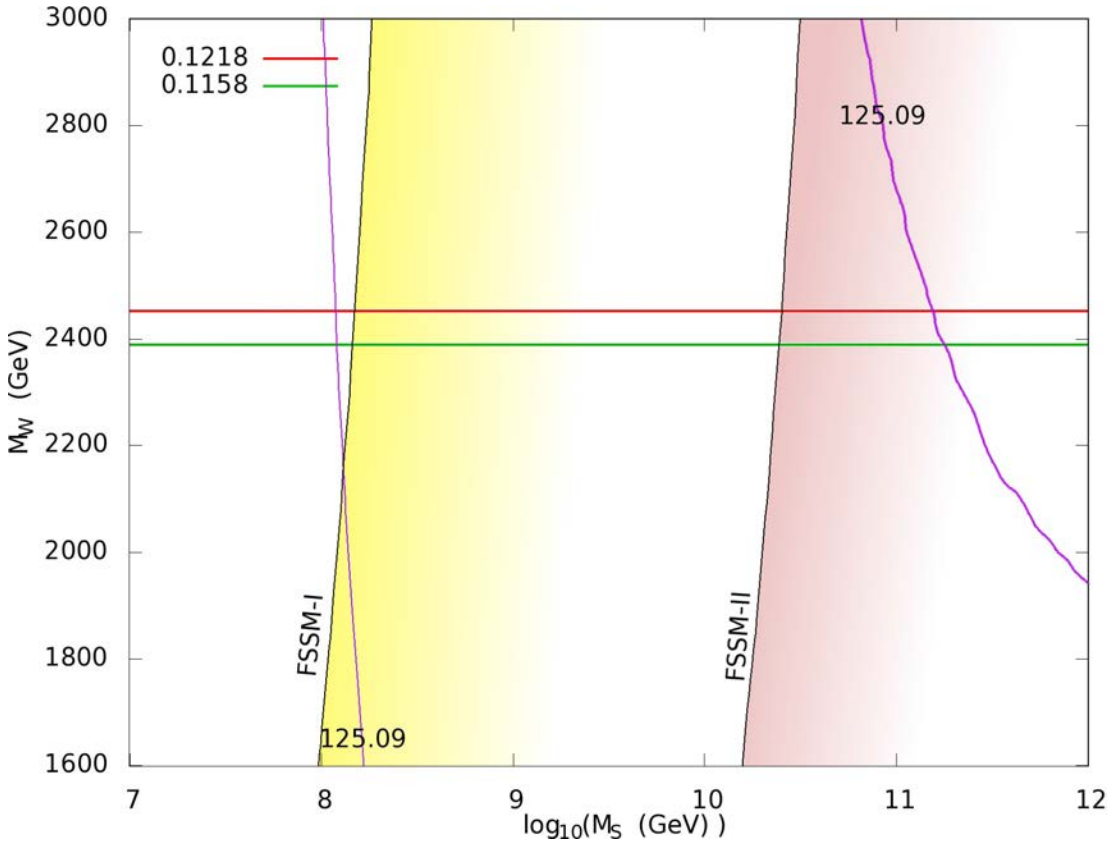

Figure 4.4: Visualisation of the constraints coming from gluino lifetime, from the requirement of a 125 GeV Higgs pole mass, and from obtaining the correct relic density in scneario $\tilde{W}|_{\rm DM}$. We use a M_S - $M_{\rm W}$ plane, where M_W is the Wino pole mass. The yellow color gradient indicate the area excluded with gluino life-time bigger than 100 s in FSSM-I. The red color gradient is the area for the FSSM-II. The bold purple line gives 125-GeV Higgs for $M_t = 173.34$, the slimmer one is the 125-Gev Higgs for a 2σ variation in M_t

Since the gauginos are not fake in the FSSM-II, this enhancement does not occur and one is left instead with the Split SUSY gluino life-time

$$\tau_{\tilde{g}'} \sim 4 \text{ sec} \times \left(\frac{M_S}{10^9 \text{GeV}}\right)^4 \times \left(\frac{1 \text{ TeV}}{m_{fg}}\right)^5 . \tag{4.39}$$

Constraints from Big Bang Nucleosynthesis (BBN) limit this lifetime to be below 100s if one relies on a standard cosmology [81]. A much longer lifetime gluino is constrained from the CMB spectrum, the gamma-ray background or even heavy-isotope searches when the gluino is stable at the scale of the age of the universe.

More precisely, for F-gluinos stable on the lifetime of the universe, remnant F-gluinos could form bound states with nuclei, which would be detectable as exotic forms of hydrogen. The relic density is very roughly approximated by

$$\Omega_{\tilde{g}} h^2 \sim \left(\frac{m_{\tilde{g}'}}{10 \text{ TeV}}\right)^2 , \tag{4.40}$$

although this assumes that the annihiliations freeze out before the QCD phase transition and are thus not enhanced by non-perturbative effects; for heavy F-gluinos this seems reasonable, but in principle the relic density could be reduced by up to three orders of magnitude. However, the constraints from heavy-isotope searches are so severe as to render this moot: the ratio of heavy isotopes to normal hydrogen X/H should be less than 10^{-29} for masses up to 1.2 TeV [83] or less than 10^{-20} for masses up to 10 TeV [84], whereas we find

$$\frac{X}{H} \sim 10^{-4} \left(\frac{m_{\tilde{g}'}}{\text{TeV}}\right) . \tag{4.41}$$

If we want to avoid these bounds, then we must either:

1. Dilute the relic abundance of F-gluinos with a late period of reheating.
2. Imagine that the reheating temperature after inflation is low enough, or that there are several periods of reheating that dilute away unwanted relics before the final one.

In both cases, we must ensure that gluinos are not produced during the reheating process itself, which may prove difficult to arrange: even if the late-decaying particle decays only to SM fields, if it is sufficiently massive then high-energy gluons may be among the first decay products, which could subsequently produce F-gluinos which would not be able to annihilate or decay away.

Overall, assuming a standard cosmology, the effect of the previous formulas with our values for the pole masses can be visualised in Figure 4.4 where we chose a Wino dark matter. We see that since the Wino pole masses must be quite heavy in order to get the correct relic density, the gluino pole mass ends up in the several TeV regime, reducing slightly the gluino lifetime. In $\tilde{W}|_{\text{DM}}$ scenarios, the (F-)gluino lifetime gives an upper bound on the possible M_S of 10^8 GeV for the FSSM-I and of 10^{10} GeV for the FSSM-II. One should not forget that the (F-)gluino pole mass is here obtained by supposing unification of the (F-)Wino and (F-)gluino masses at the GUT scale. These bounds should therefore be modified according to the previous formulas if one considers a particular SUSY breaking setup with a given ratio between (F-)gaugino masses.

2.3 Summary of the Cosmological Constraints

The direct detection for inelastic Dark Matter, the relic density, and the constraint on gluino life-time, have set bounds on four parameters of our model: the F-higgsino pole masses $\mu_{\rm pole}$, the (F-)Bino pole mass $m_{\tilde{B}}$, the (F-)Wino pole masses $m_{\tilde{W}}$ and the SUSY scale M_S.

If we take $\tan\beta = 1$, the Higgs mass gives a lower bound on the SUSY scale $M_S \gtrsim 5 \cdot 10^8$ GeV, which in the FSSM-I is in tension with the gluino lifetime. We see from Table 4.1 that the $\tilde{H}|_{\rm DM}$ scenario is also almost ruled out by direct detection constraints depending on the precise suppression of $\tilde{g}_u, \tilde{g}_d, \tilde{g}'_u$ and $\tilde{g}'_d$.

If one sticks with a standard cosmology the (F)-gluino lifetime is severely constrained, $\tau_{\tilde{g}} < 100$s [81]. Big-Bang Nucleosynthesis (BBN), the CMB spectrum and the gamma-ray background ruled out relic (F)-gluinos with lifetime between 10^2 s until 10^{17} s. When the (F)-gluino is stable at the scale of the age of the universe, heavy-isotope searches also rule out such relic (F)-gluinos. This translates into limiting the SUSY scale to be below $5 \cdot 10^8$ GeV for the FSSM-I and $5 \cdot 10^{10}$ GeV for the FSSM-II. As it has been already underlined, these constraints depends on wether or not one considers a "standard" cosmology. A late time reheating occuring before BBN could for instance dilute gluino relic. In such case, heavy-isotope searches are so stringent that they still constraint $\tau_{\tilde{g}} \lesssim 10^{16}$s but one can avoid constraints from the CMB spectrum and the gamma-ray background, allowing therefore SUSY scales up to 10^{10} GeV for the FSSM-I and 10^{14} GeV for the FSSM-II.

It is however easy to find viable dark matter candidates in FSSM. We have distinguished three scenarios :

- Scenario $\tilde{H}|_{\rm DM}$: F-higgsino LSP.
- Scenario $\tilde{W}|_{\rm DM}$: (F-)Wino LSP.
- Scenario $\tilde{B}/\tilde{H}|_{\rm DM}$: a mixed F-Bino/F-higgsino LSP, with a small splitting.

The constraints on F-higgsinos dark matter (scenario $\tilde{\mathbf{H}}|_{\rm DM}$) are in particular quite stringent. Indeed, since their couplings to the Higgs and (F)-gauginos are suppressed, the neutral higgsinos have a very small splitting. They are therefore a perfect example of inelastic dark matter and direct detection experiments constrain their mass splitting δ to be bigger than roughly 300 keV [78,79,80] (see also [85]). Estimating the splitting by

$$\delta \simeq \begin{cases} 200 \text{ keV} \cdot \mathcal{O}(1) \cdot \left(\dfrac{400 \text{ TeV}}{M_S}\right)^2 \left(\dfrac{m_{fg}}{4 \text{ TeV}}\right) & \text{for the FSSM-I} \\ 200 \text{ keV} \cdot \mathcal{O}(1) \cdot \left(\dfrac{10^7 \text{ GeV}}{M_S}\right) \left(\dfrac{\mu}{1 \text{ TeV}}\right) \left(\dfrac{4 \text{ TeV}}{m_{fg}}\right) & \text{for the FSSM-II ,} \end{cases} \tag{4.42}$$

we obtain the bounds $M_S \lesssim 5 \cdot 10^6$GeV for the FSSM-I and $M_S \lesssim 10^8$GeV for the FSSM-II.

We have summarised all the relevant constraints in Table 4.1, distinguishing between the two types of FSSM and the three dark matter scenarios we have considered.

DM type	Inelastic scattering	Relic density	Gluino lifetime
$\tilde{\mathbf{W}}\|_{\mathbf{DM}}$	None	$m_{\tilde{W}} \subset [2390, 2450]$ GeV	For multi-TeV gluinos $\begin{cases} M_S \lesssim 5 \cdot 10^8 \text{GeV} \\ \text{(for FSSM-I)} \\ \\ M_S \lesssim 2 \cdot 10^{10} \text{GeV} \\ \text{(for FSSM-II)} \end{cases}$
$\tilde{\mathbf{B}}/\tilde{\mathbf{H}}\|_{\mathbf{DM}}$	$\mu_{\text{pole}} \lesssim 900$ GeV	$m_{\tilde{B}} \simeq \mu_{\text{pole}} - (900 - \mu_{\text{pole}})/x_f$	
$\tilde{\mathbf{H}}\|_{\mathbf{DM}}$	$\begin{cases} M_S \lesssim 5 \cdot 10^6 \text{GeV} \\ \text{(for FSSM-I)} \\ \\ M_S \lesssim 10^8 \text{GeV} \\ \text{(for FSSM-II)} \end{cases}$	$\mu_{\text{pole}} \subset [1110, 1140]$ GeV	

Table 4.1: Approximate constraints on the SUSY scale and on pole masses for the Dark matter candidates. We impose a splitting between fake Higgsinos bigger than 300 keV to avoid direct detection through inelastic scattering, we require a gluino life-time smaller than 100 s to avoid hampering BBN and finally constrain the relic density (calculated at tree-level in `micrOMEGAs`) to be $\Omega h^2 \subset [0.1158, 0.1218]$. When considering constraints on M_S, gaugino masses were taken in the multi-TeV range.

3 Electroweak Baryogenesis and Thermal Effects

We close this chapter by briefly discussing the issue of baryogenesis in Fake Split SUSY models with $\tilde{\epsilon} \gtrsim 1$. In Electroweak Baryogenesis (EWBG), matter-antimatter asymmetry in the present universe is generated dynamically during the electroweak phase transition. Indeed the three Sakharov's conditions may be fulfilled simultaneously during this transition as (see e.g. [86] for a review):

- Baryon number violation can proceed through non-perturbative processes called *sphalerons* [87] at the "bubble" wall between the $SU(2) \times U(1)$ phase and the broken one.
- CP violation can for instance originate from the Bino-Higgsinos sector complementing the violation in the CKM matrix, without introducing too large Electron Dipole Moment [88].
- Out of equilibrium condition can be achieved in the vicinity of "bubble" wall if the phase transition is "strongly" first order in the sense that that we want

$$\frac{\phi_c}{T_c} \gtrsim 1 \tag{4.43}$$

  where ϕ_c is the VEV of the Higgs boson doublets at the new broken minimum and T_c is the critical temperature. This ratio governs the rate for sphaleron transitions in the broken phase and 4.43 ensures that this rate is suppressed enough so that sphalerons within the broken phase will not wash out the asymmetry produced at the bubble wall.

In the following, we will focus on the out-of-equilibrium assumption, and more precisely on (4.43) in Fake Split Models. In [89], it was argued that when the Standard Model were supplemented by Higgsinos, Winos and Binos with strong coupling to the Standard Model Higgs, one could meet (4.43), allowing for a successful baryogenesis.

Such particles correspond precisely to our F-gauginos and F-higginos in the case $\tilde{\epsilon} > 1$. In the following we show however that one cannot conciliate the Higgs mass requirement and $\tilde{\epsilon}$ large enough to obtain $\tilde{\epsilon} > 1$ without adding new, stabilising bosonic field, thereby modifying our model.

As it was already noticed in [89], for large values of $\tilde{\epsilon} > 1$, the Higgs quartic λ tends to run quickly to zero. In Figure 3.5, we have shown precisely this behaviour. We see that for a Higgs at 125 GeV, λ is zero (corresponding to the scale M_C in the Figure) at 10 TeV already for $\tilde{\epsilon} \sim 1.6$ (which corresponds to a coupling $h \sim 0.5$ in the notation of [89]). In order to solve this issue, the authors of [89] have introduced stabilising bosonic fields with vacuum masses smaller than

$$m_b^2 \leqslant \exp(\frac{m_H^2 8\pi^2}{gh^4 v^2}) m_f^2 \sim \exp(\frac{20}{gh^4}) m_f^2 \ . \tag{4.44}$$

where g is the number of fermionic degrees of freedom. For the FSSMs, supposing relatively heavy (F-)gluinos and making the additional simplifying assumption that the (F)-Bino decouple (which can be obtained easily by setting $\tilde{\epsilon}$ to zero for the $\tilde{g}'_u$ and $\tilde{g}'_d$ couplings), we have 12 degrees of freedom couplings to the Higgs, so that for $h \sim 1$, the stabilising fields are only twice heavier that the fermions. This is at odd with the Split Spectrum we have in Fake Split SUSY models.

Furthermore, for values of $\tilde{\epsilon}$ compatible with our split spectrum (namely $\tilde{\epsilon} \lesssim 1.6$), we generically found ratios $\frac{\phi_c}{T_c} \lesssim 0.1$ indicating that our fermions are not sufficiently strongly coupled to lead to a strong first order phase transition.

We conclude that EWBG is not possible in the current state of Fake Split Models as we cannot conciliate the Higgs mass with couplings strong enough to generate a strong first order phase transition. In the more general context of Dirac Gauginos and R-symmetric models, this may however be achievable [90,91] thanks to the presence of the adjoint scalars which couple to the Higgs and can strengthen the first order phase transition.

Chapter 5

The Diphoton Excess and Dirac Gauginos

The year 2015 has left the community with only but a first taste of the upcoming results of the second run of the Large Hadron Collider at center-of-mass energy of 13 TeV. This limited data set has nonetheless already yielded a promising hint for new physics. Both experiments ATLAS and CMS have detected an excess in the di-photon mass spectrum for comparable invariant masses. The CMS analysis observed it for an invariant mass of 760 GeV with a local significance of 2.6 σ [92]. Simultaneously, the ATLAS collaboration has reported a similar excess at an invariant mass of 750 GeV with a local significance of 3.6 σ [93]. Furthermore, CMS subsequently increased its data set by including the events measured with the main magnet turned off, which pushed the signal local significance to 3.4 σ [94]. While the local significance must be reduced to account for the look-elsewhere-effect, the simple fact that the two excesses occurred for almost equal invariant mass makes this anomaly one of the most promising hints seen at LHC so far.

Under the assumption that the excess is generated by the decay of spin-0 particle with a ratio decay width over mass of $\Gamma/M_S = 0.014 \times 10^{-2}$ (with M_S the pole scalar singlet mass) the combined dataset of CMS with 3.3 fb^{-1}(13 TeV) and 19.7 fb^{-1}(8 TeV) gives

$$\sigma^{13\ \mathrm{TeV}} \cdot B_{\gamma\gamma} \approx 3.7 \pm 2\mathrm{fb}. \tag{5.1}$$

A combined analysis of the two experiments performed by [95] gives more generally a best-fit cross-section for the process $S \to \gamma\gamma$ ranging from 2.6 fb for a narrow width resonance to 6.9 fb for a broad resonance with an arbitrary width. In the following, we will require for cross-section in the broad range $2 - 8$ fb.

The simplest interpretation of this excess is the production and subsequent decay of a scalar resonance[1] with mass 750 GeV. However, the decay rate of this resonance is so large that fitting is in one of the previously proposed supersymmetric extensions of the Standard Model (SM), including the MSSM, is particularly challenging.

In this chapter, we will show that the model introduced in chapter 2, the Minimal Dirac Gaugino Supersymmetric Standard Model (MDGSSM) can simultaneously:

[1] Note this resonance could also be producde by the decay of a spin-2 particle, see [96, 97, 98, 99]

explain the excess, retain perturbativity up to the GUT scale, vacuum stability and gauge couplings unification. This is furthermore achieved with the "minimal" field content for such scenarios, in the sense that we will not have to introduce "ad-hoc" fields.

Indeed, all the necessary ingredients are present in the MDGSSM:

- The singlet supermultiplet **S** introduced to give the Bino a Dirac gauging mass has a scalar component S_R which can be identified with the 750 GeV resonance. Notice that since we will not used here the pseudo-scalar component S_I, we will simplify our notation and simply note S the singlet real scalar component S_R.
- The "fake leptons" supermultiplets $\mathbf{R}_u, \mathbf{R}_d$ and $\mathbf{E'}_{1,2}$ which have been introduced as unification fields to ensure gauge couplings unification will strengthen the cross section $S \to \gamma\gamma$ by participating in the loop processes leading to the decay of S in di-photons.
- The adjoint scalar octet, which appears in the octet adjoint supermultiplets **O** will similarly increase the production rate of S through gluons fusion.

We will start this chapter by reviewing the standard results for the loop-induced processes coupling the singlet S to two photons (to account for the diphoton excuess) or two gluons (to produce the singlet by gluons fusion). We then considered the various theoretical and experimental constraints on our model. Our results will be shown in section 2. Note that the material we will covered in this chapter will be expanded and completed in [4].

1 Theoretical Considerations

In order to have a plausible supersymmetric theory describing the di-photon excess, we will have to satisfy a number of theoretical and experimental requirements. We start by considering the basics of production and decay of the scalar singlet and studing some of the collider constraints on our model. We further investigate three theoretical constraints: gauge coupling unification, perturbativity up to the GUT scale and finally vacuum stability and non-appearance of Charge or Color Breaking Vacuua.

1.1 Production and Decay in the DGMSSM

In the narrow width approximation in which the mediating S singlet is automatically on-shell, we can approximate the cross section of the complete process $pp \to S \to \gamma\gamma$ as follows:

$$\sigma(pp \to S \to \gamma\gamma) = \frac{2J+1}{sM_S\Gamma}\left[C_{gg}\Gamma(S \to gg) + \sum_q C_{q\bar{q}}\Gamma(S \to q\bar{q})\right]\Gamma(S \to \gamma\gamma)\,. \quad (5.2)$$

Assuming a spin-zero particle produced resonantly via gluon fusion, we arrive at

$$\sigma(pp \to S \to \gamma\gamma)_{13\ \mathrm{TeV}} \approx\ K_{13} \times 4.9 \times 10^6\ \mathrm{fb}\frac{\Gamma_{gg}}{\Gamma}\frac{\Gamma_{\gamma\gamma}}{\Gamma}\frac{\Gamma}{M_S} \quad (5.3)$$

$$\sigma(pp \to S \to \gamma\gamma)_{8\ \mathrm{TeV}} \approx\ K_8 \times 1.1 \times 10^6\ \mathrm{fb}\frac{\Gamma_{gg}}{\Gamma}\frac{\Gamma_{\gamma\gamma}}{\Gamma}\frac{\Gamma}{M_S} \quad (5.4)$$

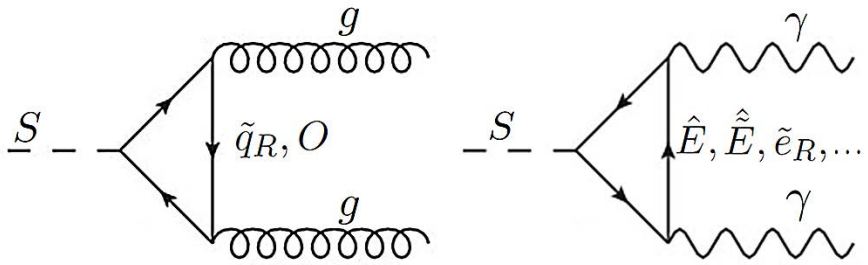

Figure 5.1: Examples of one-loop diagrams contributing to the couplings of S into two gluons and two photons.

taking $C_{gg}^{8\text{TeV}} = 174$ and $C_{gg}^{13\text{TeV}} = 2137$ as values arising from the parton distribution functions [100], respectively. An important aspect of our calculation is that for a more realistic estimation, we have taken into account the K-factors $K_{8,13}$ for the full N^{n}LO production of $H+$jet compared to the tree-level process. We have estimated $K_8 \simeq 1.9$ from the comparison of the leading-order effective vertex from `MadGraph` and the Higgs Cross-section working group value for a Standard-Model-like Higgs of 750 GeV at 8 TeV. We will take conservatively for the same value for K_{13}.

The two relevant amplitudes Γ_{gg} and $\Gamma_{\gamma\gamma}$ are obtained from one-loop diagrams of the form of Figure 5.1.

Let us first consider the coupling to two gluons. The process $S \to gg$ is a priori generated by loops of squarks, scalar octet and gluinos. The amplitude is of the form

$$\begin{aligned}\Gamma(S \to gg) &= \frac{\alpha_3^2 m_S}{8\pi^3}\left|\text{tr}\Big(\sum_f C_f \frac{g_{Sff}}{\sqrt{\tau_f}} A_{1/2}^S(\tau_f) + \sum_\phi C_\phi \frac{g_{S\phi\phi}}{2\sqrt{\tau_\phi} m_\phi} A_0^S(\tau_\phi)\Big)\right|^2 \\ &\simeq 4.3\cdot 10^{-2}\left|\text{tr}\Big(\sum \frac{g_{Sff}}{\sqrt{\tau_f}} A_{1/2}^S(\tau_f) + \frac{g_{S\phi\phi}}{2\sqrt{\tau_\phi} m_\phi} A_0^S(\tau_\phi)\Big)\right|^2 .\end{aligned} \tag{5.5}$$

where we have defined $\tau_i \equiv 4\frac{m_i^2}{m_S^2}$, the sums runs over all scalars and fermions, and

$$\begin{aligned} f(\tau) &\equiv \begin{cases} (\sin^{-1}(1/\sqrt{\tau}))^2 & \tau \geq 1 \\ -\frac{1}{4}\left[\log\frac{1+\sqrt{1-\tau}}{1-\sqrt{1-\tau}} - i\pi\right]^2 & \tau < 1 \end{cases} \\ A_0^S &= \tau(\tau f(\tau) - 1) \\ A_{1/2}^S &= 2\tau(1 + (1-\tau) f(\tau))) \ . \end{aligned}$$

and Q_f, Q_ϕ, g_{Sff} and $g_{S\phi\phi}$ are the electric charge and coupling with the singlet of the fermions and scalars participating in the triangular loops. The loop fonctions A_0^S and $A_{1/2}^S$ have a maximum at the resonant mass $M_S/2 \sim 375$ GeV. We will therefore generically require masses close to this scale in order to enhance the cross-section. The phenomenology for the squarks and scalar octet is straightforward: we need them as close from the resonance as possible and as coupled as possible. The main contributions will come from

- D-term-induced couplings between the squarks and the singlet, generated by the same contributions we discussed in chapter 2 when dealing with supersoftness. Theses couplings are proportional to the hypercharge of the squarks and the Dirac mass m_{1D}. They are sizeable only for large Dirac mass m_{1D}.

- Soft terms trilinears couplings from (2.17) between the adjoint scalar octet and the singlet. They give a strong contribution but unfortunately are strongly constrained from vacuum stability bounds.

The contribution from the Dirac gluinos is more peculiar. In fact, we observed that pure Dirac gluinos do not contribute at all to the amplitude, this point will be developped in [4]. This remark is of crucial importance for the pseudo-scalar S_I which can only couple to gluons through fermions loops as we assume CP-conserving couplings. If no Majorana masses for the original gluinos are introduced, the pseudo-scalar is practically not produced. However, if we allow for the presence of an additional Majorana mass term, the pseudo-scalar S_I can be produced and participates in the $S \to \gamma\gamma$ cross-section. This can potentially lead to a "double-peaks" scenario [4].

In the limit in which Γ_{gg} dominates the decay width (which is overly optimistic in our case as we will see in the next section), we find the following bound on $\Gamma_{\gamma\gamma}$:

$$\Gamma_{\gamma\gamma} \gtrsim 1.5 \times 10^{-4}. \tag{5.6}$$

We now turn to the amplitude to di-photon. This is given for a scalar by

$$\begin{aligned} \Gamma(S \to \gamma\gamma) &= \frac{\alpha^2 m_S}{64\pi^3} \left| \mathrm{tr}\Big(\sum_f \frac{g_{Sff}}{\sqrt{\tau_f}} Q_f^2 A_{1/2}^S(\tau_f) + \sum_\phi \frac{g_{S\phi\phi}}{2\sqrt{\tau_\phi} m_\phi} Q_\phi^2 A_0^S(\tau_\phi)\Big)\right|^2 \\ &\simeq 2.\cdot 10^{-5} \left| \mathrm{tr}\Big(\sum \frac{g_{Sff}}{\sqrt{\tau_f}} A_{1/2}^S(\tau_f) + \frac{g_{S\phi\phi}}{2\sqrt{\tau_\phi} m_\phi} A_0^S(\tau_\phi)\Big)\right|^2 \end{aligned} \tag{5.7}$$

Notice that the numerical factor in (5.7) is an order of magnitude smaller that the bound (5.6). The key issue will therefore be to populate the sums in the square terms of (5.7) since the amplitude will very roughly scale as N^2 , with N the number of particles participating in the loop.

In our case, the main contributions will come from

- D-term-induced couplings between the sleptons and the singlet, they are again proportional to the hypercharge of the sleptons and the Dirac mass m_{1D} and therefore sizeable only for large Dirac mass.

- Superpotential-induced couplings between the fake leptons and the singlet from the terms of (2.12) in chapter 2. They are the main contributions in our model.

- Soft terms trilinears couplings from (2.17) between the fake sleptons and the singlet. Similarly to the gluons case, they are strongly constrained from vacuum stability bounds.

An important remark here is that the two last contributions are mutually incompatible in presence of a preserved R-symmetry, as we have already noted in chapter 2. Indeed

the require a different R-charge for the fake leptons fields $\hat{E}$ and $\hat{E}'$ to be R-invariant. A theoretical estimation for the cross-section in the ideal case where the gluon amplitude dominate the decay width and there is no mixing between the scalar singlet and the Higgs boson is given in Figure 5.2.

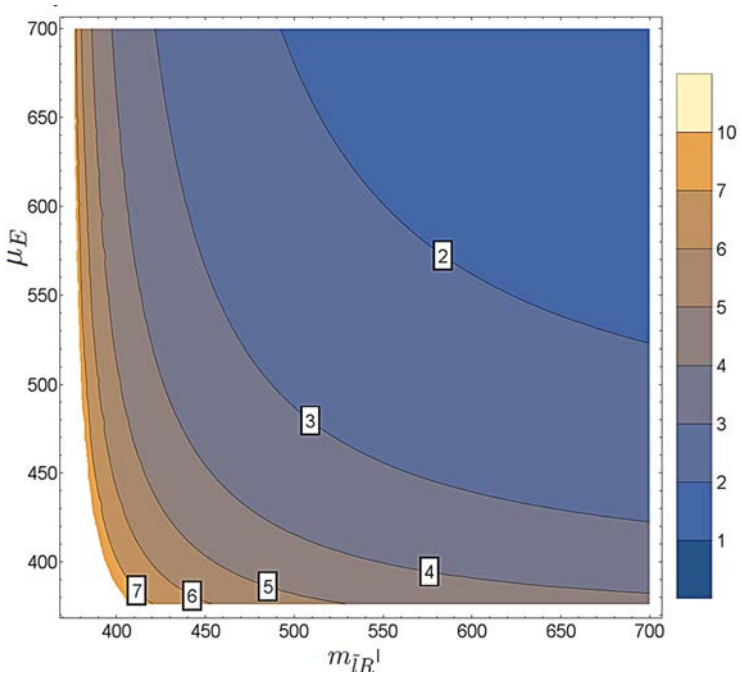

Figure 5.2: Cross-section of $S \to \gamma\gamma$ as a function of the masses m_{sl} and $m_{\tilde{E}}$ without trilinears. We assume that the gluon fusion process dominate the other processes. We have taken $\lambda_{SR} = \lambda_{ER} = 0.7$. Notice that the masses are in the axis should be understood as the pole masses.

1.2 Constraints from Higgs Mass Mixing and 8 TeV data

A crucial property of the singlet S is that it will in general mix with the Higgs eigenstate. This is in our case an undesirable feature since it will lead to tree-level decays of S into tops, W, Z or Higgs which could easily overcome the one-loop decay into photons.

Building on the notations introduced in chapter 2, we introduce

$$\begin{aligned} \tilde{m}_S^2 &= \tilde{m}_{SR}^2 + \lambda_S^2 \frac{v^2}{2} \\ \tilde{m}_T^2 &= \tilde{m}_{TR}^2 + \lambda_T^2 \frac{v^2}{2} \ , \end{aligned} \tag{5.8}$$

where the effective masses for the real parts of S and T read:

$$\tilde{m}_{SR}^2 = m_S^2 + 4m_{1D}^2 + B_S, \qquad \tilde{m}_{TR}^2 = m_T^2 + 4m_{2D}^2 + B_T \ . \tag{5.9}$$

Then, at tree level the scalar mass matrix in the basis $\{h, H, S_R, T_R^0\}$ is [29]:

$$\begin{pmatrix} M_Z^2 + \Delta_h s_{2\beta}^2 & \Delta_h s_{2\beta} c_{2\beta} & \Delta_{hS} & \Delta_{hT} \\ \Delta_h s_{2\beta} c_{2\beta} & M_A^2 - \Delta_h s_{2\beta}^2 & \Delta_{HS} & \Delta_{HT} \\ \Delta_{hS} & \Delta_{HS} & \tilde{m}_S^2 & \lambda_S \lambda_T \frac{v^2}{2} \\ \Delta_{hT} & \Delta_{HT} & \lambda_S \lambda_T \frac{v^2}{2} & \tilde{m}_T^2 \end{pmatrix} \tag{5.10}$$

where we have defined:

$$\Delta_h \;=\; \frac{v^2}{2}(\lambda_S^2 + \lambda_T^2) - M_Z^2 \tag{5.11}$$

which vanishes when λ_S and λ_T take their $N = 2$ values,

$$\Delta_{hS} = -2\frac{v_S}{v}\tilde{m}_{SR}^2, \qquad \Delta_{hT} = -2\frac{v_T}{v}\tilde{m}_{TR}^2 \tag{5.12}$$

and

$$\Delta_{HS} = g' m_{1D} v s_{2\beta}, \qquad \Delta_{HT} = -g m_{2D} v s_{2\beta} \tag{5.13}$$

.

This matrix is diagonalised by the mixing matrix S_{ij}. Of particular interest will be S_{11} which measures the lightest scalar eigenstate in Standard Model Higgs-like.

We can subsequently use the minimisation condition of v_S on the off-diagonal element Δ_{hS} of the scalar mass matrix given in (5.12) to find (see [29])

$$\begin{aligned} \Delta_{hS} =& v[v_S \lambda_S^2 - g' m_{1D} c_{2\beta} + \sqrt{2}\lambda_S \mu + \lambda_S \lambda_T v_T] \\ =& v[\sqrt{2}\lambda_S \tilde{\mu} - g' m_{1D} c_{2\beta}] \;, \end{aligned} \tag{5.14}$$

where we used the effective mass parameter

$$\tilde{\mu} \;=\; \mu + \frac{1}{\sqrt{2}}(\lambda_S\, v_S + \lambda_T\, v_T) \tag{5.15}$$

From this basic analytical calculation, we see that we can minimise the tree-level mixing by choosing:

$$\lambda_S \sim \frac{g' m_{1S} c_{2\beta}}{\sqrt{2}\tilde{\mu}} \;. \tag{5.16}$$

In general, this relation will be modified at one-loop, but the property that one value of λ_S is favored will remain and is easily observable in our coming Figures.

Such a mixing with the Standard Model Higgs will modify the Higgs sector observables. From [101] we find the latest constraint on the 125 GeV Higgs global signal strength μ_{average} to be

$$\mu_{\text{average}} = 1.09^{+0.11}_{-0.10} \;, \tag{5.17}$$

In our case this is modified by a factor of $|S_{11}|^2$, where S is the mixing matrices of the scalar sector; the above constraint gives us

$$1 - |S_{11}|^2 \leq 0.24 \leftrightarrow \sum_{k\neq 1} |S_{1k}|^2 = \sum_{k\neq 1} |S_{k1}|^2 \leq 0.24. \tag{5.18}$$

This condition is in fact satisfied quite easily, as can be seen from Figure 5.3 where we show the contours for the Higgs mass and the mixing matrix element S_{31} as a function of $\tan\beta$ and λ_S. An important comment regarding this Figure is that a 125 GeV also favors small mixing. However, the more stringent constraints arises from the

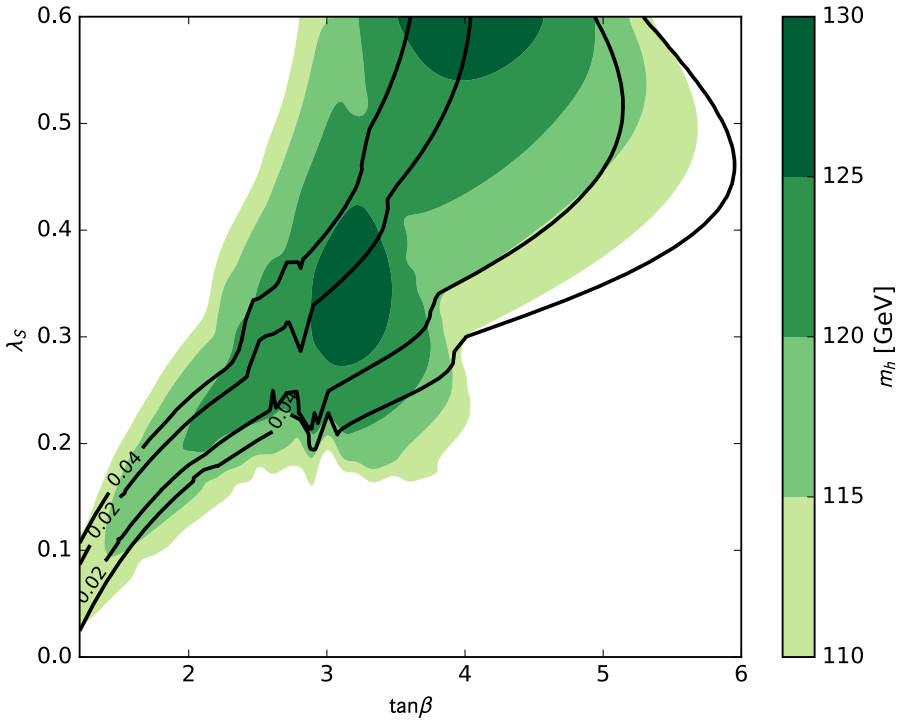

Figure 5.3: Higgs mass and mixing between h and S as a function of λ_S and $\tan\beta$ obtained from the benchmark point (5.1). The thin black lines represent the 2% and 4% mixing contour lines. The irregularities at $\tan\beta \sim 2-3$ arise since the two-loop effective potential method used to determined the Higgs mass (and scalar singlet mass) suffers from the so-called "Goldstone boson catastrophe" (see [102] for more details).

non-observation of any excess in the 8 TeV data for the ZZ, Zh and hh, dijets and WW channels. As the mixing between S and h induces a tree-level decay one naively expect a percent-level suppression to be necessary. As the S as mostly produced by gluons fusions in our scenarios, we request that (see [100]):

$$\frac{\Gamma(S \to ZZ)}{\Gamma(S \to \gamma\gamma)} \lesssim 6 \,, \tag{5.19}$$

which is the ratio we have observed to give the most stringent constraints on the mixing between S and h in our model. Note that in practice this constraints are automatically satisfied most of the time when we will have a cross-section to diphoton big enough to fit the experimental data. This will be clear in Figure 5.7.

Finally, the vev of T gives a contribution to the W boson mass and the electroweak precision data give important bounds on it. One must examine the induced correction $\Delta\rho$ to the Veltman ρ-parameter:

$$\rho \equiv \frac{M_W^2}{c_{\theta_W}^2 M_Z^2} = 1 + \Delta\rho \ , \tag{5.20}$$

with

$$\Delta\rho \sim \frac{4v_T^2}{v^2} \tag{5.21}$$

and v, the Standard Model Higgs VeV. In order to be below the experimental constraints, we need $\Delta\rho \lesssim (4.2 \pm 2.7) \times 10^{-4}$, ([29] – see also [30,31] –). At tree level, we have

$$v_T \ \simeq \ \frac{v^2}{2\tilde{m}_{TR}^2} \ \left[-g m_{2D} c_{2\beta} - \sqrt{2}\tilde{\mu}\lambda_T\right] \ , \tag{5.22}$$

with $\tilde{m}_{TR}^2 = m_T^2 + 4m_{2D}^2 + B_T$, therefore, small $\Delta\rho$ require large triplet Dirac and soft masses. This requirement can often be at odd with naturalness which prefers smaller triplet masses. Indeed, radiative corrections induced by the adjoint triplet scalars to $m_{H_{u,d}}^2$ are [29]:

$$\delta m_{H_{u,d}}^2 \supset -\frac{1}{16\pi^2}(2\lambda_T^2 m_T^2)\log\left\{\frac{\Lambda}{\text{TeV}}\right\} \tag{5.23}$$

with Λ the UV cut-off, $m_{H_{u,d}}^2, m_T^2$ the squared masses for Higgses and scalar triplet T, and λ_T the coupling defined in (2.12). For Λ at the Planck scale, a fine-tuning $\Delta_T = \delta m_H^2/m_H^2$ better than 10% translates into the constraint

$$m_T \lesssim \frac{1}{\lambda_T} 450 \text{ GeV} \ . \tag{5.24}$$

In Figure 5.4, we show the allowed region for λ_T and m_{2D} around the benchmark point (5.1). $\Delta\rho$ has been obtained at one-loop using the Spheno [66,67]) code generated by the `SARAH` (see ref. [68,69,70,71,61]). We see that the Higgs mass prefer large values of λ_T but that the following three requirements are perfectly compatible: (1) a 125 GeV Higgs, (2) a natural mass for the triplet and (3) a parameter $\Delta\rho$ compatible with the current constraints.

1.3 Unification and Landau poles

In this section, we will consider two theoretical constraints on our model: gauge coupling unification and perturbativity up to the Grand Unified Theory (GUT) scale.

Concerning the former, we note that the field content of the MDGSSM, and more precisely the two pairs of vector-like electrons $\hat{E}$ and $\hat{E}'$ as well as the doublet R_u, R_d, have been chosen to have one-loop unification by completing the $\mathbf{8}_0 + \mathbf{3}_0 + \mathbf{1}_0$ set of adjoint multiplets into a complet GUT representation of $(SU(3))^3$ (see [43]). We have

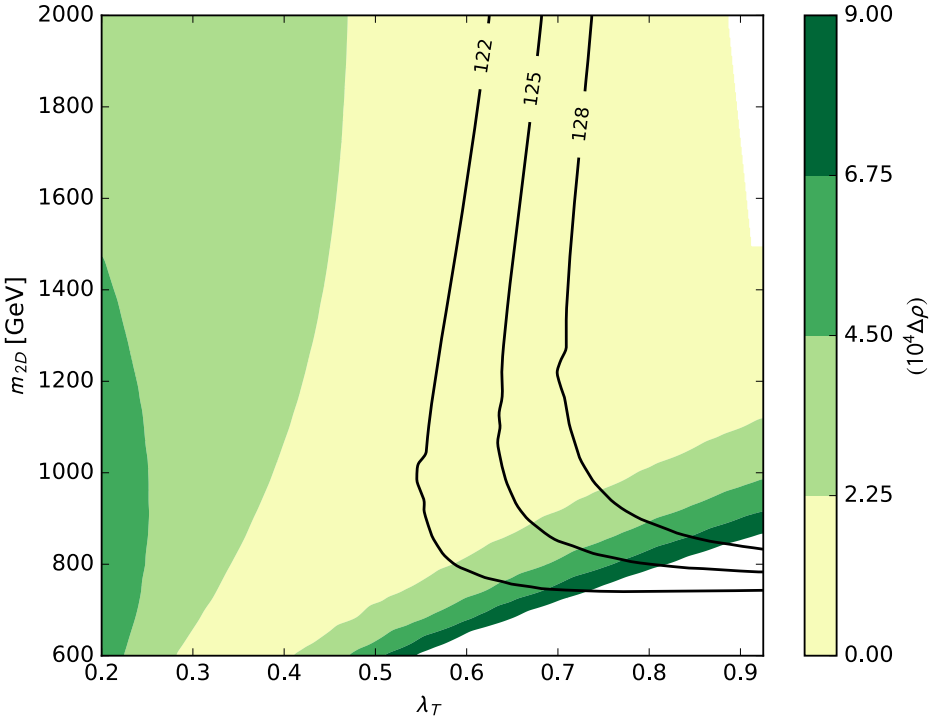

Figure 5.4: One-loop $10^4 \cdot \Delta\rho$ obtained from the benchmark point (5.1) by varying λ_T and m_{2D}. The black lines give the contours for $m_h = 122, 125, 128$ GeV

checked numerically that unification is also preserved at two-loops, albeit its precision decreases when increasing the squarks mass.

Once the GUT scale is determined, we require perturbation theory to be valide up to the GUT scale. As we will see now, this gives strong constraints on the Yukawa couplings. At one-loop, the beta functions for $\lambda_{SE}, \lambda_{SR}, \lambda_{SO}, \lambda_S$ and λ_T form a coupled system given by:

$$\beta_{\lambda_S} = \frac{1}{16\pi^2}\lambda_S[4\lambda_S^2 + 3\lambda_T^2 + 2\lambda_{SR}^2 + 2\lambda_{SE}^2 + 4\lambda_{SO}^2 - \frac{3}{5}g_1^2 - 3g_2^2 + 3y_t^2 + \dots] \quad (5.25)$$

$$\beta_{\lambda_T} = \frac{1}{16\pi^2}\lambda_T[2\lambda_S^2 + 4\lambda_T^2 - \frac{3}{5}g_1^2 - 7g_2^2 + 3y_t^2 \dots] \quad (5.26)$$

$$\beta_{\lambda_{SE}} = \frac{1}{16\pi^2}\lambda_{SE}[2\lambda_S^2 + 4\lambda_{SE}^2 + 2\lambda_{SR}^2 + 4\lambda_{SO}^2 - \frac{12}{5}g_1^2 + \dots] \quad (5.27)$$

$$\beta_{\lambda_{SR}} = \frac{1}{16\pi^2}\lambda_{SR}[2\lambda_S^2 + 2\lambda_{SE}^2 + 4\lambda_{SR}^2 + 4\lambda_{SO}^2 - \frac{3}{5}g_1^2 - 3g_2^2 + \dots] \quad (5.28)$$

$$\beta_{\lambda_{SO}} = \frac{1}{16\pi^2}\lambda_{SO}[2\lambda_S^2 + 4\lambda_{SE}^2 + 2\lambda_{SR}^2 + 6\lambda_{SO}^2 - 12g_3^2 + \dots] \,, \quad (5.29)$$

where the dots contain the contributions from the other couplings. Before studying this system numerically, we point out some peculiarities of these expressions:

- The gauge couplings contribute negatively to the beta function, increasing the stability. In particular, λ_{SO} is strongly stabilised.
- In the limit $\lambda_S \to 0$, λ_T completely decouples from the other Yukawa couplings.
- The perturbativity of the coupling λ_S will be critical as: (1) the gauge and top Yukawa already gives a positive contribution ~ 1.1 to its beta function; (2) all the other Yukawas feed intro its beta function and conversely λ_S feeds into all the beta functions.

We have numerically constrained the initial values for $\lambda_{SE}, \lambda_{SR}, \lambda_{SO}, \lambda_S$ and λ_T at the low scale (SUSY scale), so that they remain perturbative up to the GUT scale. We use the two-loop RGEs generated by the public code `SARAH` (see ref. [68, 69, 70, 71, 61] and ref. [72]). We choose as perturbativity requirement that all Yukawa couplings should remain smaller than $\sqrt{4\pi}$.[2]

In Figure 5.5, we study the case of $\lambda_{SO} = 0$, which will be relevant in our case. The perturbativity bounds are shown in the planes λ_S/λ_{SE} and λ_S/λ_T. As expected, we obtain the strongest constraints for λ_S, especially in the large λ_{SE} case, which is the one of interest in this paper. Furthermore, we recover that for $\lambda_S \to 0$, λ_T is insensitive to the other Yukawas couplings. Adding the R-violating parameter λ_{SO} will further constrain the Yukawa couplings [4].

Finally, being mass couplings, the trilinears T_{SO}, T_{SR} and T_{SE} do not develop Landau poles. Since we focus on the low-energy theory, we will not derive any constraints from their RGEs evolutions, however we will now see that their values are limited by requering the non-appearance of charge/color breaking vacuua.

[2] Notice that the precise value for perturbativity criterion is not very important since large couplings tend to grow exponentially in any case.

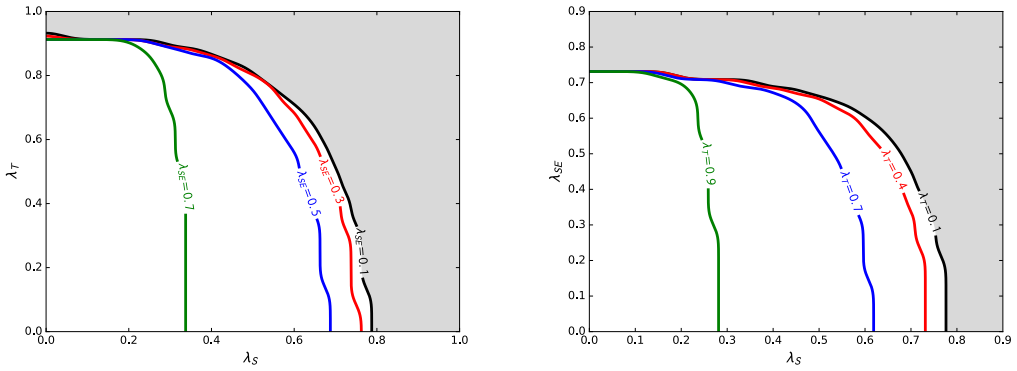

Figure 5.5: Perturbativity bounds on our model, around the first benchmark point from Table 5.1, obtained from the requirement that no couplings overtake $\sqrt{4\pi}$ before the GUT scale. We consider $\lambda_{SR} = \lambda_{SE}$. **Left plot:** Bounds for (from left to right) $\lambda_{SE} = 0.7, 0.5, 0.3, 0.1$ in the λ_S/λ_T plane, all points above the curves are excluded. **Right plot:** Bounds for (from left to right) $\lambda_T = 0.9, 0.7, 0.4, 0.1$ in the λ_S/λ_{SE} plane, all points above the curves are excluded.

1.4 Vacuum Stability

We now turn to the constraints from vacuum stability. The scalar potential can be decomposed into three main contributions:

$$V = V_g + V_W + V_{soft} \ , \tag{5.30}$$

with V_g, containing the D-terms contributions, V_W the superpotential contributions and V_{soft} the soft SUSY-breaking terms.

We have

$$V_g = \frac{1}{2}D_1^2 + \frac{1}{2}D_{2a}D_2^a + \frac{1}{2}D_{3a}D_3^a \tag{5.31}$$

where

$$\begin{aligned}
D_1 &= -2m_{1D}S_R + D_Y^{(0)} \qquad \text{with} \qquad D_Y^{(0)} = -g' \sum_j Y_j \varphi_j^\dagger \varphi_j \\
D_2^a &= -\sqrt{2}m_{2D}(T^a + T^{a\dagger}) + D_2^{a(0)} \qquad \text{with} \qquad D_2^{a(0)} = -g_2 \sum_j \varphi_j^\dagger M_j^a \varphi_j \\
D_3^a &= -\sqrt{2}m_{3D}(O^a + O^{a\dagger}) + D_3^{a(0)} \qquad \text{with} \qquad D_3^{a(0)} = -g_3 \sum_j \varphi_j^\dagger M_j^a \varphi_j \ .
\end{aligned} \tag{5.32}$$

where φ_j are the scalar components of the matter chiral superfields, possibly in the adjoint representation and M_j^a is the matrix of the gauge representation of φ_j. Let us leave aside the triplet contribution (we are considering a heavy triplet and therefore expect a near-zero VEV for it) and focus on the singlet and octet terms. Similarly, we will leave aside the squarks contribution as we are not considering large A terms and

therefore do not expect them to acquire a color-breaking VEV. We have then

$$\begin{aligned} D_1^{(0)} &= -\frac{g'}{2}(R_u^\dagger R_u - R_d^\dagger R_d) - g'(|\hat{E}i|^2 - |\hat{E}'_i|^2) \\ D_2^{a(0)} &= -g_2(R_u^\dagger \frac{\sigma^a}{2} R_u + R_d^\dagger \frac{\sigma^a}{2} R_d) \\ D_3^{a(0)} &= -g_3 O_b^\dagger (T^a)^{bc} O_c \ , \end{aligned} \tag{5.33}$$

with $(T^a)^{bc} = (-if^{abc})$ and f^{abc} the $SU(3)$ structure constants.

We now turn to the superpotential contributions (we suppress the i indices for $\hat{E}'_i$ and $\hat{E}'_j$ and the "$\cdot$" denotes $SU(2)$ indices contraction by ϵ tensors) and find:

$$\begin{aligned} V_W &= \mu_r^2(R_u^\dagger R_u + R_d^\dagger R_d) + \mu_E^2(|\hat{E}|^2 + |\hat{E}'|^2) \\ &\quad + \lambda_{SE}^2\left[|\hat{E}'\hat{E}|^2 + |S|^2(|\hat{E}|^2 + |\hat{E}'|^2)\right] + \lambda_{SR}^2\left[|R_u \cdot R_d|^2 + |S|^2(|R_u|^2 + |R_d|^2)\right] \end{aligned} \tag{5.34}$$

Adding finally the soft SUSY-breaking terms, we obtain

$$V = V_E + V_{SE} + V_{SR} + V_S + V_R + V_O + V_{SO} \ , \tag{5.35}$$

with

$$V_E = (m_E^2 + \mu_E^2)(|\hat{E}|^2 + |\hat{E}'|^2) + \lambda_{SE}^2|\hat{E}'\hat{E}|^2 + g'(|\hat{E}|^2 - |\hat{E}'|^2)^2 + B_E(\hat{E}\hat{E}' + h.c.) \tag{5.36}$$

$$V_S \supset m_S^2|S|^2 + 2m_{1D}S_R^2 + \frac{1}{2}B_S(S^2 + h.c.)$$

$$\begin{aligned} V_R &\supset (m_R^2 + \mu_r^2)(R_u^\dagger R_u + R_d^\dagger R_d) + \lambda_{SR}^2|R_u \cdot R_d|^2 + B_R(R_u \cdot R_d + h.c.) \\ &\quad + \frac{1}{8}\left[g'^2\ (R_u^\dagger R_u - R_d^\dagger R_d)^2 + g_2^2(R_u^\dagger \frac{\sigma^a}{2} R_u + R_d^\dagger \frac{\sigma^a}{2} R_d)^2\right] \end{aligned}$$

$$\begin{aligned} V_O &\supset 2m_O^2 \mathrm{tr}(O^\dagger O) + 2m_{3D}^2 \mathrm{tr}(O_R^\dagger O_R) + (B_O \mathrm{tr}(OO) + h.c.) \\ &\quad + \frac{g_3^2}{2}\left[(O_b^\dagger (T^a)^{bc} O_c)(O_b^\dagger (T_a)^{bc} O_c)\right] + \sqrt{2}g_3 m_{3D}(O + O^\dagger)^a O_b^\dagger (T_a)^{bc} O_c \ , \end{aligned}$$

and the mixed contributions

$$V_{SE} = 2g' m_{1D} S_R(|\hat{E}|^2 - |\hat{E}'|^2) + \lambda_{SE}^2|S|^2(|\hat{E}|^2 + |\hat{E}'|^2) + T_{SE}(S\hat{E}\hat{E}' + h.c.) \tag{5.37}$$

$$V_{SR} = g' m_{1D}(R_u^\dagger R_u - R_d^\dagger R_d) + \lambda_{SR}^2|S|^2(R_u^\dagger R_u + R_d^\dagger R_d)^2 + + T_{SR}(S R_u \cdot R_d + h.c.)$$

$$V_{SO} = T_{SO}(S\mathrm{tr}(OO) + h.c.) \ .$$

We will consider large trilinear couplings. As usual when looking for a charge/color breaking vacuum, we study the regions of large fields values, so that we can neglect the contributions from the mass terms.

First, we investigate the $S, \hat{E}, \hat{E}'$ sector. Furthermore we will focus on real fields for simplicity. In the large VEV limits, the minimisation equations are

$$\begin{aligned}
\frac{\partial V}{\partial S} &\simeq g'\sqrt{2}m_{1D}(|\hat{E}|^2 - |\hat{E}'|^2) + \lambda_{SE}^2 S(|\hat{E}|^2 + |\hat{E}'|^2) + T_{SE}\hat{E}\hat{E}' = 0 \qquad (5.38)\\
\frac{\partial V}{\partial \hat{E}} &= \hat{E}(m_E^2 + \mu_E^2 + \lambda_{SE}^2|S|^2 + g'm_{1D}S_R) + \hat{E}'(B_E + T_{SE}S) + \lambda_{SE}^2\hat{E}|\hat{E}'|^2 \\
&\quad + g'^2\hat{E}(|\hat{E}|^2 - |\hat{E}'|^2) \\
&= 0 \\
\frac{\partial V}{\partial \hat{E}'} &= \hat{E}'(m_E^2 + \mu_E^2 + \lambda_{SE}^2|S|^2 - g'm_{1D}S_R) + \hat{E}(B_E + T_{SE}S) + \lambda_{SE}^2\hat{E}'|\hat{E}|^2 \\
&\quad - g'^2\hat{E}'(|\hat{E}|^2 - |\hat{E}'|^2) \\
&= 0\ .
\end{aligned}$$

One should notice that the customary unstable direction $\hat{E} = \hat{E}'$ (where the potential is not protected by the quartic terms proportional to g'^2), cannot be considered here. This is due to the presence of the Dirac mass term $\pm g'\hat{E}m_{1D}S_R$ which prevent any solutions of the previous system in this direction. However, in the limit of interest for us $m_{1D} \ll T_{SE}$, we can in fact approximate this term and take $\hat{E} \simeq \hat{E}'$ so that we can also neglect the g'^2 quartic.

In this limit, we find the solution to the previous system:

$$\begin{aligned}
v_E^2 &= \frac{T_{SE}^2}{4\lambda_{SE}^2} - (m_E^2 + \mu_E^2 + B_E^2) \qquad (5.39)\\
v_S &= -\frac{T_{SE}}{2\lambda_{SE}}\ .
\end{aligned}$$

so that we have appearance of a charge-breaking vacuum if

$$\frac{T_{SE}}{2\lambda_{SE}} > \sqrt{m_E^2 + \mu_E^2 + B_E^2}\ . \qquad (5.40)$$

Similarly the condition to avoid appearance of charge-breaking vacuum in the S, R_u, R_d sector is

$$\frac{T_{SR}}{2\lambda_{SR}} > \sqrt{m_R^2 + \mu_R^2 + B_R^2}\ . \qquad (5.41)$$

In general, these bounds can be slightly relaxed by simply requiring that the second vacuum has an energy bigger than the charge-preserving one. We have found that the corresponding highest values for the trilinear compatible with fake sleptons close to 375 GeV is around 1 TeV. For such an upper bound, it is preferable to use Yukawas λ_{SE} over the trilinear in order to maximise the cross-section.

The situation is even worse for the scalar octet, since R-symmetry forbids the coupling λ_{SO}. In absence of any quartic, even the smallest trilinear term T_{SO} can lead to an Lagrangian unbounded by below. Suppose we add quartics of the schematic form

$$\frac{y_S}{2}|S|^2O_I^2 + \frac{y_O}{4}O_I^4 \qquad (5.42)$$

where we focus on the light pseudo-scalar octet we are practically using. Supposing that such couplings will be loop-generated with values of a few 10^{-2}. One can estimate the upper bound on T_{SO} compatible with a stable color-preserving vacuum. We found the (rough) bound $T_{SO} \lesssim 350$ GeV for scalar octet with masses around 500 GeV. In the following, we will conservatively consider $T_{SO} \lesssim 300$ GeV as this is sufficient to recover the measured cross-section. This issue will be discussed in more details in [4].

2 Results

Before presenting our results, let us briefly present our parameter space. While the MDGSSM has a large set of free parameters, the most relevant subset can be divided into three roughly independent sets controlling different features:

1. **Higgs and singlet masses and mixing**: $m_{1D}, m_S, B_S, \tan\beta, \mu, \lambda_S$ and λ_T.
2. **Singlet decay/production amplitude to** gg : $T_{SO}, m_O, m_{\tilde{q}}$, where $m_{\tilde{q}}$ is the soft masses for right (or left)-handed squarks.
3. **Singlet decay amplitude to** $\gamma\gamma$: T_{SE}, T_{SR}, or $\lambda_{SR}, \lambda_{SE}$ supplemented with soft masses and B terms for the fields $\hat{E}, \hat{E}', R_u$ and R_d.

The first set is dedicated to reproducing the measured Higgs boson mass as well as a 750 GeV scalar singlet. Moreover, one can adjust the value of λ_S to have a small mixing between both scalars. As we have shown, this strong requirement is tempered by the fact that this region largely overlap with the requirement $m_H \in [122, 128]$. The second set can be used to enhance the production rate of singlet through gluon fusion. The trilinears T_{SO} are crucial in this respect as they allow the scalar octet to participate in the loop-induced coupling Sgg, greatly increasing the singlet production rate. Finally, the last set of parameters is used to increase the amplitude to $\gamma\gamma$. The superpotential Yukawa couplings λ_{SE} and λ_{SR} from (2.12) are constrained to avoid the appearance of Landau poles before the GUT scale as we have discussed in section 1.3. The trilinears are mainly constrained by enforcing the scalar fields $\hat{E}, \hat{E}', R_u$ and R_d do not get a charge-breaking vacuum expectation value. In the following, we will consider a R-conserving model and choose to conserve the terms $\lambda_{SR}, \lambda_{SE}$ against the trilinears.

The singlet production proceeds mainly by gluons fusion through loops of squarks (controlled by $g' m_{1D}$) and (pseudo-)scalar octets (controlled by the trilinear T_{SO}).

Following our study of unstable vacua, we limit ourselves to low trilinear mass $T_{SO} \lesssim 300$ GeV. Since we have a Dirac masses for the gluinos $m_{3D} \gtrsim 1.8$ TeV from LHC searches, the scalar octet is a priori heavy, except if one chooses carefully a large negative B_O. On the contrary, the pseudo-scalar octet can be light. Unfortunately, recent searches in the four-tops channel leads to stringent constraint on such particles (while the scalar octet is unconstrained for sufficiently heavy gluinos). We refer to [4] for more details on this issue, the main idea is that since we are focusing on CP-conserving interactions, the pseudo-scalar octet cannot decay to two gluons so that its pair production mostly lead to four-tops signals. On the contrary, the scalar octet does couple to gluons through squarks loops which reduces its four-top signature.

In the following, we will focus on the light pseudo-scalar octet case, and require its pole mass to be above 880 GeV to evade four-tops searches. Therefore, gluons

fusion proceeds both through pseudo-scalar octet loops and an additional contribution from 800 GeV right-handed stops (left-handed squarks and left-handed sbottom are heavier at 1.75 TeV and the first two right-handed generations are at 1 TeV). As a consequence, the mass of the stop is a critical parameter in enhancing $\sigma_{\gamma\gamma}$. We illustrate this dependence in Figure 5.6 where we plot the $S \to \gamma\gamma$ cross-section as a function of the stop one-loop mass, with fake leptons and sleptons close to the resonance with masses around 400 GeV.

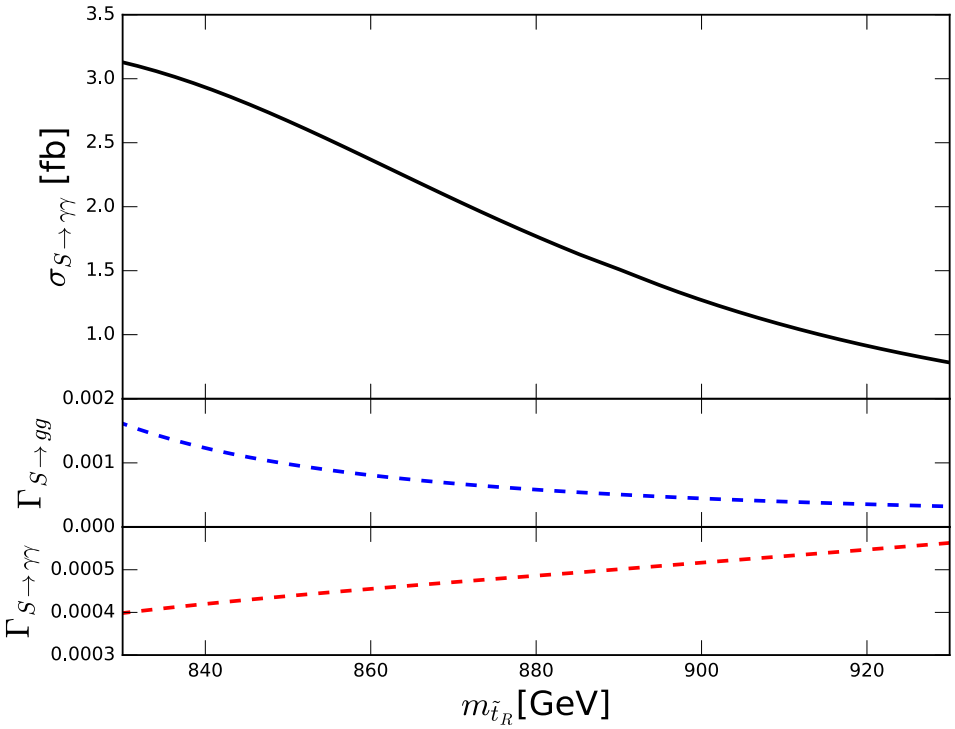

Figure 5.6: $S \to \gamma\gamma$ cross section in fb as a function of the one-loop mass for right-handed stop obtained by varying around the first benchmark point from Table 5.1. The lower part shows that the fast decrease of the amplitude to gluons is slightly counterbalanced by an increase in the amplitude to photons.

The decay $S \to \gamma\gamma$ proceeds both through loops of light right-handed sleptons (we consider left-handed sleptons above the TeV) controlled by $g' m_{1D}$ and loops of fake leptons, $\hat{E}, \hat{E}', R_u$ and R_d which are controlled by a unified Yukawa $\lambda_{SR} = \lambda_{SE} = 0.7$. Furthermore, the fake sleptons also contribute with couplings controlled by $g' m_{1D}$. In order to maximise the overall contribution, one has to take care that no cancellations occur between the various contribution (particularly for the D-terms induced couplings, which are proportional to the hypercharge of the scalar participating in the loop). Refering to Table 2.2 and 1.1 we see that one can for instance require light $\hat{E}$, R_d and $\tilde{e}_R$ and heavier $\hat{E}'$, R_u and left-handed sleptons.

In order to have a sizable contributions from the (fake) sleptons, we need reasonably large Dirac mass $m_{1D} \sim 1250$ GeV, this has the added benefit that it also enhances the squarks contribution to the scalar singlet production rate. On the other hand, it increases the tuning of λ_S necessary to have a small mixing and additionally implies that we have either a small $\tan\beta$ or a somehow large μ term as can be seen from Eq.(5.14). Overall, Figure 5.7 presents the cross-section obtained in the λ_S/μ_E plane by varying around the benchmark point of Table 5.1. Roughly speaking, this Figure combines on the x-axis the constraints from mixing with on the y-axis the requirement that the particles participating in the loop have masses close to the resonant one 750/2 GeV.[3]

We see from Figure 5.7 that the main requirement in our model is that we must consider values of λ_S tuned at the level of a few percent. This tuning is however, somehow mitigated from the fact that reproducing the Higgs mass already imposes that λ_S belongs to a limited range, as could be seen in Figure 5.3. We can also see that the constraint from the ratio $\Gamma_{ZZ}/\Gamma_{\gamma\gamma}$ are significantly weaker than the requirement on the cross-section. We further give in Table 5.1 one benchmark point, satisfying all

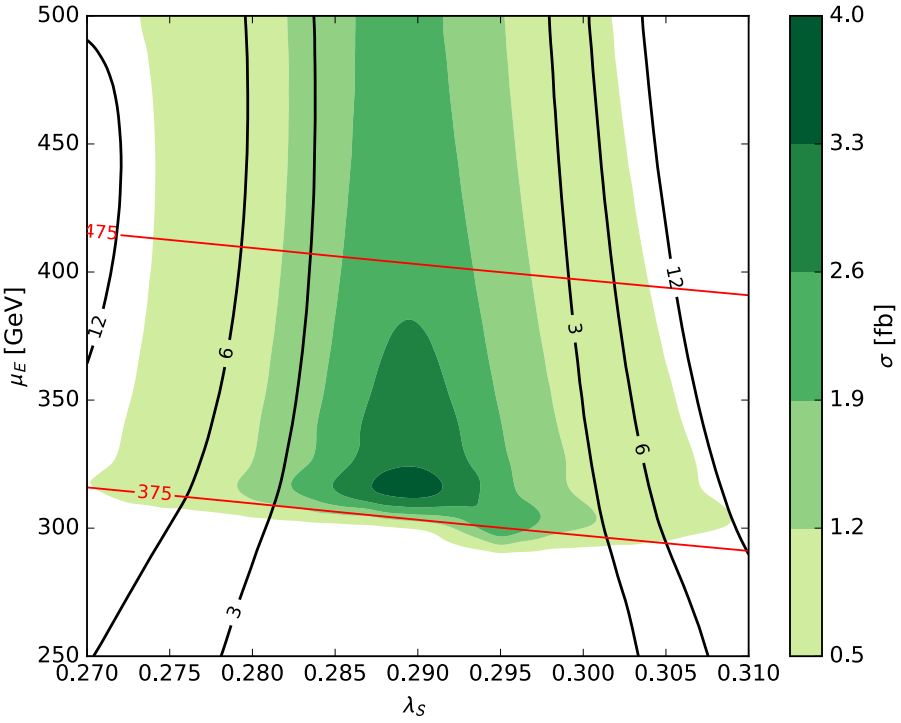

Figure 5.7: $S \to \gamma\gamma$ cross section in fb as a function of the μ_E and λ_S. The plot is based on the benchmark point of Table 5.1. The black contours show the most constraining ratio from (5.19) while the red contours shows the pole mass for the fake leptons.

[3]Notice that the fake lepton mass gets a sizeable contribution from the vev of S throught the λ_{SE} term.

the previously-mentioned constraints while retaining a $\gamma\gamma$ cross-section of order 4 fb.

	Parameter	Values
Higgs mass	μ	925 GeV
	$\tan\beta$	3
	λ_T	0.7
	m_T	500 GeV
Singlet masses and mixing	m_{1D}	1250 GeV
	m_S	500 GeV
	B_S	-2.44^2 TeV^2
	λ_S	0.29
Singlet decay /production amplitude to gg	T_{SO}	200 GeV
	m_O	1300 GeV
	$m_{\tilde{t}_R}$	500 GeV
Singlet decay amplitude to $\gamma\gamma$	$\lambda_{SR} = \lambda_{SE}$	0.7
	$m_E^2 = m_{R_{u,d}}^2$	10^2 GeV^2
	$\mu_E = \mu_{R_{u,d}}/1.4$	325 GeV
	$m_{\tilde{l}R}$	250 GeV
Outputs	Pole mass Higgs	125.5 GeV
	Pole mass S_R	750.1 GeV
	Pole mass O_I	945.5 GeV
	Pole mass $\tilde{t}_R$	820.3 GeV
	Pole mass $\tilde{l}_R$	418 GeV
	Pole mass $\hat{\tilde{E}}$	397 GeV
	$\sigma(S \to \gamma\gamma)$	**3.20 fb**
	$\Delta\rho$	0.97×10^{-4}
	v_S	151.4 GeV

Table 5.1: Benchmark point for our scenario. We further have, $B_\mu = 2.5^2$ TeV^2, the heavy left-handed squarks (as well as right-handed sbottom) have masses around 2.25 TeV. The two first generation of right-handed squarks have masses at 975 GeV, left-handed sleptons have masses at 1.5 TeV. We have $m_{2D} = 1200$ GeV, and $m_{3D} = 2.5$ TeV

3 Outlook

While the R-conserving scenario is very promising, it is nonetheless quite constrained to a small windows of values of λ_S, in order to have a small mixing with the Higgs and a sizeable cross-section to photons.

It is therefore interesting to relax the R-symmetry condition and allows for model which we can have simultaneously the couplings to the fake leptons and the trilinears T_{SE} and T_{SR}. Two promising scenarios which we will be further presented in [4] are

- $\not{R}_a$: Similar to the model presented above, but with additionally the couplings T_{SE}, T_{SR} and λ_{SO}.

- $\not{R}_b$: Similar to the model $\not{R}_a$, but we further tolerate the presence of a Majorana gluino mass term M_3.

It is interesting to note that in studying these R-conserving scenarios, we did not consider the possibility that the pseudo-scalar singlet S_I contributes to the overall cross-section. Since this field does not mix with the Higgs, it would have the additional benefit of reducing the constraints from mixing. As we have already discussed, this pseudo-scalar is not produced by gluons fusions in absence of a soft SUSY-breaking Majorana mass term for the gluinos. Since the model $\not{R}_c$ allows for the presence of such a mass, one can simultaneously produce the scalar S_R and pseudo-scalar S_I singlet and have a "double-peaks" resonance set-up.

Chapter 6

The Slow Gravitino

Lorentz symmetry is both a completely fundamental symmetry of nature and a blatantly broken one. Indeed, the boost symmetry underlying the construction of special relativity is broken as soon as one introduces a fluid whose four-velocity fixes the arrow of time. In this chapter we will see that when Lorentz symmetry as well as supersymmetry are broken by a fluid, the pseudo-particle generated by this breaking, called *phonino*, becomes the gravitino's longitudinal degrees of freedom. Crucially, these new degrees of freedom are slowed down by their interactions with the fluid while the original transverse ones are not, a feature we called "slow gravitino" in [5].

Such setups arise naturally when considering inflation in supergravity, since the scalar field describing the inflaton can be considered as an isotropic fluid. In particular it was shown in [103, 104, 105] that the equations of motion for a massive gravitino in a FLRW spacetime differed markedly between the spin-1/2 and spin-3/2 components. A feature similar to the slow "gravitino" case. These results have been successfully reproduced and extended in [106, 107, 108] using the constrained multiplet formalism of [109] (see also [110]).

On a more formal ground, constructing consistent Lagrangians for massive spin-3/2 is a difficult exercise. Indeed, apart from the supergravity gravitino, generic spin-3/2 massive particles suffer from acausal behaviour (more precisely, the Cauchy problem is not well defined) when coupled with electrodynamics, this is the Velo-Zwanziger problem [111](see also [112]). When attempting to construct massive spin-3/2 Lagrangian it makes therefore sense to try to build them *from* supergravity and to give a mass through a super-Higgs mechanism. This is precisely what we will describe in this chapter. We first show in section 1 how one can obtain a super-Higgs mechanism from thermal SUSY-breaking in supergravity. In section 2 we study the resulting Lorentz-violating Lagrangian per se, deriving the equations of motion for the physical components of the gravitino. Finally, section 3 is dedicated to the derivation of the covariant propagator.

1 Generating the Lagrangian for a Lorentz-invariant Low-energy SUSY

It has been known for a long time that supersymmetry is broken by thermal effects and is not restored in the high-temperator limit [113]. This is in line with the fact that fermions and bosons obey different statistics. It was proven in [114, 115] by working in the real time formalism that a massless goldstone fermion (goldstino) appears following supersymmetry breaking. This goldstino has been identified in certain cases with composite bilinear boson-fermion operators [116]. Later, this temperature goldstino has been called phonino [117] and has been subject to further studies where it became clear that this excitation was non-perturabative and has more to do with a "supersymmetric sound" (hence the name phonino) than with a fundamental particle (see for example [118, 119, 120, 121]).

The only feature of the phonino that is relevant for this work is that it has a non-relativistic kinetic term, dressed by the stress-energy tensor of the fluid [122], which involves the derivative $T^{\mu\nu}\gamma_{\mu}\partial_{\nu}$.

1.1 Akulov-Volkov Lagrangian for the Phonino

In section 2 chapter 1, we have presented the super-Higgs mechanism starting from the "pure" supergravity extension (see Eq.(1.19) of the same chapter) of the Akulov-Volkov Lagrangian for non-linearly realised supersymmetry. A procedure to obtain this Lagrangian was described by Deser and Zumino in [123]. We will now extend it to the case of a background fluid.

Keeping the conventions introduced in chapter 1, the usual (Lorentz invariant) Akulov-Volkov (AV) Lagrangian is given by:

$$\mathcal{L} = -\frac{1}{2}f^2 \det(W_{\mu}{}^{\nu}) \tag{6.1}$$

where f is a constant parameter and

$$W_{\mu}{}^{\nu} = \delta_{\mu}{}^{\nu} + \frac{\bar{G}}{f}\gamma_{\mu}\partial^{\nu}(\frac{G}{f}) \ .$$

This Lagrangian has been chosen such that under the supersymmetry transformation of constant parameter ϵ

$$\delta(\frac{G}{f}) = \epsilon + \xi^{\mu}\partial_{\mu}(\frac{G}{f}) \qquad \text{with} \qquad \xi^{\mu} = \bar{\epsilon}\gamma^{\mu}\frac{G}{f} \ , \tag{6.2}$$

we have $\delta(W_{\mu}{}^{\nu}) = \partial^{\nu}\xi_{\rho}W_{\mu}{}^{\rho} + \xi^{\rho}\partial_{\rho}W_{\mu}{}^{\nu}$, and

$$\delta(\mathcal{L}) = -\frac{1}{2}f^2\partial_{\mu}[\xi^{\mu}\det(W_{\rho}{}^{\sigma})] \ .$$

The Lagrangian (6.1) is therefore invariant up to total derivatives under the non-linear transformation (6.2). Expending (6.1) at first order in G^2, we obtain

$$\mathcal{L} = -\frac{1}{2}f^2 - \frac{1}{2}\bar{G}\gamma^{\mu}\partial_{\mu}G + \mathcal{O}(G^4) \ . \tag{6.3}$$

As the main new feature of the phonino is its kinetic term of the non-Lorentz-invariant form $T^{\mu\nu}\gamma_{\ \mu}\partial_\nu$, we will modify (6.3) to reproduce it. Defining T a normalisation factor, the non-linear Lagrangian yielding this kinetic term is given by:

$$\mathcal{L} \;=\; -\frac{1}{2}f^2\ \det\left[\delta_\mu^{\ \nu}-\frac{\bar{G}}{f}\frac{T_{\mu\rho}\gamma^\rho}{T}\partial^\nu(\frac{G}{f})\right]=-\frac{1}{2}f^2+\frac{1}{2}\bar{G}\frac{T^{\mu\nu}}{T}\gamma_{\ \mu}\partial_\nu G+\mathcal{O}(G^4)\ , \quad (6.4)$$

with the modified non-linear supersymmetry transformations,

$$\delta(\frac{G}{f}) \;=\; \epsilon+\xi^\mu\partial_\mu(\frac{G}{f}) \qquad \text{with} \qquad \xi^\mu \;=\; -\bar{\epsilon}\frac{T^{\mu\rho}\gamma_{\ \rho}}{T}\frac{G}{f}\ . \quad (6.5)$$

It is straightforward to verify that (6.4) transforms as a total derivative under (6.5).

1.2 Super-Higgs mechanism in a Fluid with Curved Background

The way forward is clear. First, we have to find the Lagrangian minimally coupling the AV Lagrangian (6.4) to gravity, mimicking the procedure of [123] in our Lorentz-violating case. In a second place, we will translate the calculation made in chapter 1 to realise the super-Higgs mechanism in a fluid.

a Perfect Fluid in Curved Background

To leading order in derivatives, the supergravity Lagrangian including the graviton, gravitino and goldstino fields is given by

$$\mathcal{L} \;=\; \frac{1}{2}e\left[\mathcal{L}_{\text{gravitino}}+\mathcal{L}_{\text{phonino}}+\mathcal{L}_{\text{mixing}}\right]+\mathcal{L}_{\text{f}}\ , \quad (6.6)$$

where e is the square root of the metric determinant and

$$\begin{aligned}\mathcal{L}_{\text{gravitino}} &= R-\bar{\psi}_\mu\gamma^{\mu\nu\rho}\nabla_\nu\psi_\rho\\ \mathcal{L}_{\text{phonino}} &= \bar{G}\frac{T^{\mu\nu}}{T}\gamma_{\ \mu}\nabla_\nu G\\ \mathcal{L}_{\text{mixing}} &= -\sqrt{2}\frac{T^{\mu\nu}}{\sqrt{T}M_P}\bar{G}\gamma_{\ \mu}\psi_\nu\ .\end{aligned}$$

Notice that the cosmological constant term of [123] have been replaced by an a priori unknown term $\mathcal{L}_{\text{f}}$ giving the contribution of the SUSY-breaking fluid. Since we want this Lagrangian to transform as a total derivative under the linear transformations :

$$\begin{cases}\delta e_\mu^a &= \frac{1}{2}M_P\bar{\epsilon}\gamma^{\ a}\psi_\mu\\ \delta\psi_\mu &= M_P\nabla_\mu\epsilon\\ \delta G &= \frac{\sqrt{T}}{\sqrt{2}}\epsilon\ ,\end{cases} \quad (6.7)$$

we should require

$$-2\delta(\mathcal{L}_{\text{f}}) \;=\; -M_P\bar{\epsilon}\gamma_{\ \mu}\psi_\nu[\frac{1}{M_P^2}T^{\mu\nu}]\ .$$

Let us show now that this is the case if $\mathcal{L}_{\rm f}$ describes an irrotational relativistic fluid (see [124] for a nice review). We denote by θ the scalar potential, α, β the Gauss potentials and j^μ the fluid density current. We can construct the particle number density n as

$$n \;=\; \sqrt{-g_{\mu\nu}j^\mu j^\nu}\;,$$

so that the fluid four-velocity u^μ satisfying $g_{\mu\nu}u^\mu u^\nu = -1$ is obtained from $j^\mu \equiv n\, u^\mu$.

We introduce a function $F(n)$ such that the (perfect) fluid energy density ϱ and pressure p are given as functions of n by $\varrho = F(n)$ and $p = nF'(n) - F(n)$. Then, the fluid Lagrangian can be written as:

$$\mathcal{L}_{\rm f} \;=\; -\frac{e}{M_P^2}\left[j^\mu(\partial_\mu\theta + \alpha\partial_\mu\beta) + F(n)\right] \tag{6.8}$$

in which only n is a function of the metric. The Lagrangian (6.8) is such that combined with the Einstein term $\frac{e}{2}R$ and using the equations of motion for[1] j^μ in the one for $g^{\mu\nu}$, we obtain the Einstein equations:

$$R_{\mu\nu} - \frac{1}{2}g_{\mu\nu}R \;=\; \frac{T_{\mu\nu}}{M_P^2} \;\equiv\; \frac{1}{M_P^2}\left[pg_{\mu\nu} + (\varrho + p)u_\mu u_\nu\right]\;, \tag{6.9}$$

with on the r.h.s we recognise the stress energy tensor of our perfect fluid. Notice that after integrating out j^μ, we have

$$\mathcal{L}_{\rm f} \;=\; -\frac{e}{M_P^2}\left[j^\mu(\partial_\mu\theta + \alpha\partial_\mu\beta) + F(n)\right] \;=\; \frac{ep}{M_P^2}\;. \tag{6.10}$$

The variation w.r.t α and β leads to current continuity equations describing the internal dynamics of the fluid.

The final Lagrangian (6.6) includes a "source" which will generate for instance a FLRW metric if the fluid is at rest. A similar Lagrangian has been obtained by [106] using a constrained multiplet from [109] in a minimal effective field theory for supersymmetric inflation. In that case the fluid stress energy tensor is represented by a scalar field with $p = \frac{1}{2}\dot\phi^2 - V(\phi)$. In the limit where the fluid is simply a cosmological constant, we recover the case from [125] that (6.6) can be embedded in a de Sitter supergravity action. Notice that is should be possible to construct a constrained multiplets version of the fluid Lagrangian $\mathcal{L}_f$, allowing to extend the results of [106] to a general fluid, albeit we will not attempt such construction here.

b Super-Higgs Mechanism in a Fluid

We are now ready to proceed to the super-Higgs mechanism by effectively trading the fluid part of the Lagrangian for a non-relativistic mass for the gravitino. We start by

[1] A priori, we should also include the contributions from phoninos and gravitinos. However we will always suppose that their contributions to the pressure and energy density are negligible so we can use

$$\partial_\mu\theta + \alpha\partial_\mu\beta = j_\mu\frac{F'(n)}{n}\;.$$

We have taken the convention that the pressure is negative to match the case of the cosmological constant. For a normal fluid, one should simply takes absolute value to define f.

adding to the Lagrangian above

$$-\mathcal{L}_{\rm f} + \frac{e}{2}\left[\frac{1}{2}\bar{\psi}_\mu \gamma^{\mu\nu\rho} n_{\nu\lambda}\gamma^{\lambda}\psi_\rho - \frac{T^{\mu\nu}}{2T} n_{\mu\nu}\bar{G}G\right] .$$

This is invariant under modified supergravity transformations obtained by replacing $\nabla_\mu \to \nabla_\mu - \frac{1}{2}n_{\mu\nu}\gamma^\nu$ under the condition that:

$$\gamma^{\mu\nu\rho}\ n_{\nu\lambda}\ n_{\rho\sigma}\gamma^{\lambda}\gamma^{\sigma} \ = \ \frac{2}{M_P^2}\tilde{T}^{\mu\nu}\gamma_\nu \ . \tag{6.11}$$

The total Lagrangian is given by:

$$\begin{aligned}\mathcal{L} = \frac{1}{2}e\Big[\ R + \bar{G}\frac{T^{\mu\nu}}{T}\gamma_\mu\nabla_\nu G - \sqrt{2}\frac{T^{\mu\nu}}{\sqrt{T}M_P}\bar{G}\gamma_\mu\psi_\nu - \bar{\psi}_\mu\gamma^{\mu\nu\rho}\nabla_\nu\psi_\rho \\ + \frac{1}{2}\bar{\psi}_\mu\gamma^{\mu\nu\rho}n_{\nu\lambda}\gamma^{\lambda}\psi_\rho - \frac{T^{\mu\nu}}{2T}n_{\mu\nu}\bar{G}G\ \Big] \ .\end{aligned} \tag{6.12}$$

with the supergravity transformations

$$\begin{cases}\delta e^a_\mu &= \frac{1}{2}M_P\bar{\epsilon}\gamma^a\psi_\mu \\ \delta\psi_\mu &= M_P(\nabla_\mu\epsilon - \frac{1}{2}n_{\mu\nu}\gamma^\nu\epsilon) \\ \delta G &= \frac{\sqrt{T}}{\sqrt{2}}\epsilon \ .\end{cases} \tag{6.13}$$

Notice that (6.12) is invariant under (6.13) only if we neglect derivatives in the fluid variables. A fully invariant Lagrangian can be nonetheless obtained even without neglecting them (see [126] for details). In the unitary gauge obtained by

$$\begin{cases}\delta e^a_\mu &= -\frac{1}{\sqrt{2T}}M_P\bar{G}\gamma^a\psi_\mu \\ \delta\psi_\mu &= -M_P(\nabla_\mu - \frac{1}{2}n_{\mu\nu}\gamma^\nu)\frac{\sqrt{2}G}{\sqrt{T}} \\ \delta G &= -G \ ,\end{cases}$$

the phonino is removed from the Lagrangian that becomes

$$\mathcal{L} = \frac{1}{2}e\left[\ R - \bar{\psi}_\mu\gamma^{\mu\nu\rho}(\nabla_\nu - \frac{n_{\nu\lambda}\gamma^\lambda}{2})\psi_\rho\ \right] \tag{6.14}$$

where $n_{\nu\lambda}$ satisfies (6.11). The gravitino acquires a mass similarly to the usual super-Higgs mechanism. A distinct feature, however, is that the mass terms are now space-time dependent and violates Lorentz invariance when $n_{\mu\lambda}$ is not proportional to $g_{\mu\nu}$. This Lagrangian had never been studied before and the next sections will be dedicated to thoroughly study its properties.

A key point is that we are now in *flat* space-time, the effect of the fluid on the gravitino have been completely translated in the Lorentz-violating mass term. Therefore, even if we will be using fluid-derived notations in the following, we will be in fact studying a particular Lagrangian for a massive spin-3/2 particle in flat spacetime. However, the intuitions one could gain by thinking in term of the original fluid variables will be instrumental in simplifying our equations, which explain the numerous reference to the "background" fluid in the next sections.

In general the parameter $n_{\mu\nu}$ are derived from a fluid and could be functions of space and time. However, for practical calculations, we will be interested in the case where we can neglect them. More precisely, we will require the gravitino wavelength to be smaller than the fluid scale of changes in the macroscopic variables, noted L, this imposes

$$\frac{1}{EL} \ll 1 \ . \tag{6.15}$$

This is required in order to be able to consider the gravitino as a localised particle with well-defined helicity states. Considering gravitinos with energy of the order of their mass, this last condition becomes

$$\frac{\sqrt{T}L}{M_p} \gg 1 \ . \tag{6.16}$$

In this approximation, we can neglect all derivatives of the fluid variables compared to the momentum or the mass of the gravitino.

2 Constraints and Equations of Motion for a Perfect Fluid Background

2.1 The Slow Gravitino Lagrangian

We will consider a perfect fluid with four-velocity u^μ and an equation of state

$$w \ = \ \frac{p}{\varrho} \ . \tag{6.17}$$

For $w \neq -1$ both supersymmetry and invariance under Lorentz boosts are spontaneously broken while $w = -1$ corresponds to a cosmological constant. From now on, we will neglect all derivatives of the fluid variables compared to the momentum or the mass of the gravitino and, when convenient, will trade the fluid variable w for

$$\epsilon_{\rm LV} \ \equiv \ 1 + w, \tag{6.18}$$

where $\epsilon_{\rm LV}$ measures the size of violation of Lorentz boost invariance. We also define at every point in space-time two projectors r and t by

$$\begin{aligned} r^{\mu\nu} \ &\equiv \ \eta^{\mu\nu} + u^\mu u^\nu \\ t^{\mu\nu} \ &\equiv \ (\mathbf{1} - r)^{\mu\nu} = -u^\mu u^\nu \ . \end{aligned} \tag{6.19}$$

t projects along u^μ, i.e. in the time-like direction defined by the fluid, while r projects on the vector space orthogonal to u^μ, i.e. on the spatial vector space defined by the fluid. Since our fluid is decribed by the Lagrangian (6.8), it is irrotational and its velocity does define a foliation of space-time that we can use to defined plane waves of the form $\psi^\mu \propto e^{ip^\mu x_\mu}$ with p^μ being functions of the space-time coordinates whose derivatives are neglected. This will allow us to define helicitiy eigenstates and construct the corresponding propagator.

Using the fluid foliation, we define the "spatial" and "temporal" components of the gamma matrices γ^μ and of the momentum p^μ, defined via using the projectors r and t. They are constructed as

$$\begin{aligned} r^\mu &= r^{\mu\nu}\gamma_\nu & k^\mu &= r^{\mu\nu}p_\nu \\ t^\mu &= t^{\mu\nu}\gamma_\nu & q^\mu &= t^{\mu\nu}p_\nu \ . \end{aligned}$$

r^μ and t^μ behave as γ^i and γ^0. They satisfy the relations $r^\mu r_\mu = 3$, $t^\mu t_\mu = 1$ and $t^\mu r^\nu = -r^\nu t^\mu$. We say that the fluid is "at rest" when these projections correspond to the usual spatial and temporal components, namely γ^i and γ^0 for γ^μ.

Using these objects, we can solve Eq. (6.11) and find

$$n_{\mu\nu} = \sqrt{\frac{\varrho}{3M_P^2}}\left(r_{\mu\nu} - \frac{3\epsilon_{\rm LV}-2}{2}t_{\mu\nu}\right) \ , \tag{6.20}$$

we then defined the would-be gravitino mass m as

$$m \ = \ \frac{\sqrt{3\varrho}}{4M_P}\,|\frac{4}{3} - \epsilon_{\rm LV}| \ . \tag{6.21}$$

Our Lagrangian (6.14) takes the simpler form:

$$\mathcal{L} \ = \ \frac{1}{2}\bar{\psi}_\mu\Big[\ (\gamma^{\mu\nu})(-\not{\partial} - m) + \gamma^\mu\partial^\nu - \gamma^\nu\partial^\mu - \frac{3\epsilon_{\rm LV}m}{4-3\epsilon_{\rm LV}}(r^\mu t^\nu + t^\mu r^\nu)\ \Big]\psi_\nu \ , \tag{6.22}$$

where we have defined the gravitino mass m. In (6.22) one identifies the first term with the usual Rarita-Schwinger Lagrangian and the term proportional to $\epsilon_{\rm LV}$ as the correction due to violation of Lorentz invariance.

2.2 Explicit Decomposition of a Spin-3/2 in Helicity-operator Eigenstates

The fact that we breaks Lorentz invariance makes the determination of the spin-3/2 degrees more involved. We start by deriving the explicit decomposition of a spin-3/2 particle in the case of a fluid at rest.

With our conventions $\tilde{S}^{\mu\nu}$ and $S^{\mu\nu}$ defined by

$$\tilde{S}^{\mu\nu} = \frac{\gamma^{\mu\nu}}{2} \ , \tag{6.23}$$

and

$$(S^{\mu\nu})^n_m = i(\delta^\mu_m\eta^{n\nu} - \delta^\nu_m\eta^{n\mu}) \ , \tag{6.24}$$

form a representation of the Lorentz group on the spinor and vector space respectively. The rotation generators on the spinor-vector representation are the $J_i = \frac{1}{2}\epsilon_{ijk}(\tilde{S}^{jk} + S^{jk})$, where ϵ_{ijk} is the fully antisymmetric tensor such that $\epsilon_{123} = 1$.

In particular, considering a momentum $p^\mu = (p^0, \vec{k})$ with $p^2 = k^2 - (p^0)^2$, the helicity operator along $\vec{k}$ is

$$\mathcal{S} \ \equiv \ \frac{k^i}{k}J_i = \frac{k^i}{k}(\frac{1}{2}\tilde{\Sigma}_i + \Sigma_i) \ , \tag{6.25}$$

where $k = \sqrt{k^2}$

$$\tilde{\Sigma}_i = i\gamma^0\gamma^5\gamma_i \ . \tag{6.26}$$

Eigenvectors of the helicity operator in the vector space are the ϵ'_0 and $\epsilon_0, \epsilon_+, \epsilon_-$ corresponding to $j = 0, h = 0$ and $j = 1, h = 0, +1, -1$ respectively (with helicity eigenvalues labeled by h and those of J^2 by $j(j+1)$). They are easily obtained when $\vec{k} = (0, 0, k)$ as

$$\epsilon'^{\mu}_0 = \frac{p^\mu}{|p|} \qquad \text{and} \qquad \epsilon_0{}^\mu = (\frac{k}{|p|}, 0, 0, \frac{p^0}{|p|}) \tag{6.27}$$

$$\epsilon_+{}^\mu = \frac{1}{\sqrt{2}}(0, -1, i, 0) \tag{6.28}$$

$$\epsilon_-{}^\mu = \frac{1}{\sqrt{2}}(0, 1, i, 0) \ , \tag{6.29}$$

where we have taken $|p| = \sqrt{-p^2}$. Also note that they are normalised by : $\epsilon'^{*\mu}_0 \epsilon'_{0\mu} = -1$ and $\epsilon^*_{0,+,-}{}^\mu \epsilon_{0,+,-\mu} = 1$. For a general $\vec{k}$ obtained by rotating with θ around the y axis and $-\phi$ around the z axis

$$p^\mu = \Big(p^0,\ k\cos\phi\sin\theta,\ k\sin\phi\sin\theta,\ k\cos\theta\Big) \ , \tag{6.30}$$

helicity eigenvectors are given by[2]:

$$\begin{aligned}
\epsilon'^{\mu}_0 &= \frac{p^\mu}{|p|} \\
\epsilon_+{}^\mu &= \frac{1}{\sqrt{2}}\,(0, -\cos\theta\cos\phi - i\sin\phi, -\cos\theta\sin\phi + i\cos\phi, \sin\theta) \\
\epsilon_-{}^\mu &= \frac{1}{\sqrt{2}}\,(0, \cos\theta\cos\phi - i\sin\phi, \cos\theta\sin\phi + i\cos\phi, -\sin\theta) \\
\epsilon_0{}^\mu &= \left(\frac{k}{|p|}, \frac{p^0}{|p|}\frac{\vec{k}}{k}\right) \ .
\end{aligned} \tag{6.31}$$

Finally, the spinor-vector representation of the Lorentz group (written as representation of $SU(2)_L \times SU(2)_R$ for a left-handed Weyl spinor) can be decomposed into spin representations as

$$(\frac{1}{2}, \frac{1}{2}) \otimes (\frac{1}{2}, 0) = \frac{1}{2} \oplus (1 \otimes \frac{1}{2}) = \frac{1}{2} \oplus \frac{1}{2} \oplus \frac{3}{2} \ , \tag{6.32}$$

In term of states, we can therefore decompose $|\psi\rangle$ as

$$\begin{aligned}
|\psi\rangle =& a_1 \left|\frac{1}{2}, \frac{1}{2}\right\rangle' + \tilde{a}_1 \left|\frac{1}{2}, -\frac{1}{2}\right\rangle' + a_2 \left|\frac{1}{2}, \frac{1}{2}\right\rangle + \tilde{a}_2 \left|\frac{1}{2}, -\frac{1}{2}\right\rangle \\
&+ a_3 \left|\frac{3}{2}, \frac{1}{2}\right\rangle + \tilde{a}_3 \left|\frac{3}{2}, -\frac{1}{2}\right\rangle + a_4 \left|\frac{3}{2}, \frac{3}{2}\right\rangle + \tilde{a}_4 \left|\frac{3}{2}, -\frac{3}{2}\right\rangle \ ,
\end{aligned} \tag{6.33}$$

[2]Since we have chosen the opposite signature from [127] and [128], helicity +1 and -1 eigenvectors are inverse compared to those of these authors.

where the prime notes the first spin-1/2 representation. Using the Clebsch-Gordon decomposition this last expression gives (6.43).

If we boost from the fluid rest frame to any frame, the eigenvector ϵ_0 becomes:

$$\epsilon_0^\mu = \frac{k}{|p|}u^\mu + \frac{q}{|p|k}k^\mu \ , \tag{6.34}$$

where we have $q^\mu = t^{\mu\nu}p_\nu$ and $k^\mu = r^{\mu\nu}p_\nu$ with $q = \sqrt{-q^2}$. The form of ϵ_+ and ϵ_- is complex in general, but we still have the property: $u_\mu\epsilon_\pm^\mu = 0$ since $u_\mu\epsilon_\pm^\mu$ is a Lorentz invariant.

2.3 The Constraints Equations

Since the spinor-vector representation of spin-3/2 particle contains too many degrees of freedom, we have to extract from the equations of motion the two constraints that reduce ψ_μ to the four degrees of freedom describing a massive spin-3/2 state.

The equation of motion for ψ_μ, obtained from the Lagrangian (6.22) is:

$$K^{\mu\nu}\psi_\nu = 0 \ , \tag{6.35}$$

with

$$K^{\mu\nu} \ \equiv \ (\gamma^\mu\gamma^\nu - \eta^{\mu\nu})(-\not\partial + m)\gamma^\nu\partial^\mu + \gamma^\mu\partial^\nu - \frac{3\epsilon_{\rm LV}}{4-3\epsilon_{\rm LV}}m(r^\mu t^\nu + t^\mu r^\nu) \ . \tag{6.36}$$

In the Rarita-Schwinger case, a first constraint is obtained by noting that the Lagrangian is linear in ψ_0, which therefore behaves as a Lagrange multiplier (see for example [112]). The Euler-Lagrange equation for ψ^0 gives the time component of the equation of motion. This is used as a constraint as it contains no time-derivative.

In the Lorentz-violating case, we identify the time direction as the one given by the "background fluid" four-velocity u^μ. We should therefore contract the equation of motion by u^μ to obtain the "zeroth-component". For calculation purposes we contract instead by $t^\mu = -\not u u^\mu$ and use $t^{\mu\nu} + t^\mu t^\nu = 0$ to obtain

$$[r^\mu r^\nu - r^{\mu\nu}]\,\partial_\mu\psi_\nu \ = \ -\frac{m}{1-\frac{3}{4}\epsilon_{\rm LV}}r^\rho\psi_\rho \ , \tag{6.37}$$

which indeed does not contain any time derivative (in the fluid frame).

Another constraint is obtained by contracting the equations of motion with $\mathcal{D}_\mu \equiv \partial_\mu - \frac{n_{\mu\lambda}\gamma^\lambda}{2}$. Using the condition (6.11) this constraint reduces to

$$T^{\mu\nu}\gamma_\mu\psi_\nu = 0 \ , \tag{6.38}$$

where replacing $T^{\mu\nu}$ by its expression and dividing by the energy density ϱ we obtain

$$(wr^\nu - t^\nu)\psi_\nu \ = \ 0 \ . \tag{6.39}$$

For a fluid at rest, (6.38) reads

$$\gamma^0\psi_0 = -(1-\epsilon_{\rm LV})\gamma^i\psi_i \ . \tag{6.40}$$

When taking $\epsilon_{\rm LV} = 0$, we recover the usual Rarita-Schwinger constraint:

$$\gamma^\mu \psi_\mu = 0 \ . \tag{6.41}$$

To summarise, we have exhibited two constraints (6.37) and (6.39) projecting out two spin-1/2 states. Notice that as expected there are important similarities (up to derivatives terms) of our constraints with those obtained for the case of a gravitino in a Friedmann-Robertson-Walker (FRW) space in [105].

2.4 Identification of the Spin-3/2 Degrees of Freedom

We are now ready to identify the four degrees of freedom of our spin-3/2 state and write them as two transverse (helicity-3/2) and two longitudinal (helicity-1/2) modes.

We first focus on the case where the fluid parameters are constant and work in the frame defined by the fluid background. In the last part of this section, we will generalise the result for an arbitrary fluid where both translation and rotational invariance are lost but with the extra assumption (6.16) implying that we can neglect derivatives in the "hydrodynamics" parameters.

In the constant fluid rest frame, the three-dimensional space is invariant under rotational and translation symmetries therefore both spin and helicity quantum numbers are well defined. We start with representations of the Lorentz group but, as the boosts transformations are no more symmetries, we will work with representations of the rotations symmetry group i.e. spin representations. The left-handed spinor-vector representation of the Lorentz group (written as an $SU(2)_L \times SU(2)_R$ representation) can be decomposed into spin representations as

$$(\frac{1}{2},\frac{1}{2}) \otimes (\frac{1}{2},0) = \frac{1}{2} \oplus (1 \otimes \frac{1}{2}) = \frac{1}{2} \oplus \frac{1}{2} \oplus \frac{3}{2} \ . \tag{6.42}$$

The l.h.s. expresses ψ^μ as a tensorial product of a vector times a spinor while the last expression is a spin decomposition that can be written explicitly as a linear combination of normalised spin eigenstates. Using the Clebsch-Gordon decomposition this leads to:

$$\begin{aligned}
\psi^\mu \ = \quad & \epsilon_0'^{\,\mu}\ \tilde{a}_1 \xi'_- + \epsilon_0'^{\,\mu}\ a_1 \xi'_+ \\
+ \quad & \frac{1}{\sqrt{3}} \epsilon_0{}^\mu (\tilde{a}_2 \xi_- - a_2 \xi_+) + \sqrt{\frac{2}{3}}\ (\epsilon_+^\mu\ a_2 \xi_- - \epsilon_-^\mu\ \tilde{a}_2 \xi_+) \\
+ \quad & \sqrt{\frac{2}{3}}\ \epsilon_0{}^\mu (\tilde{a}_3 \xi_- + a_3 \xi_+) + \frac{1}{\sqrt{3}} (\epsilon_+^\mu\ a_3 \xi_- + \epsilon_-^\mu\ \tilde{a}_3 \xi_+) \\
+ \quad & \epsilon_-^\mu\ \tilde{a}_4 \xi_- + \epsilon_+^\mu\ a_4 \xi_+ \ .
\end{aligned} \tag{6.43}$$

The two first lines correspond the extra spin-1/2 representations that need to be projected out of the spectrum. The third line is the helicity $\pm 1/2$ part, while the last line is the helicity $\pm 3/2$ part of the spin-3/2 representation of interest. The coefficients a_i and $\tilde{a}_i$ parametrise the decomposition as function of the product of polarisation vectors ϵ_i^μ and spinors ξ_i and ξ'_i. The indices of the latter vectors and spinors give their respective helicity eigenvalues in a self-explanatory way. The physical degrees of freedom must satisfy both constraints (6.37) and (6.39).

Let us define the useful notation n by

$$n \equiv \frac{4}{1-3w} m \ , \tag{6.44}$$

where w had been defined in (6.17). It is convenient to introduce a spinor that describes the longitudinal degrees of freedom of our spin-3/2 field. This is achieved by defining $\psi_{\frac{1}{2}}$ from our explicit construction (6.43) as

$$\psi_{\frac{1}{2}} \ \equiv \ \frac{n}{w|p|}(a_3\xi_+ + \tilde{a}_3\xi_-) \ , \tag{6.45}$$

where $|p| = \sqrt{-p^2}$. The overall coefficient ensures that $\psi_{\frac{1}{2}}$ has the canonically normalised kinetic term for a Majorana spinor.

We consider now the case of a time-varying fluid variables under the assumption (6.16). It is possible to find the corresponding form of $\psi_{\frac{1}{2}}$ either from the requirement that the constraints are satisfied or through an explicit construction. We shall use the former.

In order to identify among the various spin-1/2 representation the physical one, we consider an operator Π_μ that satisfies the constraints (6.37) and (6.39) written as:

$$\begin{array}{ll} C_1^\mu \Pi_\mu = 0 & \qquad\qquad C_1^\mu = wr^\mu - t^\mu \\ C_2^\mu \Pi_\mu = 0 & \text{with} \qquad C_2^\mu = (k^\mu - \not{k} r^\mu) + inr^\mu \ . \end{array} \tag{6.46}$$

Such Π_μ is given by

$$\Pi^\mu = (r^\mu - 3\frac{\not{k} k^\mu}{k^2}) + \frac{2}{in}k^\mu - \frac{2w}{in}\not{k} t^\mu \ , \tag{6.47}$$

and we will also define a conjugate operator as $\bar{\Pi}^\mu$ (note the change of sign of the last term)

$$\bar{\Pi}^\mu = (r^\mu - 3\frac{\not{k} k^\mu}{k^2}) + \frac{2}{in}k^\mu - \frac{2w}{in}\not{k} t^\mu \ , \tag{6.48}$$

Solutions of the constraints can then be obtained through projection by the operator $\mathcal{P}_{\frac{1}{2}}$ (note that $\mathcal{P}_{\frac{1}{2}}\mathcal{P}_{\frac{1}{2}} = \mathcal{P}_{\frac{1}{2}}$) defined by

$$\mathcal{P}_{\frac{1}{2}}^{\mu\nu} = \Pi^\mu (\bar{\Pi}^\rho \Pi_\rho)^{-1} \bar{\Pi}^\nu \ . \tag{6.49}$$

Using the constraint (6.39) we can calculate

$$\psi_{\frac{1}{2}}{}^\mu \ \equiv \ \mathcal{P}_{\frac{1}{2}}^{\mu\nu}\psi_\nu = \frac{\Pi^\mu}{2}\frac{in\not{k}}{k^2} \ r^\rho \psi_\rho \ , \tag{6.50}$$

which define the helicity-1/2 part $\psi_{\frac{1}{2}}{}^\mu$ of ψ^μ, which we exhibits in (6.43). We can write a corresponding spinor with the same degrees of freedom, a canonically normalised kinetic term in the Lagrangian, but without vector indices. It is obtained by contracting $\psi_{\frac{1}{2}}{}^\mu$ with u_μ. Comparing (6.45) with the expression we just obtain leads to

$$\psi_{\frac{1}{2}} = -\sqrt{\frac{3}{2}}\frac{n}{k}\not{u} \ r^\rho \psi_\rho \ , \tag{6.51}$$

and describes the longitudinal modes of the gravitino.

The helicity $\pm 3/2$ degrees of freedom can be identified as the remaining modes of ψ^μ after removing all three independent spin-1/2 states of the vector-spinor state. Such spinors can be constructed by applying on ψ^μ the three orthogonal projectors $\mathcal{P}_{ii}$:

$$\tilde{\mathcal{P}}^{\mu\nu}_{ii} = \frac{\tilde{\pi}^\mu_i \tilde{\pi}^\nu_i}{\tilde{\pi}^2_i} \ , \tag{6.52}$$

where $\tilde{\pi}^\mu_1$, $\tilde{\pi}^\mu_2$ and $\tilde{\pi}^\mu_3$ are orthogonal operators defined such that $\tilde{\pi}^\mu_i \tilde{\pi}_{j,\mu} = 0$ if $i \neq j$ by:

$$\begin{aligned} \tilde{\pi}^\mu_1 &= t^\mu \\ \tilde{\pi}^\mu_2 &= r^\mu \\ \tilde{\pi}^\mu_3 &= r^\mu - 3\frac{\not{k} k^\mu}{k^2} \ . \end{aligned} \tag{6.53}$$

Note that Π_μ can be expressed as a linear combination of these. The corresponding projector $\mathcal{P}_{\frac{3}{2}}$ is given by

$$\mathcal{P}^{\mu\nu}_{\frac{3}{2}} = \eta^{\mu\nu} - \tilde{\mathcal{P}}^{\mu\nu}_{33} - \tilde{\mathcal{P}}^{\mu\nu}_{22} - \tilde{\mathcal{P}}^{\mu\nu}_{11} \ , \tag{6.54}$$

and $\psi^\mu_{\frac{3}{2}} \equiv \mathcal{P}^{\mu\nu}_{\frac{3}{2}} \psi_\nu$ corresponds to the transverse degrees of freedom. This can be expressed as

$$\psi^\mu_{\frac{3}{2}} = \psi^\mu + \frac{1}{3} r^\mu r^\nu \psi_\nu + t^\mu t^\nu \psi_\nu + \frac{1}{6}(r^\mu - 3\frac{\not{k} k^\mu}{k^2})(r^\nu - 3\frac{\not{k} k^\nu}{k^2})\psi_\nu \ . \tag{6.55}$$

Using the fact that $r_\mu \psi^\mu_{\frac{3}{2}} = t_\mu \psi^\mu_{\frac{3}{2}} = k_\mu \psi^\mu_{\frac{3}{2}} = 0$, it is easy to check that $\psi^\mu_{\frac{3}{2}}$ satisfies the constraints (6.37) and (6.39) and also that $P^{\mu\nu}_{\frac{1}{2}} \psi_{\frac{3}{2}\ \nu} = 0$. We chose to keep the vector indices to remind of its spin-3/2 nature.

To summarise, in the space of solutions of the constraints (6.37) and (6.39), we have the decomposition

$$\psi^\mu = \psi^\mu_{\frac{3}{2}} + \Pi^\mu \frac{\not{k}\not{\psi}}{\sqrt{6}k} \psi_{\frac{1}{2}} = \mathcal{P}^{\mu\nu}_{\frac{3}{2}} \psi_\nu + \mathcal{P}^{\mu\nu}_{\frac{1}{2}} \psi_\nu \ , \tag{6.56}$$

where the two terms corresponds to the transverse and longitudinal modes of the spin-3/2 field.

While for the fluid at rest the helicity was defined as the projection on the globally defined direction corresponding to the space component of the particle momentum, the definition is more involved in the case of fluid not at rest as, in general, plane waves are no longer solutions of the equation of motion. However, helicity can be defined under the assumption (6.16).

In the rest frame the helicity operator is defined as:

$$\mathcal{S} \ = \ \frac{1}{2} \epsilon_{ijk} S^{ij} \partial^k \ , \tag{6.57}$$

where the $S^{\nu\rho}$ are the Lorentz generators for the spin-3/2 representation. This generalises to

$$\mathcal{S} \equiv \frac{1}{2}u^{\mu}\epsilon_{\mu\nu\rho\sigma}S^{\nu\rho}r^{\sigma\gamma}\partial_{\gamma} \ , \tag{6.58}$$

as $r^{\sigma\gamma}\partial_{\gamma}$ reduces to the space derivatives in the fluid rest frame. In a space-time varying fluid but with the assumption (6.16), locally we can treat the eigenstates wave-functions as plane waves. As a consequence, the above decomposition can be carried over and locally $\psi_{\frac{1}{2}}{}^{\mu}$ and $\psi_{\frac{3}{2}}{}^{\mu}$ appear as helicity eigenstates with eigenvalues respectively $\pm\frac{1}{2}$ and $\pm\frac{3}{2}$.

2.5 The Equations of Motion

Now that we have obtained the physical degrees of freedom $\psi_{\frac{1}{2}}$ and $\psi^{\mu}_{3/2}$, we can derive their equations of motion from the general ones (6.35) using the projector we defined in the previous sections.

The equation of motion for ψ^{μ} derived from the Lagrangian are given in (6.35). In order to extract those for the $\psi_{\frac{1}{2}}$ and $\psi^{\mu}_{3/2}$, it is useful to use the identity

$$[-\gamma^{\nu}\partial^{\mu}+\gamma^{\mu}\partial^{\nu}]\psi_{\nu}-[t^{\mu}r^{\nu}+r^{\mu}t^{\nu}](\not{\partial}-n)\psi_{\nu}=-i\bar{C}_2^{\mu}\gamma^{\nu}\psi_{\nu} \ , \tag{6.59}$$

where $\bar{C}_2^{\mu}$ is given by:

$$\bar{C}_2^{\mu}=k^{\mu}-r^{\mu}\not{k}+inr^{\mu} \ . \tag{6.60}$$

Plugging (6.59) in (6.35) leads to

$$\left[(-r^{\mu}r^{\nu}+r^{\mu\nu})(-\not{\partial}+m)+\bar{C}_2^{\mu}\gamma^{\nu}\right]\psi_{\nu}=0 \ , \tag{6.61}$$

which will be used to derive the equations of motion for both helicities 1/2 and 3/2.

We first focus on the helicity-1/2 degrees of freedom. We can get rid of the term proportional to $\bar{C}_2^{\mu}$ by contracting (6.61) with $\bar{\Pi}^{\mu}$ defined in (6.48). Two parts of the equations are obtained through splitting the derivative in the l.h.s. to the time-like and space-like parts. A bit of algebra allows to rewrite the space-like part, along with the mass term, as

$$\bar{\Pi}_{\mu}(-r^{\mu}r^{\nu}+r^{\mu\nu})(-i\not{k}+m)\psi_{\nu}=-\sqrt{6}\frac{\not{k}\not{v}}{k}(iv\not{k}-m)\psi_{\frac{1}{2}} \ . \tag{6.62}$$

On the other side, the time-like part, using the decomposition (6.56) , can be expressed as

$$-i\bar{\Pi}_{\mu}(-r^{\mu}r^{\nu}+r^{\mu\nu})\not{q}\psi_{\nu}=+i\sqrt{6}\frac{\not{k}\not{v}\not{k}}{k}\not{q}\psi_{\frac{1}{2}} \ . \tag{6.63}$$

Putting back both parts together leads to the equation of motion for the longitudinal mode:

$$(t^{\rho}\partial_{\rho}-wr^{\rho}\partial_{\rho}+m)\psi_{\frac{1}{2}}=0 \ . \tag{6.64}$$

In order to derive the equation of motion for the transverse degrees of freedom, we act on (6.61) with the operator $\mathcal{P}_{\frac{3}{2}}$ to obtain

$$(i\not{q} + i\not{k} + m)\psi_{\frac{3}{2}}{}^{\mu} = 0 \ , \tag{6.65}$$

which can be written:

$$(t^{\rho}\partial_{\rho} + r^{\rho}\partial_{\rho} \ + m)\psi_{\frac{3}{2}}{}^{\mu} = 0 \ . \tag{6.66}$$

The equations of motion (6.64) and (6.66) derived above can also be obtained from the Lagrangian

$$\mathcal{L} \ = \ \frac{1}{2}\bar{\psi}_{\frac{3}{2}\ \mu}(\gamma^{\rho}\partial_{\rho} + m)\psi_{\frac{3}{2}}{}^{\mu} + \frac{1}{2}\bar{\psi}_{\frac{1}{2}}(t^{\rho}\partial_{\rho} - wr^{\rho}\partial_{\rho} + m)\psi_{\frac{1}{2}} \ , \tag{6.67}$$

where we verify that the factors in the definition of $\psi_{\frac{1}{2}}$ were necessary for obtaining a canonically normalised kinetic term. The two spinors have obviously different dispersion relations. An important comment is that if we had not neglected the derivatives of the fluid parameters, the previous Lagrangian would not be hermitian. Furthermore an interesting consequence of these two equations of motion is that helicity-1/2 and 3/2 cannot be on-shell simultaneously when $\epsilon_{\text{LV}} \neq 0$.

3 The Covariant Spin–3/2 Propagator

If the non-relativist spin-3/2 that we have described is coupled to other particles, it will transmit the Lorentz-violation to the rest of the spectrum through loops diagrams. It is therefore particularly important to derive a complete expression for its propagator.

As in the previous sections, we assume the approximation (6.16) so that we can use plane wave solutions of momentum p^{μ}.

Our strategy will consist of writing the Lagrangian in a basis of projectors adapted to the degrees of freedom of our problem. It is convenient to use as basis the π_i^{μ}, $(i = 1, 2, 3)$ defined by

$$\begin{aligned} \pi_1^{\mu} &= p^{\mu} \\ \pi_2^{\mu} &= \not{k}(t^{\mu} - \frac{\not{q}p^{\mu}}{p^2}) \\ \pi_3^{\mu} &= r^{\mu} - \frac{\not{k}k^{\mu}}{k^2} \ . \end{aligned} \tag{6.68}$$

In making calculations, it is helpful to use the commutations or anti-commutations properties of the operators π_i with $\not{k}$, $\not{p}$ and $\not{q}$ which are (omitting the Lorentz index for clarity) given by:

$$\pi_1\not{k} = \not{k}\pi_1 \qquad \pi_1\not{q} = \not{q}\pi_1 \tag{6.69}$$

$$\pi_2\not{k} = -\not{k}\pi_2 \qquad \pi_2\not{q} = -\not{q}\pi_2 \tag{6.70}$$

$$\pi_3\not{k} = -\not{k}\pi_3 \qquad \pi_3\not{q} = -\not{q}\pi_3 \ . \tag{6.71}$$

	$\mathcal{P}_{11}$	$\mathcal{P}_{12}$	$\mathcal{P}_{13}$	$\mathcal{P}_{21}$	$\mathcal{P}_{22}$	$\mathcal{P}_{23}$	$\mathcal{P}_{31}$	$\mathcal{P}_{32}$	$\mathcal{P}_{33}$
$\mathcal{P}_{11}$	$\mathcal{P}_{11}$	$\mathcal{P}_{12}$	$\mathcal{P}_{13}$	0	0	0	0	0	0
$\mathcal{P}_{21}$	$\mathcal{P}_{21}$	$\mathcal{P}_{22}/(\pi_1^2\pi_2^2)$	$\mathcal{P}_{23}/(\pi_1^2)$	0	0	0	0	0	0
$\mathcal{P}_{31}$	$\mathcal{P}_{31}$	$\mathcal{P}_{32}/(\pi_1^2)$	$\mathcal{P}_{33}/(\pi_1^2\pi_2^2)$	0	0	0	0	0	0
$\mathcal{P}_{12}$	0	0	0	$\mathcal{P}_{11}/(\pi_1^2\pi_2^2)$	$\mathcal{P}_{12}$	$\mathcal{P}_{13}/(\pi_2^2)$	0	0	0
$\mathcal{P}_{22}$	0	0	0	$\mathcal{P}_{21}$	$\mathcal{P}_{22}$	$\mathcal{P}_{23}$	0	0	0
$\mathcal{P}_{32}$	0	0	0	$\mathcal{P}_{31}/(\pi_2^2)$	$\mathcal{P}_{32}$	$\mathcal{P}_{33}/(\pi_1^2\pi_2^2)$	0	0	0
$\mathcal{P}_{13}$	0	0	0	0	0	0	$\mathcal{P}_{11}/(\pi_1^2\pi_3^2)$	$\mathcal{P}_{12}/(\pi_3^2)$	$\mathcal{P}_{13}$
$\mathcal{P}_{23}$	0	0	0	0	0	0	$\mathcal{P}_{21}/(\pi_3^2)$	$\mathcal{P}_{22}/(\pi_3^2\pi_2^2)$	$\mathcal{P}_{23}$
$\mathcal{P}_{33}$	0	0	0	0	0	0	$\mathcal{P}_{31}$	$\mathcal{P}_{32}$	$\mathcal{P}_{33}$

Table 6.1: Contraction rules for the nine projectors $\mathcal{P}_{i,j}$, the extra-factors of π_i^2 comes from the normalisation of the nilpotent operators.

We can then define three projectors $\mathcal{P}_{i,i}$ as

$$\mathcal{P}_{i,i}^{\mu\nu} = \frac{\pi_i^\mu \pi_i^\nu}{\pi_i^2} \ , \tag{6.72}$$

and supplement them by nilpotent operators $\mathcal{P}_{i,j}$ with $i \neq j$ defined by

$$\mathcal{P}_{i,j}^{\mu\nu} = \frac{\pi_i^\mu \pi_j^\nu}{\pi_i^2 \pi_j^2} \ , \tag{6.73}$$

The contraction rules of this set of projectors is straightforward and can be summarised in Table 1. We supplemented this set of projector by $\mathcal{P}_{\frac{3}{2}}$ defined such that:

$$\mathcal{P}_{\frac{3}{2}}^{\mu\nu} + \mathcal{P}_{33}^{\mu\nu} + \mathcal{P}_{22}^{\mu\nu} + \mathcal{P}_{11}^{\mu\nu} = \eta^{\mu\nu} \ . \tag{6.74}$$

We use the identities

$$p^\mu = \pi_1^\mu \qquad\qquad \gamma^\mu = \frac{\not{p}}{p^2}\pi_1^\mu + \frac{\not{p}}{k^2}\pi_2^\mu + \pi_3^\mu \tag{6.75}$$

$$k^\mu = \frac{k^2}{p^2}\pi_1^\mu + \frac{\not{k}\not{q}}{k^2}\pi_2^\mu \qquad\qquad r^\mu = \frac{\not{k}}{p^2}\pi_1^\mu + \frac{\not{q}}{k^2}\pi_2^\mu + \pi_3^\mu \tag{6.76}$$

$$q^\mu = \frac{q^2}{p^2}\pi_1^\mu - \frac{\not{k}\not{q}}{k^2}\pi_2^\mu \qquad\qquad t^\mu = \frac{\not{q}}{p^2}\pi_1^\mu + \frac{\not{k}}{k^2}\pi_2^\mu \ , \tag{6.77}$$

and a bit algebra to express $K^{\mu\nu}$ as a function of the $\mathcal{P}_{ij}^{\mu\nu}$. We can write

$$K^{\mu\nu} = (\not{p} + m)(\mathcal{P}_{3/2}^{\mu\nu} - \mathcal{P}_{33}^{\mu\nu}) - U(\mathcal{P}_{13}^{\mu\nu} - \mathcal{P}_{31}^{\mu\nu}) + V(\mathcal{P}_{23}^{\mu\nu} - \mathcal{P}_{32}^{\mu\nu}) - W(\mathcal{P}_{12}^{\mu\nu} - \mathcal{P}_{21}^{\mu\nu}) \ , \tag{6.78}$$

with

$$W = -nk^2 \tag{6.79}$$

$$U = 2(\not{k}m + \not{q}n) \tag{6.80}$$

$$V = 2\frac{k^2}{p^2}(ip^2 + m\not{q} + n\not{k}) \ . \tag{6.81}$$

The second calculation trick is to define a conjugation relation by

$$\overline{A} = \overline{a_1 + \not{k} a_2 + \not{q} a_3} = a_1 - \not{k} a_2 - \not{q} a_3 \ , \tag{6.82}$$

this operation satisfies all the usual properties of conjugation $\overline{AB} = \overline{A}\ \overline{B}$, $\overline{A+B} = \overline{A} + \overline{B}$, and we have also

$$|A|^2 = A\overline{A} = a_1^2 + k^2 a_2^2 + q^2 a_3^3 \ , \tag{6.83}$$

which enables us to obtain the inverse as

$$A^{-1} = \frac{\overline{A}}{A\overline{A}} = \frac{a_1 - \not{k} a_2 - \not{q} a_3}{a_1^2 + k^2 a_2^2 + q^2 a_3^3} \ . \tag{6.84}$$

This formula uses the assumption that all parameters a_i are scalars. If A is such that $a_1 = a_1' + \not{k}\not{q} a_1''$ the previous formula makes little sense. However, it is always possible in this case to factorise $A = A_1 A_2$ where A_1 and A_2 have only scalar coefficients.[3]

A crucial observation is that thanks to the relations (6.69), the (anti)commutation relations between the operators π_i and A are

$$\begin{aligned} \pi_1^\mu A &= A \pi_1^\mu \\ \pi_2^\mu A &= \overline{A} \pi_2^\mu \\ \pi_3^\mu A &= \overline{A} \pi_3^\mu \ , \end{aligned} \tag{6.85}$$

which allows to make all the calculations using the A form without decomposing it in $\not{k}$ or $\not{q}$ parts. The decomposition of the propagator on the projectors basis can be written as

$$\begin{aligned} G^{\mu\nu} = \frac{m - i\not{p}}{m^2 + p^2} \mathcal{P}_{\frac{3}{2}}^{\mu\nu} + A\ \mathcal{P}_{11}^{\mu\nu} + B\ \mathcal{P}_{22}^{\mu\nu} + C\ \mathcal{P}_{33}^{\mu\nu} + D\ \mathcal{P}_{13}^{\mu\nu} + D'\ \mathcal{P}_{31}^{\mu\nu} \\ + E\ \mathcal{P}_{23}^{\mu\nu} + E'\ \mathcal{P}_{32}^{\mu\nu} + F\ \mathcal{P}_{12}^{\mu\nu} + F'\ \mathcal{P}_{21}^{\mu\nu} \ . \end{aligned} \tag{6.86}$$

The propagator satisfies

$$K_{\mu\rho} G^{\rho\nu} = \eta_\mu^{\ \nu} \ . \tag{6.87}$$

Expanded it in the projectors basis leads to a system of nine equations

$$\begin{aligned} (33) \quad & -(i\not{p} + m) C - (\pi_2 \pi_3)^{-2} V E + (\pi_1 \pi_3)^{-2} U \overline{D} = 1 \\ (32) \quad & -(i\not{p} + m) E' - (\pi_1)^{-2} U \overline{F} - V B = 0 \\ (31) \quad & -(i\not{p} + m) D' - (\pi_2)^{-2} V F' + U \overline{A} = 0 \\ (23) \quad & (i\pi_1)^{-2} W \overline{D} + V C = 0 \\ (22) \quad & (i\pi_2 \pi_3)^{-2} V E' + (\pi_1 \pi_2)^{-2} W \overline{F} = 1 \\ (21) \quad & (\pi_3)^{-2} V D' + W \overline{A} = 0 \\ (13) \quad & -(\pi_2)^{-2} W \overline{E} - U \overline{C} = 0 \\ (12) \quad & -(\pi_3)^{-2} U \overline{E}' - W \overline{B} = 0 \\ (11) \quad & -(\pi_1 \pi_3)^{-2} U \overline{D}' - (\pi_1 \pi_2)^{-2} W \overline{F}' = 1 \ . \end{aligned} \tag{6.88}$$

[3] If we had $C = c_1 + c_1' \not{k}\not{q} + c_2 \not{k} + c_3 \not{q}$, one can easily check that $C = (c_3 + c_1' \not{k} + (\frac{c_2 c_3}{c_1'} - c_1) \frac{1}{q^2} \not{q})(\frac{c_2}{c_1'} + \not{q})$ is such a decomposition.

We make the assumption that U, V and W contains no terms in $\not{k}\not{q}$ (if it was not the case, one should first factorised it, then inverse both terms using (6.84) and do the same to inverse X). We define the quantity X by

$$X = -(\not{p} + m) + \frac{1}{\pi^3 W}(VW\overline{U} - U\overline{W}V) \ . \tag{6.89}$$

This expression has no terms in $\not{k}\not{q}$. Indeed, if A and B do not have $\not{k}\not{q}$ terms, then it is easily seen that $AB + BA$ also does not have $\not{k}\not{q}$ terms and that $AB + \overline{BA}$ is a pure scalar using the product formula

$$\begin{aligned}(a_1 + a_2\not{k} + a_3\not{q})(b_1 + b_2\not{k} + b_3\not{q}) = (a_1b_1 - a_2b_2k^2 - a_3b_3q^2) + (a_2b_1 + a_1b_2)\not{k} \\ + (a_3b_1 + a_1b_3)\not{q} + (a_2b_3 - b_2a_3)\not{k}\not{q} \ .\end{aligned} \tag{6.90}$$

Since we can write

$$VW\overline{U} - U\overline{W}V = V(W\overline{U}) + (W\overline{U})V - (W\overline{U} + U\overline{W})V \ , \tag{6.91}$$

we conclude that one can apply the formula (6.84) on X and solve the system of equations as

$$\begin{aligned}
A &= \frac{\pi_1^2}{\pi_3^2}\frac{W}{|W|^2}\overline{V}\frac{X}{|X|^2}\overline{V}\frac{\overline{W}}{|W|^2} \\
B &= \frac{\pi_2^2}{\pi_3^2}\frac{W}{|W|^2}\overline{U}\frac{\overline{X}}{|X|^2}U\frac{\overline{W}}{|W|^2} \\
C &= \frac{\overline{X}}{|X|^2} \\
D &= -\pi_1^2\frac{W}{|W|^2}\overline{V}\frac{X}{|X|^2} & D' &= -\pi_1^2\frac{\overline{X}}{|X|^2}V\frac{W}{|W|^2} \\
E &= -\pi_2^2\frac{W}{|W|^2}\overline{U}\frac{\overline{X}}{|X|^2} & E' &= -\pi_2^2\frac{\overline{X}}{|X|^2}U\frac{\overline{W}}{|W|^2} \\
F &= \pi_1^2\pi_2^2(\frac{W}{|W|^2} + \frac{1}{\pi_3^2}\frac{W}{|W|^2}\overline{V}\frac{X}{|X|^2}\overline{U}\frac{W}{|W|^2}) \\
F' &= \pi_1^2\pi_2^2(-\frac{W}{|W|^2} + \frac{1}{\pi_3^2}\frac{W}{|W|^2}\overline{U}\frac{\overline{X}}{|X|^2}V\frac{W}{|W|^2})
\end{aligned} \tag{6.92}$$

Replacing these expression in the propagator, we can in fact factorise most of these terms and obtain:

$$\begin{aligned}G^{\mu\nu} = \frac{m - i\not{p}}{p^2 + m^2}\mathcal{P}^{\mu\nu}_{\frac{3}{2}} + \frac{1}{\pi_3^2}\left[\frac{W}{|W|^2}\overline{V}\pi_1^\mu + \frac{W}{|W|^2}\overline{U}\pi_2^\mu - \pi_3^\mu\right]\frac{X}{|X|^2}\left[\overline{V}\frac{\overline{W}}{|W|^2}\pi_1^\nu + \overline{U}\frac{W}{|W|^2}\pi_2^\nu - \pi_3^\nu\right] \\ + \frac{W}{|W|^2}(\pi_1^\mu\pi_2^\nu - \pi_2^\mu\pi_1^\nu) \ .\end{aligned} \tag{6.93}$$

If we replace U, V and W by their expression in our case we observe first that X simplifies in

$$X = 3(m - wi\not{k} + i\not{q}) \ , \tag{6.94}$$

which indeed does not include $\not{k}\not{q}$ terms.

Our final result can be expressed as:

$$G^{\mu\nu} = \frac{\Pi^{\mu\nu}_{\frac{3}{2}}}{p^2+m^2} + \frac{\Pi^{\mu\nu}_{\frac{1}{2}}}{w^2k^2+q^2+m^2} - \frac{3}{4}\epsilon_{\rm LV}\frac{\not{k}}{mk^2}(t^\mu k^\nu - k^\mu t^\nu) \ . \tag{6.95}$$

where the two polarisations take the form

$$\Pi^{\mu\nu}_{\frac{3}{2}} = (m - i\not{p})\mathcal{P}^{\mu\nu}_{\frac{3}{2}} \ , \tag{6.96}$$

and

$$\Pi^{\mu\nu}_{\frac{1}{2}} = \frac{2}{3}\ \Lambda^\mu\ (i\not{p} - \epsilon_{\rm LV} i\not{k} + m)\ \Lambda^\nu \ , \tag{6.97}$$

where

$$\Lambda^\mu = \gamma^\mu - i\frac{p^\mu}{n} - \frac{3}{2}(r^\mu - \frac{\not{k}k^\mu}{k^2}) - \frac{3}{4}\epsilon_{\rm LV}t^\mu \ , \tag{6.98}$$

Note that we recover again that the part corresponding to the spin-1/2 components of the spinor-vector has a pole for $m^2 + w^2k^2 + q^2 = 0$ due to a different dispersion relation. A crucial observation is that the nominator of the helicity-1/2 poles indeed projects on the physical degrees of freedom. More precisely one can show that

$$\Pi^{\mu\nu}_{\frac{1}{2}}\psi_\mu = \Pi^{\mu\nu}_{\frac{1}{2}}\psi_{\ \frac{1}{2}\ \mu} \ . \tag{6.99}$$

Furthermore, we can relate $\Pi^{\mu\nu}_{\frac{3}{2}}$ to the Rarita-Schwinger polarisation tensor $\Pi^{\mu\nu}_{RS}$ defined as

$$\Pi^{\mu\nu}_{RS} = (m - i\not{p})[\eta^{\mu\nu} - \frac{1}{3}\gamma^\mu\gamma^\nu + 2\frac{p^\mu p^\nu}{3m^2}i\frac{\gamma^\mu p^\nu - \gamma^\nu p^\mu}{3m}] \ , \tag{6.100}$$

by

$$\mathcal{P}^{\mu\nu}_{\frac{3}{2}} = \Pi^{\mu\nu}_{RS} - \frac{2}{3}[\Lambda^\mu + \frac{3}{4}\epsilon_{\rm LV}(t^\mu - i\frac{p^\mu}{m})](i\not{p} + m)[\Lambda^\nu + \frac{3}{4}\epsilon_{\rm LV}(t^\nu - i\frac{p^\nu}{m})] \ . \tag{6.101}$$

This expression makes explicit the fact that our propagator reduces to the usual Rarita-Schwinger result when $\epsilon_{\rm LV} = 0$.

The modification of the Rarita-Schwinger propagator due to Lorentz symmetry breaking appears both in the spin-3/2 and 1/2 contributions. When $\epsilon_{\rm LV} = 0$, we recover the usual Rarita-Schwinger formula [129].

We finally consider the limit of high momentum where we have the hierarchy

$$m \ \ll\ |p| \ \ll\ \mathcal{T} \ , \tag{6.102}$$

the propagator then simplifies to

$$G^{\mu\nu} \to -\mathcal{P}^{\mu\nu}_{\frac{3}{2}}\frac{i\not{p}}{p^2} - \frac{2}{3}\frac{p^\mu p^\nu}{n^2}\frac{i\not{q} - wi\not{k}}{q^2+w^2k^2} \ . \tag{6.103}$$

4 Conclusion

In this chapter, based on the super-Higgs mechanim in a fluid, we have constructed a new Lagrangian describing the propagation of a spin-3/2 with a non-Lorentz invariant mass term. We have the studied this Lagrangian per se and shown that it exhibits a feature common with spin-3/2 propagating in a curved space: the longitudinal modes ($\pm 1/2$ helicities) propagate at a slower speed, hence the "slow gravitino" name.

While we have studied our Lagrangian purely in flat space-time. The results we have found match almost perfectly the results from [103, 104, 105, 106, 107] concerning the propagation of gravitinos in a curved inflation background. It would be very interesting to understand in more details the links between the two scenarios.

From the more academic point of view our Lagrangian can be studied per se as an example of a consistent, non-Lorentz invariant, Lagrangian for a massive spin 3/2 particles. Indeed, since it is build from a super-Higgs mechanism, it should be free of the Velo-Zwanziger problem, it would be interesting to check this explicitly. Furthermore, it is clear that more investigations are needed on how this "slow" gravitino will transmit Lorentz-violating effect to our visible world and more generally, how to couple fluids to supergravity.

Chapter 7
Swift Graviton

In General Relativity, the presence of matter always tends to slow down signal propagation. A practical check of this broad statement is the Shapiro time delay, one of the classic solar system experimental verification of General Relativity. An observer on Earth sends a electromagnetic signal to bounce on another planet and measures the time needed for the return trip. The effect of the curvature of space-time will be to lengthen the trip with respect to what would have expected in Newtonian gravity corresponding to flat space-time.

The intuitive definition for a "fast" (namely superluminal) travel, would be to compare the observed propagation speed in a given setup with the one in flat Minkowski space-time. To do so, however, one would need a way to compare "locations" between two different spacetimes, a notoriously difficult exercise due to diffeomorphism invariance. An additional difficulty is that one can construct *any* spacetime once sufficiently exotic matter is considered, as the Einstein equations only related the curvature tensors to the stress-energy one. Therefore, we must always consider that a definition of fast travel should come together with a condition on what "reasonable" matter should look like. One such energy condition is the weak (resp. null) energy condition which requires the stress-energy tensor $T_{\mu\nu}$ to satisfy:

$$T_{\mu\nu}k^\mu k^\nu \geqslant 0 \ , \tag{7.1}$$

where k^μ is a time-like (resp. null) vector. Armed with these inequalities, one can then write various theorems about "fast travel" in General Relativity based on the study of null geodesics.

In extended gravity, when General Relativity is modified, the boundary of the causal future of a point p are in general not determined by null geodesics but by the characteristics hypersurfaces passing by p. Loosely speaking, characteristics are defined as the hypersurfaces on which the Cauchy problem is not well-defined. In general these hypersurfaces are different from null hypersurfaces, leading to the possibility of superluminal propagation, even when the appropriate energy conditions are considered. This has been known for a long time in the simple case of Lovelock theories [130, 131]. In this chapter, we will consider extended gravity theories described by Lagrangians in D spacetime dimensions of the form ($c = \hbar = 1$):

$$\mathcal{L} = \frac{1}{16\pi\ell_P^{D-2}}\sqrt{-g}(R + \ell_2^2\left[R^2\right] + \ell_3^4\left[R^3\right] + \ell_4^6\left[R^4\right]), \tag{7.2}$$

where g is the determinant of the metric $g_{\mu\nu}$, ℓ_P is the Planck length, l_i are dimensionful coupling constants and $[R^n]$ is a linear combination of contractions of n Riemann tensors.[1] We will focus on theories with $\ell_i \gg \ell_P$, and consider the propagation of gravitons of energy $E \sim \ell_i^{-1}$, in which case all the different terms in (7.2) are important.

1 The Background Metric and Graviton Equations of Motion

Since our goal is to study extended gravity theories as generic as possible, we must consider a background as simple as possible so that it could remain a solution of the extended Einstein equations. We will consider the background metric induced by an axisymmetric source beam. The idea is to model a stream of massless relativistic particle, being photons or gravitons.

1.1 The Beam Metric

Our ansatz for the line element will have a rotation symmetry around the x_{D-1} axis:

$$ds^2 = -dudv + h_0(r)du^2 + \sum_{i=1}^{D-2}(dx_i)^2. \tag{7.3}$$

We use light-cone coordinates defined as $u = t - x_{D-1}$, $v = t + x_{D-1}$ where t and x_i denote the time and space coordinates, respectively. We also define the transverse distance: $r \equiv (\sum_{i=1}^{D-2}(x_i)^2)^{\frac{1}{2}}$.

The only non zero Christoffel symbols are given by:

$$\Gamma^i{}_{uu} = -\frac{1}{2}\partial^i h_0, \qquad \Gamma^v{}_{iu} = -\partial^i h_0, \tag{7.4}$$

the non-zero components of the Riemann and Ricci tensors are:

$$R_{iuju} = -\frac{1}{2}\partial_i\partial_j h_0, \qquad R_{uu} = -\frac{1}{2}\partial_i\partial^i h_0, \tag{7.5}$$

and the Ricci scalar vanishes.

The source is taken to be a "Bonnor beam" [132], namely an infinitely long straight beam of radius r_0, propagating at the speed of light in the direction of the v axis. It corresponds to the energy momentum tensor:

$$T_{uu} = \begin{cases} \rho & r \le r_0 \\ 0 & r > r_0 \end{cases}, \qquad T^{vv} = \begin{cases} 4\rho & r \le r_0 \\ 0 & r > r_0 \end{cases}, \tag{7.6}$$

while all the other components vanish and $\rho > 0$. The Einstein equations of motion reduce to:

$$\partial_i\partial^i h_0 = -16\pi\ell_P^{D-2}\, T_{uu}\ . \tag{7.7}$$

[1] The $[R^3]$ term includes in addition to all possible contractions of three Riemann tensors also those of two covariant derivatives and two Riemann tensors.

The solution to Eq. (7.7) for $D > 4$ is given by:

$$h_0(r) = \begin{cases} \dfrac{16\pi\rho\,\ell_P^{D-2}\,r_0^2}{(D-4)(D-2)}\left[\dfrac{r_0}{r}\right]^{D-4} & r > r_0 \\ \dfrac{8\pi\rho\,\ell_P^{D-2}\,r_0^2}{(D-4)}\left[1-\left(\dfrac{D-4}{D-2}\right)\dfrac{r^2}{r_0^2}\right] & r \le r_0 \end{cases} . \tag{7.8}$$

This solution belongs to a class of solutions called "plane fronted waves with parallel rays" (or *pp*-waves) and enjoys a superposition property, meaning that the linear sum of two parallel *pp*-waves propagating in the same direction is still a solution. Away from the beam, at $r > r_0$, h_0 satisfies

$$\partial_i\partial^i h_0 = 0 . \tag{7.9}$$

It will be convenient to define R_b as

$$R_b^{D-4}(\rho, r_0) \equiv \frac{16\pi}{(D-4)(D-2)}\;\rho\;\ell_P^{D-2}\;r_0^{D-2} , \tag{7.10}$$

such that for $r > r_0$:

$$h_0 = \left(\frac{R_b}{r}\right)^{D-4} . \tag{7.11}$$

In the limit $r_0 \to 0$, the linear density of energy λ_ρ is kept fixed by taking $\rho r_0^{D-2} \to \lambda_\rho \frac{\Gamma(D/2)}{\pi^{(D-2)/2}}$. The background (7.8) then becomes:

$$\begin{aligned} h_0(x_i) \to\; & \frac{16\pi\ell_P^{D-2}}{(D-4)(D-2)}\;\left(\frac{\lambda_\rho\Gamma(\frac{D}{2})}{\pi^{\frac{D-2}{2}}}\right)\;\frac{1}{r^{D-4}} \\ =\; & \frac{4}{\pi^{(D-4)/2}}\Gamma\left(\frac{D-4}{2}\right)\frac{\lambda_\rho\ell_P^{D-2}}{r^{D-4}} , \end{aligned} \tag{7.12}$$

which corresponds to:

$$T_{uu} = \lambda_\rho\delta^{D-2}(x^i) . \tag{7.13}$$

We choose the energy density and beam radius such that:

$$h_0 \sim \ell_P^{D-2}\rho r_0^2 \ll 1 , \tag{7.14}$$

so that we are considering a small perturbation to flat spacetime. We stress that our background is nonetheless in general a full solution of the extended gravity theories we will be considering, so we will not rely on (7.14) to make a perturbative analysis.

1.2 Equations of Motion for the Probe Graviton

Since we are interested in the propagation of probe gravitons in the background metric (7.3), we will allow for a small perturbation of the form:

$$\delta g_{ij} = h_{ij}(u, v) . \tag{7.15}$$

Let us first derive the equations of motion for this probe graviton in General Relativity. We work in the light-cone gauge, $g_{vv} = g_{vi} = g_{ui} = 0$ (see e.g. [133]). We will restrict the discussion to gravitons $h_{ij}(u, v)$ having transverse and traceless polarisation ϵ_{ij}.[2] The tracelessness restriction simplifies the equations of motion but, in contrast to the case of flat spacetime, it is not enough to solve all the constraints given by the Einstein equations.

For ease of use, we have listed in Appendix 1.1 the metric components, the non vanishing Christoffel symbols, Riemann and Ricci tensor components and Ricci scalar up to first order in the probe graviton contribution. Let us simply quote here the most useful results for our calculations:

$$\begin{aligned} &R_{iuju} = -\frac{1}{2}h_{0\,,ij} - \frac{1}{2}h_{ij,uu}, \qquad R_{ivjv} = -\frac{1}{2}h_{ij,vv}, \qquad R_{iujv} = -\frac{1}{2}h_{ij,uv}, \\ &R_{ij} = 2(h_{ij,uv} + h_0 h_{ij,vv}), \quad R_{iu} = \partial^j h_0 h_{ij,v}, \quad R_{uu} = -\frac{1}{2}(h_{0\,,ii} - h^{ij}h_{0\,,ij}), \\ &\qquad\qquad R = 0\ . \end{aligned} \tag{7.16}$$

We are now ready to study the Einstein equation. For general relativity on this background, the it takes the form (away from the beam):

$$2\,(h_{ij,uv} + h_0 h_{ij,vv}) = 0 \qquad (ij)\ , \tag{7.17}$$

$$\partial^j h_0 h_{ij,v} = 0 \qquad (iu)\ , \tag{7.18}$$

$$-\frac{1}{2}(h_{0\,,ii} - h^{ij}h_{0\,,ij}) = 0 \qquad (uu)\ , \tag{7.19}$$

and the other components vanish identically.

Eq. (7.17) is the wave equation describing the propagation of the probe graviton and will be used to extract the causal cone of the theory using the method of characteristics. This will be discussed extensively in the next sections.

The second equation, Eq. (7.18) should not come as a surprise. Indeed, we have consider a perturbation independ from the transverse coordinates, even tough the gravitational interaction of the graviton with the beam shoud deflect it. The solution is straightforward: introduce a second identical beam so that the graviton is propagating right in the middle between the two beams without deflection, making Eq. (7.18) automatically satisfied.

Since any linear combination of *pp*-waves sharing the same Killing vector is also a solution of Einstein equations, we do not have to impose any condition on the distance between the beams to ensure they do not influence each other. The background line element is then given by:

$$ds^2 = -dudv + (h_0^{(1)} + h_0^{(2)})du^2 + \sum_{i=1}^{D-2}(dx_i)^2\ , \tag{7.20}$$

where $h_0^{(1)}$ and $h_0^{(2)}$ are of the form (7.8) with the appropriate distances r and $\hat{r}$. We concentrate on the behaviour of gravitons propagating between the two beams, such

[2] In $D = 4$, such a restriction implies that the polarisations space is two-dimensional. However, the additional constraint (7.23) will further constrain the polarisation space to be one-dimensional. We discuss this issue in detail in Section 6.

that the impact parameter $\vec{b}_1$ with respect to the first beam and $\vec{b}_2$ with respect to the second one are opposite, $\vec{b}_1 + \vec{b}_2 = 0$. This restriction leads to numerous simplification in our calculations. Indeed, at these points of spacetime:

$$\partial_i (h_0^{(1)} + h_0^{(2)})\Big|_{\vec{b}_1+\vec{b}_2=0} = \partial_i\partial_j\partial_k (h_0^{(1)} + h_0^{(2)})\Big|_{\vec{b}_1+\vec{b}_2=0} = 0 \ . \tag{7.21}$$

As a consequence, any instance of a zero order Christoffel symbol which is not differentiated by a partial derivative vanishes. In what follow, we will always put ourselves in this configuration, and so, h_0 should be understood as $h_0 \equiv h_0^{(1)} + h_0^{(2)}$.

Finally, the last equation Eq. (7.19) is a modification of the zeroth order one Eq. (7.7) that determines our background. There, the additional first order term in h^{ij} indicates that the probe graviton can back-react on the background metric unless:

$$h^{ij} h_{0\,,ij} = (4-D)\frac{R_b^{D-4}}{b^D}(b^2 h^{ij}\delta_{ij} - (D-2)h^{ij}b_i b_j) = 0 \ . \tag{7.22}$$

Since h^{ij} is traceless, this reduces to:

$$\epsilon^{ij} b_i b_j = 0 \ . \tag{7.23}$$

Notice that this is an additional constraint. It implies that we are missing one degree of freedom, consisting in an excitation backreacting on the beam. This degree of freedom will be sorely missing when we will consider the four-dimensional case, as we will see in section 6.

To conclude, our equations describe the motion of a graviton propagating right in the middle between two beams. For this particular trajectory, one can find $D(D-3)/2-1$ traceless transverse polarisations which satisfy all the components of the Einstein equations, identically except for the ij components which describe the propagation along the trajectory.

In order to observe swift behaviour, we must require "close fly-by" of our test graviton, namely $b \sim \ell_n$. The condition that we look at gravitons propagating outside of our beam ($b > r_0$) then implies:

$$r_0 \lesssim \ell_n \ , \tag{7.24}$$

where l_n are the coupling constants of equation (7.2).

While in this section we have dealt with the Einstein-Hilbert action, we will show in section 4 that the constraints (7.21) and (7.23) will remain sufficient to solve the uu and ui components of the equations of motion for the extended gravity theories under consideration.

2 A first look into time advance in Extended gravity theories

As we have already underlined, in extended gravity theories, there is no reason that the fastest trajectories follow null geodesics. A consequence is that the usual Shapiro time delay, experienced by a particle moving in a space-time curved by some matter distribution, can transform in a time *advance*. This effect is particularly marked for a

space-time called "shock-wave" which can be used to describe the effect of a high-energy graviton on the surrounding spacetime. In this case, the spacetime is Minkowski expect in a localised region, making the definition of time-shift simpler. Before introducing our results for a curved background and the numerous complications involved, we will review in this section the work of Camanho, Edelstein, Maldacena and Zhiboedov in [134] which show time-advance statements for this metric and link them to the form of the graviton three-points function.

2.1 Time Advance and Shock-Wave

We use the "shock-wave" metric, whose line element is similar to the one introduced in (7.3) with h_0 given by

$$h_0(x_i) = \frac{4}{\pi^{(D-4)/2}}\Gamma\left(\frac{D-4}{2}\right)\frac{-P_u\delta(u)\ell_P^{D-2}}{r^{D-4}} \ , \tag{7.25}$$

with P_u the momentum of a single high-energy graviton.

Consider as a first step a scalar field ϕ propagating in this curved space-time. Its equation of motion can be derived straightforwardly as

$$\partial_u\partial_v\phi + h_0\partial_v\partial_v\phi - \frac{1}{4}\vec{\partial}^2\phi = 0 \ . \tag{7.26}$$

At the vicinity of the shock, for $u \sim 0$, the variation in v is far bigger than the one in the transverse variable, so that we can neglect the last term of (7.26) and integrate the equation. Noting b the impact parameter of the scalar field with respect to the shock, we obtain

$$\phi(0^+, v, \vec{x}) = e^{-\Delta v\partial_v}\phi(0^-, v, \vec{x}) \ , \tag{7.27}$$

where we recognise the generator of translations acting on $\phi(0^-)$ and

$$\Delta v = \frac{4}{\pi^{(D-4)/2}}\Gamma\left(\frac{D-4}{2}\right)\frac{|P_u|\ell_P^{D-2}}{b^{D-4}} \ . \tag{7.28}$$

We see that the scalar field undergoes a shift toward positive v, thereby it feels a time *delay*.

Let us see how this picture is modified when considering a graviton propagating in the shock-wave background for Gauss-Bonnet Gravity. The Gauss-Bonnet action takes the form

$$\mathcal{L} = \frac{1}{16\pi\ell_P^{D-2}}\sqrt{-g}\left[R + \varepsilon_\pm\ell_2^2(R^2 - 4R^{\mu\nu}R_{\mu\nu} + R^{\mu\nu\rho\sigma}R_{\mu\nu\rho\sigma})\right] \ , \tag{7.29}$$

where $\varepsilon_\pm$ stands for the sign of the Gauss-Bonnet term, and the corresponding equations of motion take the form:

$$G_{\mu\nu} + \varepsilon_\pm\ell_2^2 H_{\mu\nu} = 0 \ , \tag{7.30}$$

where:

$$G_{\mu\nu} = R_{\mu\nu} - \frac{1}{2}g_{\mu\nu}R \ , \tag{7.31}$$

is the usual Einstein tensor and:

$$\begin{aligned} H_{\mu\nu} = \; & 2(RR_{\mu\nu} - 2R_{\mu}{}^{\alpha}R_{\alpha\nu} - 2R^{\alpha\beta}R_{\mu\alpha\nu\beta} + R_{\mu}{}^{\alpha\beta\gamma}R_{\nu\alpha\beta\gamma}) \\ & - \frac{1}{2}g_{\mu\nu}(R^2 - 4R^{\alpha\beta}R_{\alpha\beta} + R^{\alpha\beta\gamma\delta}R_{\alpha\beta\gamma\delta}) \ , \end{aligned} \tag{7.32}$$

is the additional Gauss-Bonnet contribution. We will consider a transverse traceless graviton mode h_{ij} propagating on the shock-wave background. From (7.30) its equations of motion are

$$\partial_u\partial_v h_{ij} + h_0[\partial_v^2 h_{ij} + 4\varepsilon_\pm \ell_2^2 \ \partial_k\partial_{(i}h_0 \ \partial_v^2 h_{j)}{}^{k} \,] = 0 \ , \tag{7.33}$$

we will show later on that this equation is in fact diagonal in h_{ij}, so that noting ϵ_{ij} the polarisation tensor of h_{ij}, we can contract eq. (7.33) by ϵ^{ij}. Integrating at the vicinity of the shock we finally obtain

$$\Delta v = \frac{4}{\pi^{(D-4)/2}}\Gamma\left(\frac{D-4}{2}\right)\frac{|P_u|\ell_P^{D-2}}{b^{D-4}}\left[1 + 4\varepsilon_\pm\ell_2^2\frac{(D-4)(D-2)}{b^2}\left(\frac{\epsilon^i{}_k\epsilon^{kj}b_ib_j}{b^2} - \frac{1}{D-2}\right)\right] . \tag{7.34}$$

Therefore by choosing $b^2 \sim \ell_2^2$ and the polarisation tensor we can choose the sign of Δv at will, irrespectively of the sign of $\varepsilon_\pm$. Indeed, we can take without loosing generality $\vec{b} = (1, 0, 0, \ldots)$. Then, labelling the transverse coordinates by x_i, $\ i = 1, 2, 3, \ldots$, we see that for ϵ of the form $\epsilon^{1b} = \epsilon^{b1} = 1/\sqrt{2}$, the last parenthesis is positive while for $\epsilon^{ab} = \epsilon^{ba} = 1/\sqrt{2}$ with $a, b \neq 1$ it is negative.

For action with equation of motion with only second-order derivatives, the authors of [134] have traced down the appearance of the time-advance behaviour to the form of the graviton three-point vertex.

2.2 Graviton three-point function

Consider a two-by-two graviton scattering process $13 \to 24$ mediated by the exchange of another graviton I and notes the amplitude for this process $\mathcal{A}_4$. Then [134] focused on the following kinematics:

$$p_{1\,\mu} = \left(p_u, \frac{q^2}{16p_u}, \frac{\vec{q}}{2}\right) \qquad p_{2\,\mu} = \left(\frac{q^2}{16p_v}, p_v, -\frac{\vec{q}}{2}\right) \tag{7.35}$$

$$p_{3\,\mu} = \left(-p_u, -\frac{q^2}{16p_u}, \frac{\vec{q}}{2}\right) \qquad p_{4\,\mu} = \left(-\frac{q^2}{16p_v}, -p_v, \frac{\vec{q}}{2}\right) \tag{7.36}$$

in the eikonal limit $t/s \ll 1$ with

$$s \simeq \ 4p_up_v \qquad t = -q^2 \ . \tag{7.37}$$

The eikonal amplitude obtained by resumming the horizontal ladder diagrams is then given by [135] as

$$i\mathcal{A}_{eik} = 2s\int d^{D-2}\vec{b}e^{-i\vec{q}\cdot\vec{b}}\left[e^{i\chi} - 1\right] \tag{7.38}$$

where we used the phase χ given by

$$\chi = \frac{1}{2s}\int \frac{d^{D-2}\vec{q}}{(2\pi)^{D-2}} e^{i\vec{q}\cdot\vec{b}}\mathcal{A}_4 \ , \tag{7.39}$$

It was shown in [136] that the wave packet of the gravitons undergoing the scattering process experiences a time shift proportional to $\frac{\partial\chi}{\partial s}$. The road ahead is clear: we must first give an expression for $\mathcal{A}_4$, then calculate the phase χ to extract the nature of the time-shift. All four external legs are on-shell and the exchanged graviton is associated to a propagator proportional to $\frac{1}{q^2}$. More precisely, in the De Donder gauge we have

$$\mathcal{A}_4 = \mathcal{A}^{13I}_{\mu\nu}\frac{1}{2q^2}[\eta^{\mu\alpha}\eta^{\nu\beta}+\eta^{\nu\alpha}\eta^{\mu\beta}-\frac{2}{D-2}\eta^{\mu\nu}\eta^{\alpha\beta}]\mathcal{A}^{24I}_{\alpha\beta} \ . \tag{7.40}$$

where $\mathcal{A}^{13I}_{\mu\nu}$ and $\mathcal{A}^{24I}_{\alpha\beta}$ are the three-point amplitude with one free leg corresponding to the mediator graviton I. Three forms of three-points function were considered in [134]. Given the kinematics (7.35), the dominant contribution for $\mathcal{A}_4$ goes like $p_u^2 p_v^2$ and can be obtained from $\mathcal{A}_4 \supset \mathcal{A}^{13I}_{uu}\frac{4}{q^2}\mathcal{A}^{24I}_{vv}$, with three possibilities for $\mathcal{A}^{13I}_{uu}$ (we omit the uu and vv metric indices in the following for simplicity):

$$\mathcal{A}^{13I}_{R} = \sqrt{32\pi G}[p_u^2 \epsilon_1{}^{ij}\epsilon_{3\,ij}]^2 \tag{7.41}$$

$$\mathcal{A}^{13I}_{R^2} = \sqrt{32\pi G}[p_u^2 \epsilon_1{}^{ik}\epsilon_{3\,jl}q_k q_l] \tag{7.42}$$

$$\mathcal{A}^{13I}_{R^3} = \sqrt{32\pi G}[p_u^2 \epsilon_1{}^{ij}\epsilon_3{}^{kl}q_i q_j q_k q_l]^2, \tag{7.43}$$

and similarly for $24I$ by replacing p_u by p_v. Replacing in (7.39) we obtained

$$\chi = \frac{1}{2s}\int \frac{d^{D-2}\vec{q}}{(2\pi)^{D-2}} e^{i\vec{q}\cdot\vec{b}}\mathcal{A}^{13I}(\vec{q})\frac{4}{q^2}\mathcal{A}^{24I}(\vec{q}) \tag{7.44}$$

$$= \frac{2\mathcal{A}^{13I}(-i\vec{\partial})\mathcal{A}^{24I}(-i\vec{\partial})}{s}\int \frac{d^{D-2}\vec{q}}{(2\pi)^{D-2}} e^{i\vec{q}\cdot\vec{b}}\frac{4}{q^2} \tag{7.45}$$

$$= \frac{2\mathcal{A}^{13I}(-i\vec{\partial})\mathcal{A}^{24I}(-i\vec{\partial})}{s}\left(\frac{\Gamma\left(\frac{D-4}{2}\right)}{4\pi^{(D-4)/2}}\frac{1}{b^{D-4}}\right) \ . \tag{7.46}$$

Replacing the expressions for the three-point functions, we obtain

$$\chi = Gs\frac{\Gamma\left(\frac{D-4}{2}\right)}{\pi^{(D-4)/2}}\left[1-a_2\epsilon_1{}^{i}{}_{k}\epsilon_3^{kj}\partial_i\partial_j + a_4\epsilon_1^{ij}\epsilon_3^{kl}\partial_i\partial_j\partial_k\partial_l\right] \tag{7.47}$$

$$\times\left[1-a_2\epsilon_2{}^{i}{}_{k}\epsilon_4^{kj}\partial_i\partial_j + a_4\epsilon_2^{ij}\epsilon_4^{kl}\partial_i\partial_j\partial_k\partial_l\right]\frac{1}{b^{D-4}} \ , \tag{7.48}$$

where a_2 and a_4 parameterise the most general three-point function one can build from $\mathcal{A}_R$, $\mathcal{A}_{R^2}$ and $\mathcal{A}_{R^3}$ of (7.41). A straightforward calculation then leads to the expression of the phase for the various three-point functions. It was shown in [134] that while the first one, corresponding to General Relativity, only leads to the Shapiro time delay, the two others exhibit the same behaviour that what we have seen in the Gauss-Bonnet case for the shock-wave metric: a possible time-advance for certain polarisations.

In the following, we will generalise this result to a large class of extended gravity theories.

3 Characteristics, Swiftness and Causal Structure

Replacing the simple shock-wave background by the complete "Bonnor beam" metric (7.3) leads to numerous complications. First, we must be careful about the notion of "fast propagation" we want to use. Second, we need an effective way of deriving the causal structure which does not rely on integrating the equations of motion at the vicinity of the shock wave.

3.1 Defining time-shifts in General Relativity

As a first step toward dealing with the first point, we will review the classic results concerning time-shifts in General Relativity.

Let us start with the result from Visser, Basset and Liberati in [137], where stationary perturbations of Minkowski spacetime in the harmonic gauge were considered. It was shown that null geodesics of the total metric always lie inside the light-cone of flat spacetime. The main calculations go as follow. In the harmonic gauge, the equation for small perturbation of $h_{\mu\nu}$ of the flat spacetime metric $\eta_{\mu\nu}$ is

$$\Delta h_{\mu\nu} = -16\pi G \bar{T}_{\mu\nu} \equiv \ -16\pi G[T_{\mu\nu} - \frac{1}{2}\eta_{\mu\nu}T^{\rho}_{\rho}] \ , \tag{7.49}$$

which can be formally solved with a retarded potential integral as

$$h_{\mu\nu} = 4G \int d^3\vec{y} \frac{\bar{T}_{\mu\nu}(\vec{y}, t - |\vec{x} - \vec{y}|)}{|\vec{x} - \vec{y}|} \ . \tag{7.50}$$

From (7.50) one can see straightforwardly that

$$g_{\mu\nu}k^{\mu}k^{\nu} \geqslant 0 \ , \tag{7.51}$$

for all k^{μ} such that $k^{\mu}k^{\mu}\eta_{\mu\nu} = 0$, a result which can be seen as showing that the null cone of the perturbed metric lies within the null cone of flat space-time.

This result is however highly gauge dependent. As it was noted in Gao and Wald [138], one can take a suitable pure gauge change of the schematic form:

$$h_{\mu\nu} \to \tilde{h}_{\mu\nu} = h_{\mu\nu} + \partial_{\mu}(\frac{\alpha r_{\nu}}{2 + g(r)}) + \partial_{\nu}(\frac{\alpha r_{\mu}}{2 + g(r)}) \ , \tag{7.52}$$

where r_{μ} is the radially pointing-outward vector, α a small constant and g a function given by

$$g(r) = \begin{cases} r \text{ for } r \geqslant 1/2 \\ r^2 \text{ for } r \leqslant 1/2 \end{cases} \ . \tag{7.53}$$

Such a gauge choice can "open" the null cone since

$$\tilde{h}_{\mu\nu}k^{\mu}k^{\nu} = h_{\mu\nu}k^{\mu}k^{\nu} + \left[\frac{2\alpha}{(2 + g(r))^2}\left(rg'(r)\frac{\vec{k}\cdot\vec{r}}{r^2} - (2 + g)k^2\right)\right] \ , \tag{7.54}$$

since the second term is always negative for our choice of function g, one can always engineer $\tilde{h}_{\mu\nu}k^{\mu}k^{\nu} < 0$. Obviously this new gauge does not satisfies the harmonic

gauge in agreement with the results [137]. In the passive vision of the diffeomorphism gauge freedom, the choice of (7.52) amounts to "stretch" locally the coordinates in the curved space-time so that comparing with the unstreched ones of flat space-time, signals appears to be propagating faster.

The authors of [138] therefore argued that the previous constraints could not give a good definition of "fast" travel as one would like such a notion to be gauge-invariant, or equivalently, not relying on a comparison with flat space-time. One such statement had been first derived in [139], albeit with a rather intricated characterisation of time-delay. Instead, Gao and Wald chose to focus on the asymptotic structure of a given spacetime. Loosely speaking, they showed in [138] that signals prefer travelling on the boundary of a space-time. More precisely, they show that given a compact K, one can find a second compact K' such that: *for every two points $M_1, M_2 \not\subset K'$ with M_2 at the edge of the causal future of M_1, the null geodesics connecting M_1 and M_2 does not cross K*. The main limitation being that one has no control over the size of K'. The proof being quite technical, we will only give here the main underlying arguments.

- Consider a geodesically complete space-time satisfying the null energy condition[3]. Then every null geodesic contain a pair of conjugate points[4] (see the proof in [140]).

- Then [138] shows that the null energy condition implies that the map $\mathcal{H}$ which associates a point p with its first conjugate q is continuous at the vicinity of p.

- Given a point M and a null geodesic γ from M generated by the vector V_M, assume we can find the first pair of conjugate point p then q on γ in the causal future of M. We can then consider the smallest ball [5] $\mathcal{B}_M$ containing the three points as well as the null geodesic linking them. The continuity of the exponential map coupled with the continuity of $\mathcal{H}$ then implies that by taking an arbitrary small $\mathcal{O}$ neighbourhood around (M, V_M), the conjugate pairs from geodesics originating from this neighbourhood will lie in a ball with radius arbitrarily close to $\mathcal{B}$. This proves the upper-semicontinuity of the function f associating (M, V_M) to the radius of $\mathcal{B}_M$).

- Given a compact region K, since f is upper-semicontinuous, we can then take the maximum of f on K. We can then use it to define a new compact K' containing all the conjugate pairs associated to each geodesics crossing K. This means that if a geodesic cross K, it must have a conjugate pair somewhere in K'. The main points of the previous arguments is in fact to show that K' is indeed a compact.

Let us now check that given K, the compact K' satisfies the above theorem. Consider two points $M_1, M_2 \not\subset K'$ with M_2 at the edge of the causal future of M_1, the null geodesic linking M_1 and M_2 cannot contain any conjugate pairs (see [140]). Now γ can cross K' but not K since if it did, it should necessarily contain a pair of conjugate points in K', contradicting the previous assumption. The null geodesics must then

[3] plus the so-called null generic condition, supposed to hold in almost all physical spacetime [140]

[4] Two points p and q are conjugate if there exist a Jacobi field which vanishes at both p and q, this roughly corresponds to geodesics starting from p crossing again at q.

[5] The ball is defined in geodesics distance from M

travel outside of the compact K, asserting our previous assertion that fastest null geodesics prefer "travelling on the boundary".

An interesting development regarding "fast" propagation was obtained in [141] by Palmer and Marolf. They considered a static spherically symmetric spacetimes. The crucial idea is that by restricting the complete gauge freedom to the subset conserving the symmetry of the problem, one can define unambiguously a comparison between all space-time with the same symmetry. In [141] they considered spherical cavities, therefore all gauge transformation must respecting the spherical symmetry must: (i) conserve the angle (ii) map a sphere into another sphere, potentially with another radius. It is then possible to compare the proper time required to cross a cavity according to an observer sitting on the sphere with a given radius R in two space-time and compare it. This criterium was successfully used by Papallo and Reall in [142] to prove that time-advance occurred in Gauss-Bonnet gravity for gravitons scattering on a Schwarzschild black hole. Such symmetry protection will be important in deriving our notion of swift propagation, as we will see below.

Notice finally that in the context of extended gravity theories, we could a priori simply compare the fastest propagation speed in this theory with the fastest null geodesics in the Standard Model. If the spacetime we are studying is a solution of both theories, there is no obstruction in comparing them. However, it is more interesting to find extended gravity setups in which no only is propagation faster than the one in General Relativity, but also "fast" as defined by the previous theorems, even when considering matter satisfying energy conditions.

3.2 Method of Characteristics

The previous theorems considered exclusively General Relativity where the fastest trajectories for massless particles always follow null geodesics, making them (relatively) simple to study. In order to analyse the causal structure for theories of extended gravity. We have instead to study their characteristic hypersurfaces. Those can be deduced from the equations of motion for a probe graviton in the background (7.3), as we will describe now.

Consider a linear equation of motion for a scalar field ϕ of the form

$$P(\partial)\phi = 0 \ , \tag{7.55}$$

where P is a polynomial in ∂ of order n with constant coefficients. We denote by P_n the truncation of this polynomial to its highest derivative terms in P (P_n is often called the principal part of P). Each 1-form ξ such that:

$$P_n(\xi) = 0 \ , \tag{7.56}$$

is normal to a codimension-1 hypersurface called a characteristic hypersurface. On characteristic hypersurfaces a full set of initial Cauchy data including all inner pointing derivatives and the first $n-1$ outward pointing derivatives does not fully determine the value of the n-th order outward pointing derivative. In particular, the n-th order outward pointing derivative can be discontinuous, allowing for the propagation of shock waves. For illustrative purposes, we explain the idea behind the method of characteristic for a scalar field in appendix 1.2.

Since characteristic hypersurfaces are boundaries of the causal development of an initial hypersurface $\mathcal{I}$, they give the edges of the region where the physics is fixed by the initial data on $\mathcal{I}$. As a consequence of these properties, the characteristic hypersurfaces also determine the trajectories of signals with the highest propagation speed in the theory considered.

To use the method of characteristics with the equations of motion for our probe graviton, one should take into account the following two subtleties. First, the coefficients of the PDEs could in principle be (non-constant) functions of the spacetime coordinates. However, since we are considering a setup in which the test graviton has a constant impact parameter, it remains static in the transverse directions and therefore its equations of motion admit constant coefficients. Second, we are considering a tensor field, hence (7.56) should be modified to a determinant of the set of characteristic equations corresponding to the different polarisations of the probe graviton. However, we will take the basis of polarisation such that the system of equations of motion becomes diagonal.[6] We can therefore consider each polarisation individually and look for those exhibiting a swift behaviour. The detailed choices of polarisations that we take are described at the beginning of section 5.

Since we are only considering the equations of motion in the (u, v) plane, we cannot check that the full equations of motion are hyperbolic.[7] This property is required to make sure that the notion of causal structure is well-defined, as we review in the next section 3.5. If we assume that the causal cone does exist, then our results give locally its projection to the (u, v) plane. We therefore only investigate swift propagation of gravitons restricted to this plane.

We find that the projected causal cone can be degenerate in theories with terms of the form $(\text{Riemann})^4$ where the characteristic equation has one root with degeneracy four. In this situation, we use a theorem stated in section 3.5 to prove that the full equations of motion cannot be hyperbolic with respect to the time direction when expanded around our background, and therefore the initial value problem is not well-posed. The theorem relates the degeneracy of the roots of different truncations of the characteristic polynomial. We leave the complete proof to the appendix. Three comments are in order. First, in this degenerate case, the hyperbolicity depends on the complete equations, and not only on the terms at highest order in derivatives. Second, in our proof, we rely on the fact that our action always includes the Einstein-Hilbert term. Third, the non-hyperbolicity is a local statement because we are only considering probe gravitons propagating in the middle between the two beams.

3.3 Time Shift and Swift Propagation

We chose our background such that h_0 goes to zero at infinity, which is obtained by taking the beams to be generated by a small density of energy as explained in the previous section, with a big but finite length so that our metric is locally a very good approximation. This metric is furthermore static and invariant by translation in the

[6] This means that the Einstein equations do not mix different polarisations and we have the form: $E_{ij} \propto \epsilon_{ij}$.

[7] The precise definition of hyperbolicity is given in 3.5. In [143], it was shown that Lovelock theories, for instance, are hyperbolic around pp-wave solutions.

direction of the beam. Therefore, we are considering a problem with translational symmetry in the u and v direction.

When dealing with generic extended gravity theory, it is very difficult to solve completely the characteristic equations. We therefore cannot to use the criterion for superluminality of [138] since it requires the complete knowledge of the causal structure of the theory to find the fastest path. We do not have this information in the case of our background.

In order to define "superluminal" or "infraluminal" speeds, we will compare the characteristic hypersurfaces with those asymptotically far away, in the limit $r \to \infty$. In our gauge, these are those of Minkowski spacetime, therefore we are effectively applying the naive criterium of comparint propagation speed in the plane u, v in a given background h_0 to the propagation speed in a flat Minkowski spacetime which is obtained in the limit $h_0 \to 0$. Gravitons propagating faster than the asymptotical characteristic hypersurfaces are then called "swift gravitons".

This definition is in fact non-ambiguous for all gauge choice compatible with linearised gravity and with the two translational symmetries in u and v of our problem. Indeed, writing $h_{0\,\mu\nu}$ is a small perturbation of flat space-time, the gauge ambiguity can written as

$$h_{0\,\mu\nu} \to h_{0\,\mu\nu} + \partial_\mu \xi_\nu + \partial_\nu \xi_\mu \ . \tag{7.57}$$

where ξ_μ is a small perturbation. Requiring that the gauge transformed metric do not depend on u and v forces ξ_u and ξ_v to depend only linearly on u and v. Furthermore, since we are considering perturbative gravity, the we must have $\partial_\mu \xi_\nu + \partial_\nu \xi_\mu \ll 1$ at every point in spacetime. This further fix the possible gauges to

$$\xi_u = au + bv + f(\vec{x}) \tag{7.58}$$

$$\xi_v = bv + du + g(\vec{x}) \ , \tag{7.59}$$

where a and b are small constants which do not depend on the transverse variables. Consequently, the metric elements $h_{0\,uu}, h_{0\,uv}$ and $h_{0\,vv}$ which are relevant to discuss the swiftness according to our definition, can only be modified by *small constant* terms. Such term is easily eliminated when comparing with the characteristic hypersurfaces asymptotically far away, so that our definition of swiftness does not depend on the gauge choice.

It seems plausible that one can use similar arguments to this section and to [141] to compare non-equivocally propagation speed in certain cases between two spacetimes sharing the same symmetries. For instance, in our case, we could have used the rotational symmetry around the beam coupled with the two translational symmetries to compare un-ambiguously cylinders around the beam with the same length and radius with other cylinders in another spacetime sharing the axisymmetry property. We will not push this idea further in this thesis.

In $D > 4$, we can proceed straightforwardly and define swiftness by comparing the characteristic hypersurfaces with the flat spacetime light-cone corresponding to the limit $r \to \infty$. Suppose that we find that one of the characteristic is of the form $(\xi_u = -\Delta c, \xi_v = 1)$ with $|\Delta c| \ll 1$, then swift propagation occurs for $\Delta c < 0$.

In $D = 4$, the situation is more delicate and we need to use the fact that the beams have a finite length L. In the relevant limit where this length is very large compared to the other length scales in the problem, our background is of the form $h_0 \sim \log \frac{L}{r}$ where the beam length plays the role of an IR cut off. Because of the logarithmic growth of this metric, we remain in the limit $h_0 \ll 1$ for all practical purposes. We find that in that case, Δc is of the form $\Delta c = a(\log \frac{\Lambda}{r} + \frac{N\ell^m}{r^m})$ where N is a $\mathcal{O}(1)$ number which can be either positive or negative depending on the polarisation of the probe graviton, a is a constant depending on the source beam, ℓ^m is the coupling constant of the extended gravity terms and $m \geqslant 4$ an integer which depends on the extended gravity theory. As was already pointed out in [134], it is always possible to find a setup in which the logarithm is overtaken by the other terms such that we can focus on the sign of their contribution to determine if we have swift propagation.

3.4 Characteristic Equations: Structure and Examples

For concreteness, let us describe the characteristic equations we will considered in the rest of this chapter and apply to them the "swiftness" criterion that we have just defined.

We are interested in equations of motion of the form:

$$\partial_u \partial_v h + a\partial_v^2 h + b\partial_v^4 h + c\partial_u \partial_v^3 h = 0 \ , \tag{7.60}$$

with three different cases:

1. When $c = b = 0$, we have a situation similar to Einstein gravity. Our equations of motion are second order in derivatives of the probe graviton and we have two distinct roots for the characteristic equation. Swift propagation occurs if $a < 0$.

2. When $b \neq 0$ and $c = 0$, we have only one characteristic $\xi_v = 0$. The causal cone is degenerate, we are in the situation discussed in the previous subsection.

3. When $b \neq 0$ and $c \neq 0$, we have a causal cone whose boundaries are the two characteristics given by $\xi_u = -\xi_v b/c$ and $\xi_v = 0$. Swift propagation occurs if $b/c < 0$.

We start by studying the example of a graviton propagating in Einstein gravity described by the equations of motion (7.17). The characteristic equations read:

$$2\xi_u \xi_v \epsilon^{ij} + 2h_0 \xi_v^2 \epsilon^{ij} = 0 \ . \tag{7.61}$$

These equations are diagonal in the polarisations (i.e. they satisfy $E_{ij} \propto \epsilon_{ij}$). Therefore, we can consider each polarisation separately. The equations have two solutions, independent of the polarisation of the graviton, giving two characteristic hypersurfaces:

$$(\xi_u = 1, \xi_v = 0) \text{ and } (\xi_u = -\frac{h_0}{1 + {h_0}^2}, \xi_v = \frac{1}{1 + {h_0}^2}). \tag{7.62}$$

Since $h_0 > 0$, gravitons propagating in the negative x_{D-1} direction suffer a time delay and their propagation is infraluminal. This is the Shapiro time delay. Graviton propagating in the positive x_{D-1} directions remains unaffected.

As a second example we consider an abelian gauge field in $D > 4$ non-minimally coupled to gravity:

$$\mathcal{L} = \sqrt{-g}\left(\frac{1}{16\pi\ell_P^{D-2}}R + \frac{1}{4}F_{\mu\nu}F^{\mu\nu} + \frac{1}{4}\ell_R^2 R^{\mu\nu\rho\sigma}F_{\mu\nu}F_{\rho\sigma}\right) . \tag{7.63}$$

We suppose that the background metric is of the form (7.3) and is induced by two parallel beams. We are interested in a particle propagating in the middle between the two beams. The equations of motion for A^μ simplify to:

$$\partial_\rho\partial^\rho A^\mu - \partial^\mu\partial_\rho A^\rho - 2\ell_R^2 R^{\mu\nu\rho\sigma}\partial_\nu\partial_\rho A_\sigma = 0 . \tag{7.64}$$

We focus on a field A^μ with only transverse modes and suppose that it does not depend on the transverse coordinates. The only relevant components of the equation of motion are:

$$\partial_u\partial_v A^i + (\delta^{ij}h_0 + \ell_R^2\partial^i\partial^j h_0)\partial_v^2 A_j = 0 . \tag{7.65}$$

The unit vector ξ^μ normal to a characteristic hypersurface satisfies:

$$\xi_u\xi_v A^i + (\delta^{ij}h_0 + \ell_R^2\partial^i\partial^j h_0)\xi_v^2 A_j = 0 . \tag{7.66}$$

We choose the impact parameter $\vec{b} = (b, 0, \dots)$ and we consider two choices of polarisations:

- (A): A^1 non zero and all the other components vanish,
- (B): A^2 non zero and all the other components vanish.

We get:

$$\xi_v(\xi_u + \mathcal{C}\xi_v) = 0 , \tag{7.67}$$

where $\mathcal{C} \in \{\mathcal{C}_{(\mathrm{A})}, c_\beta\}$ depends on the polarisation of A^i:

$$\mathcal{C}_{(\mathrm{A})} = \left(\frac{R_b}{b}\right)^{D-4}\left[1 + \ell_R^2\frac{(D-4)(D-3)}{b^2}\right] , \tag{7.68}$$

and

$$c_\beta = \left(\frac{R_b}{b}\right)^{D-4}\left[1 - \ell_R^2\frac{D-4}{b^2}\right] . \tag{7.69}$$

Taking b small enough such that $\dfrac{\ell_R}{b} > 1$, $\mathcal{C}_{(\mathrm{A})}$ and c_β have opposite signs. Therefore we can have $\mathcal{C} < 0$ regardless of the sign of ℓ_R^2.[8] The two characteristic hypersurfaces are given by:

$$(\xi_u = 1, \xi_v = 0) \text{ and } (\xi_u = -\frac{\mathcal{C}}{1+\mathcal{C}^2}, \xi_v = \frac{1}{1+\mathcal{C}^2}) . \tag{7.70}$$

Hence, when $\mathcal{C} < 0$, A^i propagates toward decreasing x_{D-1} at a superluminal speed. Note that the relative size of R_b compared to b, affects only the strength of the time shift effect. Its advance or delay nature is determined by the polarisation of A^i and by the impact parameter. Therefore, swift propagation can happen even in the weak curvature regime when $\left(\frac{R_b}{b}\right)^{D-4} \ll 1$.

[8]Note, that the notation ℓ_R^2 is made to match the conventions in the literature. We do not need to assume it is of positive sign for our argument in this subsection.

3.5 Causality and Hyperbolicity

Finally we will summarise in this section some useful notions regarding causality and hyperbolicity. This includes a formal definition of hyperbolicity and its relation to well-posed initial value problems, the definition of the causal cone and the notion of causality [144, 145]. We also quote a theorem which will be used to demonstrate that when the projection of the causal cone to the (u, v) plane is degenerate the full equations of motion are not hyperbolic. This result will be particularly revelant for $[R^4]$ extended gravity theories.

Let us start by defining hyperbolicity. Let $P(\partial)$ be a differential operator of order m: $P(\partial) = \sum_{i=0}^{m} P_i(\partial)$, where all terms of order i are regrouped in P_i. The highest order terms, $P_m(\partial)$ are called the principal part. The operator $P(\partial)$ is said to be hyperbolic with respect to a vector ξ if all the following conditions are satisfied:

1. ξ is not a root of the principal part: $P_m(\xi) \neq 0$.
2. $P_m(V+\tau\xi) = 0$ has only real roots in τ where V is a real vector. We furthermore define the cone $\Gamma(P, \xi)$ by $V \in \Gamma(P, \xi)$ if and only if all the previous roots are strictly negative.
3. P_m is stronger than the remaining terms in P in the sense that there exists $C \in \mathbb{R}$ positive such that $\forall i \in [0, m]$ and $\forall \xi \in \mathbb{R}^D$

$$\frac{\sum_{\alpha \geqslant 0, i} |P_i^{(\alpha)}(\xi)|^2}{\sum_{\alpha \geqslant 0} |P_m^{(\alpha)}(\xi)|^2} < C \ , \tag{7.71}$$

where we use the usual parenthesis notation for the derivative of order α with respect to all possible parameters.

Notice that the last condition is automatically satisfied if $P = P_m$, so that the principal part of P is hyperbolic if it satisfies the two first conditions.

We also define the causal cone $\Gamma^0(P, \xi)$ more formally as follows. $\Gamma^0(P, \xi)$ is the set of all vectors inside $\Gamma(P, \xi)$. That is, every element V in $\Gamma^0(P, \xi)$ is such that $V \cdot \theta \geqslant 0$ for all $\theta \in \Gamma(P, \xi)$. It can usually be obtained by considering the cone bounded by the characteristics in the direction of ξ (in the future-time direction if ξ is taken to be the time direction).

Suppose we fix the boundary conditions on a hyperspace $\mathcal{I}$ with normal ξ, if the initial conditions are non-zero only on a compact convex subset K of $\mathcal{I}$, then causality is the requirement that the solution to our Cauchy problem vanishes outside $K + \Gamma^0(P_m, \xi)$. This requirement holds as long as P is hyperbolic [145].

Next, we quote a theorem which applies to hyperbolic systems and which we find useful in arguing that our system is not hyperbolic in the case of a degenerate causal cone. The theorem states that for a hyperbolic system $P = P_m + P_{m-1} + \ldots$ with respect to a vector ξ, if V is not proportional to ξ and τ_0 is a root of $P_m(V + \tau\xi)$ of degeneracy μ then $V + \tau_0\xi$ is a root of degeneracy $\mu - j$ of P_{m-j}, $j = 0, \ldots, m-1$.

To show that for the cases we study in this paper a system with a degenerate causal cone cannot be hyperbolic we use the following argument. Suppose we decompose the characteristics polynomial $P(\xi)$ as follows:

$$P(\xi) = Q(\xi_u, \xi_v) + R(\xi_u, \xi_v, \xi_i) \ , \tag{7.72}$$

where $R(\xi_u, \xi_v, 0) = 0$. In this paper, we have studied the term Q, since we have restricted the motion of our probe graviton to the (u, v) plane. For the case of a degenerate causal cone, we have shown that Q takes the generic form:

$$Q(\xi_u, \xi_v) = \xi_u \xi_v + a\xi_v^2 h + b\xi_v^4 \ , \tag{7.73}$$

where a, b are real non-zero constants. Suppose the full equations of motion are hyperbolic with respect to $\tilde{\xi} = (\xi_u, \xi_v, 0, \dots)$, with $\xi_v \neq 0$ (this includes for instance the time direction $\xi_{time} \propto (1, 1, 0, \dots)$). Given $V = (V_u, V_v, 0, \dots)$ not proportional to ξ we have:

$$P_m(V + \tau\xi) = Q_m(V + \tau\xi) = b(V_v + \tau\xi_v)^4 \ . \tag{7.74}$$

We find that $\tau_0 = -V_v/\xi_v$ is a root of $P_m(V + \tau\xi)$ of degeneracy four. The previous theorem then implies that τ_0 must be a second order root of $P_2(V + \tau\xi) = Q_2(V + \tau\xi)$, if P is hyperbolic. Since $Q_2(\xi_u, \xi_v) = \xi_u \xi_v + a\xi_v^2$ and V is not proportional to ξ, τ_0 is only a first order root, contradicting the result of the previous theorem. We therefore conclude that the full equations of motion are not hyperbolic with respect to ξ. This proves that in the case of a degenerate causal cone (at least in the context of the cases studied in this paper), the full equations of motion are not hyperbolic with respect to the time direction when evaluated locally in between the two beams.

4 Equations of Motion in Theories of Extended Gravity

We can finally start studying theories of extended gravity in $D > 4$. For the cases in which the background (7.3) with h_0 defined in (7.8) remains a solution, we derive the equations of motion for a propagating probe graviton of the form (7.15).

Since our background (7.3) is a very simple line element, we will see that it is automatically a solution of almost all the possible extended gravity we will considered, except for few cases that we will classified explicitly. However, even if we will not be able to check for swift propagation for them it is easy to show that gravitons propagating around flat background in these theories will have equations of motion with terms which contain four or six derivatives acting on the probe graviton, so that these theories are very likely to develop Ostrogradsky instabilities.

Since deriving equations of motion for extended gravity theories is a lengthy process, most of the results of this section were derived using *Mathematica* and the rules listed in appendix 1.3.

4.1 General Considerations

As we have seen in section 1.2, the components ij of the equations are the most interesting ones, since they are the one used to find the equation of propagation. However, the other components have been found to lead to additional constraints on h^{ij}. We will show now that the tracelessness condition along with the constraint (7.23):

$$\epsilon^{ij} b_i b_j = 0 \ , \tag{7.75}$$

are enough to satisfy automatically all the equations of motion except for the propagation one.

Indeed, the uu, uv and vv components in extended gravity theories can only contain factors of the form:

$$h_0^l |b|^{2m} b^i b^j \partial_{u,v}^n h_{ij} \ , \tag{7.76}$$

where m, k and l are natural numbers, and $\partial_{u,v}^n$ stands for any number of u and v derivatives. These factors vanish when (7.75) is imposed.

Furthermore, the ui and vi equations of motion must involve at least one h_0 acted on by an odd number of derivatives. This is since h_{ij} indices come in even numbers. Therefore, the contributions of the two beams always cancel each other when the graviton propagates in the middle between them (see Eq. (7.21)) and the equations are identically satisfied.

4.2 Deriving the Equations of Motion

We now study systematically all possible gravity actions containing terms of the form $[R^2]$ $[R^3]$, $[R\nabla^2 R]$ and $[R^4]$ theories. We will first derive numerically the transverse equations of motion for each possible term, then classify their resulting contributions to the equations of motion of a generic extended gravity theory.

There are three possible curvature squared terms which we can consider: R^2, $R^{\mu\nu}R_{\mu\nu}$ and $R^{\mu\nu\rho\sigma}R_{\mu\nu\rho\sigma}$. We list their contributions to the background equations of motion and those of the probe graviton in Table 7.1. Since we want to keep the form (7.8) for h_0, we require that the zeroth order background equations remain the same as those of general relativity. The actions satisfying this condition can be read from Table 7.1 and include $f(R)$ gravity, Einstein-Gauss-Bonnet and any linear combination thereof. The equations of motion of all those theories are found to be either vanishing or proportional to:

$$\mathcal{T}_0^{ij} \equiv h_{0,}{}^{k(i} h^{j)}{}_{k,vv} \ , \tag{7.77}$$

at first order in the probe graviton contribution.

Action	Background equations	EoM at first order in h^{ij}
R^2	0	0
$R_{ab}R^{ab}$	$-\frac{1}{2}\vec{\partial}^4 h_0$	$-\frac{1}{2}\Delta_d^2 h^{ij}$
$R_{abcd}R^{abcd}$	$-2\vec{\partial}^4 h_0$	$-2\Delta_d^2 h^{ij} + 8h_{0,}{}^{k(j}\ \partial_v^2 h^{i)}{}_k$

Table 7.1: Contributions of the possible $[R^2]$ actions to the zeroth and first order equations of motion. Orange color indicates fourth order derivatives acting on h^{ij}. We have defined $\Delta_d \equiv -4(\partial_u\partial_v + h_0\partial_v^2)$.

The equations of motion for Einstein-Gauss-Bonnet gravity have been presented in (7.30) when dealing with the shock-wave background. One can read directly the transverse equations of motion for the probe graviton from Table 7.1 and obtain:

$$E_{ij} = h_{ij,uv} + h_0 h_{ij,vv} + 4\varepsilon_\pm \ell_2^2\ h_{0,k(i}\ h_{j)}{}^k{}_{,vv} = 0 \ . \tag{7.78}$$

We will study the characteristics hypersurfaces for this equation in the next section.

At higher order, the calculations cannot practically be done by hand. Therefore, for the equations of motion for actions containing contributions of the forms R^3, $R\nabla^2 R$ and R^4 we used xAct [146,147,148] and xTras [149], tensor algebra packages for *Mathematica*. We followed the steps bellow:

1. Generate all possible contractions of three Riemann tensors, four Riemann tensors, and two Riemann tensor and two covariant derivatives.
2. Select an independent basis of actions, taking into account integration by parts and various geometric identities.
3. Compute the full equations of motion for each of the above actions using xTras.
4. Check if the background equations defining h_0 are modified.
5. Expand around h_0 given by (7.8) and use the rules detailed in Appendix 1.3 to simplify and evaluate these equations of motion at first order in perturbation theory.

Most of the rules derived in Appendix 1.3 are due to the peculiar form of our background and the possible number of instances and placements of the u and v indices.

We list out results for the equations of motion of $R\nabla^2 R$ and R^3 actions in Table 7.2. We obtain that all contributions of dimension six to the equations of motion of the probe graviton are linear combinations of two possible terms:

$$\mathcal{T}_1^{ij} \equiv h_{0,}{}^{k(j}\ \Delta_d \partial_v^2 h^{i)}{}_k \ , \tag{7.79}$$

and

$$\mathcal{S}_0^{ij} \equiv h_{0,}{}^{ijkl}\ \partial_v^2 h_{kl} \ , \tag{7.80}$$

where we have defined the derivative operator Δ_d by:

$$\Delta_d = -4(\partial_u \partial_v + h_0 \partial_v \partial_v) \ . \tag{7.81}$$

$\mathcal{T}_1^{ij}$ is simply the Δ_d derivative of the $\mathcal{T}_0^{ij}$ term that we already encountered in the context of the Gauss-Bonnet action. We will study both contributions in the next section and show that they lead to swift propagation for certain polarisations of the graviton.[9]

Similarly, we can consider actions built from four Riemann tensors. The background equations are not modified in this case. All actions including at least one Ricci tensor or Ricci scalar have equations of motion which are identically satisfied for the probe graviton. Our results for the equations of motion of the test graviton are summarised in Table 7.3.

There are three possible contributions to the equations of motion of $[R^4]$ terms, each with four derivatives acting on h^{ij} given by:

$$\mathcal{U}_0^{(ij)} \equiv h_{0,}{}^{lk} h_{0,k}{}^{(i} h^{j)}{}_{l,v^4} \ , \tag{7.82}$$

[9] In Table 7.2, we also have a $\Delta_d^3 h_{ij}$ contribution, however, the action term which generates it, $R^{ab}\nabla_c\nabla^c R_{ab}$, also modifies the background equations of motion, rendering our analysis irrelevant.

Action	Background equations	EoM at first order in h^{ij}
$R_a{}^c R^{ab} R_{bc}$	0	0
$R R^{ab} R_{ab}$	0	0
R^3	0	0
$R^{ab} R^{cd} R_{acbd}$	0	0
$R R_{abcd} R^{abcd}$	0	$-8 h_{0,}{}^{ijkl}\ \partial_v^2 h_{kl}$
$R^{ab} R_a{}^{cde} R_{bcde}$	0	$-2 h_{0,}{}^{ijkl}\ \partial_v^2 h_{kl} + 4 h_{0,}{}^{k(i}\ \Delta_d \partial_v^2 h_k{}^{j)}$
$R_a{}^e{}_c{}^f R^{abcd} R_{bedf}$	0	$3 h_{0,}{}^{ijkl}\ \partial_v^2 h_{kl}$
$R_{ab}{}^{ef} R^{abcd} R_{cdef}$	0	$24 h_{0,}{}^{k(i}\ \Delta_d \partial_v^2 h_k{}^{j)}$
$R \nabla_c \nabla^c R$	0	0
$R^{ab} \nabla_c \nabla^c R_{ab}$	$-\frac{1}{2} \vec{\partial}^6 h_0$	$-\frac{1}{2} \Delta_d^3 h^{ij}$

Table 7.2: Various contributions from the possible dimension-six terms constructed from Riemann tensors and covariant derivatives. Orange color indicates the presence of fourth order derivatives acting on h^{ij} and red the presence of sixth order derivatives.

$$\mathcal{W}_0^{ij} \equiv h_{0,}{}^{ik} h_{0,}{}^{jl} h_{kl,v^4} \ , \tag{7.83}$$

and

$$\mathcal{V}_0^{ij} \equiv h_{0,}{}^{kl} h_{0,kl} h^{ij}{}_{,v^4} \ . \tag{7.84}$$

Action	EoM at first order in h^{ij}
$R_{ab}{}^{ef} R^{abcd} R_{ce}{}^{hg} R_{dfhg}$	$-32 h_{0,}{}^{lk} h_{0,k}{}^{(i} \partial_v^4 h^{j)}{}_l$
$R_a{}^e{}_c{}^f R^{abcd} R_b{}^h{}_e{}^g R_{dhfg}$	$-8 h_{0,}{}^{lk} h_{0,k}{}^{(i} \partial_v^4 h^{j)}{}_l - 4 h_{0,}{}^{kl} h_{0,kl} \partial_v^4 h^{ij}$
$R_{ab}{}^{ef} R^{abcd} R_c{}^h{}_e{}^g R_{dhfg}$	0
$R_{ab}{}^{ef} R^{abcd} R_{cd}{}^{hg} R_{efhg}$	$-64 h_{0,}{}^{ik} h_{0,}{}^{jl} \partial_v^4 h_{kl}$
$R_{abc}{}^e R^{abcd} R_d{}^{fhg} R_{efhg}$	$-16 h_{0,}{}^{ik} h_{0,}{}^{jl} \partial_v^4 h_{kl} - 16 h_{0,}{}^{lk} h_{0,k}{}^{(i} \partial_v^4 h^{j)}{}_l$
$R_a{}^e{}_c{}^f R^{abcd} R_b{}^h{}_d{}^g R_{ehfg}$	$-8 h_{0,}{}^{ik} h_{0,}{}^{jl} \partial_v^4 h_{kl} - 8 h_{0,}{}^{kl} h_{0,kl} \partial_v^4 h^{ij}$
$R_{abcd} R^{abcd} R_{efhg} R^{efhg}$	0

Table 7.3: Various contributions from the possible $[R^4]$ terms. The contributions to the background equations of motion vanish.

As an example we consider the third and fourth order Lovelock theories.

$$\begin{aligned} \mathcal{L}_3 = \sqrt{-g} \Big(& R^3 + 16 R_a{}^c R_{ab} R^{bc} + 24 R_{ab} R^{cd} R_{acbd} + 3 R R^{abcd} R_{abcd} \\ & - 12 R R_{ab} R^{ab} - 24 R^{ab} R_a{}^{cde} R_{bcde} + 8 R_a{}^e{}_c{}^f R^{abcd} R_{bfde} + 2 R_{ab}{}^{ef} R^{abcd} R_{cdef} \Big) \ , \end{aligned} \tag{7.85}$$

and

$$\begin{aligned}\mathcal{L}_4 = \sqrt{-g}\Big(&96R_a{}^e{}_c{}^f R^{abcd} R_b{}^h{}_e{}^i R_{dhfi} + 96R_{ab}{}^{ef} R^{abcd} R_c{}^h{}_e{}^i R_{difh} \\ &- 6R_{ab}{}^{ef} R^{abcd} R_{cd}{}^{hi} R_{efhi} + 48R_{abc}{}^e R^{abcd} R_d{}^{fhi} R_{efhi} \\ &-48R_a{}^e{}_c{}^f R^{abcd} R_b{}^h{}_d{}^i R_{ehfi} - 3\left(R_{abcd}R^{abcd}\right)^2\Big) + \mathcal{F}(R^{ab}, R).\end{aligned} \tag{7.86}$$

Using the results of Tables 7.2 and 7.3 we find that both the contributions to the background equations of motion and those to the equations of motion for the test graviton vanish. This is expected since the E_{ij} components of the equations of motion in Lovelock theories take the form:

$$\sum_{n\geq 2} \lambda_n \delta^{i\rho_1\dots\rho_{2p}}_{j\sigma_1\dots\sigma_{2p}} R_{\rho_1\rho_2}{}^{\sigma_1\sigma_2} \dots R_{\rho_{2p-1}\rho_{2p}}{}^{\sigma_{2p-1}\sigma_{2p}} \tag{7.87}$$

where δ is the generalised Kronecker delta. In particular, for $n > 2$, we must have at least two Riemann tensors at zeroth order in perturbation theory and therefore must absorb four upper u / lower v indices. However, the generalised Kronecker delta can only absorb two upper u / lower v indices since it is fully antisymmetric, and so, the contributions from Lovelock terms of order $n > 2$ vanish.

5 Swift Behaviour and degenerate causal cone

We now use the equations of motion derived in the previous section to find the characteristics hypersurfaces for the probe graviton and check for swift propagation. We only consider cases with $D > 4$ as the case $D = 4$ will lead to significantly weaker results, presented in section 6. We will additionally find that for the $[R^4]$ terms, one can obtain a situation in which the characteristics hypersurfaces are all degenerate, we will argue that this denotes a non-hyperbolicity of the equation of motion.

We know from our previous study of the shock wave background that we are likely to find a polarisation-dependent effect. We therefore start by choosing a consistent basis of polarisations for the probe graviton before fully classifying the possible swift propagation resulting from the operators found in the previous section.

5.1 Choosing a Basis of Polarisations

We can choose without loss of generality the impact parameter to be $\vec{b} = (b, 0, \dots)$ where we label the transverse coordinates by x_i, $i = 1, 2, 3, \dots$. The index structure forces all contributions to our equations of motion to be of the form:

$$F\epsilon^{ij} + Gb^k b^{(i}\epsilon^{j)}_{\ k}\,, \tag{7.88}$$

where F and G may contain v and u derivatives. Given the restriction (7.23) and the fact that the polarisation is traceless, for gravitons propagating in the middle between the two beams, we can use the following basis of polarisations:

- $\oplus$ polarisations – these are polarisations of the form $\epsilon^{aa} = -\epsilon^{bb} = 1/\sqrt{2}$ with the requirement that $a, b \neq 1$ (as a consequence of (7.23)) and all other components vanish.

- $\otimes$ polarisations – these are polarisations of the form $\epsilon^{ab} = \epsilon^{ba} = 1/\sqrt{2}$ and all other components vanish.

It is then easy to see that the second term of (7.88) vanishes for $\oplus$ polarisations and that it is non zero only for $\otimes$ polarisations of the form $\epsilon^{1b} = \epsilon^{b1} = 1/\sqrt{2}$. Hence we identify two different classes of $\otimes$ polarisation: those for which the second term of (7.88) vanishes and those for which it does not. Picking one representative for each class, we have:

- Class (A): $\otimes$ polarisation with $\epsilon^{21} = \epsilon^{12} = 1/\sqrt{2}$.
- Class (B): $\otimes$ polarisation with $\epsilon^{23} = \epsilon^{32} = 1/\sqrt{2}$.

Notice that the operator $F\delta^{ik}\delta^{jl} + Gb^k b^{(i}\delta^{j)l}$ is diagonal for this basis of polarisations (i.e. $E_{ij} \sim \epsilon_{ij}$ since $\epsilon^{k(i}b^{j)}b_k = b^2\epsilon^{ij}/2$ for class (A) and 0 for class (B)). This validates the choice we made in section 2.1 of contracting the equations of motion by the polarisation tensor. Furthermore, we are in the case discussed in section 3 so that we can consider the characteristic equation for each type of polarisation separately.

5.2 Swift Behaviour of Second and Third Order Actions

Since the equations of motion are linear in the probe graviton it is possible to study the characteristic equations of each type of contribution to the equations of motion separately. We use $\mathcal{C}_{(\mathrm{A})}$ and c_β to denote contribution to the characteristic equations for gravitons with polarisations (A) and (B), respectively.

First, let us consider the contribution to the characteristic equations from the Einstein-Hilbert term $\mathcal{E}_{ij} = -\frac{1}{2}\Delta_d h_{ij}$ of Eq. (7.17):

$$\mathcal{C}_{(\mathrm{A})/(\mathrm{B})}\left[\mathcal{E}_{ij}\right] = 2\xi_v\left(\xi_u + \left(\frac{R_b}{b}\right)^{D-4}\xi_v\right)\epsilon_{ij} \ . \tag{7.89}$$

As we have already seen before, the characteristics hypersurfaces are given by Eq. (7.62) and indicates infraluminal propagation (Shapiro time delay) independent of the choice polarisation.

We move next to terms which are quadratic in derivatives of the probe graviton. We have seen in the previous section that these are the $\mathcal{T}_0^{ij} = h_{0,}{}^{k(i}h^{j)}{}_{k,vv}$ and $\mathcal{S}_0^{ij} = h_{0,}{}^{ijkl}h_{kl,vv}$ terms of Eqs. (7.77) and (7.80). Their contributions to the characteristic equations are given by:

$$\begin{aligned}
\mathcal{C}_{(\mathrm{A})}\left[\mathcal{T}_0^{ij}\right] &= \epsilon_{ij}\left(\frac{R_b}{b}\right)^{D-4}\frac{(D-4)^2}{2b^2}\xi_v^2, \\
c_\beta\left[\mathcal{T}_0^{ij}\right] &= -\epsilon_{ij}\left(\frac{R_b}{b}\right)^{D-4}\frac{(D-4)}{b^2}\xi_v^2,
\end{aligned} \tag{7.90}$$

and

$$\begin{aligned}
\mathcal{C}_{(\mathrm{A})}\left[\mathcal{S}_0^{ij}\right] &= -\epsilon_{ij}\left(\frac{R_b}{b}\right)^{D-4}\frac{2(D-4)(D-2)(D-1)}{b^4}\xi_v^2, \\
c_\beta\left[\mathcal{S}_0^{ij}\right] &= \epsilon_{ij}\left(\frac{R_b}{b}\right)^{D-4}\frac{2(D-4)(D-2)}{b^4}\xi_v^2.
\end{aligned} \tag{7.91}$$

Note that the signs of these contributions depend on the polarisation of the probe graviton.

We illustrate the swift behaviour of the probe graviton by studying two examples in details. These are Gauss-Bonnet gravity and an action of the form $R-\frac{\lambda_3\ell_3^4}{8}RR_{abcd}R^{abcd}$. For Gauss-Bonnet gravity, we obtained the following equations of motion (see Eq. (7.78)):

$$h_{ij,uv}+h_0h_{ij,vv}+4\varepsilon_\pm\ell_2^2h_{0\,,k(i}\,h_{j)}^{\ k}{}_{,vv}=0. \tag{7.92}$$

Using the previous results, we can show that the characteristic equation for the polarisation (A) is:

$$\xi_v\left(\xi_u+\left(\frac{R_b}{b}\right)^{D-4}[1+2\frac{\varepsilon_\pm\ell_2^2(D-4)^2}{b^2}]\xi_v\right)=0 \tag{7.93}$$

and for the polarisation (B):

$$\xi_v\left(\xi_u+\left(\frac{R_b}{b}\right)^{D-4}[1-4\frac{\varepsilon_\pm\ell_2^2(D-4)}{b^2}]\xi_v\right)=0 \tag{7.94}$$

The solutions correspond to two characteristic hypersurfaces:

$$\xi_v=0,\qquad \xi_u=-h_0\left[1-4\gamma_{(A)/(B)}\frac{\varepsilon_\pm\ell_2^2(D-4)}{b^2}\right]\xi_v, \tag{7.95}$$

where

$$\gamma_{(A)}=\frac{4-D}{2}\quad\text{ and }\quad\gamma_{(B)}=1. \tag{7.96}$$

The second solution is inside the flat spacetime light-cone when ξ_u is negative. This is the case if $\ell_2^2=0$ (Einstein gravity) since R_b is a positive constant. For $b\sim\sqrt{|\varepsilon_\pm|}\ell_2$ we can always adjust ξ_u to be positive for either the (A) or (B) polarisations depending on the sign of $\varepsilon_\pm$. This shows that Einstein-Gauss-Bonnet gravity allows for swift propagation regardless of sign of the Gauss-Bonnet coefficient. If we would have considered instead the term $h_{0\,,}^{\ ijkl}h_{kl,vv}$, which is produced by an action of the form $R-\frac{\lambda_3\ell_3^4}{8}RR_{abcd}R^{abcd}$ (where λ_3 stands for the sign of this correction), we would have obtained the characteristics:

$$\xi_v=0,\qquad \xi_u=-h_0\left[1-\tilde\gamma_{(A)/(B)}\frac{(D-4)(D-2)}{b^4}\lambda_3\ell_3^4\right]\xi_v, \tag{7.97}$$

where

$$\tilde\gamma_{(A)}=D-1\qquad\text{and}\qquad\tilde\gamma_{(B)}=-1\ . \tag{7.98}$$

These two examples can be matched to the two types of extended gravity amplitudes considered in [134] (see their Eq. (3.17)).

Finally, returning to Table 7.2, the only term that we have not discussed so far (and is not associated with a modification of the background) is $\mathcal{T}_1^{ij}=h_{0\,,}^{\ k(i}\,\Delta_d\partial_v^2h_k^{\ j)}$

of equation (7.79). This is simply the derivative of one of the terms that we have already studied. However, since it has four derivatives acting on the probe graviton it dominates the characteristic equations, which are determined from the principal part of the characteristic polynomial (as already mentioned in subsection 3.2). In this case the characteristic hypersurfaces do not depend on the polarisation and are given by:

$$\xi_v = 0, \qquad \xi_u = -\xi_v h_0 = -\xi_v \left(\frac{R_b}{b}\right)^{D-4}, \tag{7.99}$$

so that we recover the usual Shapiro time delay. Such a theory with equations of motion which are fourth order derivatives theory can suffer however from Ostrogradsky instabilities. We summarise our results in Table 7.4 for an independent basis of actions of the forms $[R^2]$, $[R^3]$ and $[R\nabla^2 R]$ sorting them according to the four following categories:

- Category 1 contains terms which do not modify the Hilbert-Einstein equations for the background and for the probe graviton. In this category, we have for instance $f(R)$ gravity and the Lovelock terms of order higher than two.
- Category 2 contains terms that do not modify the background equations, but do modify the equations for the probe graviton in a way that leads to swift propagation. These are specified up to addition of terms from category 1.
- Category 3 contains terms that do not modify the background equations, but their equations for the probe graviton are fourth-order in derivatives with characteristic hypersurfaces similar to Einstein-Hilbert gravity. These are specified up to addition of terms from categories 1 and 2.
- Category 4 contains terms which have modified background equations, implying that we cannot apply our analysis in this case. These are specified up to addition of terms from categories 1,2 and 3.

5.3 Swift Behaviour of Fourth Order Actions

Let us now consider the behaviour of $[R^4]$ terms. As can be read from Table 7.3, the equations of motion of $[R^4]$ actions are linear combinations of the following three contributions:

$$\begin{aligned} \mathcal{V}_0{}^{ij} &\equiv h_{0,}{}^{kl} h_{0,kl} h^{ij}{}_{,v^4}, \\ \mathcal{U}_0{}^{ij} &\equiv h_{0,}{}^{kl} h_{0,k}{}^{(i} h^{j)}{}_{l,v^4}, \\ \mathcal{W}_0{}^{ij} &\equiv h_{0,}{}^{ik} h_{0,}{}^{jl} h_{kl,v^4}, \end{aligned} \tag{7.100}$$

that lead to the following contributions to the characteristic equations. For $\mathcal{V}_0^{ij}$ we have:

$$\mathcal{C}_{(\mathrm{A})}\left[\ \mathcal{V}_0^{ij}\ \right] = c_\beta[\ \mathcal{V}_0^{ij}\ ] = \left(\frac{R_b}{b}\right)^{2(D-4)} \frac{(D-2)(D-3)(D-4)^2}{b^4} \xi_v^4\, \epsilon_{ij}\ , \tag{7.101}$$

Category 1 (no contribution)	$R^2,\ R^3,\ R\nabla_c\nabla^c R$ $R_a{}^c R^{ab} R_{bc}\ ,\ RR^{ab}R_{ab}$ $R^{ab}\nabla_c\nabla^c R_{ab}$ $RR_{abcd}R^{abcd} - 4R^{ab}R_a{}^{cde}R_{bcde} + \frac{2}{3}R_{ab}{}^{ef}R^{abcd}R_{cdef}$ $RR_{abcd}R^{abcd} + \frac{8}{3}R_a{}^e{}_c{}^f R^{abcd}R_{bedf}$
Category 2 (swift propagation)	$RR_{abcd}R^{abcd}$ $R_{abcd}R^{abcd} - 4R_{ab}R^{ab}$
Category 3 (higher derivative operators, infraluminal)	$R_{ab}{}^{ef}R^{abcd}R_{cdef}$
Category 4 (background modified)	$R^{ab}\nabla_c\nabla^c R_{ab}$ $R^{ab}R_{ab}$

Table 7.4: Basis of $[R^2]$, $[R^3]$ and $[R\nabla^2 R]$ action terms, sorted by categories as detailed in the text. Our analysis is relevant as long as the background equations are not modified, i.e., for the terms in categories 1,2 and 3.

which does not depend on the polarisation. For $\mathcal{U}_0^{ij}$ we have:

$$\begin{aligned}\mathcal{C}_{(\mathrm{A})}\left[\,\mathcal{U}_0^{ij}\,\right] &= \left(\frac{R_b}{b}\right)^{2(D-4)}\frac{(D-4)^2}{b^4}\left[1+\frac{(D-2)(D-4)}{2}\right]\xi_v^4\,\epsilon_{ij},\\ c_\beta\left[\,\mathcal{U}_0^{ij}\,\right] &= \left(\frac{R_b}{b}\right)^{2(D-4)}\frac{(D-4)^2}{b^4}\xi_v^4\,\epsilon_{ij}\ ,\end{aligned} \tag{7.102}$$

where the contributions of the two polarisations behave differently, but have the same sign, so that in general the sign cannot be adjusted by picking the appropriate polarisation. Finally, for $\mathcal{W}_0{}^{ij} \equiv h_{0,}{}^{ik}h_{0,}{}^{jl}h_{kl,v^4}$ we get:

$$\begin{aligned}\mathcal{C}_{(\mathrm{A})}\left[\,\mathcal{W}_0^{ij}\,\right] &= -\left(\frac{R_b}{b}\right)^{2(D-4)}\frac{(D-4)^2}{b^4}(D-3)\xi_v^4\,\epsilon_{ij},\\ c_\beta\left[\,\mathcal{W}_0^{ij}\,\right] &= \left(\frac{R_b}{b}\right)^{2(D-4)}\frac{(D-4)^2}{b^4}\xi_v^4\,\epsilon_{ij}\ .\end{aligned} \tag{7.103}$$

For this term we can adjust the sign by choosing an appropriate polarisation.

None of these three terms $\mathcal{V}_0$, $\mathcal{U}_0$, $\mathcal{W}_0$ can appear alone in the equations of motion. This is because they have fourth order derivatives of the form ∂_v^4 acting on the probe graviton. The characteristic equations are dominated by these ξ_v^4 contributions, and if no other four derivative terms are present, the causal cone is locally degenerate.

We have discuss this situation in detail in section 3.5 and show that in this case the full equations of motion cannot be hyperbolic with respect to the time direction when expanded around our background. The initial value problem is therefore not well-posed for gravitons propagating in the middle between the two beams.

Consider for instance the action:

$$\mathcal{L}_{ss4} = \frac{\sqrt{-g}}{16\pi\ell_P^{D-2}}\left[R + \frac{\zeta(3)\ell_4^6}{8}R^{abcd}\left(R_a{}^e{}_c{}^f R_b{}^h{}_e{}^g R_{dhfg} - \frac{R_{ab}{}^{ef}R_{ce}{}^{hg}R_{dfhg}}{4}\right)\right], \quad (7.104)$$

present in the effective action originating from superstring theory as presented by [150].[10] Using the results of section 4, the equations of motion read:

$$2h^{ij}{}_{,uv} + 2h_0 h^{ij}{}_{,v^2} - \ell_4^6\frac{\zeta(3)}{2}h_0{}_,{}^{kl}h_{0,kl}h^{ij}{}_{,v^4} = 0\ , \quad (7.105)$$

and have a degenerate causal cone as discussed above. However, this can be fixed by adding extra, lower order terms to the action which have equations of motion with four derivatives acting on the probe graviton. Table 7.2 reveals two such terms, $R^{ab}R_a{}^{cde}R_{bcde}$ and $R_{ab}{}^{ef}R^{abcd}R_{cdef}$, which do not modify the background equations. We therefore modify our action to:

$$\mathcal{L}_{mod} = \frac{\sqrt{-g}}{16\pi\ell_P^{D-2}}\Big[R + \ell_3^4 R^{ab}R_{acde}R_b{}^{cde} + \ell_4^6\frac{\zeta(3)}{8}R^{abcd}\left(R_a{}^e{}_c{}^f R_b{}^h{}_e{}^g R_{dhfg} - \frac{1}{4}R_{ab}{}^{ef}R_{ce}{}^{hg}R_{dfhg}\right)\Big] \quad (7.106)$$

which reduces to the previous one in the limit $\ell_3 \to 0$. We can use our previous results to find that the characteristic equations have the following solutions:

$$\xi_v = 0, \qquad \xi_u = -h_0\left[1 - \gamma_{(A)/(B)}\frac{\zeta(3)\ell_4^6}{16b^2\ell_3^4}(D-2)(D-3)\right]\xi_v\ , \quad (7.107)$$

where

$$\gamma_{(A)} = -1 \qquad \text{and} \qquad \gamma_{(B)} = \frac{D-4}{2}\ . \quad (7.108)$$

Since the sign of γ can be chosen to be either positive or negative, we have swift propagation if:

$$\frac{\ell_3^4 b^2}{\ell_4^6} < \frac{\zeta(3)}{8}(D-2)(D-3)|\gamma| \quad (7.109)$$

therefore when varying $\frac{\ell_3^4 b^2}{\ell_4^6}$ from infinity (no fourth order term) to zero (only fourth order term), the theory starts infraluminal, then admits swift propagation and finally the causal cone collapses and becomes degenerate.

Below a critical value:

$$b_c \sim h_0\sqrt{\left|\frac{\ell_4^6}{\ell_3^4}\right|} \quad (7.110)$$

[10] It differs from the expression of [151] by factors of $\mathcal{L}_4$, the fourth order Lovelock Lagrangian. Such factors are irrelevant in our analysis since they do not influence the equations of motion for the probe graviton on our background.

the local causal cone envelops a region including slices of constant time.

We close this section by supplementing the unitarity and analyticity constraints of [152] with some constraints implied by requiring the absence of a degenerate causal cone in actions composed of the Einstein-Hilbert action supplemented by quartic corrections only. We then obtain two algebraic relations between the coefficients c_i of [152] that are complementary to their positivity requirements. These are:

$$\begin{aligned} 2(c_7 + 2c_2 + 4c_4) &= -2(D-3)(2c_6 + c_7), \\ 2(c_6 + 2c_2 + 8c_3) &= -(D-3)(D-4)(2c_6 + c_7). \end{aligned} \tag{7.111}$$

6 Four Dimensional Case

We close this chapter by considering in more details the case $D = 4$ we had left aside in the previous sections. Since we have only 2 transverse dimensions there are a priori only two possible polarisations state for a massless transverse graviton. However, the additional constraint (7.23) remove one of these two degrees of freedom, so that we only have one polarisation. This implies that we cannot choose the nature of the time shift by going from type (A) to type (B) polarisations (the only possible polarisation is straightforwardly seen to be $\epsilon^{12} = \epsilon^{21}$). The presence or absence of a swift propagation therefore depends on the particular sign of the coupling constants of the extended gravity theory.

Solving the Einstein equation (7.7) in four dimensions gives:

$$h_0(x_i) = \begin{cases} 8\pi\rho\ell_P^2 r_0^2 \log\dfrac{\Lambda}{r} & r > r_0 \\ 4\pi\rho\ell_P^2 r_0^2 \left[1 + 2\log\dfrac{\Lambda}{r_0} - \dfrac{r^2}{r_0^2}\right] & r \leq r_0 \end{cases} . \tag{7.112}$$

Where Λ is a positive constant which is not fixed by the Einstein equations. Following the discussion of Section 3.3, we view this as an IR cutoff to our theory related to the length of the beams, indicating that we should take $r < \Lambda$.

Defining the constant a by

$$a \equiv 8\pi\rho\ell_P^2 r_0^2 > 0 \tag{7.113}$$

we obtain

$$\begin{aligned} h_0(\vec{b}) &= a \log\frac{\Lambda}{r} \\ \partial_i\partial_j h_0(\vec{b}) &= -\frac{a}{b^4}(b^2\delta_{ij} - 2b_i b_j) \\ \partial_i\partial_j\partial_k\partial_l h_0(\vec{b}) &= \frac{2a}{b^8}\left[-4b^2(\delta_{ij}b_k b_l + \dots) + b^4(\delta_{kl}\delta_{ij} + \dots)\right. \\ &\qquad \left. +24 b_i b_j b_k b_l\right], \end{aligned} \tag{7.114}$$

where the $\dots$ stand for all index permutations of a given tensor structure.

The results of Tables 7.1, 7.2 and 7.3 are left unchanged (since we have not used the particular form of h_0 there).

Next, we compute the characteristic equations for the various contributions to the equations of motion (suppressing the ϵ^{ij}):

$$\begin{aligned}
&\mathcal{C}_{(\mathrm{A})}\left[-\frac{1}{2}\Delta_d h^{ij}\right] = 2\xi_u\xi_v + 2\xi_v^2 a\log\frac{\Lambda}{r},\\
&\mathcal{C}_{(\mathrm{A})}\left[h_{0,}{}^{k(i}h^{j)}{}_{k,vv}\right] = 0,\\
&\mathcal{C}_{(\mathrm{A})}\left[h_{0,}{}^{k(j}\ \Delta_d\partial_v^2 h^{i)}{}_{k}\right] = 0,\\
&\mathcal{C}_{(\mathrm{A})}\left[h_{0,}{}^{ijkl}\ \partial_v^2 h_{kl}\right] = -\frac{12a}{b^4}\xi_v^2\\
&\mathcal{C}_{(\mathrm{A})}\left[h_{0,}{}^{lk}h_{0,k}{}^{(i}h^{j)}{}_{l,v^4}\right] = \frac{a^2}{b^4}\xi_v^4\\
&\mathcal{C}_{(\mathrm{A})}\left[h_{0,}{}^{ik}h_{0,}{}^{jl}h_{kl,v^4}\right] = -\frac{a^2}{b^4}\xi_v^4\\
&\mathcal{C}_{(\mathrm{A})}\left[h_{0,}{}^{kl}h_{0,kl}h^{ij}{}_{,v^4}\right] = \frac{2a^2}{b^4}\xi_v^4
\end{aligned} \tag{7.115}$$

Using the results of Table 7.1 one can easily check that the Gauss-Bonnet combination gives a vanishing contribution in $D = 4$. This is expected since the Euler density is topological in $D = 4$. Furthermore, we see that the only non-vanishing contribution from $[R^3]$ terms is $h_{0,}{}^{ijkl}\ \partial_v^2 h_{kl}$, which is present in the equations of motion derived from $RR_{abcd}R^{abcd}$, $R^{ab}R_a{}^{cde}R_{bcde}$ and $R_a{}^e{}_c{}^f R^{abcd}R_{bedf}$. The most general Lagrangian build from $[R^2]$ and $[R^3]$ terms for which our background (7.112) is a solution is then of the form:

$$\mathcal{L} = \frac{\sqrt{-g}}{16\pi\ell_P^2}\left[R + \ell_3^4(d_1 RR_{abcd}R^{abcd}R^{ab} + d_2 R_a{}^{cde}R_{bcde} + d_3 R_a{}^e{}_c{}^f R^{abcd}R_{bedf}) + (\dots)\right]\ ,$$

where the $(\dots)$ includes all the $[R^2]$ and $[R^3]$ terms with vanishing contributions to the characteristic equations (see Eq. (7.115) and Table 7.2). We obtain the characteristic equation:

$$\xi_u\xi_v + \xi_v^2 a\left[\log\frac{\Lambda}{b} + \frac{6\ell_3^4}{b^4}(8d_1 + 2d_2 + 3d_3)\right] = 0\ . \tag{7.116}$$

The presence of the logarithm and how to deal with it has been discussed at the end of Section 3.3. The presence of swift propagation for $b \sim \ell_3$ then depends on the sign of the last term in Eq. (7.116). We observe swift propagation if:

$$8d_1 + 2d_2 + 3d_3 < 0\ . \tag{7.117}$$

Since we are in four dimension, we have redundancy between the different operators listed in Table 7.2. For instance, the fact that the third order Lovelock theory (7.85) is topological implies that we can trade one of the d_i for the two others.

We have thus seen the in $D = 4$ we have somehow weaker conclusions than in the general case $D > 4$. There is a noteworthy exception: turning to the $[R^4]$ terms, we see that we get once more a degenerate causal cone. In $D = 4$ it is however not possible to fix this behaviour by adding $[R^3]$ terms as we did in Section 5.3, we readily conclude that this issue can only be solved by adding *higher* order terms in the actions.

7 Conclusions

In this chapter we have been interested in a simple, albeit not exhaustive, way of studying the local causal structure of a large variety of extended gravity theories. By considering perturbations propagating in parallel to two beams described by the stress-energy tensor (7.6), we found that many extended gravity theories allow for swift propagation, namely the fact that gravitons propagate close to a beam of massless relativistic particles faster than they would at the boundary of our spacetime. With our gauge choice, this is in fact equivalent to comparing directly their speed to the speed of light in a flat Minkowsky spacetime.

The background beams were chosen to mimic the successive scattering events of gravitons that [134] used to find a sizeable time-shift. In this sense, we recover and extend the results of [134] in an alternative fashion. We have further studied all possible theories based on $[R^2]$, $[R^3]$, $[R\nabla^2 R]$ and $[R^4]$ terms around our background (7.8). We have shown that swiftness appears to be a quite general feature. Noteworthy exceptions are $f(R)$ theories and Lovelock theories with order higher than three, which have the same local causal structure as general relativity around our background. The case of Gauss-Bonnet gravity appears to be an exception. This comes as a surprise as it was in this theories that the characteristics were first found to be different from the null geodesics. It may well be that for Lovelock theories at order larger than two, one needs a more complex background to exhibit swift propagation.

Most of the $[R^4]$ terms that we have studied have equations of motion with four derivatives acting on the probe graviton. We stress that from the point of view of causality, this should not be considered a game-ending property since these theories can be shown to be nonetheless hyperbolic in certain cases. However, we have found that for terms that we have classified, the projection of the characteristic hypersurfaces on the u, v plane can be degenerate. This situation have been proven to lead the non hyperbolicity of the equations of motion.

Many of the theories we consider have equations of motion with more than two derivatives acting on the probe graviton and hence may be subject to Ostrogradsky instabilities. Common solutions include looking for theories with degenerate higher derivative terms like $f(R)$ theories (see [153]), restricting to actions with equations of motion with no more than two derivatives, like Lovelock theories, or adding constraints to remove the instabilities [154]. The swift propagation issue we have discuss here is a priori unrelated and can further constrain the well-behaved extended gravity actions as they do for the case of Gauss-Bonnet gravity.

1 Swift Graviton

1.1 List of Metric Components, Christoffel Symbols and Riemann Components

We denote $x^\mu = (u, v, \vec{x})$. The zeroth order metric components are given by:

$$g^{(0)}_{\mu\nu} = \begin{pmatrix} h_0(\vec{x}) & -\frac{1}{2} & \\ -\frac{1}{2} & 0 & \\ & & \delta_{ij} \end{pmatrix}, \qquad g^{(0)\mu\nu} = \begin{pmatrix} 0 & -2 & \\ -2 & -4h_0(\vec{x}) & \\ & & \delta^{ij} \end{pmatrix}, \tag{.118}$$

where $h_0(\vec{x})$ is given by Eq. (7.8). As a rule of thumb at zeroth order in the probe graviton contribution:

$$\begin{aligned} V^u &= -2V_v, \qquad V^v = -2V_u - 4h_0 V_v, \\ V_u &= h_0 V^u - \frac{1}{2}V^v, \qquad V_v = -\frac{1}{2}V^u, \end{aligned} \tag{.119}$$

and so, a vector that only has a lower u component will only have an upper v component and the other way around.

a Zeroth Order in the Probe Graviton Contribution

The non-vanishing Christoffel symbols are given by:[11]

$$\begin{aligned} \Gamma^{(0)}_{iuu} &= -\frac{1}{2}\partial_i h_0, \qquad \Gamma^{(0)}_{uiu} = \frac{1}{2}\partial_i h_0, \\ \Gamma^{i(0)}_{uu} &= -\frac{1}{2}\partial_i h_0, \qquad \Gamma^{v(0)}_{iu} = -\partial_i h_0. \end{aligned} \tag{.120}$$

Those vanish when summing right in the middle between two beams. The non-vanishing Riemann components are:

$$\begin{aligned} R^{(0)}_{iuku} &= -\frac{1}{2}\partial_k\partial_i h_0, \\ R^i{}_{uku} &= -\frac{1}{2}\partial_k\partial^i h_0, \qquad R^v{}_{iku} = -\partial_k\partial_i h_0, \\ R^{(0)ivkv} &= -2\partial^k\partial^i h_0. \end{aligned} \tag{.121}$$

The non vanishing Ricci tensor components are:

$$R^{(0)}_{uu} = -\frac{1}{2}\partial_i\partial^i h_0, \qquad R^{(0)vv} = -2\partial_i\partial^i h_0, \tag{.122}$$

those vanish outside the beam. And the Ricci scalar vanishes identically:

$$R^{(0)} = 0. \tag{.123}$$

[11] The others are implied by symmetry or vanish.

b First Order in the Probe Graviton Contribution

We allow for a probe graviton of the form:

$$\delta g^{(1)}_{ij} = h_{ij}(u,v), \qquad \delta g^{(1)ij} = -h_{ij}(u,v). \tag{.124}$$

Which leads to the following non-vanishing Christoffel symbols:

$$\begin{aligned} \Gamma^{(1)}_{uij} &= -\frac{1}{2}\partial_u h_{ij}, \qquad \Gamma^{(1)}_{iuj} = \frac{1}{2}\partial_u h_{ij}, \\ \Gamma^{(1)}_{vij} &= -\frac{1}{2}\partial_v h_{ij}, \qquad \Gamma^{(1)}_{ivj} = \frac{1}{2}\partial_v h_{ij}, \end{aligned} \tag{.125}$$

or alternatively:

$$\begin{aligned} &\Gamma^{i(1)}_{uu} = \frac{1}{2}h^{ij}\partial_j h_0, \qquad \Gamma^{i(1)}_{uj} = \frac{1}{2}\partial_u h_{ij}, \\ &\Gamma^{v(1)}_{ij} = \partial_u h_{ij} + 2h_0\partial_v h_{ij}, \qquad \Gamma^{i(1)}_{vj} = \frac{1}{2}\partial_v h_{ij}, \qquad \Gamma^{u(1)}_{ij} = \partial_v h_{ij}. \end{aligned} \tag{.126}$$

The non vanishing components of the Riemann tensor are given by:

$$\begin{aligned} &R^{u(1)}_{iju} = -\partial_u\partial_v h_{ij}, \qquad R^{u(1)}_{ijv} = -\partial_v^2 h_{ij}, \qquad R^{u(1)}_{uiu} = -\frac{1}{2}\partial_k h_0\,\partial_v h_{ik}, \\ &R^{v(1)}_{kij} = \partial_i h_0\partial_v h_{kj} - \partial_j h_0\partial_v h_{ki}, \qquad R^{v(1)}_{uuj} = h_0\partial_i h_0\partial_v h_{ij}, \\ &R^{v(1)}_{kuj} = \partial_u^2 h_{kj} + 2h_0\partial_u\partial_v h_{kj}, \qquad R^{v(1)}_{kvj} = \partial_v\partial_u h_{ij} + 2h_0\partial_v^2 h_{ij}, \\ &R^{v(1)}_{iuv} = -\frac{1}{2}\partial_k h_0\partial_v h_{ik}, \qquad R^{v(1)}_{vuj} = -\frac{1}{2}\partial_i h_0\partial_v h_{ij}, \\ &R^{i(1)}_{ujk} = -\frac{1}{2}\partial_v h_{ij}\partial_k h_0 + \frac{1}{2}\partial_v h_{ik}\partial_j h_0, \\ &R^{i(1)}_{uuk} = \frac{1}{2}\partial_u^2 h_{ik} - \frac{1}{2}h^{ij}\partial_k\partial_j h_0, \qquad R^{i(1)}_{vuk} = \frac{1}{2}\partial_u\partial_v h_{ik}, \\ &R^{i(1)}_{juk} = \frac{1}{2}\partial_v h_{ik}\partial_j h_0 - \frac{1}{2}\partial_v h_{jk}\partial_i h_0, \qquad R^{i(1)}_{uvk} = \frac{1}{2}\partial_u\partial_v h_{ik}, \\ &R^{i(1)}_{vvk} = \frac{1}{2}\partial_v^2 h_{ik}, \qquad R^{i(1)}_{uuv} = -\frac{1}{4}\partial_v h^{ij}\partial_j h_0, \end{aligned} \tag{.127}$$

or alternatively:

$$\begin{aligned} &R^{(1)}_{ukij} = \frac{1}{2}(\partial_j h_0\partial_v h_{ki} - \partial_i h_0\partial_v h_{kj}), \qquad R^{(1)}_{uvui} = \frac{1}{4}\partial_j h_0\partial_v h_{ij}, \\ &R^{(1)}_{ukui} = -\frac{1}{2}\partial_u^2 h_{ki}, \qquad R^{(1)}_{ukvi} = -\frac{1}{2}\partial_v\partial_u h_{ki}, \qquad R^{(1)}_{vijv} = \frac{1}{2}\partial_v^2 h_{ij}. \end{aligned} \tag{.128}$$

The non vanishing Ricci tensor components are given by:

$$\begin{aligned} &R^{(1)}_{ij} = 2\partial_u\partial_v h_{ij} + 2h_0\partial_v^2 h_{ij}, \qquad R^{(1)}_{ui} = \partial_v h_{ij}\partial_j h_0 - \frac{1}{2}\partial_i h_0\partial_v h^k_k, \\ &R^{(1)}_{uu} = \frac{1}{2}h^{kj}\partial_k\partial_j h_0 - \frac{1}{2}\partial_u^2 h^k_k, \qquad R_{uv} = -\frac{1}{2}\partial_u\partial_v h^k_k, \qquad R_{vv} = -\frac{1}{2}\partial_v^2 h^k_k. \end{aligned} \tag{.129}$$

If we assume that the perturbation is traceless we are left with:

$$R^{(1)}_{ij} = 2\partial_u\partial_v h_{ij} + 2h_0\partial_v^2 h_{ij}, \qquad R^{(1)}_{ui} = \partial_v h_{ij}\partial_j h_0, \qquad R^{(1)}_{uu} = \frac{1}{2}h^{kj}\partial_k\partial_j h_0. \quad (.130)$$

Note that there are no lower v indices and hence no upper u indices. The Ricci scalar reads:

$$R^{(1)} = 4\partial_u\partial_v h^k_k + 4h_0\partial_v^2 h^k_k, \quad (.131)$$

and vanishes for a traceless perturbation:

$$R^{(1)} = 0. \quad (.132)$$

1.2 Characteristic Method - a Detailed Example

In this appendix, we explicitly show the property quoted in section 3 that characteristics surfaces can be obtained from the vanishing of the characteristic form in a particular example of interest. We consider the equation

$$\partial_u\partial_v h + a\partial_v^2 h + b\partial_v^4 h = 0\ , \quad (.133)$$

where h is a scalar function of the two variables u and v and a and b are two constants. Suppose that $\xi = (\xi_u, \xi_v)$ is the unit normal vector to the curve $\mathcal{C}$ on which we are given the Cauchy data. Inner derivatives on $\mathcal{C}$ can be obtained by $-\xi_v\partial_u + \xi_u\partial_v$ and normal derivative to $\mathcal{C}$ by $\xi_u\partial_u + \xi_v\partial_v$. In order to find all partial derivatives of h up to third order, we have to solve successively the following systems :

$$\begin{cases} -\xi_v\partial_u h + \xi_u\partial_v h & = \partial_{\mathcal{C}} h \\ \xi_u\partial_u h + \xi_v\partial_v h & = \partial_\perp h \end{cases}$$

$$\begin{cases} -\xi_v\partial_u^2 h + \xi_u\partial_u\partial_v h & = \partial_{\mathcal{C}}\partial_u h \\ -\xi_v\partial_u\partial_v h + \xi_u\partial_u\partial_v h & = \partial_{\mathcal{C}}\partial_v h \\ (\xi_u\partial_u + \xi_v\partial_v)^2 h & = \partial_\perp^2 h \end{cases}$$

$$\begin{cases} -\xi_v\partial_u^3 h + \xi_u\partial_u^2\partial_v h & = \partial_{\mathcal{C}}\partial_u^2 h \\ -\xi_v\partial_u^2\partial_v h + \xi_u\partial_u\partial_v^2 h & = \partial_{\mathcal{C}}\partial_u\partial_v h \\ -\xi_v\partial_u\partial_v^2 h + \xi_u\partial_v^3 h & = \partial_{\mathcal{C}}\partial_v^2 h \\ (\xi_u\partial_u + \xi_v\partial_v)^3 h & = \partial_\perp^3 h \end{cases}$$

where all partial derivatives are evaluated on $\mathcal{C}$ and $\partial_{\mathcal{C}}$ ($\partial_\perp$) denotes the inner (outer) derivative to $\mathcal{C}$. Since these systems have determinants respectively $-(\xi_u^2 + \xi_v^2) = -1$, $(-\xi_u^2 - \xi_v^2)^2 = 1$ and , $(-\xi_u^2 - \xi_v^2)^3 = -1$, they are solvable and gives all partial derivatives up to third order.

Fourth order partial derivatives must be obtained from

$$\begin{cases} -\xi_v \partial_u^4 h + \xi_u \partial_u^3 \partial_v h & = \partial_{\mathcal{C}} \partial_u^3 h \\ -\xi_v \partial_u^3 \partial_v h + \xi_u \partial_u^2 \partial_v^2 h & = \partial_{\mathcal{C}} \partial_u^2 \partial_v h \\ -\xi_v \partial_u^2 \partial_v^2 h + \xi_u \partial_u \partial_v^3 h & = \partial_{\mathcal{C}} \partial_u \partial_v^2 h \\ -\xi_v \partial_u \partial_v^3 h + \xi_u \partial_v^4 h & = \partial_{\mathcal{C}} \partial_v^3 h \\ b \partial_v^4 h = -\partial_u \partial_v h + a \partial_v^2 h & \end{cases}$$

whose determinant is precisely the characteristic form $b\xi_v^4$. Since all higher order partial derivatives can be derived from the previous system by partial derivations, the vanishing of the characteristic form indicated that Cauchy data on $\mathcal{C}$ do not fix uniquely the solution of eq.133.

1.3 Replacement Rules

In this appendix we detail some of the replacement rules which we used in *Mathematica* in order to obtain our results.

a Zeroth Order Equations of Motion

We consider a background of the form $h_0 = \left(\frac{R_b}{r}\right)^{D-4}$, as in equation (7.8) for $r > r_0$, with $D > 4$ and where R_b was defined in (7.10) and is a positive constant. We denote by $\vec{b}$ the impact parameter, that is, the location in which we evaluate our equations of motion. The value and first derivatives of h_0 at this point are given by:

$$\begin{aligned} h_0(\vec{b}) &= \left(\frac{R_b}{b}\right)^{D-4}, \\ \partial_i h_0(\vec{b}) &= -\left(\frac{R_b}{b}\right)^{D-4} \frac{(D-4)}{b^2} b_i, \\ \partial_i \partial_j h_0(\vec{b}) &= -\left(\frac{R_b}{b}\right)^{D-4} \frac{(D-4)}{b^4} (b^2 \delta_{ij} - (D-2) b_i b_j), \\ \partial_i \partial_j \partial_k h_0(\vec{b}) &= \left(\frac{R_b}{b}\right)^{D-4} \frac{(D-4)(D-2)}{b^6} \Big[b^2 (\delta_{ij} b_k + \delta_{jk} b_i + \delta_{ik} b_j) \\ &\qquad - D b_i b_j b_k \Big], \\ \partial_i \partial_j \partial_k \partial_l h_0(\vec{b}) &= \left(\frac{R_b}{b}\right)^{D-4} \frac{(D-4)(D-2)}{b^8} \Big[-b^2 D (\delta_{ij} b_k b_l + \dots) \\ &\qquad + b^4 (\delta_{kl} \delta_{ij} + \dots) + D(D+2) b_i b_j b_k b_l \Big], \end{aligned} \tag{.134}$$

where the $\dots$ stands for all index permutations of a given tensor structure. At the midpoint between two identical beams we obtain:

$$\begin{aligned} \partial_i h_0(\vec{b}) &\to \partial_i (h_0 + \hat{h}_0)(\vec{b}) = \partial_i (h_0(\vec{b}) + h_0(-\vec{b})) = 0, \\ \partial_i \partial_j h_0(\vec{b}) &\to \partial_i \partial_j (h_0 + \hat{h}_0)(\vec{b}) = 2 \partial_i \partial_j h_0(\vec{b}), \\ \partial_i \partial_j \partial_k h_0(\vec{b}) &\to \partial_i \partial_j \partial_k (h_0 + \hat{h}_0)(\vec{b}) = 0, \\ \partial_i \partial_j \partial_k \partial_l h_0(\vec{b}) &\to \partial_i \partial_j \partial_k \partial_l (h_0 + \hat{h}_0)(\vec{b}) = 2 \partial_i \partial_j \partial_k \partial_l h_0(\vec{b}). \end{aligned} \tag{.135}$$

Before we start, we reiterate a number of useful facts. First, (.135) implies that the zeroth order Christoffel symbols (.120) and any even number of derivatives acting on them vanish when evaluated at the midpoint between the two beams. With a little abuse of notation we write:

$$\Gamma^{(0)}_{\mu\nu\rho}(\vec{b}) = 0, \qquad \partial_\alpha\partial_\beta\Gamma^{(0)}_{\mu\nu\rho}(\vec{b}) = 0, \qquad \text{etc.} \tag{.136}$$

Similarly any odd number of derivatives acting on a zeroth order Riemann tensor vanishes at the midpoint:

$$\partial_\mu R^{(0)}_{\alpha\beta\gamma\delta}(\vec{b}) = 0, \qquad \text{etc.} \tag{.137}$$

Finally, notice that there are no zero order quantities with lower v or upper u indices.

In order to make sure that $h_{_0}$ given in (7.8) is indeed a valid background we have to make sure that it solves the equations of motion of the full extended gravity theory. A sufficient condition is that the zeroth order equations of motion take the form (7.7). This is the case for many of the theories studied in this paper. Since all zeroth order quantities have two lower u indices and no lower v indices and since h_0 does not depend on u and v we have at most one h_0 (and therefore, one Riemann or Ricci tensor) contribution to the E_{uu} equation of motion and no contributions to the other components of the equations of motion. This is because we are left with lower u indices which cannot be contracted. However it is always possible to have contributions to the equations of motion of the form $\partial^4 h_0$, $\partial^6 h_0$ from additional space derivatives acting on the Riemann tensor. We can use the following replacement rules:

$$\nabla_\alpha\nabla^\alpha R^{\mu\nu} = -\frac{1}{2}\vec{\partial}^4 h_{_0}, \tag{.138}$$

$$\nabla^\alpha\nabla_\alpha\nabla^\beta\nabla_\beta R^{\mu\nu} = -\frac{1}{2}\vec{\partial}^6 h_{_0}. \tag{.139}$$

For polynomials of third and fourth order in the Riemann or Ricci tensors we get that the zeroth order equations of motion are automatically satisfied by our background since they contain at least two instances of the Riemann or Ricci tensors. The contributions to the zeroth order equations of motion for all independent gravity actions containing one or two Riemann tensors and at most two covariant derivatives are listed in Table .5.[12]

b First Order Equations of Motion

In this subsection we detail the rules used to simplify the equations of motion at first order in the probe graviton contribution. We address separately rules which are relevant for the equations of motion of actions with two and three Riemann tensors and those which are relevant for actions with four Riemann tensors.

As explained in subsection 4.1, on our background and with the assumptions we take regarding the polarisations, the only components of the higher curvature gravity equations which are not automatically satisfied are E_{ij}. We will use a set of rules to simplify possible structures of E_{ij}.

[12] We did not consider as independent, gravity actions which are related by integration by parts, use of the second Bianchi identity or the addition of R^3 terms which do not contribute to the equations of motion at zeroth order in the probe graviton.

Action	Background equations
R	$-\frac{1}{2}\vec{\partial}^2 h_0$
R^2	0
$R_{ab}R^{ab}$	$-\frac{1}{2}\vec{\partial}^4 h_0$
$R_{abcd}R^{abcd}$	$-2\vec{\partial}^4 h_0$
$R\nabla_c\nabla^c R$	0
$R^{ab}\nabla_c\nabla^c R_{ab}$	$-\frac{1}{2}\vec{\partial}^6 h_0$

Table .5: Contributions to the zero order equations of motion.

Actions with Two or Three Riemann Tensors Using the statements of the previous subsection and the list of metric components, Christoffel symbols and Riemann components found in appendix 1.1 one can derive the following set of rules for the possible structures of E_{ij}. We implemented these rules in *Mathematica* to obtain the results of section 4.

The vanishing of $R^{(0)}$, $R^{(1)}$ and $R^{(0)}_{\mu\nu}$ implies that up to first order in h_{ij}, any contraction of an expression with the following tensor structure should vanish:

$$R = 0, \qquad R_{\alpha\beta}R_{\gamma\delta} = 0, \qquad R_{\alpha\beta}\nabla_\gamma\nabla_\delta R_{\epsilon\zeta} = 0. \tag{.140}$$

The fact that there are no zero order quantities with lower v or upper u indices implies that all expressions of the form:

$$R^{\alpha\beta\gamma\delta}R^{\rho\sigma\kappa\mu}R^{\nu\zeta\lambda\xi} = 0, \tag{.141}$$

with all indices except for two of them contracted, vanish when they appear in the E_{ij} component of the equations of motion. This is only to be used in the R^3 and $R\nabla^2 R$ actions. The reason is the following: after extracting all the metric factors, two of the Riemann tensor are at zero order. Each one of them carries two lower u indices. Since the only metric term with upper u indices is g^{uv}, this leaves us with four lower v indices. Since no zero order terms have such indices and the first order Riemann tensor can only absorb two of them, such contributions do not arise. The polarisation condition $\epsilon_{ij}b^i b^j = 0$ implies:

$$R^{\alpha\beta\gamma\delta}R_{\alpha\beta\gamma\delta} = 0. \tag{.142}$$

Using (.136) and (.137) it is also easy to show that:

$$\begin{aligned} &\nabla_\alpha R_{\beta\gamma\delta\rho}\nabla^\sigma R^{\mu\nu\zeta\lambda} = 0, \\ &\nabla_\alpha R_{\beta\gamma}\nabla^\sigma R^{\mu\nu\zeta\lambda} = 0, \\ &\nabla^\alpha R^{\beta\gamma}\nabla^\sigma R^{\mu\nu} = 0. \end{aligned} \tag{.143}$$

Finally for the non-zero terms we denote:

$$\begin{aligned}
\mathcal{T}_0{}^{ij} &\equiv h_{0,}{}^{kj}\ h^i{}_{k,vv}, \\
\mathcal{T}_1{}^{ij} &\equiv \Delta_d \mathcal{T}_0{}^{ij}, \\
\mathcal{S}_0^{ij} &\equiv h_{0,}{}^{ijkl}\ h_{kl,vv},
\end{aligned} \tag{.144}$$

where $\Delta_d \equiv -4(\partial_u\partial_v + h_0\partial_v^2)$, and obtain the following rules for terms of dimension four:

$$\begin{aligned}
&R^{\alpha\beta}R^{\mu}{}_{\alpha}{}^{\nu}{}_{\beta} = 0, \\
&R^{\mu\alpha\beta\gamma}R^{\nu}{}_{\alpha\beta\gamma} = 2\mathcal{T}_0{}^{\mu\nu} + 2\mathcal{T}_0{}^{\nu\mu}, \\
&R^{\mu\alpha\beta\gamma}R^{\nu}{}_{\beta\alpha\gamma} = \mathcal{T}_0{}^{\mu\nu} + \mathcal{T}_0{}^{\nu\mu}, \\
&\nabla_\alpha\nabla^\alpha R^{\mu\nu} = -\frac{1}{2}\Delta_d^2 h^{\mu\nu},
\end{aligned} \tag{.145}$$

and of dimension six

$$\begin{aligned}
&R^{\nu}{}_{\alpha\beta\gamma}\nabla^\gamma\nabla^\beta R^{\mu\alpha} = 0, \\
&R^{\mu}{}_{\alpha}{}^{\nu}{}_{\beta}\nabla_\gamma\nabla^\gamma R^{\alpha\beta} = 0, \\
&R^{\alpha\beta}\nabla_\gamma\nabla^\gamma R^{\mu}{}_{\alpha}{}^{\nu}{}_{\beta} = 0, \\
&R^{\alpha\beta}\nabla_\alpha\nabla_\beta R^{\mu\nu} = 0, \\
&R^{\nu}{}_{\alpha\beta\gamma}\nabla^\gamma\nabla^\mu R^{\alpha\beta} = 0, \\
&R^{\alpha\beta\gamma\delta}\nabla_\beta\nabla^\mu R^{\nu}{}_{\alpha\gamma\delta} = -2\,\mathcal{S}^{\mu\nu}, \\
&R^{\alpha\beta\gamma\delta}\nabla_\delta\nabla_\beta R^{\mu}{}_{\alpha}{}^{\nu}{}_{\gamma} = \mathcal{S}^{\mu\nu}, \\
&R^{\nu\alpha\beta\gamma}\nabla_\rho\nabla^\rho R^{\mu}{}_{\alpha\beta\gamma} = 2\,\mathcal{T}_1{}^{\mu\nu}, \\
&R^{\nu\gamma\alpha\beta}\nabla_\gamma\nabla_\beta R^{\mu}{}_{\alpha} = \mathcal{T}_1{}^{\mu\nu}, \\
&R^{\nu\beta\alpha\gamma}\nabla_\gamma\nabla_\beta R^{\mu}{}_{\alpha} = \mathcal{T}_1{}^{\mu\nu}, \\
&R^{\alpha\beta\gamma\delta}\nabla^\mu\nabla^\nu R_{\alpha\beta\gamma\delta} = 4\,\mathcal{S}^{\mu\nu}, \\
&R^{\alpha\beta\gamma\delta}\nabla^\mu\nabla^\nu R_{\alpha\gamma\beta\delta} = 2\,\mathcal{S}^{\mu\nu}, \\
&R^{\alpha\beta\gamma\delta}\nabla_\delta\nabla^\mu R^{\nu}{}_{\alpha\beta\gamma} = \mathcal{S}^{\mu\nu}, \\
&R^{\nu\alpha\beta\gamma}\nabla_\delta\nabla^\delta R^{\mu}{}_{\beta\alpha\gamma} = \mathcal{T}_1{}^{\mu\nu}, \\
&\nabla^\alpha\nabla_\alpha\nabla^\beta\nabla_\beta R^{\mu\nu} = -\frac{1}{2}\Delta_d^3 h^{\mu\nu},
\end{aligned} \tag{.146}$$

with μ and ν restricted to the transverse directions. We derive the rules for the terms of dimension six as follows. Splitting the covariant derivatives to partial derivatives and Christoffel symbols, we obtain four different kinds of contributions: $R\partial^2 R$, $R^2\partial\Gamma$, $R\Gamma\partial R$ and $R^2\Gamma^2$. Due to the relations (.136) and (.137) the contributions of the form $R\Gamma\partial R$ and $R\Gamma^2 R$ vanish at first order in the probe graviton contribution. The contributions of the form $R^2\partial\Gamma$ are also always vanishing. This however, requires working out explicitly the relevant index structures. The first contribution, of the form $R\partial^2 R$, does not vanish and gives the results listed above. We would also like to point out that terms of the form $g^{ij}\phi$, where ϕ is a scalar are automatically vanishing using the same reasoning as in subsection 4.1.

c Actions with Four Riemann Tensors

For actions with four Riemann tensors, the equations of motion can contain either four Riemann (or Ricci) tensors, or alternatively three Riemann tensors and two covariant derivatives. Terms in the equations of motion that contain four Riemann tensors have vanishing contribution when evaluated on our background (7.8). This follows from the fact that such contributions would have three h_0 factors, accompanied by six lower u indices. To contract them properly one must be able to absorb six lower v indices. However we can absorb at most two lower v indices in the only Riemann tensor which is first order in the probe graviton and two in the free indices of the equation of motion.

For the second possible type of contributions with three Riemann tensors and two covariant derivatives we are only left with structures of the form $R^2\partial^2 R$. This is derived using (.143) which is still valid due to the two beams setup. Focusing on contributions to the transverse equations of motion E_{ij}, we have two of the Riemann tensors that have to be of zero order in the probe graviton contributions and are therefore associated with four lower u indices. We are left with four lower v indices that need to be absorbed. Two of them can be absorbed in a first order term and the two others in the derivatives. As such, the derivatives cannot have free indices and have to be of the form ∂_v.

Requiring two v indices to be absorbed by a first order term forces it to be a Riemann tensor (since the Ricci tensor cannot absorb such v indices). We therefore have:

$$\begin{aligned}
&R^{\alpha\beta\gamma\delta}R^{\rho\sigma\kappa\mu}\nabla^\zeta\nabla^\lambda R^{\nu\xi} = 0,\\
&R^{\alpha\beta}R^{\rho\sigma\kappa\mu}\nabla^\zeta\nabla^\lambda R^{\nu\xi} = 0,\\
&R^{\alpha\beta}R^{\rho\sigma}\nabla^\zeta\nabla^\lambda R^{\nu\xi} = 0,\\
&R^{\alpha\beta}R^{\rho\sigma}\nabla^\zeta\nabla^\lambda R^{\gamma\delta\nu\xi} = 0,\\
&R^{\alpha\beta}R^{\rho\sigma\kappa\mu}\nabla^\zeta\nabla^\lambda R^{\nu\xi\gamma\delta} = 0.
\end{aligned} \tag{.147}$$

The requirement the derivatives must absorb two lower v indices automatically forbids terms of the form $RR\nabla_\alpha\nabla^\alpha R$, $RR\nabla\nabla^\mu R$ and $RR\nabla^\mu\nabla^\nu R$ where μ and ν are the free transverse indices of the equation of motion.

We also notice that the two Riemann tensors outside of the derivatives must be at zeroth order. This is because the derivative of a zeroth order quantity with respect to v is vanishing, which forces the Riemann inside the derivatives to be first order. Hence we cannot contract indices which are not transverse between the two Riemann tensors outside the derivatives. Remembering that the free indices are transverse we obtain:

$$\begin{aligned}
&R_\alpha{}^{\delta\rho\sigma}R^{\nu\alpha\beta\gamma}\nabla_\sigma\nabla_\gamma R^\mu{}_{\delta\beta\rho} = 0,\\
&R_\alpha{}^{\delta\rho\sigma}R^{\nu\alpha\beta\gamma}\nabla_\gamma\nabla_\beta R^\mu{}_{\delta\rho\sigma} = 0,\\
&R_\alpha{}^{\delta\rho\sigma}R^{\nu\alpha\beta\gamma}\nabla_\delta\nabla_\gamma R^\mu{}_{\beta\rho\sigma} = 0,\\
&R_\alpha{}^{\delta\rho\sigma}R^{\nu\alpha\beta\gamma}\nabla_\sigma\nabla_\delta R^\mu{}_{\rho\beta\gamma} = 0,\\
&R^{\nu\alpha\beta\gamma}R_\alpha{}^{\delta\rho\sigma}\nabla_\sigma\nabla_\gamma R^\mu{}_{\rho\beta\delta} = 0.
\end{aligned} \tag{.148}$$

Direct calculation then leads to

$$R_\beta{}^{\delta\rho\sigma}R^{\nu\alpha\beta\gamma}\nabla_\sigma\nabla_\gamma R^\mu{}_{\rho\alpha\delta}=0,$$
$$R_\beta{}^{\delta\rho\sigma}R^{\nu\alpha\beta\gamma}\nabla_\sigma\nabla_\alpha R^\mu{}_{\rho\gamma\delta}=0, \tag{.149}$$

$$R^{\mu\alpha\beta\gamma}R^{\nu\delta\rho\sigma}\nabla_\gamma\nabla_\beta R_{\alpha\delta\rho\sigma}=0,$$
$$R^{\nu\alpha\beta\gamma}R_\alpha{}^{\delta\rho\sigma}\nabla_\gamma\nabla_\beta R^\mu{}_{\delta\rho\sigma}=0, \tag{.150}$$

$$R^{\mu\alpha\nu\beta}R^{\gamma\delta\rho\sigma}\nabla_\delta\nabla_\alpha R_{\beta\gamma\rho\sigma}=0,$$
$$R^{\mu\alpha\nu\beta}R^{\gamma\delta\rho\sigma}\nabla_\delta\nabla_\beta R_{\alpha\gamma\rho\sigma}=0, \tag{.151}$$

$$R^{\mu\alpha\nu\beta}R^{\gamma\delta\rho\sigma}\nabla_\beta\nabla_\alpha R_{\gamma\delta\rho\sigma}=0,$$
$$R^{\mu\alpha\nu\beta}R^{\gamma\delta\rho\sigma}\nabla_\sigma\nabla_\delta R_{\alpha\gamma\beta\rho}=0, \tag{.152}$$

$$R^{\alpha\beta\gamma\delta}R_{\alpha\beta}{}^{\rho\sigma}\nabla_\sigma\nabla_\delta R^\mu{}_\gamma{}^\nu{}_\rho=0, \tag{.153}$$

$$R^{\alpha\beta\gamma\delta}R_\alpha{}^{\rho\sigma\xi}\nabla_\xi\nabla_\rho R_{\beta\gamma\delta\sigma}=0, \tag{.154}$$

Finally, defining:

$$\begin{aligned}\mathcal{U}_0{}^{ij}&=h_{0,}{}^{lk}h_{0,k}{}^{j}h^i{}_{l,v^4}\ ,\\ \mathcal{W}_0{}^{ij}&=h_{0,}{}^{ik}h_{0,}{}^{jl}h_{kl,v^4}\ ,\\ \mathcal{V}_0{}^{ij}&=h_{0,}{}^{kl}h_{0,kl}h^{ij}{}_{,v^4}\ ,\end{aligned} \tag{.155}$$

the non-vanishing contributions are given by:

$$R_{\alpha\beta\gamma\delta}R^{\rho\beta\sigma\delta}\nabla_\sigma\nabla^\gamma R^{\mu\alpha\nu}{}_\rho=-2\,\mathcal{V}_0{}^{\mu\nu},$$
$$R_\alpha{}^\rho{}_\gamma{}^\sigma R^{\alpha\beta\gamma\delta}\nabla_\sigma\nabla_\rho R^\mu{}_\beta{}^\nu{}_\delta=-2\,\mathcal{V}_0{}^{\mu\nu},$$
$$R_\alpha{}^\rho{}_\gamma{}^\sigma R^{\alpha\beta\gamma\delta}\nabla_\sigma\nabla_\delta R^\mu{}_\beta{}^\nu{}_\rho=-2\,\mathcal{V}_0{}^{\mu\nu},$$
$$R_\alpha{}^\rho{}_\gamma{}^\sigma R^{\alpha\beta\gamma\delta}\nabla_\rho\nabla_\delta R^\mu{}_\beta{}^\nu{}_\sigma=-2\,\mathcal{V}_0{}^{\mu\nu}, \tag{.156}$$

$$R_{\alpha\beta\gamma\delta}R^{\nu\sigma\alpha\rho}\nabla_\sigma\nabla_\rho R^{\mu\beta\gamma\delta}=-4\,\mathcal{U}_0{}^{\mu\nu}, \tag{.157}$$

$$R_\beta{}^{\delta\rho\sigma}R^{\nu\alpha\beta\gamma}\nabla_\sigma\nabla_\gamma R^\mu{}_{\delta\alpha\rho}=2\,\mathcal{U}_0{}^{\mu\nu},$$
$$R_\beta{}^{\delta\rho\sigma}R^{\nu\alpha\beta\gamma}\nabla_\sigma\nabla_\delta R^\mu{}_{\alpha\gamma\rho}=2\,\mathcal{U}_0{}^{\mu\nu},$$
$$R_\beta{}^{\delta\rho\sigma}R^{\nu\alpha\beta\gamma}\nabla_\sigma\nabla_\alpha R^\mu{}_{\delta\gamma\rho}=2\,\mathcal{U}_0{}^{\mu\nu},$$
$$R_\beta{}^{\delta\rho\sigma}R^{\nu\alpha\beta\gamma}\nabla_\sigma\nabla_\delta R^\mu{}_{\gamma\alpha\rho}=2\,\mathcal{U}_0{}^{\mu\nu}, \tag{.158}$$

$$R_\beta{}^{\delta\rho\sigma}R^{\nu\alpha\beta\gamma}\nabla_\gamma\nabla_\alpha R^\mu{}_{\delta\rho\sigma}=-4\,\mathcal{U}_0{}^{\mu\nu},$$
$$R_\beta{}^{\delta\rho\sigma}R^{\nu\alpha\beta\gamma}\nabla_\delta\nabla_\gamma R^\mu{}_{\alpha\rho\sigma}=-4\,\mathcal{U}_0{}^{\mu\nu},$$
$$R_\beta{}^{\delta\rho\sigma}R^{\nu\alpha\beta\gamma}\nabla_\delta\nabla_\alpha R^\mu{}_{\gamma\rho\sigma}=-4\,\mathcal{U}_0{}^{\mu\nu}, \tag{.159}$$

$$R^{\mu\alpha\beta\gamma}R^{\nu\delta\rho\sigma}\nabla_\gamma\nabla_\alpha R_{\beta\delta\rho\sigma}=-4\,\mathcal{W}_0{}^{\mu\nu}, \tag{.160}$$

$$R^{\mu\alpha\beta\gamma}R^{\nu\delta\rho\sigma}\nabla_\sigma\nabla_\gamma R_{\alpha\rho\beta\delta}=2\,\mathcal{W}_0{}^{\mu\nu}, \tag{.161}$$

$$R^{\mu\alpha\beta\gamma}R^{\nu\delta\rho\sigma}\nabla_\delta\nabla_\alpha R_{\beta\gamma\rho\sigma}=-8\,\mathcal{W}_0{}^{\mu\nu}, \tag{.162}$$

where some of the rules are related using the second Bianchi identity.

List of Figures

Bibliography

[1] K. Benakli, L. Darmé, M. D. Goodsell, and P. Slavich, "A Fake Split Supersymmetry Model for the 126 GeV Higgs," *JHEP* **1405** (2014) 113.

[2] K. Benakli, L. Darmé, and M. D. Goodsell, "(O)Mega Split," *JHEP* **11** (2015) 100, arXiv:1508.02534 [hep-ph].

[3] K. Benakli and L. Darmé, "Off-trail SUSY," *PoS* **PLANCK2015** (2015) 019, arXiv:1511.02044 [hep-ph].

[4] K. Benakli, L. Darmé, M. D. Goodsell, and J. Harz, "The Di-Photon Excess in a Perturbative SUSY Model," arXiv:1605.05313 [hep-ph].

[5] K. Benakli, L. Darmé, and Y. Oz, "The Slow Gravitino," *JHEP* **10** (2014) 121, arXiv:1407.8321 [hep-ph].

[6] K. Benakli, S. Chapman, L. Darmé, and Y. Oz, "On Swift Gravitons," arXiv:1512.07245 [hep-th].

[7] N. Arkani-Hamed and S. Dimopoulos, "Supersymmetric unification without low energy supersymmetry and signatures for fine-tuning at the LHC," *JHEP* **06** (2005) 073, arXiv:hep-th/0405159 [hep-th].

[8] G. F. Giudice and A. Romanino, "Split supersymmetry," *Nucl. Phys.* **B699** (2004) 65–89, arXiv:hep-ph/0406088 [hep-ph]. [Erratum: Nucl. Phys.B706,65(2005)].

[9] N. Arkani-Hamed, S. Dimopoulos, G. F. Giudice, and A. Romanino, "Aspects of split supersymmetry," *Nucl. Phys.* **B709** (2005) 3–46, arXiv:hep-ph/0409232 [hep-ph].

[10] P. H. Chankowski, K. Kowalska, S. Lavignac, and S. Pokorski, "Flavor changing neutral currents and inverted sfermion mass hierarchy," in *Proceedings, 40th Rencontres de Moriond, 2005 Electroweak interactions and unified theories*, pp. 267–276. 2005. arXiv:hep-ph/0507133 [hep-ph]. http://inspirehep.net/record/687130/files/arXiv:hep-ph˙0507133.pdf.

[11] M. Badziak, E. Dudas, M. Olechowski, and S. Pokorski, "Inverted Sfermion Mass Hierarchy and the Higgs Boson Mass in the MSSM," *JHEP* **07** (2012) 155, arXiv:1205.1675 [hep-ph].

[12] G. F. Giudice and A. Romanino, "Split supersymmetry," *Nucl.Phys.* **B699** (2004) 65–89.

[13] N. Bernal, A. Djouadi, and P. Slavich, "The MSSM with heavy scalars," *JHEP* **07** (2007) 016, arXiv:0705.1496 [hep-ph].

[14] G. F. Giudice and A. Strumia, "Probing High-Scale and Split Supersymmetry with Higgs Mass Measurements," *Nucl. Phys.* **B858** (2012) 63–83, arXiv:1108.6077 [hep-ph].

[15] A. Arvanitaki, N. Craig, S. Dimopoulos, and G. Villadoro, "Mini-Split," *JHEP* **02** (2013) 126, arXiv:1210.0555 [hep-ph].

[16] E. Bagnaschi, G. F. Giudice, P. Slavich, and A. Strumia, "Higgs Mass and Unnatural Supersymmetry," *JHEP* **09** (2014) 092, arXiv:1407.4081 [hep-ph].

[17] J. P. Vega and G. Villadoro, "SusyHD: Higgs mass Determination in Supersymmetry," *JHEP* **07** (2015) 159, arXiv:1504.05200 [hep-ph].

[18] P. Fayet, "MASSIVE GLUINOS," *Phys. Lett.* **B78** (1978) 417.

[19] J. Polchinski and L. Susskind, "Breaking of Supersymmetry at Intermediate-Energy," *Phys. Rev.* **D26** (1982) 3661.

[20] L. J. Hall and L. Randall, "U(1)-R symmetric supersymmetry," *Nucl. Phys.* **B352** (1991) 289–308.

[21] P. J. Fox, A. E. Nelson, and N. Weiner, "Dirac gaugino masses and supersoft supersymmetry breaking," *JHEP* **08** (2002) 035, arXiv:hep-ph/0206096 [hep-ph].

[22] I. Antoniadis, K. Benakli, A. Delgado, M. Quiros, and M. Tuckmantel, "Split extended supersymmetry from intersecting branes," *Nucl. Phys.* **B744** (2006) 156–179, arXiv:hep-th/0601003 [hep-th].

[23] I. Antoniadis, A. Delgado, K. Benakli, M. Quiros, and M. Tuckmantel, "Splitting extended supersymmetry," *Phys.Lett.* **B634** (2006) 302–306.

[24] S. Abel and M. Goodsell, "Easy Dirac Gauginos," *JHEP* **06** (2011) 064, arXiv:1102.0014 [hep-th].

[25] R. Davies, "Dirac gauginos and unification in F-theory," *JHEP* **10** (2012) 010, arXiv:1205.1942 [hep-th].

[26] K. Benakli, "Dirac Gauginos: A User Manual," *Fortsch. Phys.* **59** (2011) 1079–1082, arXiv:1106.1649 [hep-ph].

[27] K. Benakli and M. D. Goodsell, "Dirac Gauginos in General Gauge Mediation," *Nucl.Phys.* **B816** (2009) 185–203.

[28] C. Csaki, J. Goodman, R. Pavesi, and Y. Shirman, "The $m_D - b_M$ problem of Dirac gauginos and its solutions," *Phys. Rev.* **D89** no. 5, (2014) 055005, arXiv:1310.4504 [hep-ph].

[29] M. D. Goodsell, F. Staub, and K. Benakli, "Dirac Gauginos and the 125 GeV Higgs," *JHEP* **1306** (2013) 073.

[30] E. Bertuzzo, C. Frugiuele, T. Gregoire, and E. Ponton, "Dirac gauginos, R symmetry and the 125 GeV Higgs," *JHEP* **04** (2015) 089, arXiv:1402.5432 [hep-ph].

[31] H. Beauchesne and T. Gregoire, "Electroweak precision measurements in supersymmetric models with a $U(1)_R$ lepton number," *JHEP* **05** (2014) 051, arXiv:1402.5403 [hep-ph].

[32] L. J. Hall, D. Pinner, and J. T. Ruderman, "A Natural SUSY Higgs Near 126 GeV," *JHEP* **04** (2012) 131, arXiv:1112.2703 [hep-ph].

[33] K. Benakli, M. D. Goodsell, and A.-K. Maier, "Generating mu and Bmu in models with Dirac Gauginos," *Nucl. Phys.* **B851** (2011) 445–461, arXiv:1104.2695 [hep-ph].

[34] G. D. Kribs and A. Martin, "Supersoft Supersymmetry is Super-Safe," *Phys. Rev.* **D85** (2012) 115014, arXiv:1203.4821 [hep-ph].

[35] J. Hisano, M. Nagai, T. Naganawa, and M. Senami, "Electric Dipole Moments in PseudoDirac Gauginos," *Phys. Lett.* **B644** (2007) 256–264, arXiv:hep-ph/0610383 [hep-ph].

[36] G. D. Kribs, E. Poppitz, and N. Weiner, "Flavor in supersymmetry with an extended R-symmetry," *Phys. Rev.* **D78** (2008) 055010, arXiv:0712.2039 [hep-ph].

[37] A. Kumar, D. Tucker-Smith, and N. Weiner, "Neutrino Mass, Sneutrino Dark Matter and Signals of Lepton Flavor Violation in the MRSSM," *JHEP* **09** (2010) 111, arXiv:0910.2475 [hep-ph].

[38] R. Fok and G. D. Kribs, "μ to e in R-symmetric Supersymmetry," *Phys. Rev.* **D82** (2010) 035010, arXiv:1004.0556 [hep-ph].

[39] E. Dudas, M. Goodsell, L. Heurtier, and P. Tziveloglou, "Flavour models with Dirac and fake gluinos," *Nucl. Phys.* **B884** (2014) 632–671, arXiv:1312.2011 [hep-ph].

[40] K. Hsieh, "Pseudo-Dirac bino dark matter," *Phys. Rev.* **D77** (2008) 015004, arXiv:0708.3970 [hep-ph].

[41] G. Belanger, K. Benakli, M. Goodsell, C. Moura, and A. Pukhov, "Dark Matter with Dirac and Majorana Gaugino Masses," *JCAP* **0908** (2009) 027.

[42] K. Benakli and M. D. Goodsell, "Dirac Gauginos, Gauge Mediation and Unification," *Nucl. Phys.* **B840** (2010) 1–28, arXiv:1003.4957 [hep-ph].

[43] K. Benakli, M. Goodsell, F. Staub, and W. Porod, "Constrained minimal Dirac gaugino supersymmetric standard model," *Phys.Rev.* **D90** (Aug., 2014) 045017.

[44] M. Heikinheimo, M. Kellerstein, and V. Sanz, "How Many Supersymmetries?," *JHEP* **04** (2012) 043, arXiv:1111.4322 [hep-ph].

[45] S. Y. Choi, D. Choudhury, A. Freitas, J. Kalinowski, J. M. Kim, and P. M. Zerwas, "Dirac Neutralinos and Electroweak Scalar Bosons of N=1/N=2 Hybrid Supersymmetry at Colliders," *JHEP* **08** (2010) 025, arXiv:1005.0818 [hep-ph].

[46] S. Y. Choi, J. Kalinowski, J. M. Kim, and E. Popenda, "Scalar gluons and Dirac gluinos at the LHC," *Acta Phys. Polon.* **B40** (2009) 2913–2922, arXiv:0911.1951 [hep-ph].

[47] T. Plehn and T. M. P. Tait, "Seeking Sgluons," *J. Phys.* **G36** (2009) 075001, arXiv:0810.3919 [hep-ph].

[48] D. Goncalves-Netto, D. Lopez-Val, K. Mawatari, T. Plehn, and I. Wigmore, "Sgluon Pair Production to Next-to-Leading Order," *Phys. Rev.* **D85** (2012) 114024, arXiv:1203.6358 [hep-ph].

[49] S. Calvet, B. Fuks, P. Gris, and L. Valery, "Searching for sgluons in multitop events at a center-of-mass energy of 8 TeV," *JHEP* **04** (2013) 043, arXiv:1212.3360 [hep-ph].

[50] L. Beck, F. Blekman, D. Dobur, B. Fuks, J. Keaveney, and K. Mawatari, "Probing top-philic sgluons with LHC Run I data," *Phys. Lett.* **B746** (2015) 48–52, arXiv:1501.07580 [hep-ph].

[51] K. Benakli, M. Goodsell, F. Staub, and W. Porod, "Constrained minimal Dirac gaugino supersymmetric standard model," *Phys. Rev.* **D90** no. 4, (2014) 045017, arXiv:1403.5122 [hep-ph].

[52] K. Benakli and M. D. Goodsell, "Dirac Gauginos, Gauge Mediation and Unification," *Nucl.Phys.* **B840** (2010) 1–28.

[53] C. Csaki, J. Goodman, R. Pavesi, and Y. Shirman, "The m_d-b_m problem of Dirac gauginos and its solutions," *Phys.Rev.* **D89** (Mar., 2014) 055005.

[54] ATLAS and C. collaborations, "Combined Measurement of the Higgs Boson Mass in pp Collisions at $\sqrt{s}=7$ and 8 TeV with the ATLAS and CMS Experiments," *Phys.Rev.Lett.* **114** (May, 2015) 191803.

[55] **Particle Data Group** Collaboration, J. Beringer *et al.*, "Review of Particle Physics (RPP)," *Phys. Rev.* **D86** (2012) 010001.

[56] **Tevatron Electroweak Working Group, CDF, D0** Collaboration, M. Muether, "Combination of cdf and do results on the mass of the top quark using up to 8.7 fb^{-1} at the tevatron," arXiv:1305.3929 [hep-ex].

[57] J. Fleischer, F. Jegerlehner, O. V. Tarasov, and O. L. Veretin, "Two loop QCD corrections of the massive fermion propagator," *Nucl. Phys.* **B539** (1999) 671–690, arXiv:hep-ph/9803493 [hep-ph]. [Erratum: Nucl. Phys.B571,511(2000)].

[58] L. V. Avdeev and M. Yu. Kalmykov, "Pole masses of quarks in dimensional reduction," *Nucl. Phys.* **B502** (1997) 419–435, arXiv:hep-ph/9701308 [hep-ph].

[59] M. Binger, "Higgs boson mass in split supersymmetry at two-loops," *Phys. Rev.* **D73** (2006) 095001, arXiv:hep-ph/0408240 [hep-ph].

[60] C. Tamarit, "Decoupling heavy sparticles in hierarchical SUSY scenarios: Two-loop Renormalization Group equations," arXiv:1204.2292 [hep-ph].

[61] F. Staub, "SARAH 4: A tool for (not only SUSY) model builders," *Comput.Phys.Commun.* **185** (2014) 1773–1790.

[62] F. Lyonnet, I. Schienbein, F. Staub, and A. Wingerter, "PyR@TE: Renormalization Group Equations for General Gauge Theories," *Comput. Phys. Commun.* **185** (2014) 1130–1152, arXiv:1309.7030 [hep-ph].

[63] A. Sirlin and R. Zucchini, "Dependence of the Quartic Coupling H(m) on M(H) and the Possible Onset of New Physics in the Higgs Sector of the Standard Model," *Nucl. Phys.* **B266** (1986) 389.

[64] G. Degrassi, S. Di Vita, J. Elias-Miro, J. R. Espinosa, G. F. Giudice, G. Isidori, and A. Strumia, "Higgs mass and vacuum stability in the Standard Model at NNLO," *JHEP* **08** (2012) 098, arXiv:1205.6497 [hep-ph].

[65] D. Buttazzo, G. Degrassi, P. P. Giardino, G. F. Giudice, F. Sala, A. Salvio, and A. Strumia, "Investigating the near-criticality of the Higgs boson," *JHEP* **12** (2013) 089, arXiv:1307.3536 [hep-ph].

[66] W. Porod, "SPheno, a program for calculating supersymmetric spectra, SUSY particle decays and SUSY particle production at e+ e- colliders," *Comput.Phys.Commun.* **153** (2003) 275–315.

[67] W. Porod and F. Staub, "SPheno 3.1: Extensions including flavour, CP-phases and models beyond the MSSM," *Comput.Phys.Commun.* **183** (2012) 2458–2469.

[68] F. Staub, "SARAH,".

[69] F. Staub, "Automatic Calculation of supersymmetric Renormalization Group Equations and Self Energies," *Comput.Phys.Commun.* **182** (2011) 808–833.

[70] F. Staub, "From Superpotential to Model Files for FeynArts and CalcHep/CompHep," *Comput.Phys.Commun.* **181** (2010) 1077–1086.

[71] F. Staub, "SARAH 3.2: Dirac Gauginos, UFO output, and more," *Comput.Phys.Commun.* **184** (2013) pp. 1792–1809.

[72] M. D. Goodsell, "Two-loop RGEs with Dirac gaugino masses," *JHEP* **1301** (2013) 066.

[73] T. P. collaboration, "Planck 2015 results. XIII. Cosmological parameters,".

[74] E. W. Kolb and M. S. Turner, "The Early Universe," *Front. Phys.* **69** (1990) 1–547.

[75] K. Griest and D. Seckel, "Three exceptions in the calculation of relic abundances," *Phys. Rev.* **D43** (1991) 3191–3203.

[76] N. Arkani-Hamed, A. Delgado, and G. F. Giudice, "The Well-tempered neutralino," *Nucl.Phys.* **B741** (2006) 108–130.

[77] G. Belanger, F. Boudjema, A. Pukhov, and A. Semenov, "micrOMEGAs_3: A program for calculating dark matter observables," *Comput.Phys.Commun.* **185** (2014) 960–985.

[78] N. Nagata and S. Shirai, "Higgsino Dark Matter in High-Scale Supersymmetry," *JHEP* **1501** (Jan., 2015) 029.

[79] X. collaboration, "Implications on Inelastic Dark Matter from 100 Live Days of XENON100 Data," *Phys.Rev.* **D84** (2011) 061101.

[80] L. collaboration, "First results from the LUX dark matter experiment at the Sanford Underground Research Facility," *Phys.Rev.Lett.* **112** (Mar., 2014) 091303.

[81] A. Arvanitaki, C. Davis, P. W. Graham, A. Pierce, and J. G. Wacker, "Limits on split supersymmetry from gluino cosmology," *Physical Review D* **72** no. 7, (2005) 075011. http://prd.aps.org/abstract/PRD/v72/i7/e075011.

[82] P. Gambino, G. F. Giudice, and P. Slavich, "Gluino decays in split supersymmetry," *Nucl.Phys.* **B726** (2005) 35–52.

[83] T. K. Hemmick *et al.*, "A Search for Anomalously Heavy Isotopes of Low Z Nuclei," *Phys. Rev.* **D41** (1990) 2074–2080.

[84] P. F. Smith, J. R. J. Bennett, G. J. Homer, J. D. Lewin, H. E. Walford, and W. A. Smith, "A SEARCH FOR ANOMALOUS HYDROGEN IN ENRICHED D-2 O, USING A TIME-OF-FLIGHT SPECTROMETER," *Nucl. Phys.* **B206** (1982) 333–348.

[85] A. De Simone, V. Sanz, and H. P. Sato, "Pseudo-Dirac Dark Matter Leaves a Trace," *Phys. Rev. Lett.* **105** (2010) 121802, arXiv:1004.1567 [hep-ph].

[86] M. Quiros, "Finite temperature field theory and phase transitions," in *High energy physics and cosmology. Proceedings, Summer School, Trieste, Italy, June 29-July 17, 1998*, pp. 187–259. 1999. arXiv:hep-ph/9901312 [hep-ph]. http://alice.cern.ch/format/showfull?sysnb=0302087.

[87] G. 't Hooft, "Computation of the Quantum Effects Due to a Four-Dimensional Pseudoparticle," *Phys. Rev.* **D14** (1976) 3432–3450. [Erratum: Phys. Rev.D18,2199(1978)].

[88] Y. Li, S. Profumo, and M. Ramsey-Musolf, "Bino-driven Electroweak Baryogenesis with highly suppressed Electric Dipole Moments," *Phys. Lett.* **B673** (2009) 95–100, arXiv:0811.1987 [hep-ph].

[89] M. Carena, A. Megevand, M. Quiros, and C. E. M. Wagner, "Electroweak baryogenesis and new TeV fermions," *Nucl.Phys.* **B716** (2005) 319–351.

[90] P. Kumar and E. Ponton, "Electroweak Baryogenesis and Dark Matter with an approximate R-symmetry," *JHEP* **11** (2011) 037, arXiv:1107.1719 [hep-ph].

[91] R. Fok, G. D. Kribs, A. Martin, and Y. Tsai, "Electroweak Baryogenesis in R-symmetric Supersymmetry," *Phys. Rev.* **D87** no. 5, (2013) 055018, arXiv:1208.2784 [hep-ph].

[92] **CMS Collaboration** Collaboration, "Search for new physics in high mass diphoton events in proton-proton collisions at $\sqrt{s} = 13$ TeV," Tech. Rep. CMS-PAS-EXO-15-004, CERN, Geneva, 2015. https://cds.cern.ch/record/2114808.

[93] "Search for resonances decaying to photon pairs in 3.2 fb^{-1} of pp collisions at $\sqrt{s} = 13$ TeV with the ATLAS detector," Tech. Rep. ATLAS-CONF-2015-081, CERN, Geneva, Dec, 2015. http://cds.cern.ch/record/2114853.

[94] **CMS Collaboration** Collaboration, "Search for new physics in high mass diphoton events in 3.3 fb^{-1} of proton-proton collisions at $\sqrt{s} = 13$ TeV and combined interpretation of searches at 8 TeV and 13 TeV," Tech. Rep. CMS-PAS-EXO-16-018, CERN, Geneva, 2016. https://cds.cern.ch/record/2139899.

[95] H. P. Nilles and M. W. Winkler, "750 GeV Diphotons and Supersymmetric Grand Unification," arXiv:1604.03598 [hep-ph].

[96] C. Han, H. M. Lee, M. Park, and V. Sanz, "The diphoton resonance as a gravity mediator of dark matter," *Phys. Lett.* **B755** (2016) 371–379, arXiv:1512.06376 [hep-ph].

[97] J. L. Hewett and T. G. Rizzo, "750 GeV Diphoton Resonance in Warped Geometries," arXiv:1603.08250 [hep-ph].

[98] V. Sanz, "Theoretical interpretation of a spin-two diphoton excess," arXiv:1603.05574 [hep-ph].

[99] B. M. Dillon and V. Sanz, "A Little KK Graviton at 750 GeV," arXiv:1603.09550 [hep-ph].

[100] R. Franceschini, G. F. Giudice, J. F. Kamenik, M. McCullough, A. Pomarol, R. Rattazzi, M. Redi, F. Riva, A. Strumia, and R. Torre, "What is the gamma gamma resonance at 750 GeV?," arXiv:1512.04933 [hep-ph].

[101] T. ATLAS and C. Collaborations, "Measurements of the Higgs boson production and decay rates and constraints on its couplings from a combined ATLAS and CMS analysis of the LHC pp collision data at $\sqrt{s} = 7$ and 8 TeV,".

[102] M. Goodsell, K. Nickel, and F. Staub, "Generic two-loop Higgs mass calculation from a diagrammatic approach," *Eur. Phys. J.* **C75** no. 6, (2015) 290, arXiv:1503.03098 [hep-ph].

[103] G. F. Giudice, I. Tkachev, and A. Riotto, "Nonthermal production of dangerous relics in the early universe," *JHEP* **9908** (1999) 009.

[104] G. F. Giudice, A. Riotto, and I. Tkachev, "Thermal and nonthermal production of gravitinos in the early universe," *JHEP* **9911** (1999) 036.

[105] R. Kallosh, L. Kofman, A. D. Linde, and A. Van Proeyen, "Gravitino production after inflation," *Phys.Rev.* **D61** (2000) 103503.

[106] Y. Kahn, D. A. Roberts, and J. Thaler, "The goldstone and goldstino of supersymmetric inflation," *JHEP* **10** (2015) 001, arXiv:1504.05958 [hep-th].

[107] S. Ferrara, R. Kallosh, and J. Thaler, "Cosmology with orthogonal nilpotent superfields," *Phys. Rev.* **D93** no. 4, (2016) 043516, arXiv:1512.00545 [hep-th].

[108] E. Dudas, S. Ferrara, A. Kehagias, and A. Sagnotti, "Properties of Nilpotent Supergravity," *JHEP* **09** (2015) 217, arXiv:1507.07842 [hep-th].

[109] Z. Komargodski and N. Seiberg, "From Linear SUSY to Constrained Superfields," *JHEP* **09** (2009) 066, arXiv:0907.2441 [hep-th].

[110] G. Dall'Agata, E. Dudas, and F. Farakos, "On the origin of constrained superfields," arXiv:1603.03416 [hep-th].

[111] G. Velo and D. Zwanziger, "Propagation and quantization of Rarita-Schwinger waves in an external electromagnetic potential," *Phys. Rev.* **186** (1969) 1337–1341.

[112] S. Deser, V. Pascalutsa, and A. Waldron, "Massive spin 3/2 electrodynamics," *Phys.Rev.* **D62** (2000) 105031.

[113] A. K. Das and M. Kaku, "SUPERSYMMETRY AT HIGH TEMPERATURES," *Phys. Rev.* **D18** (1978) 4540.

[114] K. Tesima, "SUPERSYMMETRY AT FINITE TEMPERATURES," *Phys. Lett.* **B123** (1983) 226.

[115] D. Boyanovsky, "Supersymmetry Breaking at Finite Temperature: The Goldstone Fermion," *Phys. Rev.* **D29** (1984) 743.

[116] H. Aoyama and D. Boyanovsky, "Goldstone Fermions in Supersymmetric Theories at Finite Temperature," *Phys. Rev.* **D30** (1984) 1356.

[117] V. V. Lebedev and A. V. Smilga, "SUPERSYMMETRIC SOUND," *Nucl. Phys.* **B318** (1989) 669–704.

[118] R. G. Leigh and R. Rattazzi, "Supersymmetry, finite temperature and gravitino production in the early universe," *Phys.Lett.* **B352** (1995) 20–28.

[119] K. Kratzert, "Finite temperature supersymmetry: The Wess-Zumino model," *Annals Phys.* **308** (2003) 285–310.

[120] K. Kratzert, "Supersymmetry breaking at finite temperature,".

[121] P. Kovtun and L. G. Yaffe, "Hydrodynamic fluctuations, long time tails, and supersymmetry," *Phys.Rev.* **D68** (2003) 025007.

[122] C. Hoyos, B. Keren-Zur, and Y. Oz, "Supersymmetric sound in fluids," *JHEP* **1211** (2012) 152.

[123] S. Deser and B. Zumino, "Broken Supersymmetry and Supergravity," *Phys.Rev.Lett.* **38** (1977) 1433–1436.

[124] R. Jackiw, V. P. Nair, S. Y. Pi, and A. P. Polychronakos, "Perfect fluid theory and its extensions," *J. Phys.* **A37** (2004) R327–R432, arXiv:hep-ph/0407101 [hep-ph].

[125] E. A. Bergshoeff, D. Z. Freedman, R. Kallosh, and A. Van Proeyen, "Pure de Sitter Supergravity," *Phys. Rev.* **D92** no. 8, (2015) 085040, arXiv:1507.08264 [hep-th]. [Erratum: Phys. Rev.D93,no.6,069901(2016)].

[126] K. Benakli, Y. Oz, and G. Policastro, "The Super-Higgs Mechanism in Fluids," *JHEP* **1402** (2014) 015.

[127] P. R. Auvil and J. J. Brehm, "Wave functions for particles of higher spin," *Phys. Rev.* **145** (1966) 1152.

[128] T. Moroi, "Effects of the gravitino on the inflationary universe,".

[129] P. Van Nieuwenhuizen, "Supergravity," *Phys.Rept.* **68** (1981) 189–398.

[130] C. Aragone, "STRINGY CHARACTERISTICS OF EFFECTIVE GRAVITY," in *SILARG 6: 6th Latin American Symposium on Relativity and Gravitation Rio de Janeiro, Brazil, July 13-18, 1987*. 1987. http://alice.cern.ch/format/showfull?sysnb=0093487.

[131] Y. Choquet-Bruhat, "The Cauchy Problem for Stringy Gravity," *J. Math. Phys.* **29** (1988) 1891–1895.

[132] W. Bonnor, "The gravitational field of light," *Communications in Mathematical Physics* **13** no. 3, (1969) 163–174.

[133] M. Goroff and J. H. Schwarz, "D-dimensional Gravity in the Light Cone Gauge," *Phys. Lett.* **B127** (1983) 61–64.

[134] X. O. Camanho, J. D. Edelstein, J. Maldacena, and A. Zhiboedov, "Causality Constraints on Corrections to the Graviton Three-Point Coupling," *JHEP* **02** (2016) 020, arXiv:1407.5597 [hep-th].

[135] D. N. Kabat and M. Ortiz, "Eikonal quantum gravity and Planckian scattering," *Nucl. Phys.* **B388** (1992) 570–592, arXiv:hep-th/9203082 [hep-th].

[136] M. Ciafaloni and D. Colferai, "Rescattering corrections and self-consistent metric in Planckian scattering," *JHEP* **10** (2014) 85, arXiv:1406.6540 [hep-th].

[137] M. Visser, B. Bassett, and S. Liberati, "Superluminal censorship," *Nucl. Phys. Proc. Suppl.* **88** (2000) 267–270, arXiv:gr-qc/9810026 [gr-qc].

[138] S. Gao and R. M. Wald, "Theorems on gravitational time delay and related issues," *Class. Quant. Grav.* **17** (2000) 4999–5008, arXiv:gr-qc/0007021 [gr-qc].

[139] K. D. Olum, "Superluminal travel requires negative energies," *Phys. Rev. Lett.* **81** (1998) 3567–3570, arXiv:gr-qc/9805003 [gr-qc].

[140] S. W. Hawking and G. F. R. Ellis, *The Large Scale Structure of Space-Time*. Cambridge Monographs on Mathematical Physics. Cambridge University Press, 2011.

[141] B. C. Palmer and D. Marolf, "On fast travel through spherically symmetric space-times," *Phys. Rev.* **D67** (2003) 044012, arXiv:gr-qc/0211045 [gr-qc].

[142] G. Papallo and H. S. Reall, "Graviton time delay and a speed limit for small black holes in Einstein-Gauss-Bonnet theory," *JHEP* **11** (2015) 109, arXiv:1508.05303 [gr-qc].

[143] H. Reall, N. Tanahashi, and B. Way, "Causality and Hyperbolicity of Lovelock Theories," *Class.Quant.Grav.* **31** (2014) 205005.

[144] R. Courant and D. Hilbert, *Methods of Mathematical Physics*, vol. 2. Wiley, New York, 1962.

[145] L. Hormander, *The analysis of linear partial differential operators, Vol I and II*. Classics in Mathematics. Springer-Verlag, Berlin, 1983. Distribution theory and Fourier analysis.

[146] J. M. Martin-Garcia, R. Portugal, and L. R. U. Manssur, "The Invar Tensor Package," *Comput.Phys.Commun.* **177** (2007) 640–648.

[147] J. M. Martin-Garcia, D. Yllanes, and R. Portugal, "The Invar tensor package: Differential invariants of Riemann," *Comput.Phys.Commun.* **179** (2008) 586–590.

[148] J. M. Martin-Garcia, "xPerm: fast index canonicalization for tensor computer algebra," *Computer physics communications* **179** no. 8, (2008) 597–603.

[149] T. Nutma, "xTras: A field-theory inspired xAct package for mathematica," *Comput.Phys.Commun.* **185** (June, 2014) 1719–1738.

[150] A. A. Tseytlin, "R**4 terms in 11 dimensions and conformal anomaly of (2,0) theory," *Nucl.Phys.* **B584** (2000) 233–250.

[151] D. J. Gross and E. Witten, "Superstring Modifications of Einstein's Equations," *Nucl.Phys.* **B277** (1986) 1.

[152] B. Bellazzini, C. Cheung, and G. N. Remmen, "Quantum Gravity Constraints from Unitarity and Analyticity," *Phys. Rev.* **D92** (2015) 125009, arXiv:1509.00851 [hep-th].

[153] R. P. Woodard, "Avoiding dark energy with 1/r modifications of gravity," *Lect. Notes Phys.* **720** (2007) 403–433, arXiv:astro-ph/0601672 [astro-ph].

[154] T.-j. Chen, M. Fasiello, E. A. Lim, and A. J. Tolley, "Higher derivative theories with constraints: Exorcising Ostrogradski's Ghost," *JCAP* **1302** (2013) 042, arXiv:1209.0583 [hep-th].

Luc DARMÉ **09/06/2016**

Sujet : Unconventional particle behaviours in supersymmetric theories and gravity

Résumé : Nous étudions dans un premier temps deux théories supersymétriques basées sur la présence de Gauginos de Dirac à travers deux scénarios à la phénoménologie bien distincte. La première, dite de "Fake Split SUSY", se caractérise par un spectre de particules scindé entre une partie à l'échelle électrofaible et l'autre plus lourde. Ces modèles prédisent avec une grande précision la masse du boson de Higgs et sont compatibles avec de nombreux résultats de cosmologie, au prix d'un spectre très peu naturel. La seconde présente un scénario supersymétrique dont l'un des boson scalaire pourrait être identifié avec la résonance à 750 GeV observée au LHC.

Dans un second temps, nous analysons d'abord la propagation d'un champ massif de spin 3/2 dans un fluide sous-jacent (par exemple le gravitino lorsque la supergravité est couplée au fluide). Nous montrons que les degrés de liberté correspondant aux différentes hélicités se propagent avec des vitesses distinctes. Nous étudions ensuite la question de la vitesse des gravitons dans les théories de gravité étendue dans lesquelles, en sus du Lagrangien d'Einstein-Hilbert, nous ajoutons des opérateurs construits à partir de tenseurs de Riemann.

Subject : Unconventional particle behaviours in supersymmetric theories and gravity

Abstract : We will first focus on supersymmetric theories with Dirac Gaugino masses. We investigate two advantages of such models. First, the possibility to reconcile the measured Higgs mass with an arbitrary large scale of supersymmetry breaking. Second, we show how the scalar singlet present in such models is a sound candidate for a resonance explaining the 750 GeV diphoton excess observed by the LHC experiments.

In a second part, we start by discussing the propagation of a massive spin 3/2 state in a fluid (for instance the gravitino when supergravity is coupled to a background fluid). We show that the degrees of freedom corresponding to different helicities travel with different velocities. We then discuss the separate issue of graviton speed in extended gravity theories where the usual Einstein-Hilbert Lagrangian is supplemented by various higher order terms constructed from Riemann tensors.